

# Final Report

February 1975

## Design, Fabrication, and Test of Lightweight Shell Structure

(NASA-CR-120605) DESIGN, FABRICATION AND  
TEST OF LIGHTWEIGHT SHELL STRUCTURE Final  
Report (Martin Marietta Corp.) 155 p HC  
46.25 CSCL 20K

N75-19731

Unclass

63/39 11849

**MARTIN MARIETTA**

MCR-75-10  
Contract NAS8-29979

Final  
Report

February 1975

---

DESIGN, FABRICATION AND  
TEST OF LIGHTWEIGHT  
SHELL STRUCTURE

Author

John R. Lager

Prepared for

National Aeronautics and  
Space Administration  
George C. Marshall Space  
Flight Center  
Huntsville, Alabama

MARTIN MARIETTA CORPORATION  
P.O. Box 179  
Denver, Colorado 80201



## FOREWORD

---

This final report was prepared by the Denver Division of Martin Marietta Corporation under Contract NAS8-29979. The report covers work performed from September 1973 to February 1975. The program was sponsored by the National Aeronautics and Space Administration, George C. Marshall Space Flight Center, Huntsville, Alabama, with Mr. Carl Loy, the Contracting Officers' Representative (COR). The program was performed by the Stress, Test, and Advanced Structures Section, Structures and Materials Engineering, Martin Marietta Corporation, Denver, Colorado, with Mr. John R. Lager serving as Program Manager (PM).

The following Martin Marietta personnel were principal contributors to the program: Joseph W. Maccalous and Bernard M. Burke, Composite Fabrication; Alan E. Muhl, Metal Fabrication; Arthur Feldman, Materials; Joseph M. Toth, Jr. and Alvin A. Holston, Design and Analysis; and Major L. Sansam and Richard Brown, Structural Test.

## ABSTRACT

---

A cylindrical shell structure 3.66 m (144 in.) high by 4.57 m (180 in.) diameter was designed using a wide variety of materials and structural concepts to withstand design ultimate combined loading of 1225.8 N/cm (700 lb/in.) axial compression and 245.2 N/cm (140 lb/in.) torsion. The overall cylinder geometry and design loading are representative of that expected on a high performance Space Tug vehicle. The relatively low design load level results in designs that use thin gage metals and fibrous-composite laminates. Fabrication and structural test of small panels and components representative of many of the candidate designs served to demonstrate proposed fabrication techniques and to verify design and analysis methods. Three of the designs evaluated, honeycomb sandwich with aluminum faceskins, honeycomb sandwich with graphite/epoxy faceskins, and aluminum truss with fiber-glass meteoroid protection layers were selected for further evaluation. Successful compression and shear tests of larger panels verified the structural integrity of these three candidate design concepts. These concepts result in overall cylinder structural weight in the range 2.59 to 3.08 kg/m<sup>2</sup> (0.53 to 0.63 lb/ft<sup>2</sup>).



## CONTENTS

---

	<u>Page</u>
I. INTRODUCTION . . . . .	I-1
II. MATERIALS . . . . .	II-1
A. Material Properties . . . . .	II-1
B. Ultrathin Composite Materials Study . . . . .	II-1 thru II-11
III. DESIGN AND ANALYSIS . . . . .	III-1
A. Structural Concepts . . . . .	III-2
B. Analysis Methods . . . . .	III-2
C. Structural Design . . . . .	III-11
D. HOLBOAT Program Modification . . . . .	III-21 thru III-26
IV. FABRICATION DEVELOPMENT . . . . .	IV-1
A. Small Phase I Structures . . . . .	IV-1
B. Large Phase II Structures . . . . .	IV-27 thru IV-54
V. QUALITY NDE--SANDWICH PANEL . . . . .	V-1 thru V-6
VI. STRUCTURAL TEST . . . . .	VI-1
A. Small Phase I Structures . . . . .	VI-1
B. Large Phase II Structures . . . . .	VI-28 thru VI-39
VII. CONCLUSIONS AND RECOMMENDATIONS . . . . .	VII-1
A. Conclusions . . . . .	VII-1
B. Recommendations . . . . .	VII-3 thru VII-5
VIII. REFERENCES . . . . .	VIII-1 and VIII-2
APPENDIX	
CONVERSION FACTORS . . . . .	A-1

## Figure

---

II-1	Recommended and Actual Cure Cycles for Laminate B414-2 . . . . .	II-6
II-2	Recommended and Actual Cure Cycles for Laminate EG-8-1 . . . . .	II-7
II-3	Recommended and Actual Cure Cycles for Laminate AS12-1 . . . . .	II-8
II-4	Recommended and Actual Cure Cycles for Laminate B414-1 . . . . .	II-9
II-5	Comparison of Lamina Arrangements for Laminate Styles B410-1 and B410-2 . . . . .	II-11
III-1	Shell Structure and Design Loading . . . . .	III-1
III-2	Isotropic Stiffened Shell Configuration . . . . .	III-6
III-3	Skin/Stringer Detail . . . . .	III-7
III-4	Element of Isogrid Rib Grid . . . . .	III-10
III-5	Honeycomb Sandwich Concept Design Conditions . . . . .	III-12
III-6	Truss, Finite Element Model . . . . .	III-14
III-7	Aluminum Truss Member Geometry, Sections . . . . .	III-15
III-8	Aluminum Lightweight Shell Isogrid, Flat Test Panel . . . . .	III-16
III-9	Design Concept Summary . . . . .	III-20
III-10	Stiffened Cylinder Construction . . . . .	III-24
III-11	Example of Typical Stiffening Member Composed of Straight and Circular Elements of Symmetric, Balanced Laminate Construction . . . . .	III-24
III-12	Shell Construction Combination . . . . .	III-25
IV-1	Specimen Geometry . . . . .	IV-2
IV-2	Composite Stiffener Straps . . . . .	IV-3
IV-3	Graphite/Epoxy Truss Strut, Overall Geometry . . . . .	IV-5
IV-4	Graphite/Epoxy Truss Strut, Center and End Regions . . . . .	IV-6
IV-5	Boron/Graphite/Epoxy Truss Strut Finished Component . . . . .	IV-7
IV-6	FM-24 Reticulated Adhesive . . . . .	IV-9
IV-7	Aluminum Honeycomb Core Damage . . . . .	IV-11
IV-8	Machined Honeycomb Core . . . . .	IV-13
IV-9	Laminate Configurations . . . . .	IV-14
IV-10	Vacuum Bag System . . . . .	IV-16
IV-11	Time/Temperature/Pressure Cure Cycle . . . . .	IV-16
IV-12	Cured Laminates . . . . .	IV-17
IV-13	Sandwich Faceskin Configurations . . . . .	IV-18
IV-14	Face Skin Layup Tool . . . . .	IV-19
IV-15	Composite Development Test Panels Type I-GL-18-1 . . . . .	IV-21
IV-16	Honeycomb Sandwich Test Panels, 10X Photomicrographs . . . . .	IV-22
IV-17	Honeycomb Sandwich Test Panels, Photomicrographs . . . . .	IV-23
IV-18	Isogrid Test Panel . . . . .	IV-24
IV-19	Aluminum Truss Components . . . . .	IV-26
IV-20	Aluminum Truss Joint . . . . .	IV-26
IV-21	Structural Concept Selection for Phase II Work . . . . .	IV-28
IV-22	Graphite/Epoxy Panel Configuration . . . . .	IV-29
IV-23	Graphite/Epoxy Faceskin Layup . . . . .	IV-29
IV-24	Graphite/Epoxy Faceskins Vacuum Bag System . . . . .	IV-30



IV-25	Graphite/Epoxy Sandwich Panel Layup . . . . .	IV-31
IV-26	Graphite/Epoxy Faceskin Cure Cycle . . . . .	IV-32
IV-27	Cured Graphite/Epoxy Faceskin . . . . .	IV-33
IV-28	Graphite/Epoxy Sandwich Panels . . . . .	IV-35
IV-29	Sandwich Panel Vacuum Bag System . . . . .	IV-37
IV-30	Graphite/Epoxy Sandwich Panel Layup . . . . .	IV-37
IV-31	Cure Cycle for Graphite/Epoxy Sandwich Panel CP-Type I-Gr-16 . . . . .	IV-38
IV-32	Graphite/Epoxy Compression Test Panel CP-Type I-GR-16 . . . . .	IV-38
IV-33	Graphite/Epoxy Shear Test Panel SP-Type I-GR-6 . . . . .	IV-39
IV-34	Shear Panel Damage and Repair . . . . .	IV-39
IV-35	Aluminum Panel Configuration . . . . .	IV-40
IV-36	Aluminum Sheet before Immersion into Chem-Mill Etchant Solution . . . . .	IV-42
IV-37	Aluminum Sheet Being Removed from Chem-Mill Etchant Solution . . . . .	IV-42
IV-38	Aluminum Sandwich Panels . . . . .	IV-45
IV-39	Modified FM-24 Cure Cycle for Aluminum Sandwich Panels . . . . .	IV-47
IV-40	Aluminum Sandwich Compression Panel CP-Alum-10 . . . . .	IV-48
IV-41	Aluminum Sandwich Shear Panel SP-Alum-10 . . . . .	IV-48
IV-42	Aluminum Truss Configuration . . . . .	IV-50
IV-43	Aluminum Truss Component Chem Milling . . . . .	IV-52
IV-44	Aluminum Truss Members . . . . .	IV-52
IV-45	Aluminum Truss Stringer Weld-Bond . . . . .	IV-53
IV-46	Aluminum Truss Joint Assembly . . . . .	IV-54
IV-47	Aluminum Truss Assembly Fixture . . . . .	IV-54
IV-48	Aluminum Truss Compression Test Panel without Fiberglass Cloth . . . . .	IV-56
IV-49	Aluminum Truss with Fiberglass Meteoroid Protection Layers . . . . .	IV-56
V-1	Aluminum Sandwich Panel Quality NDE Standards Panel . . . . .	V-2
V-2	Quality NDE Standards Panel Aluminum Core . . . . .	V-2
V-3	Quality NDE Standards Panel F7-24 Adhesive Film . . . . .	V-3
V-4	Quality NDE Standards Panel Aluminum Faceskin . . . . .	V-4
V-5	Ultrasonic C Scan Aluminum Honeycomb Sandwich Panel Quadrant A, FM-24 Splice . . . . .	V-4
V-6	Ultrasonic C Scan Aluminum Honeycomb Sandwich Panel Quadrant B, Core Damage . . . . .	V-4
V-7	Ultrasonic C Scan Aluminum Honeycomb Sandwich Panel Quadrant B, Skin Damage . . . . .	V-5
V-8	Ultrasonic C Scan Aluminum Honeycomb Sandwich Panel Quadrant D, Bond Anomaly . . . . .	V-5
V-9	X-Ray Aluminum Honeycomb Sandwich Panel Quadrant B, Core Damage . . . . .	V-6
VI-1	Failed Flat Bond Tensile Specimens, Panel 15 Unreticulated . . . . .	VI-1
VI-2	Sandwich Stiffener Location . . . . .	VI-3
VI-3	Test Setup . . . . .	VI-4
VI-4	Composite Stiffner Straps, Load Deflection Curves . . . . .	VI-5

VI-5	Failed Specimens . . . . .	VI-5
VI-6	Graphite/Epoxy Truss Strut Test Specimen . . . . .	VI-7
VI-7	Test Setup . . . . .	VI-7
VI-8	Local Deflection Curves, Graphite/Epoxy Columns . . .	VI-8
VI-9	Strain Gage Plots . . . . .	VI-8
VI-10	Failed Section, Specimen 1 . . . . .	VI-9
VI-11	Strain Gage Locations . . . . .	VI-11
VI-12	Axial Compression Test Setup . . . . .	VI-12
VI-13	Load Deflection Curves, Honeycomb Sandwich Compression Tests . . . . .	VI-12
VI-14	Typical Failures, Honeycomb Sandwich Compression Tests . . . . .	VI-13
VI-15	Long Beam Bending Test Setup . . . . .	VI-15
VI-16	Load Deflection Curves, Honeycomb Sandwich Long Beam Bending Tests . . . . .	VI-17
VI-17	Typical Failures, Honeycomb Sandwich Long Beam Bending Tests . . . . .	VI-20
VI-18	Short Beam Shear Test Setup . . . . .	VI-21
VI-19	Load Deflection Curves, Honeycomb Sandwich Short Beam Shear Tests . . . . .	VI-22
VI-20	Failed Short Beam Shear Specimen . . . . .	VI-24
VI-21	Aluminum Isogrid Test Panel . . . . .	VI-25
VI-22	Aluminum Isogrid Panel Test Setup . . . . .	VI-25
VI-23	Aluminum Isogrid Instrumentation . . . . .	VI-26
VI-24	Load Deflection Curves, Aluminum Isogrid Panel . . . .	VI-26
VI-25	Strain Gage Plots, Aluminum Isogrid Panel . . . . .	VI-27
VI-26	Failed Panel, Aluminum Isogrid . . . . .	VI-27
VI-27	Sandwich Panel Compression Test Fixture . . . . .	VI-34
VI-28	Southwell Plot, Aluminum Panel Compression Test, CP-Alum-10 . . . . .	VI-34
VI-29	Southwell Plot, Graphite/Epoxy Panel Compression Test, CP-TypeI-Gr-16 . . . . .	VI-37
VI-30	Aluminum Truss Compression Test Local Stringer Buckling . . . . .	VI-37
VI-31	Aluminum Sandwich Shear Panel Failed Specimen . . . .	VI-38
VI-32	Graphite/Epoxy Sandwich Shear Panel Failed Specimen . . . . .	VI-38
VI-33	Aluminum Truss Shear Test Local Buckling Failure . . .	VI-39

Table

II-1	Material Properties, Metallic Materials . . . . .	II-2
II-2	Material Properties, Composite Materials . . . . .	II-3
II-3	Ultrathin Composite Materials Study, Laminate Styles . . . . .	II-5
II-4	Ultrathin Composite Laminate Characterization . . . .	II-10
III-1	Stiffness Matrices Skin/Stringer/Frame Construction . . . . .	III-8
III-2	Stiffness Matrices Truss Construction . . . . .	III-10
III-3	Selected Honeycomb Sandwich Designs . . . . .	III-17



III-4	Selected Shirt Truss Designs . . . . .	III-18
III-5	Selected Skin/Stringer/Frame and Isogrid Design . . . .	III-19
IV-1	Graphite/Epoxy Faceskins . . . . .	IV-33
IV-2	Aluminum Faceskins . . . . .	IV-41
VI-1	Honeycomb Sandwich Flat Tension Test Results . . . . .	VI-2
VI-2	Test Results . . . . .	VI-4
VI-3	Honeycomb Panel Definition . . . . .	VI-10
VI-4	Honeycomb Sandwich Compression . . . . .	VI-14
VI-5	Honeycomb Sandwich Long Beam Bending Test Results . . .	VI-19
VI-6	Honeycomb Sandwich Short Beam Shear Test Results . . . .	VI-23
VI-7	Material Properties . . . . .	VI-33
VI-8	Theoretical and Experimental Panel Loads . . . . .	VI-35

## I. INTRODUCTION

---

During Phase I of Contract NAS8-29979, Design, Fabrication, and Test of Lightweight Shell Structure, a cylindrical shell skirt structure 4.57 m (180 in.) in diameter and 3.66 m (144 in.) high was subjected to a design and analysis study using a wide variety of structural materials and concepts. The design loading of 1225.8 N/cm (700 lb/in.) axial compression and 245.2 N/cm (140 lb/in.) torsion is representative of that expected on a typical Space Tug skirt section. Structural concepts evaluated included honeycomb sandwich, truss, isogrid, and skin/stringer/frame. The materials considered include a wide variety of structural metals as well as glass, graphite, and boron-reinforced composites. The most unique characteristic of the candidate designs is that they involve the use of very thin-gage material. Fabrication and structural test of small panels and components representative of many of the candidate designs served to demonstrate proposed fabrication techniques and to verify design and analysis methods. Three of the designs evaluated, honeycomb sandwich with aluminum faceskins, honeycomb sandwich with graphite/epoxy faceskins, and aluminum truss with fiberglass meteoroid protection layers were selected for further evaluation. These concepts result in overall cylinder structural weight in the range 2.59 to 3.08 kg/m<sup>2</sup> (0.53 to 0.63 lb/ft<sup>2</sup>). Phase I work is only summarized in this report because a thorough coverage was given in the Interim Report, MCR-74-92, March 1974.<sup>1</sup>

During Phase II, Fabrication and Test, three structural components of each of the three selected structural concepts were fabricated. A development panel with approximately 1.83 by 0.915 m (6 by 3 ft) overall dimensions was first fabricated for each structural concept. These panels served to verify fabrication techniques and were not subjected to structural test. Successful fabrication of the development panels was followed by fabrication of 1.83 by 0.915 m (6 by 3 ft) compression panels that were subjected to axial compression test loading. A 0.915 by 0.915 m (3 by 3 ft) panel of each concept was also fabricated and subjected to pure shear test loading. In addition, the computer program used to predict the overall buckling of anisotropic cylinders under combined loading was modified to include cylinders with discrete stringers and frames and theoretical/experimental correlation factors.



## II. MATERIALS

---

### A. MATERIAL PROPERTIES

The material properties used in the design study are listed in Tables II-1 and II-2 with references to the data sources. The materials considered included conventional materials such as aluminum and fiberglass along with less frequently used materials such as beryllium and advanced fibrous composites. In general, it was expected that the materials with the highest values of stiffness/density would be the most efficient for the cylindrical structure being studied--provided the strengths were reasonable. However, the useful minimum gage of each material, as determined by availability, discrete ply thicknesses of composites, manageability, fabricability, material quality, and cost had to be considered in only a qualitative way. Because material thickness directly affects weight, minimum available gages and ply thicknesses could be a more important consideration than the other properties for a material with adequate strength and stiffness. These properties are, therefore, listed in Tables II-1 and II-2.

In Table II-1, the mechanical properties taken from the *Aerospace Structural Metals Handbook* and the MIL-HDBK-5B are B-basis values. The properties for boron/aluminum and beryllium/titanium are average properties. Information on available minimum gages was obtained directly from vendors. In Table II-2, the values come either from MIL-HDBK-17A or are vendor data (or other average values), modified to account for the thickness of the laminates where they were to be applied. Thin laminates unavoidably have higher resin contents and generally seem to have lower strengths and stiffnesses.<sup>2,3</sup> One goal of this program is to determine what penalty must be applied to thick laminate data for use with thin laminates and whether or not this penalty can be reduced by innovative design and fabrication techniques.

### B. ULTRATHIN COMPOSITE MATERIALS STUDY

A material process development program was performed on ultrathin fibrous composite laminates. Symmetric laminates embodying epoxy preimpregnated layers of graphite, boron, and glass fibers singly or in combination were manufactured with a range of thicknesses from 0.165 to 0.470 mm (0.0065 to 0.018 in.), respectively. The effect of processing parameters on the quality of the laminates

Table II-1 Material Properties, Metallic Materials

Material and Alloy	Density, gm/cm <sup>3</sup> (lb/in. <sup>3</sup> )	Elastic Modulus, E, 10 <sup>6</sup> N/cm <sup>2</sup> (10 <sup>6</sup> psi)	Shear Modulus, G, 10 <sup>6</sup> N/cm <sup>2</sup> (10 <sup>6</sup> psi)	Poisson's Ratio, $\nu$	Compressive Yield Strength, 10 <sup>3</sup> N/cm <sup>2</sup> (10 <sup>3</sup> psi)	Shear Strength, 10 <sup>3</sup> N/cm <sup>2</sup> (10 <sup>3</sup> psi)	Minimum Commercially-Available Thickness, mm (in.)
Aluminum <sup>a</sup>							
2014-T6	2.80 (0.101)	7.4 (10.7)	2.8 (4.0)	0.33	41 (60)	28 (40)	0.254 (0.010)
7075-T6	2.80 (0.101)	7.2 (10.5)	2.7 (3.9)	0.33	49 (71)	32 (47)	0.254 (0.010)
7178-T6	2.82 (0.102)	7.2 (10.5)	2.7 (3.9)	0.33	52 (75)	35 (51)	0.254 (0.010)
Titanium <sup>a</sup>							
6Al-4V	4.43 (0.160)	11.3 (16.4)	4.3 (6.2)	0.31	106 (154)	69 (100)	0.178 (0.007)
8Al-1Mo-1V	4.37 (0.158)	12.4 (18.0)	4.6 (6.7)	0.32	98 (143)	63 (91)	0.406 (0.016)
Maraging Steel <sup>b</sup>							
200	8.00 (0.289)	18.1 (26.2)	7.2 <sup>d</sup> (10.4)	0.264	--	--	0.381 (0.015)
250	8.03 (0.290)	19.6 to 21.4 (28.5 to 31.0)	7.5 to 8.1 <sup>d</sup> (10.9 to 11.8)	0.31	165 to 171 (239 to 245)	109 to 110 (158 to 160)	0.381 (0.015)
300	8.03 (0.290)	19.3 to 20.0 (28.0 to 29.0)	7.4 to 7.6 <sup>d</sup> (10.7 to 11.1)	0.31	180 to 186 (261 to 270)	118 to 119 (172 to 173)	0.381 (0.015)
Beryllium <sup>a,b</sup>	1.85 (0.067)	29.3 (42.5)	13.8 (20.0)	0.03	16 (23)	8 <sup>e</sup> (11.5)	0.508 (0.020)
Lockalloy <sup>b,c</sup>	2.09 (0.0756)	20.0 (29.0)	8.6 (12.5)	0.30	21 (31)	16 (24)	0.635 (0.025)
Boron/Aluminum <sup>f</sup>	2.63 (0.095)	22.9 <sup>g</sup> (33.2) 13.8 <sup>h</sup> (20.1)	4.8 (7.0)	0.25	429 <sup>i</sup> (623)	15 (22)	0.178 <sup>j</sup> (0.007)
Beryllium/Titanium <sup>k</sup>	2.85 (0.103)	21.5 <sup>g</sup> (31.2) 18.0 <sup>h</sup> (26.1)	10.1 (14.6)	0.17	132 <sup>i</sup> (192)	41 (60)	0.635 (0.025)
<p>Note: <sup>a</sup> "Metallurgical Materials and Elements for Aerospace Vehicle Structures", MIL-HDBK-5B, September 1, 1971.  <sup>b</sup> Aerospace Structural Metals Handbook. AFML-TR-68-115, Belfour Stulen, Inc. 1973.  <sup>c</sup> Beryllco Lockalloy Extrusions. Bulletin No. 2200, Beryllco, Inc.  <sup>d</sup> Computed from <math>G = E/2(1 + \nu)</math>.  <sup>e</sup> Assumed.  <sup>f</sup> Cairo and Tarczyner: Graphite/Epoxy, Boron-Graphite/Epoxy Hybrid, and Boron/Aluminum Design Allowables. AFML-TR-72-232. December 1972.  <sup>g</sup> Longitudinal.  <sup>h</sup> Transverse.  <sup>i</sup> Ultimate strength value.  <sup>j</sup> Cured ply thickness.  <sup>k</sup> V. L. Goodwin: Beryllium/Titanium Composites. Brush Wellman, Inc., September 13, 1972.</p>							

Table I-2 Material Properties, Composite Materials

Material	Density, gm/cm <sup>3</sup> , (lb/in. <sup>3</sup> )	Longitudinal Young's Modulus, E <sub>11</sub> , 10 <sup>6</sup> N/cm <sup>2</sup> (10 <sup>6</sup> psi)	Transverse Young's Modulus, E <sub>22</sub> , 10 <sup>6</sup> N/cm <sup>2</sup> (10 <sup>6</sup> psi)	Shear Modulus, G <sub>12</sub> , 10 <sup>6</sup> N/cm <sup>2</sup> (10 <sup>6</sup> psi)	Principal Poisson's Ratio, ν <sub>12</sub>	Compressive Strength, σ <sub>11</sub> , 10 <sup>3</sup> N/cm <sup>2</sup> (ksi)	Shear Strength, 10 <sup>3</sup> N/cm <sup>2</sup> (ksi)	Minimum Cured Ply Thickness, mm (in.)
Glass Fabric (112)/Epoxy <sup>a,d</sup>	2.08 (0.075)	3.10 (4.5)	3.10 (4.5)	1.03 <sup>e</sup> (1.5)	0.30	34 (50)	21 <sup>c</sup> (30 <sup>c</sup> )	0.076 (0.003)
Glass Fabric (104)/Epoxy <sup>b,d</sup>	2.08 (0.075)	2.52 (3.65)	2.52 (3.65)	0.62 (0.9)	0.30	34 (50)	21 <sup>c</sup> (30 <sup>c</sup> )	0.038 (0.0015)
Boron/Epoxy <sup>f</sup>	2.01 (0.0725)	18.8 (27.3)	1.88 (2.73)	0.76 (1.1)	0.25	125 (182)	8	0.140 (0.0055)
A/S Graphite/ Epoxy <sup>h</sup>	1.52 (0.055)	11.2 (16.2)	0.69 (1.0)	0.28 (0.4)	0.30	93 (135)	8	0.127 (0.005)
H1-Modmor I Graphite/Epoxy <sup>f</sup>	1.63 (0.059)	15.9 (23.1)	0.69 (1.0)	0.28 (0.4)	0.30	41 (60)	8	0.152 (0.006)
Thornel 300 Graphite/Epoxy <sup>f</sup>	1.52 (0.055)	11.7 (17.0)	0.69 (1.0)	0.28 (0.4)	0.30	93 (135)	47 <sup>c</sup> (67.5 <sup>c</sup> )	0.051 (0.002)

Note: a. Style 112 woven-glass fabric.  
b. Style 104 woven-glass fabric, 2-ply (±45°) balanced layup, minimum 2-ply thickness = 0.038 mm (0.0015 in.).  
c. ±45° laminate.  
d. Extrapolated from MIL-HDBK-17A "Plastics for Aerospace Vehicles," Part 1, Reinforced Plastics, January 1971.  
e. Stability of Filament-Wound Cylinders under Combined Loading, AFFDL-TR-67-55. May 1967.  
f. Modified vendor data.  
g. Not used for shear applications.  
h. Modified from: Advanced Development of Not-Critical-to-Flight-Safety Advanced Composite Aircraft Structures. Northrop Corp., Aircraft Division, Quarterly Progress Report No. 5, July 31, 1973. Contract F33615-72-C-1781.

as measured by the surface roughness, void content and distribution, resin content, and fiber arrangement was investigated. Nine styles of laminates, as shown in Table II-3, were studied. Processing parameters included initial resin content, resin removal techniques, and curing schedule. A total of twelve 30.5 by 35.6-cm (12 by 14-in.) panels were made, distributed among the nine laminate styles. Various combinations of changes in processing parameters were made in the three duplicated styles dictated by our expectations of the effects. Resin content determinations were made on each panel and photomicrographs were taken of the cross-sections.

The resin system to be used for impregnating the all fiberglass laminates was SR-5700, which is the resin used in the Narmco Rigidite 5208 style of graphite/epoxy prepregs. The fiberglass layers on the outside of the other laminates were not impregnated initially. Instead, we wished to see whether bleed-through during the initial stages of curing would carry enough resin out of the primary material and into the glass layers. If so, then, of course, there would be only one resin in any laminate. The attempt to use the resin in the middle layers of prepreg to wet the outer layers and thus obtain high fiber contents was only partially successful. The technique worked for HM10-1, however. The other laminates in which it was tried had resin-starved surfaces. These laminates were remade using prepregged glass.

When resin systems are mixed, a compromise curing scheme may be required. One such scheme, recommended by Narmco, is shown in Fig. II-1 along with the actual cure cycle obtained on laminate B414-2. The vendor-recommended cure cycles for unmixed laminates of Narmco 5208, Hercules 3501, and Avco 5505 are shown in Fig. II-2, through II-4, respectively, along with the actual cure cycles obtained for representative styles incorporating these respective systems. The designation 2373 refers to the resin used in the Avco 5505 composite system. All laminae were at room temperature at the time of layup and there were no debulking cycles. Diagrams of the arrangement of the bleed system used for each laminate are included on the comprehensive data sheets referred to below.

Table II-4 lists all 12 laminates made in this study with the prepreg and cured laminate thicknesses and constituent contents. It is apparent that estimates of thickness resulting from the laminate orientations being studied must be revised upward about 5 to 10% and that the minimum resin content by volume for good graphite and boron laminates is over 40% but can probably be held below 45%. The very thin all-glass laminates probably require higher resin contents because they are woven, with no unidirectional layers, and weaving inherently creates additional spaces that must be filled by resin. As expected, those remade styles using prepregged rather than dry glass had slightly higher average resin contents. The additional resin required to make the difference between a laminate with a resin-starved surface appearance and one with a good, smooth, void-free surface is only 1 to 2%.

Table II-3 Ultrathin Composite Materials Study, Laminate Styles

Style	Primary Material	Layer Arrangement	Estimated Thickness, mm (in.)
EG06	Woven E-glass, Style 108/SR-5700	1 each at 0°, 90°, 0°	0.152 (0.006)
EG08	Woven E-glass, Style 108/SR-5700	1 each at 0°, 90°, 90°, 0°	0.203 (0.008)
EG10	Woven E-glass/SR-5700	1 of Style 104 at +45° 1 of Style 181 1 of Style 104 at +45°	0.254 (0.010)
HM10	Graphite/Epoxy Type I/5208 (Narmco)	1 of 104 E-Glass at 0° 1 at 0°, 2 at 90°, 1 at 0° 1 of 104 E-Glass at 0°	0.254 (0.010)
AS12	Graphite/Epoxy A/S-3501 (Hercules)	1 of 104 E-Glass at +45° 1 of 104 E-Glass at -45° 8 mil at 0° 1 of 104 E-Glass at -45° 1 of 104 E-Glass at +45°	0.305 (0.012)
HM14	Graphite/Epoxy Type I/5208 (Narmco)	1 of 104 E-Glass at +45° 1 of 104 E-Glass at -45° 10 mil at 0° 1 of 104 E-Glass at -45° 1 of 104 E-Glass at +45°	0.356 (0.014)
B408	Boron/Epoxy 5505/4 (Avco)	1 of 104 E-Glass at +45° 1 of 104 E-Glass at 0° 1 at 0° (including 104 scrim) 1 of 104 E-Glass at +45°	0.203 (0.008)
B410	Boron/Epoxy 5505/4 (Avco)	1 of 108 E-Glass at +45° 1 of 104 E-Glass at 0° 1 at 0° (including 104 scrim) 1 of 108 E-Glass at +45°	0.254 (0.010)
B414	Boron/Epoxy 5505/4 (Avco)	1 of 108 E-Glass at +45° 2 at 0° with 104 scrims on outside (boron face-to- face) 1 of 108 E-Glass at +45°	0.356 (0.014)



HYBRID #1 (5208/2373)

Specimen B 414-2

1. Full Vacuum.
2. Heat to  $240 \pm 6^\circ\text{F}$ ,  $389 \pm 3^\circ\text{K}$ , at  $5 \pm 1^\circ\text{F}$ ,  $3 \pm 0.5^\circ\text{K}$ , per minute.
3. Dwell 30 minutes after Reaching  $235^\circ\text{F}$ ,  $386^\circ\text{K}$ .
4. Apply 100 psi, 69 N/cm<sup>2</sup>
5. Vent Bag to Atmosphere.
6. Heat to  $355 \pm 8^\circ\text{F}$ ,  $452 \pm 8^\circ\text{K}$ , at  $5 \pm 1^\circ\text{F}$ ,  $3 \pm 0.5^\circ\text{K}$ , per minute.
7. Cure 2 Hours.
8. Cool under Pressure to  $140^\circ\text{F}$ ,  $333^\circ\text{K}$ , or Less.

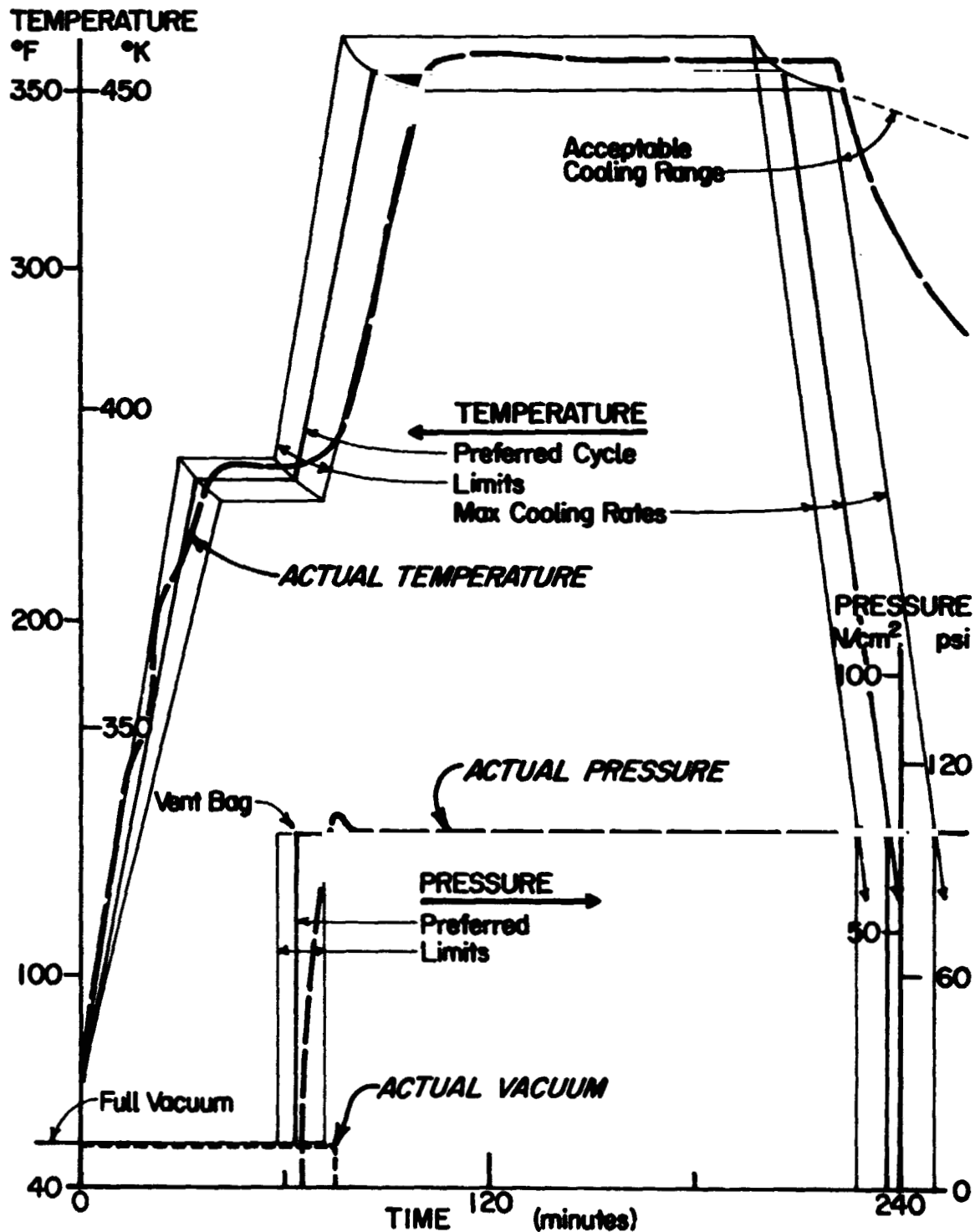


Fig. II-1 Recommended and Actual Cure Cycles for Laminate B414-2

NARMCO 5208

Specimen EG 08 - 1

1. Full Vacuum.
2. Heat to  $275 \pm 5^\circ\text{F}$ ,  $408 \pm 3^\circ\text{K}$ , at  $5 \pm 1^\circ\text{F}$ ,  $3 \pm 0.5^\circ\text{K}$ , per minute.
3. Dwell 60 minutes after Reaching  $265^\circ\text{F}$ ,  $402^\circ\text{K}$ .
4. Add 100 psi,  $69 \text{ N/cm}^2$ .
5. Vent Bag to Atmosphere.
6. Heat to  $355 \pm 5^\circ\text{F}$ ,  $452 \pm 3^\circ\text{K}$ , at  $5 \pm 1^\circ\text{F}$ ,  $3 \pm 0.5^\circ\text{K}$ , per minute.
7. Cure 2 Hours at  $355 \pm 5^\circ\text{F}$ ,  $452 \pm 3^\circ\text{K}$ .

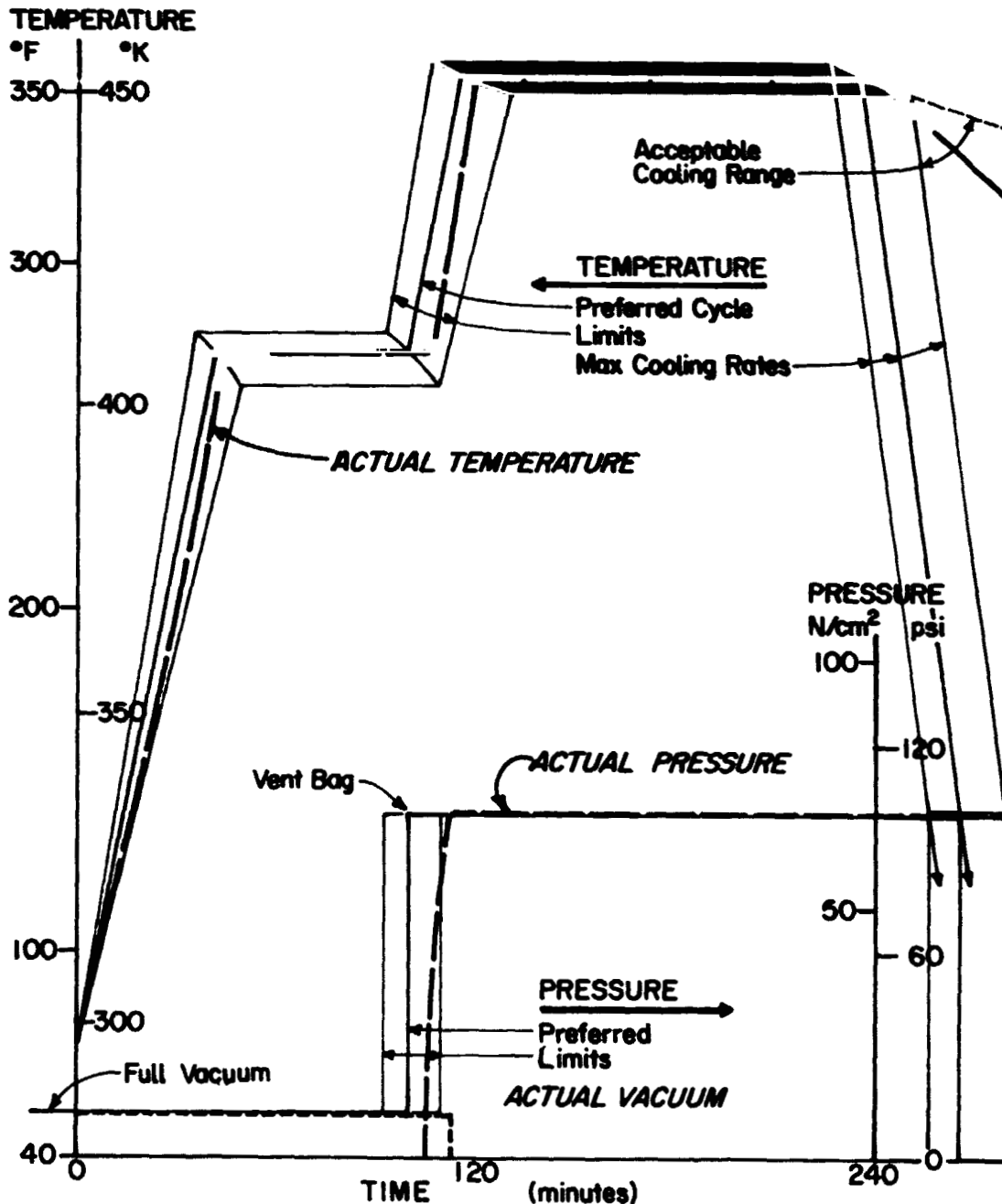


Fig. II-2 Recommended and Actual Cure Cycles for Laminate EG-8-1

HERCULES 3501

Specimen A/S 12-2

1. Full Vacuum.
2. Heat to  $350 \pm 5^\circ\text{F}$ ,  $450 \pm 3^\circ\text{K}$ , at  $2.5 \pm 0.5^\circ\text{F}$ ,  $1.5 \pm 0.3^\circ\text{K}$ , per minute.
3. When at  $225^\circ\text{F}$ ,  $380^\circ\text{K}$ , Apply 85-100 psi, 59-69 N/cm<sup>2</sup>.
4. Cure at  $350 \pm 5^\circ\text{F}$ ,  $450 \pm 3^\circ\text{K}$ , for One Hour with Full Vacuum and 85-100 psi, 59-69 N/cm<sup>2</sup>.
5. Cool to  $150^\circ\text{F}$ ,  $339^\circ\text{K}$ , or Lower at  $13 \pm 2^\circ\text{F}$ ,  $7 \pm 1^\circ\text{K}$ , per minute.

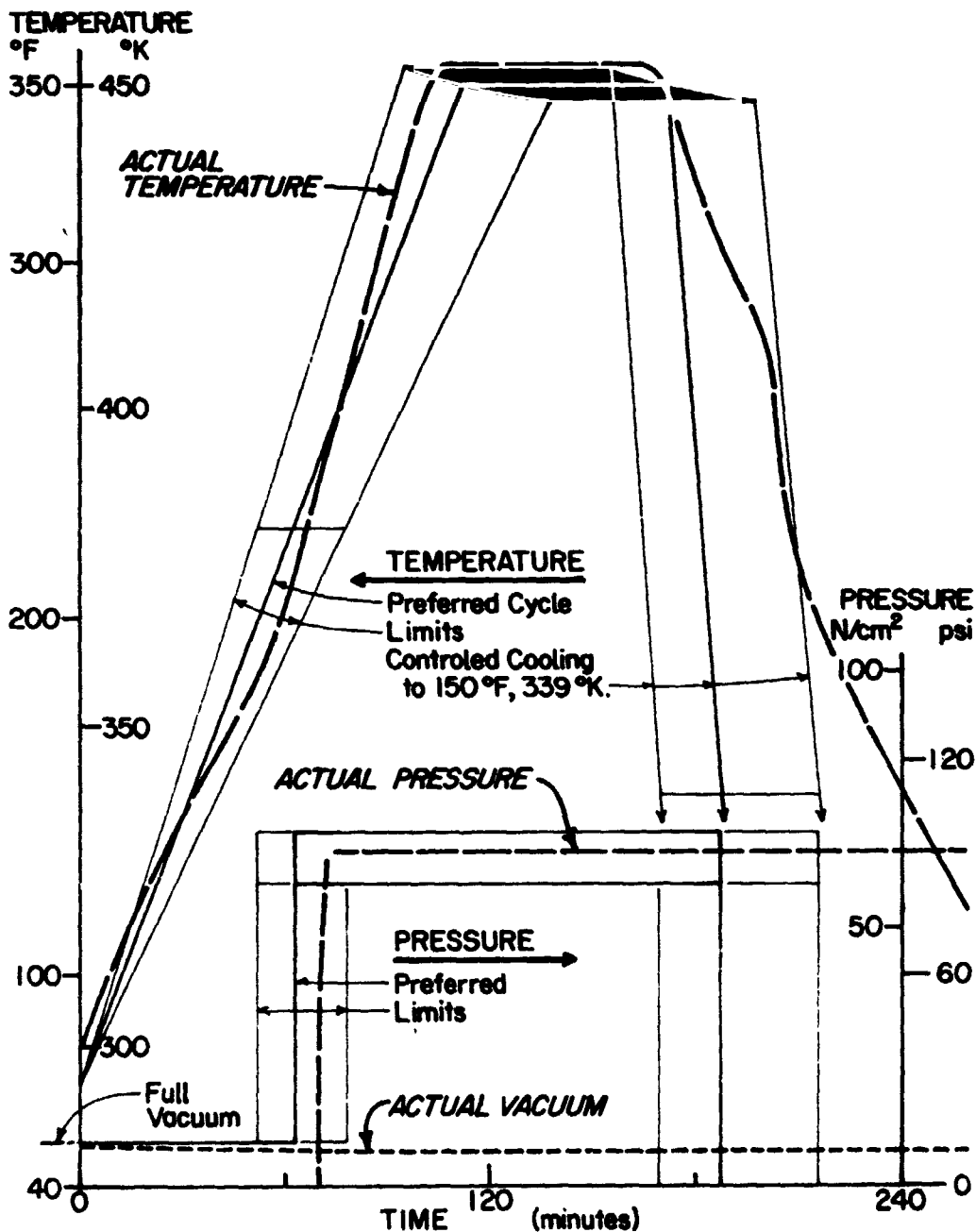


Fig. II-3 Recommended and Actual Cure Cycles for Laminate AS12-1

AVCO 5505 (2373)

Specimen B 414 - 1

1. Full Vacuum
2. Apply 100 psi, 69 N/cm<sup>2</sup>.
3. Heat to 350 ± 10°F, 450 ± 6°K, at 3-5°F, 2-3°K, per minute.
4. Cure 90-120 minutes at 350 ± 10°F, 450 ± 6°K.
5. Cool under Pressure to 125°F, 325°K, or Less in a Minimum of 40 minutes.

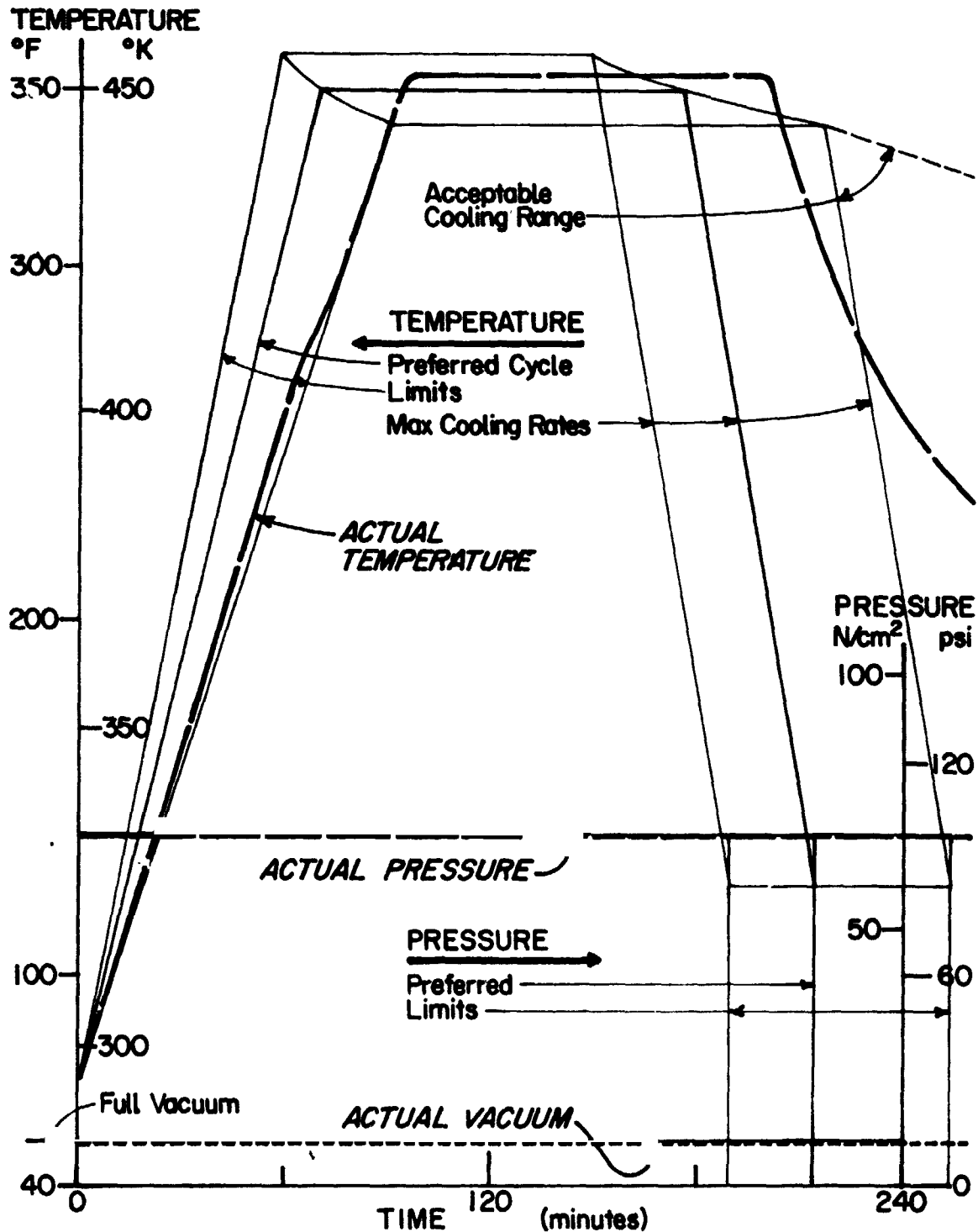


Fig. II-4 Recommended and Actual Cure Cycles for Laminar B414-1

Table II-4 Ultrathin Composite Laminate Characterization

Prepreg			Cured Laminate, Average Values						General Appearance
Specimen	Resin Wt, %	Thickness, mm (mils)	Fiber, %		Resin, %		Thickness, mm (mils)		
			Vol	Wt	Vol	Wt	Target	Actual	
EG06-1 108 Glass	46	0.0635 to 0.0762 (2.5 to 3)	49.2	66.2	49.5	33.8	0.152 (6)	0.165 (6.5)	Good
EG08-1 108 Glass	46	0.0635 to 0.0762 (2.5 to 3)	50.6	67.3	49.4	32.7	0.203 (8)	0.216 (8.5)	Good
EG10-1 181 Glass	27	0.33 (13)	58.6	74.5	40.3	25.5	0.254 (10)	0.267 (10.5)	Some Warpage
104 Glass	40	0.0381 (1.5)							
HM10-1 Mod I Graphite	53	0.152 to 0.178 (6 to 7)	50.1	59.7	44.5	34.3	0.254 (10)	0.432 to 0.462 (17 to 19)†	Good
104 Glass	40	0.0381 (1.5)	4.0	6.0					
AS12-1 A Graphite	42	0.152 to 0.178 (6 to 7)					0.305 (12)	0.356 (14)	Poor - Extreme lack of resin on surface
104 Glass	0	0.0254 (1)*							
AS12-2 A Graphite	42	0.152 to 0.178 (6 to 7)	50.2	54.1	39.8	30.9	0.305 (12)	0.356 (14)	Fair - Slight resin starvation
104 Glass	40	0.0381 (1.5)	9.8	15.0					
HM14-1 Mod I Graphite	53	0.152 to 0.178 (6 to 7)	44.6	51.3	44.5	34.0	0.356 (14)	0.368 (14.5)	Good
104 Glass	0	0.0254 (1)*	9.9	14.7					
B408-1 Boron	42.5	0.152 (6)	42.5	53.6	39.9	24.7	0.203 (8)	0.216 (8.5)	Good
104 Glass	40	0.0381 (1.5)	17.6	21.7					
B410-1 Boron	42.5	0.152 (6)	33.5	43.2	42.4	26.3	0.254 (10)	0.274 (10.8)	Resin starved in glass layers
108 Glass	46	0.0635 to 0.0762 (2.5 to 3)	24.2	30.5					
104 Glass	0	0.254 (1)*							
B410-2 Boron	42.5	0.152 (6)	32.4	42.2	43.4	27.2	0.254 (10)	0.274 (10.8)	Tool side good; bleed side slight- ly starved
108 Glass	46	0.0635 to 0.0762 (2.5 to 3)	24.2	30.7					
104 Glass	40	0.0381 (1.5)							
B414-1 Boron	42.5	0.152 (6)	46.6	58.4	36.8	21.8	0.356 (14)	0.368 (14.5)	Slight resin star- vation in glass layers
108 Glass	0	0.0508 (2)*	16.2	19.8					
B414-2 Boron	42	0.152 (6)	43.1	55.2	41.7	25.7	0.356 (14)	0.376 (14.8)	Tool side good; bleed side slight- ly starved
108 Glass	49	0.0762 (3)	15.2	19.1					

\*Thickness of dry cloth.  
†Ultrathin prepreg thickness of delivered material was considerably greater than expected.

\*Thickness of dry cloth.

†Ultrathin prepreg thickness of delivered material was considerably greater than expected.

ORIGINAL PAGE IS  
OF POOR QUALITY

As stated above, three of the laminates that were made with dry fiberglass cloth on the surface, AS12-1, B410-1, and B414-1, were remade using prepregged fiberglass. Although a considerable improvement in laminate quality was achieved with this change, AS12-2 was still slightly resin-starved on the bleed-cloth side. Laminate B410-2 differed from B410-1 in two aspects. The layer of style 104 fiberglass was prepregged rather than dry, and the layup assembly was turned over (see Fig. II-5). It was expected that this would place and keep more resin on the tool side of the laminate, which it did. The tool side of B410-2 was excellent; however, the bleed-cloth side, although improved, was still slightly resin-starved.

Laminate B414-2 differed from B414-1 in three aspects. The style 108 glass cloth used was prepregged instead of dry; only two plies of 120 bleed-cloth were used instead of three; and a layer of perforated Teflon was inserted between the "pink" release bleed-cloth and the untreated 120 bleed-cloth, in order to reduce the amount of resin removed. Again, there was considerable improvement in the appearance of the laminate and apparent distribution of the resin, but the bleed-cloth side still exhibited slight resin starvation.

Photomicrographs were taken of samples cut from 11 of the 12 laminates made as part of this study. (Laminate AS12-1 was too resin-starved to justify characterization). The most pertinent photomicrographs along with appropriate information on the lamina arrangement, resin extraction system, sample location, and constituent proportions were presented and discussed in the Interim Phase I Report.<sup>1</sup>

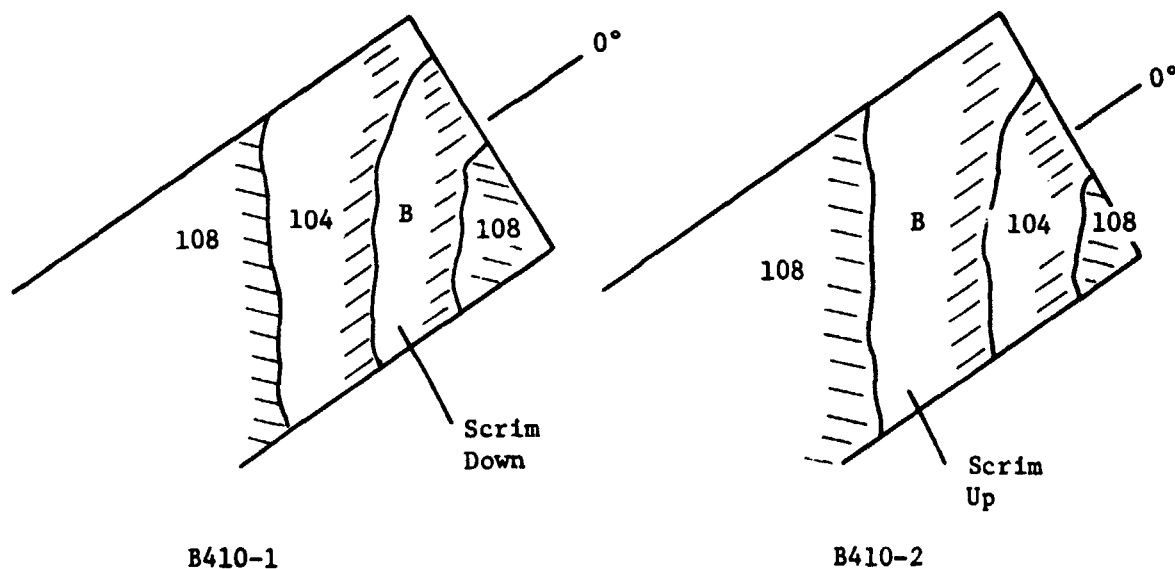


Fig. II-5  
Comparison of Lamina Arrangements for Laminate Styles B410-1 and B410-2

### III. DESIGN AND ANALYSIS

---

The high mass fraction required for the Space Tug system makes it necessary to minimize structural weight while maintaining reasonable design guidelines concerning cost, fabricability, reliability etc. The design and analysis study conducted during Phase I considered a wide variety of structural concepts and materials in the design of a lightweight cylindrical shell structure 3.66 m (144 in.) high and 4.57 m (180 in.) in diameter. The design ultimate loading was 1225.8 N/cm (700 lb/in.) axial compression and 245.2 N/cm (140 lb/in.) torsion. The overall size and design loading, shown in Fig. III-1, were selected to be representative of a skirt or body structure for the Space Tug vehicle.

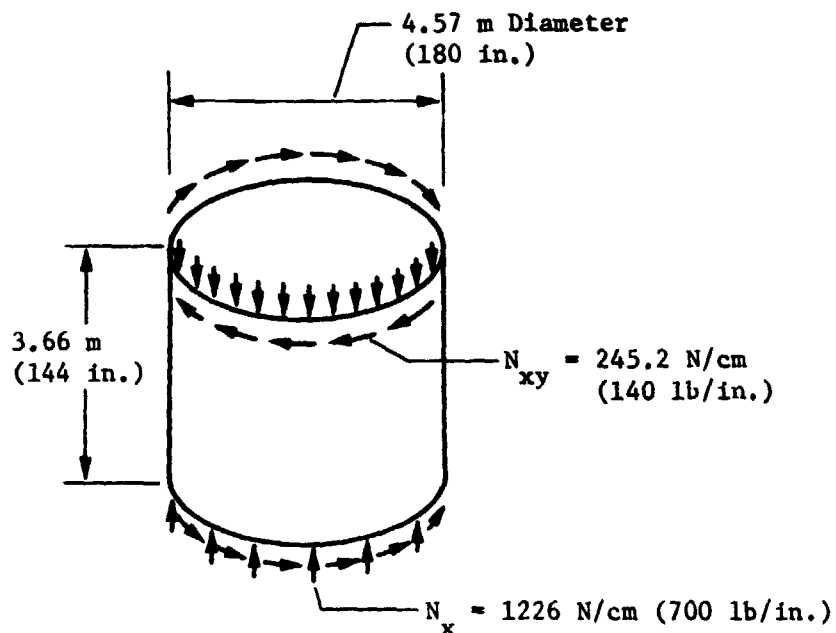


Fig. III-1 Shell Structure and Design Loading



## A. STRUCTURAL CONCEPTS

Four basic structural concepts were subjected to detailed evaluation during Phase I; they were: (1) honeycomb sandwich; (2) skin/stringer/frame; (3) truss; and (4) isogrid.

- 1) The honeycomb sandwich concept uses a lightweight aluminum Hexcel core material with thin, 0.020 to 0.046-cm (0.008 to 0.018-in.) faceskins. A wide variety of faceskin materials were considered in the design. The low design loads dictated that the minimum useful gage of most candidate materials be determined. The core/faceskin bond was accomplished in all cases with 0.009-cm (0.0035-in.) thick FM-24 film adhesive.
- 2) The stiffened skin concept using hat-section stringers and frames was evaluated using a variety of metals. Attachment of the stringers and frames to the skin was assumed in each case to be accomplished using a weld-bonding technique. Typical sheet metal gages for this concept were 0.038 to 0.076-cm (0.015 to 0.030-in.).
- 3) A truss skirt concept was considered using aluminum members in one case and graphite/epoxy members in another. Two different aluminum member cross-sectional geometries were evaluated; a closed rectangular section and an I section. The graphite/epoxy member geometry was basically a closed square section with local titanium shim reinforcement in the truss joint region. The truss openings are covered with two 0.010-cm (0.004-in.) laminates for meteoroid penetration protection.
- 4) The cylindrical shell structure was also designed using an integrally-stiffened waffle construction designated "isogrid." Only unflanged reinforcing ribs were evaluated because of the thin gage of aluminum involved.

## B. ANALYSIS METHODS

The general approach taken in investigating the various constructions was to establish the stability characteristics and then check the strength of the structure. For an efficient design, panel stability and local stability of the components were equated to provide a starting point. General stability was then checked for the composite or built-up structure. Gross structural stresses were then determined for the structural components.

Due to the combined axial compression and torsion loading on the structure, it was necessary to consider the effect of load interaction on stability and gross stress. The NASA Space Vehicle Design Criteria Monograph on the buckling of thin-walled circular cylinders<sup>4</sup> recommends the use of a linear interaction relationship, i.e.,

$$R_c + R_t = 1$$

where

$$R_c = N_x / (N_x)_{cr},$$

$$N_x = \text{applied axial load,}$$

$$(N_x)_{cr} = \text{critical axial load,}$$

$$R_t = N_{xy} / (N_{xy})_{cr},$$

$$N_{xy} = \text{applied torsional load,}$$

$$(N_{xy})_{cr} = \text{critical torsional load.}$$

For the given geometry and loading, a linear interaction relationship was also indicated from the results of the Martin Marietta Corporation orthotropic shell stability analysis (HOLBOAT<sup>5</sup>) to be described later. The linear relationship was used throughout this study.

As for stresses, MIL-HDBK-5<sup>6</sup> states that practically all structural (columnar) members made from thin materials fail through instability; this is particularly true for torsion of thin tubes. To provide a conservative approach to gross stress interaction, a linear relationship was used, i.e.,

$$f_c + f_t = 1$$

where

$$f_c = \sigma_c / \sigma_y \text{ or } \sigma_c / \sigma_{ult},$$

$$\sigma_c = \text{applied axial stress,}$$

$$\sigma_y = \text{compressive yield stress,}$$

$$\sigma_{ult} = \text{compressive ultimate stress,}$$

$$f_t = \tau_{xy} / (\tau_{xy})_{cr},$$

$$\tau_{xy} = \text{applied torsional shear stress,}$$

$$(\tau_{xy})_{cr} = \text{allowable shear stress.}$$

The linear interaction relationship was used throughout the study. Only one of the constructions was found to be strength-critical by this criterion. Due to the built-up character of the evaluated designs, it would be expected that localized buckling failures would occur before material failure of the primary load carrying elements.

For all of the design/analyses performed in this study, to provide a consistent basis for comparison, all of the relationships were based on theoretical considerations. No reduction factors, correlation factors, knockdown factors or similar factors were used.

#### 1. Honeycomb Sandwich

The honeycomb sandwich constructions which were evaluated consisted of two faceskins of equal thickness and a low-density aluminum honeycomb core. The construction was checked for two modes of instability failure: (1) general instability where the shell fails with the core and faces acting together; (2) local instability taking the form of intercell buckling of the faceskins. Gross structural stresses were checked to prevent interaction material failure.

Analysis of the general stability of the parametric designs was made using HOLBOAT. HOLBOAT is an orthotropic cylindrical shell stability analysis based on a theory originally established by the work of Cheng and Ho.<sup>7,8</sup> Cheng and Ho formulated their basic equations from classical thin shell theory and Flugge's<sup>9</sup> differential equations of equilibrium. The assumptions used are: (1) the ratio of thickness of the shell to its radius of curvature is small compared to unity; (2) the displacements are small compared with the shell thickness; and (3) the elements normal to the undeformed middle surface are normal to the deformed middle surface and suffer no extension.

Each layer or structural component of the shell construction contributes to the overall stiffness of the construction through its constitutive equations linking stress and strain. Summing these individual contributions then results in overall stiffnesses (i.e., extensional, coupling, and bending) for the entire shell. These stiffness matrices are designated [A], [B], and [D], respectively. The HOLBOAT computer program has the option of either being given the elastic constants, thicknesses, and orientations of the layers (or components) and internally generating the individual and combined stiffnesses, or accepting combined stiffnesses that have been generated externally to the program. The present internal generating capabilities of HOLBOAT are limited to laminar constructions. It is necessary to generate externally the stiffness matrices for constructions such as skin/stringer/frame and truss/gridwork. A modification of the HOLBOAT program to include internal generation of stiffness matrices for panels stiffened with discrete

stringers and frames was accomplished under a contract add-on near the end of Phase I. This modification is summarized in Section III.D of this report and fully defined in a User's Manual, MCR-74-428, October 1974.<sup>10</sup>

Solution of the stability equation in HOLBOAT is made using the available stiffness matrices. The equation contains the wave numbers in the axial and circumferential directions as coefficients; therefore, minimizing the buckling load with respect to these wave numbers.

Local stability of the facesheets for the intercell buckling mode of failure was made assuming that the facesheet acted as a simply supported wide column over the length of the cell.

## 2. Skin/Stringer/Frame

The configuration studied was that shown in Fig. III-2 and III-3. Components of the configuration include a skin, hat-section stiffeners, and hat-section frames. Hat-sections were selected because they offered closed-section torsional stiffness when attached to the skin, and for the thin gages contemplated, a closed-section with no outstanding free edges (e.g., in contrast to a channel section).

Two design criteria approaches were taken: (1) the cylinder components were assumed to be designed on a noninteraction basis, i.e., the skin would resist all of the torsional load and the stringers would resist all of the axial load; and (2) the cylinder components were assumed to be designed on a limited interaction basis, i.e., the skin would resist all of the torsional load and the stringers, together with an effective width of skin, would resist the axial load. In both cases, the frames were to be designed to provide adequate radial stiffness to force the stringers/skin into panel instability mode shapes. The above conditions provided for the evaluation of local stability requirements. Governing equations were listed and discussed in the Interim Report.<sup>1</sup>

HOLBOAT was used to evaluate the general stability of the built-up panel between frames and the overall cylinder stability including frames. The orthotropic shell analysis is the only viable method of satisfactorily evaluating these failure modes. However, the orthotropic shell analysis is only appropriate if the stringer and frame sizes and spacings are sufficiently small so that when these reinforcing elements are averaged over their respective areas, a fictitious orthotropic sheet has the same structural stiffnesses. This was the case for the designs in this program.

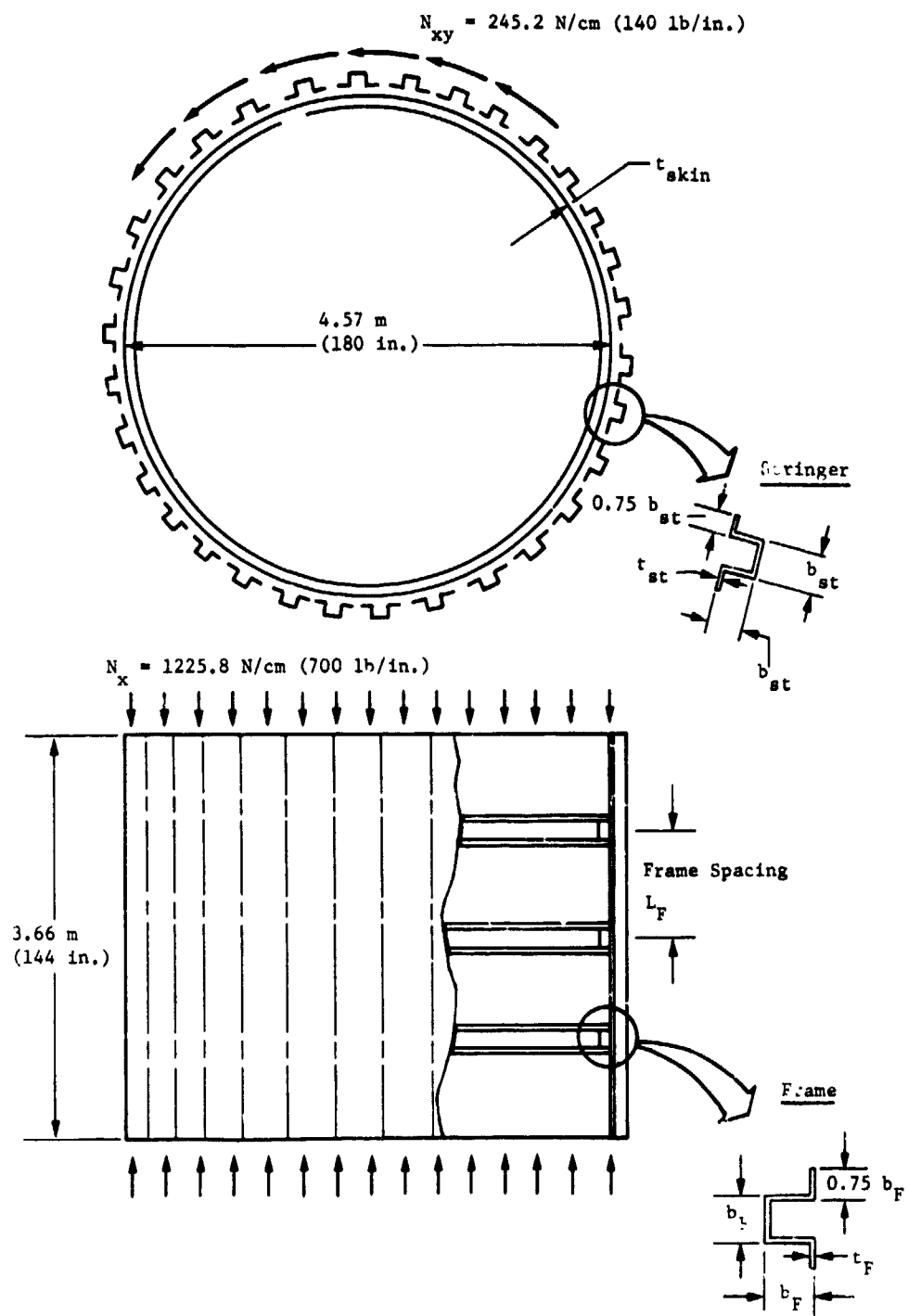


Fig. III-1 Isotropic Stiffened Shell Configuration

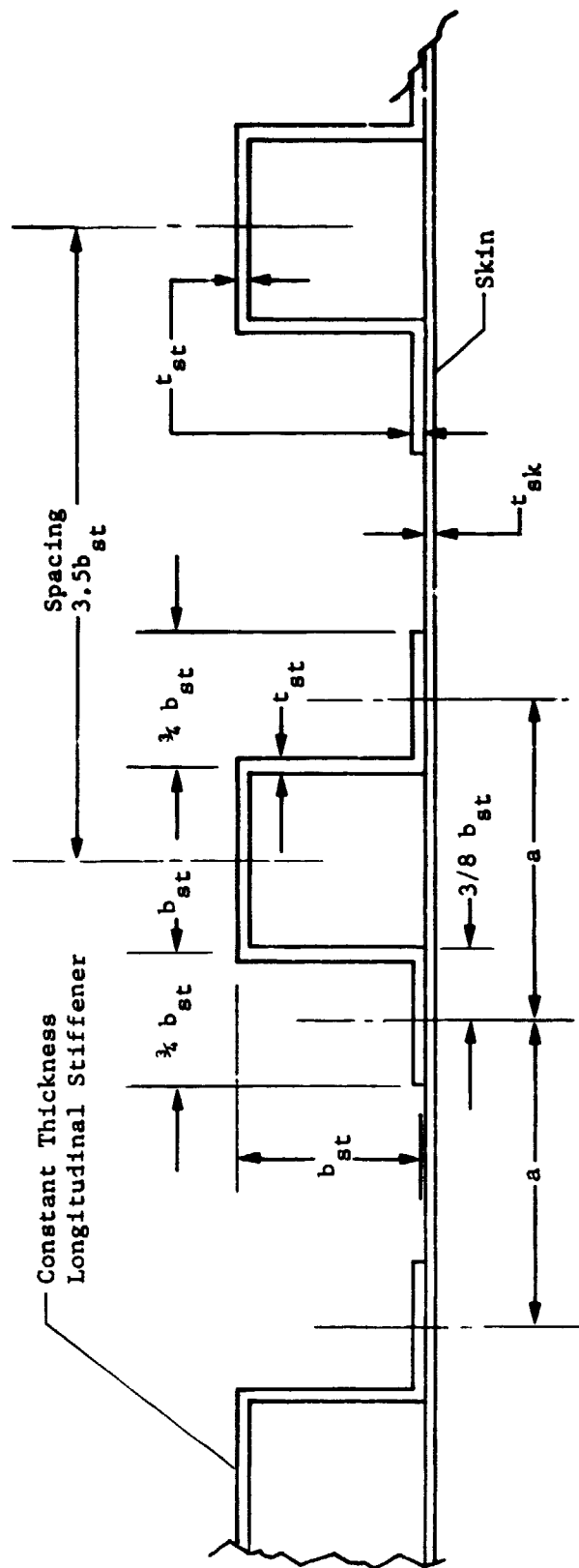


Fig. III-3

Fig. III-3 Skin/Stringer Detail

The extensional, coupling, and bending stiffnesses of the shell configuration were required as input to the program. The parameters in the matrices were obtained using the equations given in<sup>4</sup> for isotropic-skinned cylinders with stiffeners and rings. The stiffness matrices are shown in Table III-1.

Table III-1 Stiffness Matrices Skin/Stringer/Frame Construction

Extensional Stiffness	Bending Stiffness	Coupling Stiffness
$A_{11} = \frac{E_{sk} t_{sk}}{1 - \nu_{sk}^2} + \frac{E_{st} A_{st}}{c_{st}}$	$D_{11} = \frac{E_{sk} t_{sk}^3}{12(1 - \nu_{sk}^2)} + \frac{E_{st} I_{st}}{c_{st}} + \gamma_{st}^2 \frac{E_{st} A_{st}}{c_{st}}$	$B_{11} = \gamma_{st} \frac{E_{st} A_{st}}{c_{st}}$
$A_{22} = \frac{E_{sk} t_{sk}}{1 - \nu_{sk}^2} + \frac{E_F A_F}{L_F}$	$D_{22} = \frac{E_{sk} t_{sk}^3}{12(1 - \nu_{sk}^2)} + \frac{E_F I_F}{L_F} + \gamma_F^2 \frac{E_F A_F}{L_F}$	$B_{22} = \gamma_F \frac{E_F A_F}{L_F}$
$A_{12} = \frac{\nu_{sk} E_{sk} t_{sk}}{1 - \nu_{sk}^2}$	$D_{12} = \nu_{sk} \left[ \frac{E_{sk} t_{sk}^3}{12(1 - \nu_{sk}^2)} \right]$	$B_{12} = B_{66} = B_{16} = B_{26} = 0$
$A_{66} = \frac{E_{sk} t_{sk}}{2(1 + \nu_{sk})}$	$D_{66} = \frac{E_{sk} t_{sk}^3}{6(1 + \nu_{sk})} + \frac{G_{st} K_{st}}{c_{st}} + \frac{G_F K_F}{L_F}$	
$A_{16} = A_{26} = 0$	$D_{16} = D_{26} = 0$	
<p>where</p> <div style="display: flex; justify-content: space-between;"> <div> <p>E - Modulus of elasticity</p> <p>G - Shear modulus</p> <p><math>\nu</math> - Poisson's ratio</p> <p>t - Thickness</p> <p>A - Area</p> <p>I - Moment of Inertia</p> <p><math>\gamma</math> - Distance from the center of the skin to the centroid of the reinforcing element. Radial outward is the positive direction.</p> </div> <div> <p>K - Torsional constant</p> <p><math>c_{st}</math> - Stiffener spacing</p> <p><math>L_F</math> - Frame spacing</p> <p>sk - Denotes skin property</p> <p>st - Denotes stringer property</p> <p>F - Denotes frame property</p> </div> </div>		



### 3. Truss

A potential lightweight structural concept for the given design conditions is a small-grid rigid-joint truss with thin sheet material applied to the inner and outer surfaces to provide meteoroid protection.

The initial concept was to use wide-flange members as the structural components; the later effort indicated the advantageous use of tubular members. Because of the work completed earlier in the program with honeycomb sandwich shells, a rough estimate was known of the required longitudinal and transverse extensional and bending stiffnesses to prevent general instability. Panel sizing could then be made using Euler buckling of the members. Stability of the members in the circumferential direction of the shell was to be provided by attachment of the members to the meteoroid protection skins.

Member stresses were determined by analyzing finite element stress of one-fourth of the shell. These stresses could then be compared to the gross material stress (e.g., compressive yield) and to the local buckling stress of the member elements (i.e., flange and web). Local buckling stresses were determined using the NASA Structures Manual.<sup>11</sup> For the wide-flange struts, the local buckling stress is given by

$$\sigma_{cst} = \frac{k_w \pi^2 E}{12(1-\nu^2)} \left( t_w / b_w \right)^2$$

where

$t_w$  = web thickness

$b_w$  = web length

and  $k_w$  is determined from Fig. C4.2.2-4.<sup>11</sup> For the tubular struts, the local buckling stress is given by

$$\sigma_{cst} = \frac{k_h \pi^2 E}{12(1-\nu^2)} \left( \frac{t_{h'}}{h'} \right)^2$$

where

$t_{h'}$  = web thickness

$h'$  = web height

and  $k_h$  is determined from Fig. C4.2.2-5.<sup>11</sup>

General stability analyses of the truss designs were made using the HOLBOAT program. The extensional, coupling, and bending stiffnesses were required as inputs to the program. These stiffnesses were modeled using the principles established for orthotropic shell construction given in<sup>4</sup>. The stiffness matrices used are shown in Table III-2.

Table III-2 Stiffness Matrices Truss Construction

Extensional Stiffness	Bending Stiffness	Coupling Stiffness
$A_{11} = \frac{E_V A_V}{d}$	$D_{11} = \frac{E_V I_V}{d}$	All B's = 0
$A_{22} = \frac{E_H A_H}{d}$	$D_{22} = \frac{E_H I_H}{d}$	
$A_{66} = \frac{E_D A_D}{2d}$	$D_{66} = \frac{G_V K_V}{d} + \frac{G_H K_H}{d} + \frac{G_D K_D}{\sqrt{2}d}$	
$A_{12} = A_{16} = A_{26} = 0$	$D_{12} = D_{16} = D_{26} = 0$	
<p>where</p> <div style="display: flex; justify-content: space-between;"> <div> <p>E - Modulus of elasticity</p> <p>G - Shear modulus</p> <p><math>\nu</math> - Poisson's ratio</p> <p>A - Area</p> <p>I - Moment of Inertia</p> <p>K - Torsional constant</p> </div> <div> <p>d - Length of square-panel vertical and horizontal members</p> <p>V - Denotes vertical member property</p> <p>H - Denotes horizontal member property</p> <p>D - Denotes diagonal member property</p> </div> </div>		

#### 4. Isogrid

The isogrid construction consists of a structural skin stiffened with 60° triangularly oriented rib components (Fig. III-4). Gross structural behavior of the construction is essentially that of an isotropic plate. As a result, recognized analytical techniques for homogeneous, isotropic materials can be used in the design/analysis. Considerations in the design process include: overall cylinder instability, triangular panel (skin) instability, rib instability, and strength. The detailed design procedures set forth in the Isogrid Design Handbook<sup>12</sup> were followed in this study and will not be repeated here.

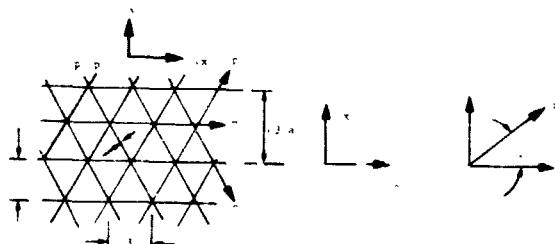


Fig. III-4 Element of Isogrid Rib Grid

## C. STRUCTURAL DESIGNS

Designs were prepared for the four constructions; honeycomb sandwich, skin/stringer/frame, truss, and isogrid. The material properties of the materials used in the design study were given in Tables II-1 and II-2 of the Materials Chapter. Detailed tabulated results for all of the designs were presented in the Phase I Interim Report<sup>1</sup>, and, therefore, will not be duplicated here.

### 1. Honeycomb Sandwich

Seven isotropic metallic skin and four composite skin constructions were evaluated during the study. The metallic skins were:

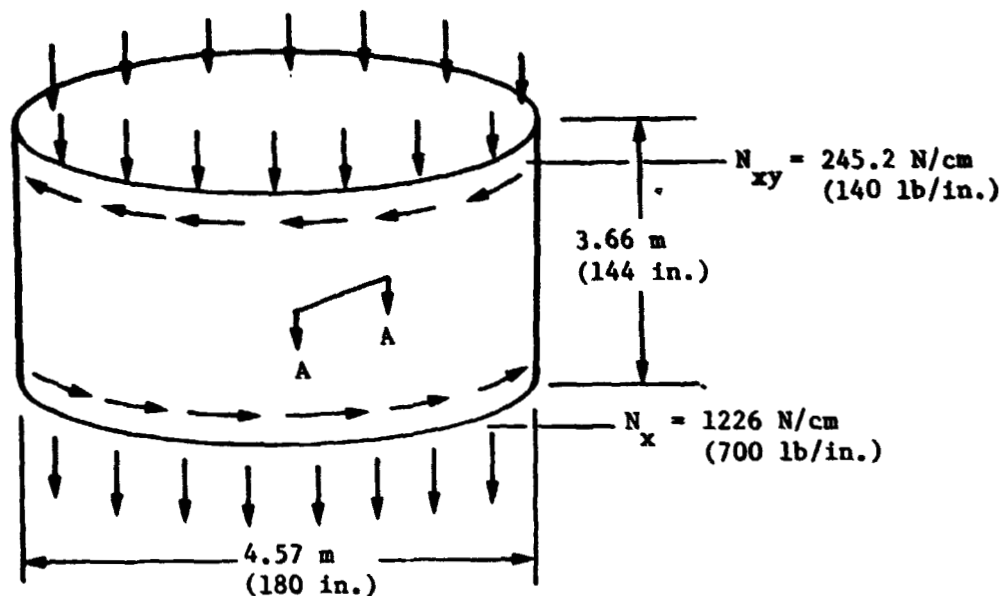
Aluminum  
Titanium  
Maraging Steel  
Beryllium  
Lockalloy  
Boron/Aluminum  
Beryllium/Titanium

The composite skins were:

Fiberglass/Boron/Fiberglass  
Fiberglass/Type AS Graphite/Fiberglass  
Fiberglass/HM-Modmor Graphite/Fiberglass  
T 300 Graphite/HM-Modmor Graphite/T 300 Graphite

The design conditions for these constructions are given in Fig. III-5.

Design of the composite material skin sandwich was more involved than that for the isotropic skins. It was assumed that the primary axial load-carrying skin component was the unidirectional 0° tape material. This component was one of these three materials; boron, Type A/S graphite, or HM-Modmor graphite. It was assumed that the primary torsional load-carrying skin component was the 45° material. This component was one of the following: Style 104 woven-glass fabric, Style 112 woven-glass fabric, or continuous unidirectional Thornel 300 graphite filament tape. The thin 0.019 mm (0.00075 in.) Style 104 fabric and Thornel 300 tape are both



- Note:**
1. Honeycomb core, aluminum 1/8-5052-0.0007,  $49.7 \text{ kg/m}^3$  ( $3.1 \text{ lb/ft}^3$ ).
  2. Core/face skin adhesive, Bloomingdale Corp., reticulating FM-24 epoxy, 0.0127 cm (0.005-in.) thick.
  3. No edge weight included.
  4.  $0^\circ$  orientation lies along the cylinder axis.
  5. Buckling loads are classical theoretical values without reduction factor.



Fig. III-5 Honeycomb Sandwich Concept Design Conditions

unbalanced basic constructions and must be balanced during laminate fabrication to provide adequate shear strength. The Style 112 fabric is balanced and provides a good structural laminate when used at 45° to the loading axis.

## 2. Skin/Stringer/Frame

Seven isotropic skin/stringer/frame designs were evaluated during the study. All seven of the designs were prepared using the previously described Design Criteria 1. A design for aluminum 2014-T6 was also prepared using Design Criteria 2. For three of the materials (i.e., Ti-8Al-1Mo-1V, "250" Maraging steel, and Lock-alloy), two thicknesses were used because the theoretically required gages were below those readily commercially available.

## 3. Truss

Results of the design/analysis of previous constructions pointed to the use of aluminum as the most weight-efficient material for use in the truss. The finite element model of one-fourth of the cylindrical shell is shown in Fig. III-6 and member cross-sections are shown in Fig. III-7. Due to the long running times necessary for a stress analysis using the finite element program, only two cases were run and stresses for the remaining conditions were extrapolated from these two cases. The use of tubular-closed cross-section struts greatly enhances the stability of the truss compared with using wide-flange struts.

## 4. Isogrid

As with the truss construction, the only material evaluated with the isogrid construction was 2014-T6 aluminum. The resulting configuration is shown in the drawing for the small test panel shown in Fig. III-8. The weight of this construction is 4.502 kg/m<sup>2</sup> (0.922 lb/ft<sup>2</sup>).

## 5. Design Summary

A total of 11 structural designs were chosen as candidates for consideration during Phase I fabrication development work. A summary of these designs is given in Tables III-3 thru III-5. The cylindrical skirt weight expressed in Kg/m<sup>2</sup> (lb/ft<sup>2</sup>) for each of these designs is shown in Fig. III-9. The solid portion of the bars shown indicates the basic skirt weight; the added-on cross-hatched bar indicates the additional weight due to an edge attachment weight increment. The edge weight increment is based on a preliminary design of a candidate attachment structural concept. All of the honeycomb sandwich designs shown, in addition to the aluminum isogrid and the graphite/epoxy truss design, were subjected to small component structural tests to aid in concept evaluation.

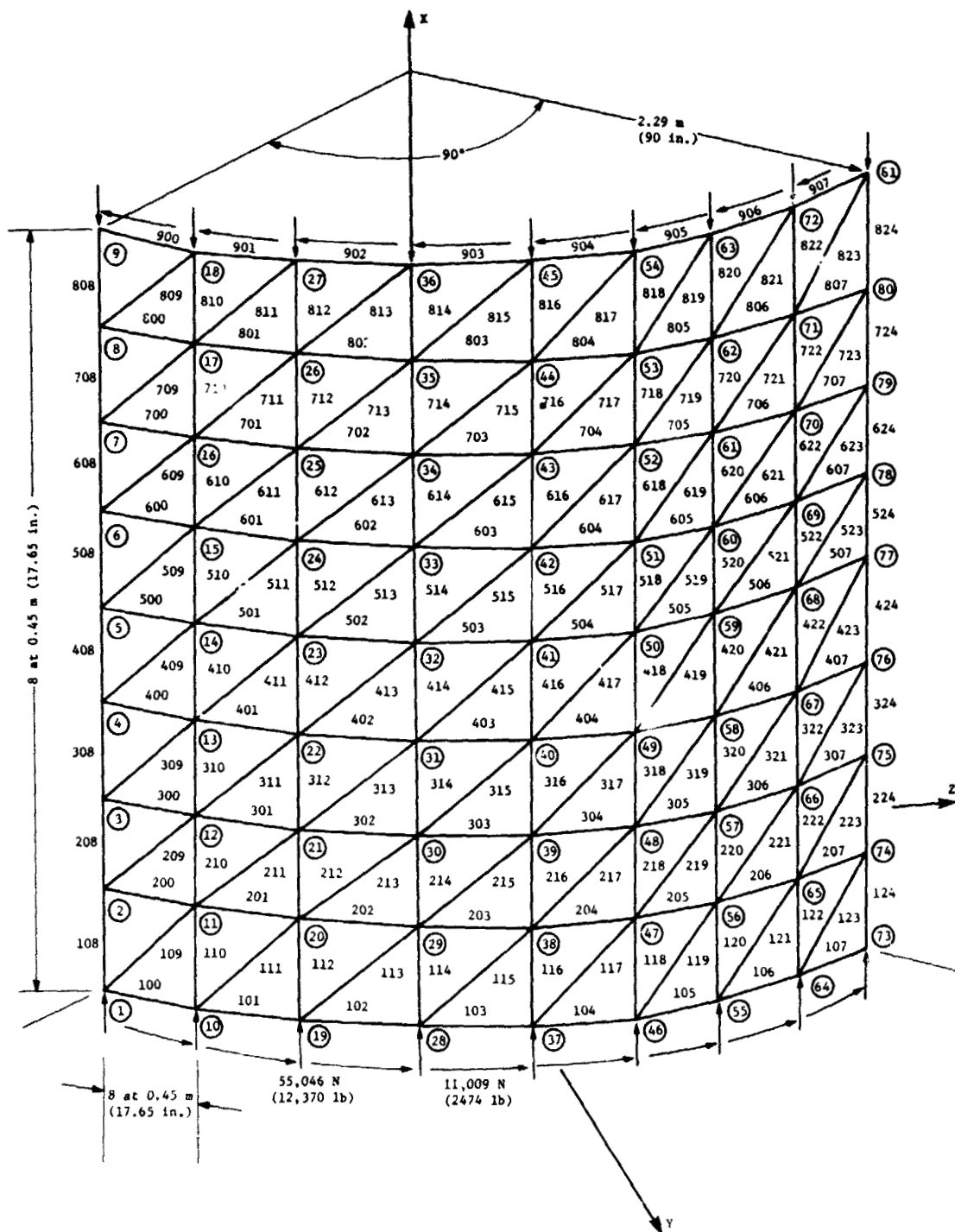


Fig. III-6 Truss, Finite Element Model

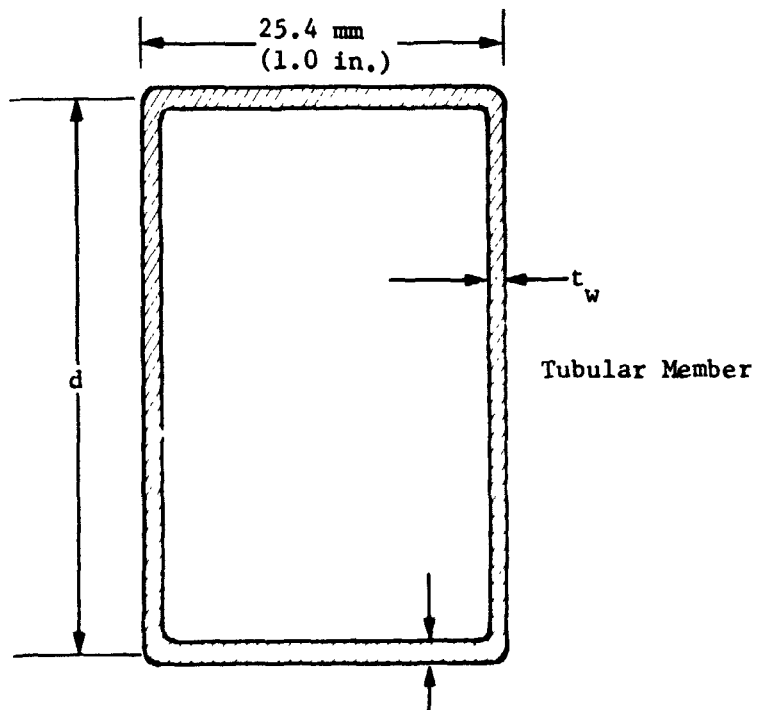
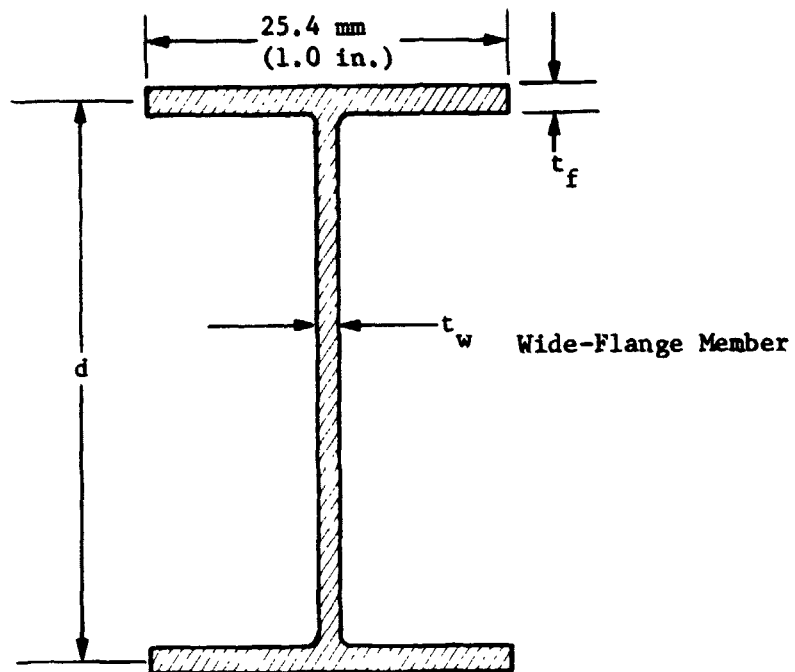


Fig. III-7 Aluminum Truss Member Geometry, Sections



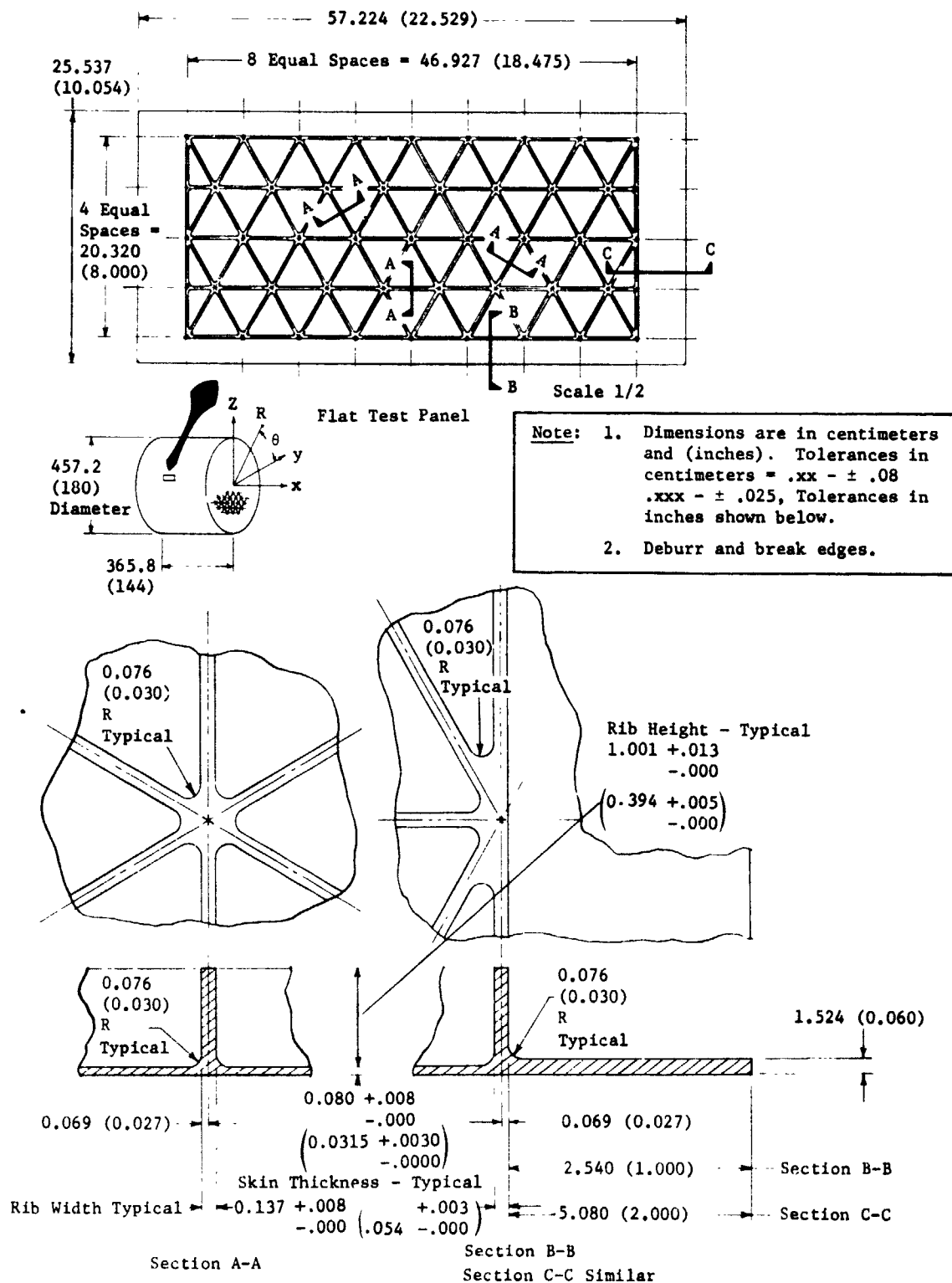


Fig. III-8 Aluminum Lightweight Shell Isogrid, Flat Test Panel

Table III-3 Selected Honeycomb Sandwich Designs

Panel Designation	Face Skin Material		Total Face Skin Thickness, cm (in.)	Core Thickness, cm (in.)	Structural Weight		
					Basic Panel, kg/m <sup>2</sup> (lb/ft <sup>2</sup> )	Edge Attachment Delta, kg/m <sup>2</sup> (lb/ft <sup>2</sup> )	Total, kg/m <sup>2</sup> (lb/ft <sup>2</sup> )
Type I-GR-20	Modmor Type I/5208 Graphite/Epoxy	T300/5208 Graphite/Epoxy	0.0393 (0.0155)	1.510 (0.595)	2.185 (0.448)	6.400 (0.082)	2.585 (0.530)
Type I-GL-18	Modmor Type I/5208 Graphite/Epoxy	Style 112 Fiberglass Cloth/5208	0.368 (0.0145)	2.145 (0.845)	2.490 (0.509)	0.415 (0.085)	2.905 (0.594)
Boron-GL-17	Narmco 5505/4 Boron/Epoxy	Style 112 Fiberglass Cloth/5208	0.0380 (0.0150)	1.660 (0.654)	2.512 (0.515)	0.405 (0.083)	2.917 (0.598)
A/S-GL-18	Hercules A/S-3501 Graphite/Epoxy	Style 112 Fiberglass Cloth/5208	0.0406 (0.0160)	2.410 (0.948)	2.512 (0.515)	0.424 (0.087)	2.936 (0.602)
Alum-12	2014-T6 Aluminum		0.0254 (0.0100)	1.485 (0.585)	2.270 (0.465)	0.302 (0.062)	2.572 (0.527)
Titan-10	6Al-4V Titanium		0.0203 (0.0080)	1.280 (0.505)	2.572 (0.525)	0.298 (0.061)	2.870 (0.586)

Note: All designs use 1/8-5052-0.0007-3.1 aluminum Hexcel core and 0.085 cm (0.0035 in.) thick FM-24 core/face skin bond. Edge attachment weight increment calculated using geometry shown:

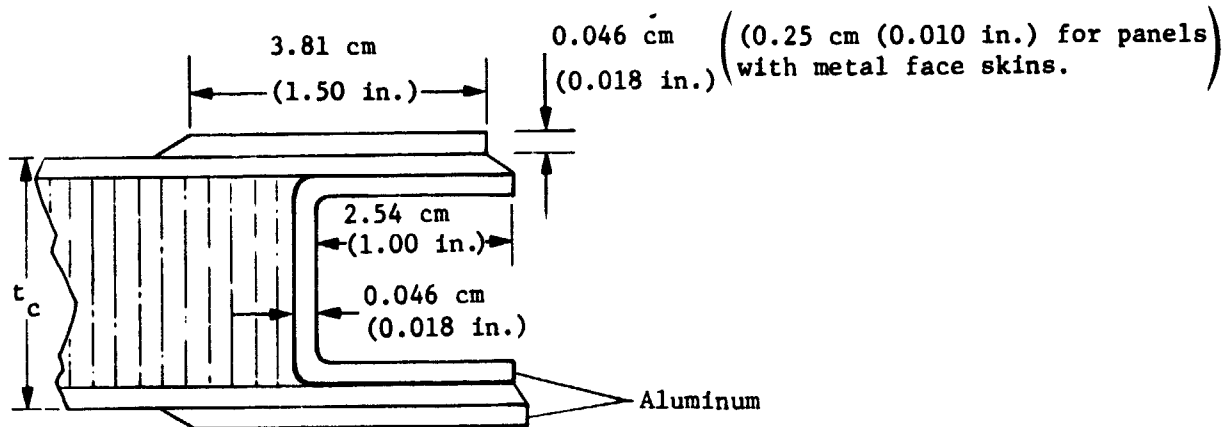


Table III-4

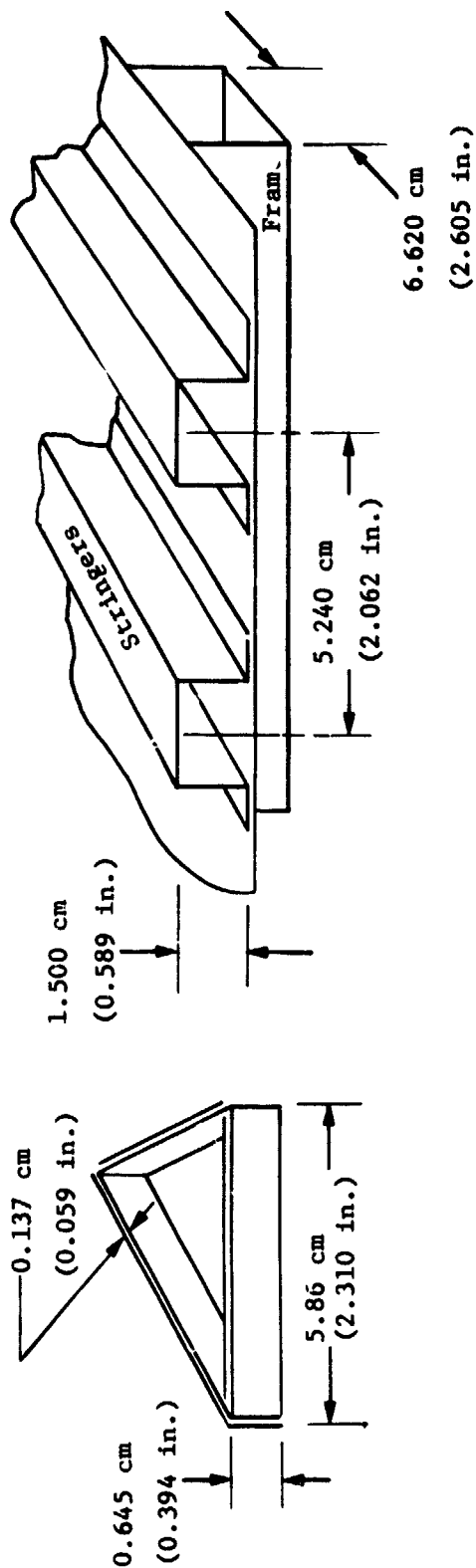
Table III-4 Selected Skirt Truss Designs

Truss Designation	Primary Material	Truss Member Geometry						Structural Weight		
		Stringers		Horizontals		Diagonals		Basic Truss, $\text{kg/m}^2$ (lb/ft $^2$ )	Edge Attachment Delta, $\text{kg/m}^2$ (lb/ft $^2$ )	Total, $\text{kg/m}^2$ (lb/ft $^2$ )
		$t_w$ , cm (in.)	$t_f$ , cm (in.)	$t_w$ , cm (in.)	$t_f$ , cm (in.)	$t_w$ , cm (in.)	$t_w$ , cm (in.)			
Aluminum	2014-T6	0.089 (0.035)	0.165 (0.065)	0.064 (0.025)	0.076 (0.030)	0.076 (0.030)	0.076 (0.030)	3.070 (0.628)	0.122 (0.025)	3.192 (0.653)
Graphite/Epoxy	Alur num • Modmor Type I/5208 Graphite/Epoxy	0.104 (0.041)	0.142 (0.056)	0.104 (0.041)	0.04 (0.041)	0.104 (0.041)	0.104 (0.041)	2.320 (0.475)	0.171 (0.035)	2.491 (0.510)
Aluminum/ Boron/Epoxy	2014-T6 Aluminum with Narmco 5505/4 Boron/Epoxy on stringer flanges	0.089 (0.035)	0.102 (0.040)	0.064 (0.025)	0.076 (0.030)	0.076 (0.030)	0.076 (0.030)	2.835 (0.581)	0.122 (0.025)	2.957 (0.606)

Note: 1. All truss members are square with inside dimensions of 3.175 by 3.175 cm (1.25 by 1.25 in.)  
 2. Basic truss weight includes truss joint weight and edge attachment weight. Delta is due to provision to introduce cylinder end loading.

Table III-5 Selected Skin/Stringer/Frame and Isogrid Designs

Structure Designation	Primary Material	Skin Thickness, cm (in.)	Skin Reinforcement (See Figure Below)	Structural Weight		
				Basic Truss kg/m <sup>2</sup> (lb/ft <sup>2</sup> )	Edge Attachment Delta kg/m <sup>2</sup> (lb/ft <sup>2</sup> )	Total kg/m <sup>2</sup> (lb/ft <sup>2</sup> )
Isogrid	2014-T6 Aluminum	0.081 (0.032)	Isogrid Rectangular Sections	4.500 (0.922)	0.151 (0.031)	4.651 (0.953)
Skin/Stringer/Frame	2014-T6 Aluminum	0.033 (0.013)	Hat Section Stringers and Frames	3.510 (0.719)	0.127 (0.026)	3.637 (0.745)



Note: 1. Stringers: Stringer flange width equals web height. Constant thickness of 0.43 cm (0.017 in.).  
 2. Frames: Frame flange width equals web height. Constant Thickness of 0.046 cm (0.018 in.)

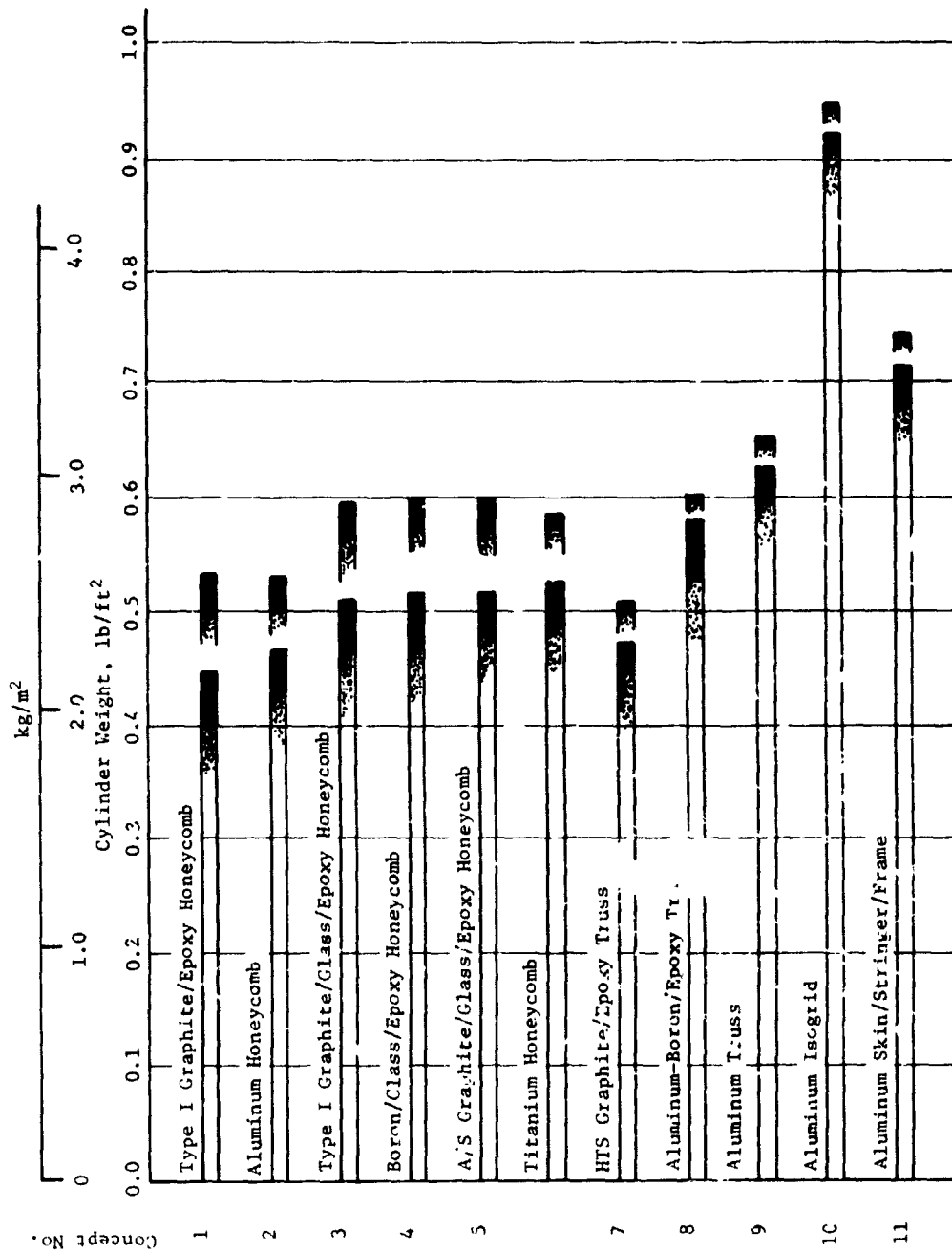


Fig. III-9 Design Concept Summary

#### D. HOLBOAT\* PROGRAM MODIFICATION

The computer program HOLBOAT<sup>5</sup> calculates buckling loads of inhomogeneous anisotropic cylinders under combined loads. It is based on the Kirchhoff-Love hypothesis, generally anisotropic constitutive equations, and Flugg's differential equations of equilibrium. It was developed under contract to AFFDL and has been improved since then (circa 1967).

Cheng and Ho<sup>7</sup> developed the basic equations for buckling by pressure, axial load and torsion. Their analysis was extended to include bending<sup>13</sup>. Thus, any combination of pressure, axial load, torsion, and bending can be analyzed with the program and theoretical interactions determined.

The inhomogeneity considered is that which arises in a laminated cylinder due to different layers having different elastic properties and/or orientations. The elastic properties of each layer are input, along with its orientation and thickness. Then the program internally calculates the required shell stiffness. Each individual layer may be isotropic, orthotropic, or generally anisotropic and a symmetric or balanced arrangement of layers is not required.

Simple support boundary conditions are satisfied for "specially orthotropic" cylinders. For generally anisotropic configurations, no homogeneous boundary conditions are satisfied on sections perpendicular to the axis. If the cylinder is long or has a small axial stiffness, then these constraints will not greatly affect the buckling loads. However, short cylinders and those with high axial stiffness may be affected by boundary constraints.

Input to the program is via "Namelist." This means that the user does not have to have his input in "Format" but merely writes the name of the input variable, an equal sign, and the numerical value of the variable. This input may be in any sequence. The program can also run multiple problems and the user has only to input values of variables which changed from the previous problem. This feature is most useful in performing parametric studies. Program input consists of cylinder geometry, elastic properties of each layer, load combinations, wave number ranges, and buckling load type.

---

\*General Instability Analysis of Inhomogeneous, Anisotropic, Stiffened Cylinders under Combined Loadings.

Output is shell stiffness, buckling load, and buckling mode shape. Two buckling loads are given for each wave number set; one based on "Flügge type" theory and the second from a Donnell theory. The minimum buckling load and corresponding wave numbers are also printed for each data set.

Two major improvements were made to HOLBOAT that will enhance the program usefulness in obtaining more efficiently designed structures and free the user from performing some tedious input calculations. The areas modified were (1) extension to stiffened cylinders and (2) incorporation of "knockdown" or reduction factors to obtain critical design loads.

#### 1. Stiffened Cylinders

A cylinder with closely spaced stiffeners, inside, outside, or both, may be treated by "smearing" the stiffeners into an anisotropic sheet in the analysis. In this technique one determines a set of average stiffnesses for the stiffened cylinder and then determines buckling loads based on the average stiffnesses. The resulting buckling wave lengths are then compared with stiffener spacing to verify the smearing assumption.

*a. Operating Modes* - Three operating modes are available to the user:

- 1) Input of experimentally determined values of stiffness from isolated axial compression, torsion, and internal pressure tests. The analysis for this mode and a detailed discussion of input parameters are given in<sup>3</sup>. Sample Problem 1 in Appendix A of the User's Manual illustrates the input and output information.
- 2) Input of cylinder geometry and wall construction. This input mode is more widely used than either of the other two and is directly related to the recent modifications. Sample Problems 2 through 4 in the User's Manual illustrate the input and output information.
- 3) Direct input of stiffness matrices. The analysis for this mode and a detailed discussion of input parameters are given in<sup>3</sup>. Sample Problem 5 in the User's Manual illustrates the input and output information.

*b. Geometry* - Right circular cylinders or segments of right circular cylinders are treated. Vertical and circumferential stiffening members may be included in the modeling (Fig. III-10). Stringers or rings may be on the inside or outside of the cylinder.

c. *Wall Construction* - 1 construction consists of a skin reinforced with stiffening members.

The skin may be a laminated cylinder constructed of layers of different materials having different elastic properties or orientations. Each individual layer may be isotropic or orthotropic and a symmetric or balanced arrangement of layers is not required.

The stiffening members consisting of vertical stringers and/or circumferential rings are treated in the analysis by smearing the stiffeners into an orthotropic sheet. The stiffnesses of the stiffening elements are then added to the skin stiffnesses. These additions are made only in relation to their principal directions<sup>14</sup>. That is, the vertical stringers contribute only to the vertical skin stiffness and to the torsional stiffness and the rings contribute only to the circumferential skin stiffnesses and to the torsional stiffness. For applicability of the smearing assumption, the buckling wavelengths must be compared to the stiffener spacing to assure that the wavelengths are several times greater than the stiffener spacing.

Each stiffening member may be composed of a number of straight or circular elements (Fig. III-11) on equidistant spacings around the circumference and equidistant spacings along the length of the cylinder. Each stiffening member element may be composed of a laminate of layers of orthotropic material, each layer having different orthotropic properties, orientation, and thickness. It is emphasized that the stiffening member laminates must be symmetric and balanced.

The skin and stiffening member construction combinations that can be evaluated are shown in Fig. III-12.

d. *Boundary Conditions* - Simple-support boundary conditions are satisfied for "specially orthotropic" cylinders. For generally anisotropic configurations, no homogeneous boundary conditions are satisfied on sections perpendicular to the axis. If the cylinder is long or has a small axial stiffness, these constraints will not greatly affect the buckling loads; however, short cylinders and those with high axial stiffness may be affected by boundary constraints.

e. *Loadings* - The buckling calculations for any combination of pressure, uniform axial compression, and torsion are similar. Any two of the loads may be input and the remaining load to cause buckling is calculated. In the case of bending, any of the above three loadings are input and the program calculates the bending load to cause buckling.



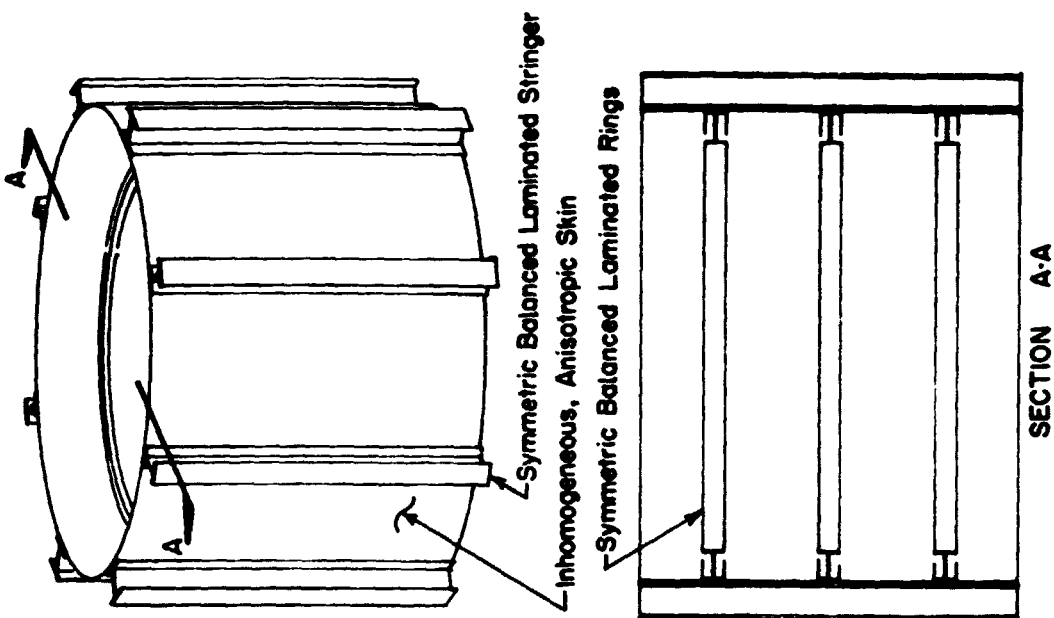


Fig. III-10

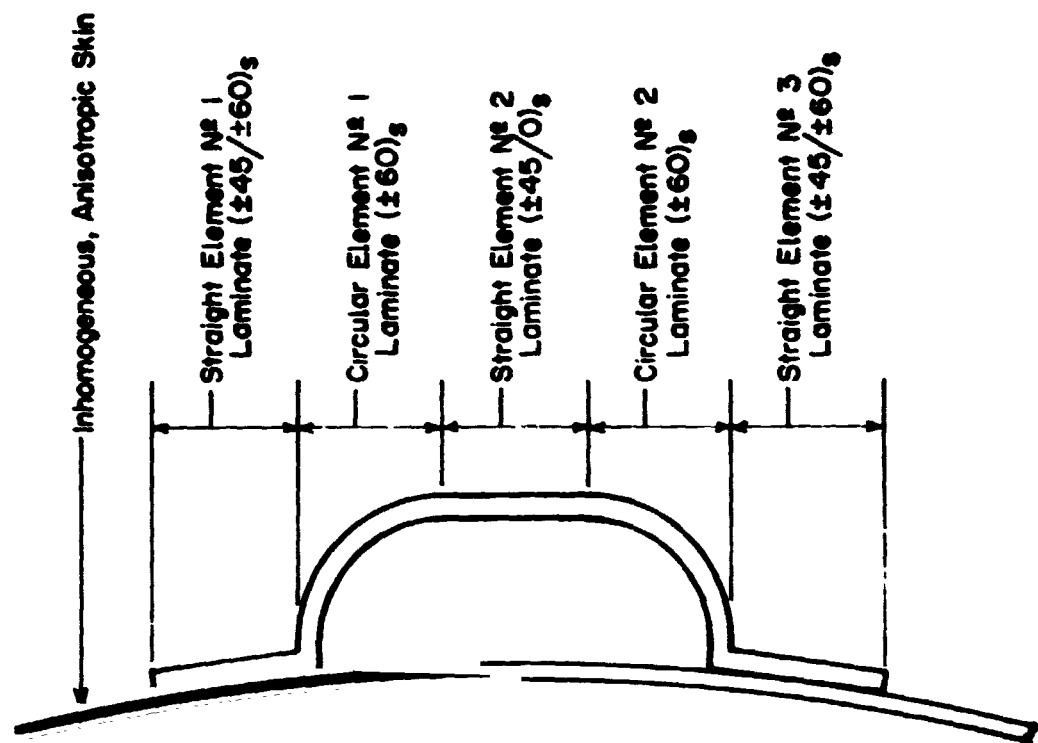


Fig. III-11

Fig. III-11  
Example of Typical Stiffening Member Composed of  
Straight and Circular Elements of Symmetric,  
Balanced Laminates Construction

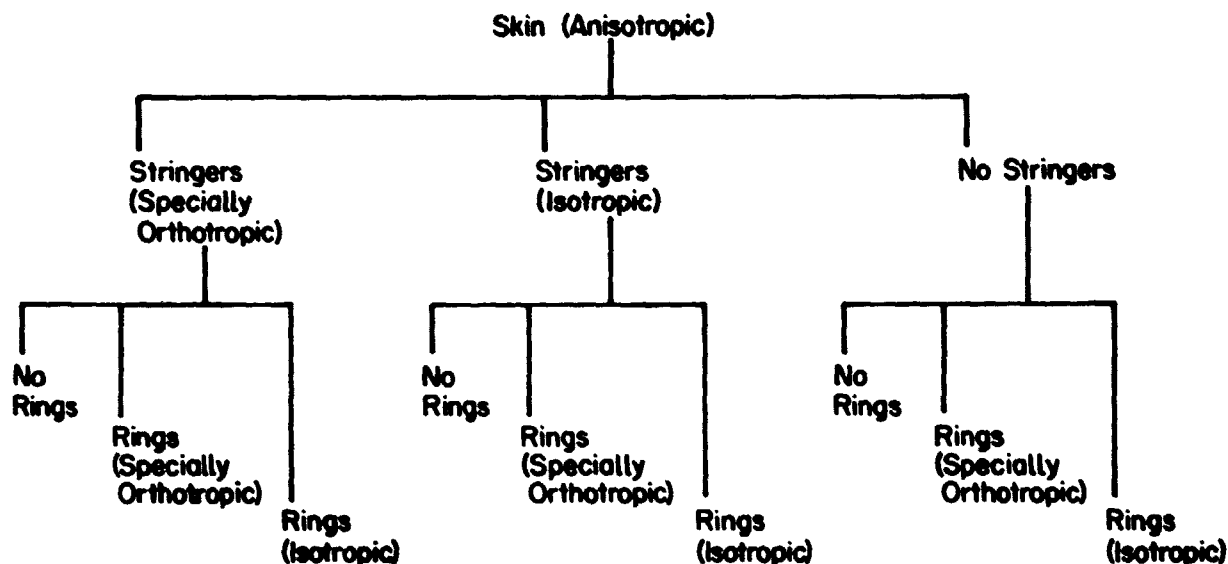


Fig. III-12 Shell Construction Combinations

## 2. Correlation Coefficients

A design buckling load is obtained by multiplying the theoretical buckling load by a "knockdown" factor. These factors are obtained from previously obtained test data and correlation studies and they reflect differences between theory and test. Both initial imperfections and boundary conditions have been shown to be significant in causing these discrepancies. Most test data are not specific with regard to imperfections or boundary conditions; thus, the data from similar specimens and loadings are usually combined. Lower bound or statistical correlation curves are then drawn to provide the correlation coefficients. HOLBOAT uses the expressions for correlation coefficients given in the NASA Space Vehicle Design Criteria Monograph, NASA SP-8007<sup>15</sup>, which provide for differences in loading condition and cylinder construction, as follows:

[1] Correlation coefficient  $\gamma = 1 - C_1 (1 - e^{-\phi})$

where

[2]  $C_1 = 0.901$  for axial load

[3]  $C_1 = 0.731$  for bending load

and

[4]  $\phi = \frac{1}{C_2} \sqrt{a/h}^*$

where

[5]  $C_2 = 16$  for isotropic constructions

and

$$[6] \quad \phi = \frac{1}{C_2} \left[ \frac{a}{\left( \frac{D_{11} \ D_{22}}{A_{11} \ A_{22}} \right)^{\frac{1}{4}}} \right]^{\frac{1}{2} *}$$

where

[7]  $C_2 = 29.8$  for orthotropic constructions.

Print out of the computed correlation coefficient in the summary of the problem permits the program user to tailor the "design" buckling load to his specific design uncertainties. The generated correlation coefficient is applied to only the calculated buckling load; it is not applied to any of the input loads.

Specific information concerning the use of the computer program along with several worked example problems are presented in a User's Manual, HOLBOAT Computer Program, MCR-74-426, October 1974<sup>10</sup>, provided to NASA-MSFC.

---

\*a = cylinder radius  
h = cylinder thickness  
 $D_{11}, D_{22}, A_{11}, A_{22}$  = cylinder stiffnesses

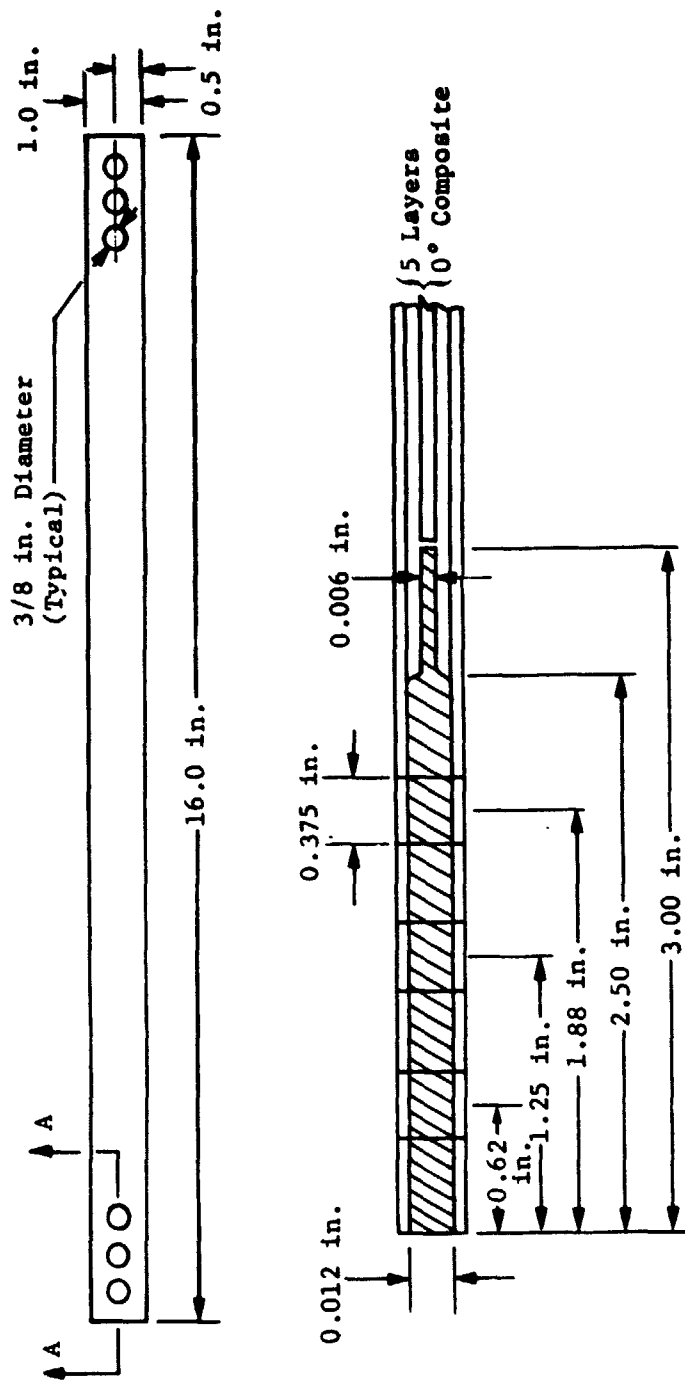
#### IV. FABRICATION DEVELOPMENT

##### A. SMALL PHASE I STRUCTURES

The fabrication effort during Phase I was to demonstrate the fabricability of the wide variety of structural concepts subjected to design evaluation. The honeycomb sandwich concept involved lightweight aluminum honeycomb core with a variety of thin faceskins using fibrous composites as well as metals. Thin fibrous-composite stiffener straps for reinforcement of the sandwich panels were also considered. Candidate truss skirt concepts used were: graphite/epoxy, boron/graphite/epoxy, and aluminum truss members. The isogrid concept evaluated involved integrally machined aluminum with thin stiffener and skin gages. Success or difficulty in fabricating relatively small test panels and components aided in selection of concepts to be further evaluated during Phase II.

##### 1. Composite Stiffener Straps

A modified honeycomb sandwich cylindrical shell design uses closely spaced, thin, unidirectional composite stiffener straps oriented axially and bonded directly to or directly underneath the sandwich faceskins. The geometry of three candidate stiffener straps is shown in Fig. IV-1. The ends of each specimen were reinforced with a thin titanium shim insert. These inserts were chem-milled at the ends to provide steps for bonding the composite layers. Three different kinds of composite material were used, Rigidite 5505 boron/epoxy, HM/X-904 graphite/epoxy, and HTS/X-904 graphite/epoxy. The graphite/epoxy specimens also contained style 104 glass cloth between each graphite/epoxy layer to provide transverse strength. The boron/epoxy prepreg tape already contained style 104 glass scrim carrier cloth and, therefore, additional glass cloth was not added to these specimens. The individual layers contained in one of the graphite/epoxy specimens and a completed specimen are shown in Figure IV-2. The cure cycle used for each of the composite material types was that recommended by the material supplier. Three 3/8-in. diameter holes were cut in each end of the cured specimens. These holes were made using a Roto-Punch machine, which provides a high quality hole in thin materials. The finished straps were sent to the structural test laboratory for determination of their ultimate tensile strength.



Specimen Number	1D	2E	3D
0° Composite Material	Boron/Epoxy	HM Graphite/Epoxy	HTS Graphite/Epoxy
Measured Thickness	0.028 in.	0.020 in.	0.029 in.

Fig. IV-1 Specimen Geometry

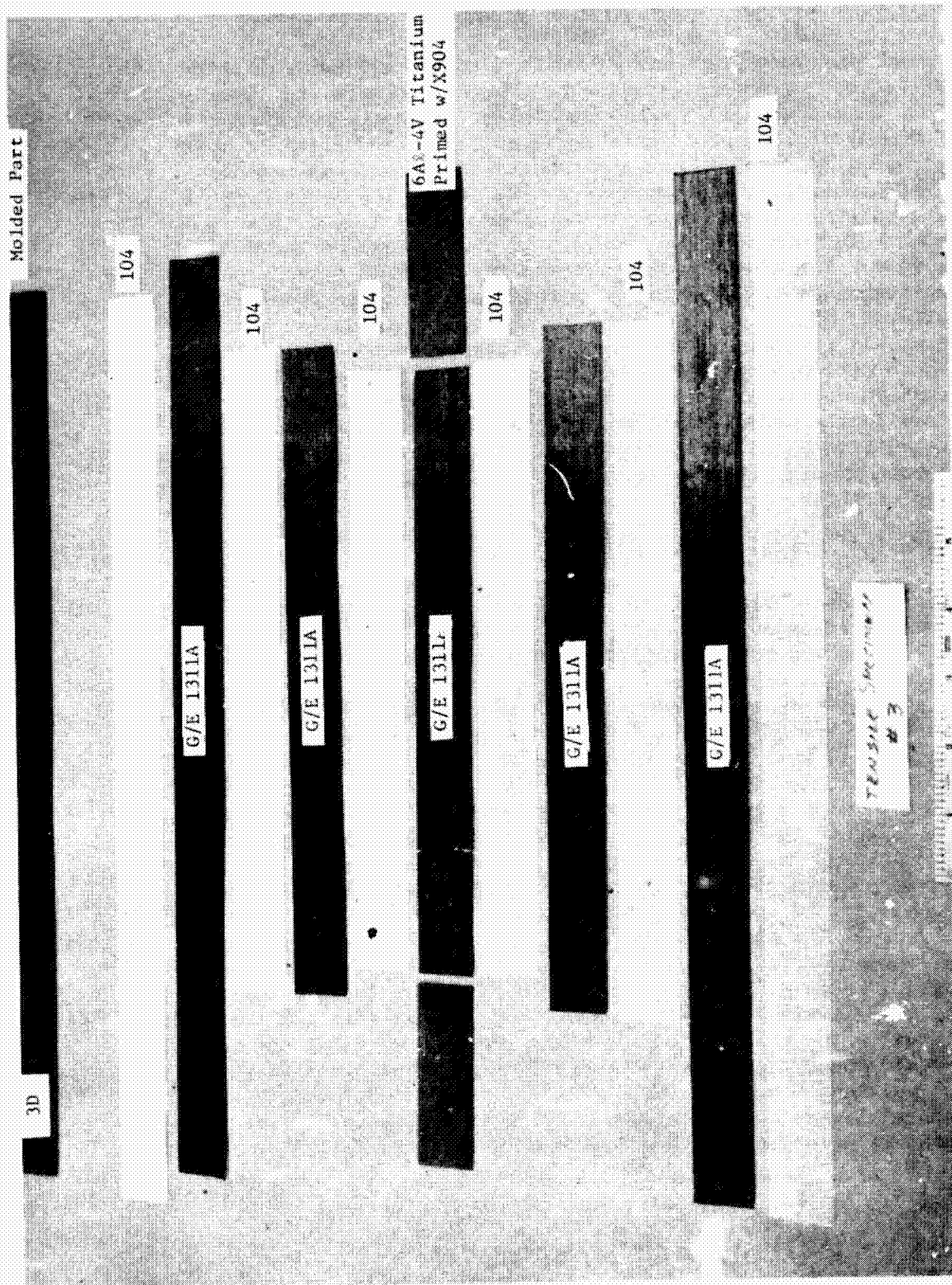


Fig. IV-2

Fig. IV-2 Composite Stiffener Straps

## 2. Graphite Epoxy Truss Struts

Two graphite/epoxy truss struts related to the cylindrical skirt truss concept were fabricated. The overall geometry and layer definition is shown in Fig. IV-3. The struts contained titanium shim end reinforcement inserts as shown for introduction of axial compression load. The type of graphite/epoxy used was Hercules A/S-3501 continuous 7.6-cm (3-in.) wide tape. The layup mandrel used consisted of Brak-Away plaster bonded to a 1.6-cm (5/8-in.) diameter aluminum tube and machined to the dimensions shown in Fig. IV-3. The graphite/epoxy layers were applied using a hand layup technique with the titanium shims added to the appropriate locations. The titanium shims were prepared for bonding by using a Pasa-Jell treatment. The layup was compacted several times prior to cure by using wrapped-on shrink tape. Final cure was accomplished with an external vacuum bag and using an autoclave for application of external pressure and temperature. One of the finished struts and sections through the center and end regions are shown in Fig. IV-4. The specimen was cut into sections following structural test.

## 3. Boron/Graphite/Epoxy Truss Strut

Another truss strut with boron/epoxy flanges and graphite/epoxy webs was fabricated to verify proposed fabrication techniques. This article was for demonstration purposes only; and, therefore, did not contain provisions for load introduction. The truss strut webs consisted of two graphite/epoxy channel sections, shown in Fig. IV-5, 45.7 cm (18.0 in.) long by 2.54 cm (1.0 in.) high with 1.52 cm (0.60 in.) flange legs. The basic layup consisted of eight layers of HTS/X904 graphite/epoxy in a balanced  $\pm 45^\circ$  configuration with a single layer of style 104 fiberglass scrim cloth added to the inner and outer surfaces. The average cured wall thickness was 0.119 cm (0.047 in.) for each part. The parts were laminated over a machined aluminum male molding tool and subjected to the vendor-recommended vacuum bag, autoclave cure cycle. The strut flanges consist of two boron/epoxy laminates, shown in Fig. IV-5, 45.7 cm (18.0 in.) long by 3.81 cm (1.50 in.) wide and 0.127 cm (0.050 in.) thick. These flanges contain 10 layers of Rigidite 5505/4 boron/epoxy with all fibers oriented in the axial direction. They were cured using the vendor-recommended vacuum bag, autoclave cure cycle. The finished strut section, also shown in Fig. IV-5, was made by bonding the flange strips to the web channels using FM-24 film adhesive. The components were secured in a tool during bonding.

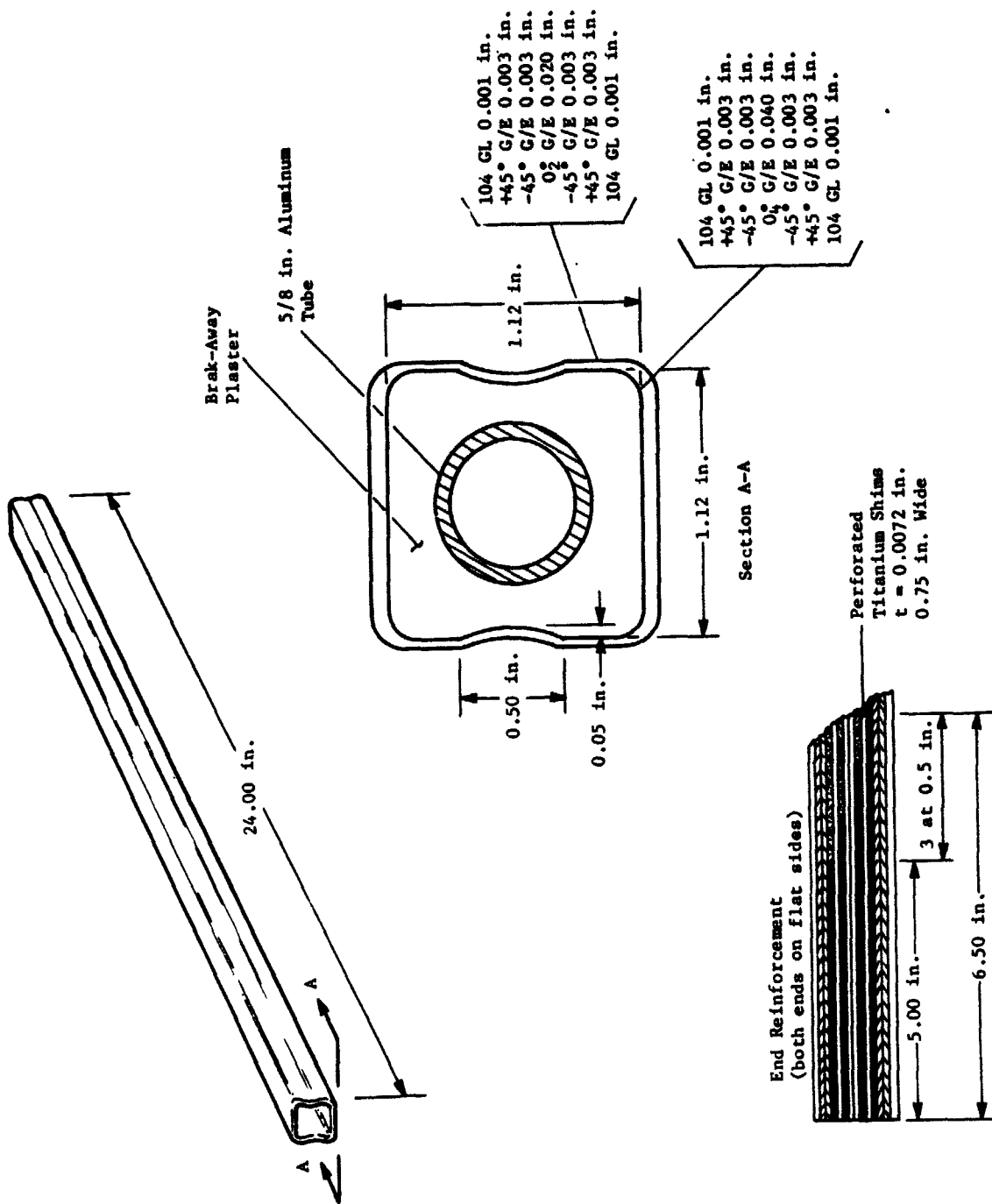


Fig. IV-3 Graphite/Epoxy Truss Strut, Overall Geometry



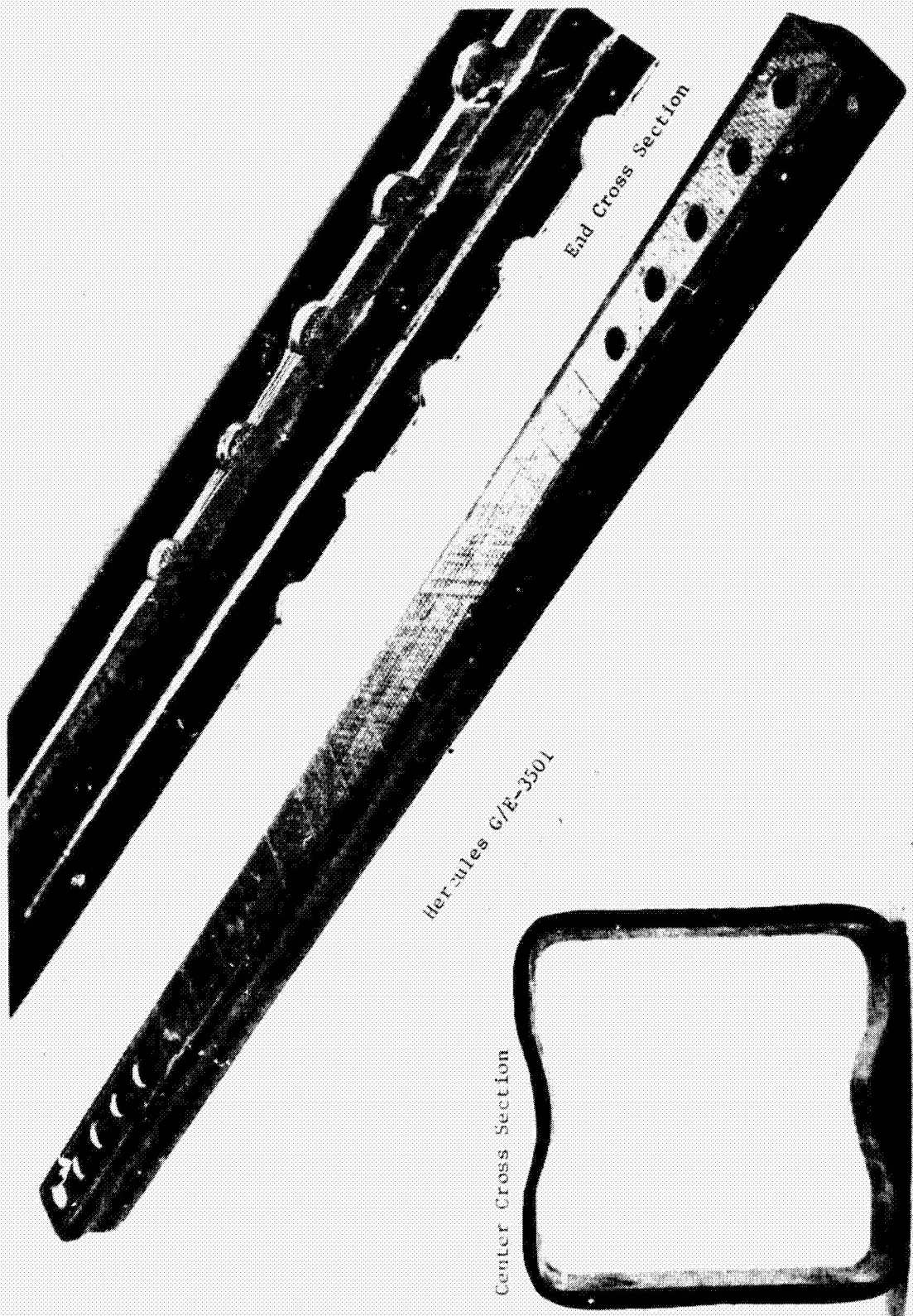


Fig. IV-4  
IV-6

Fig. IV-4 Graphite/Epoxy Truss Sturt, Center and End Regions

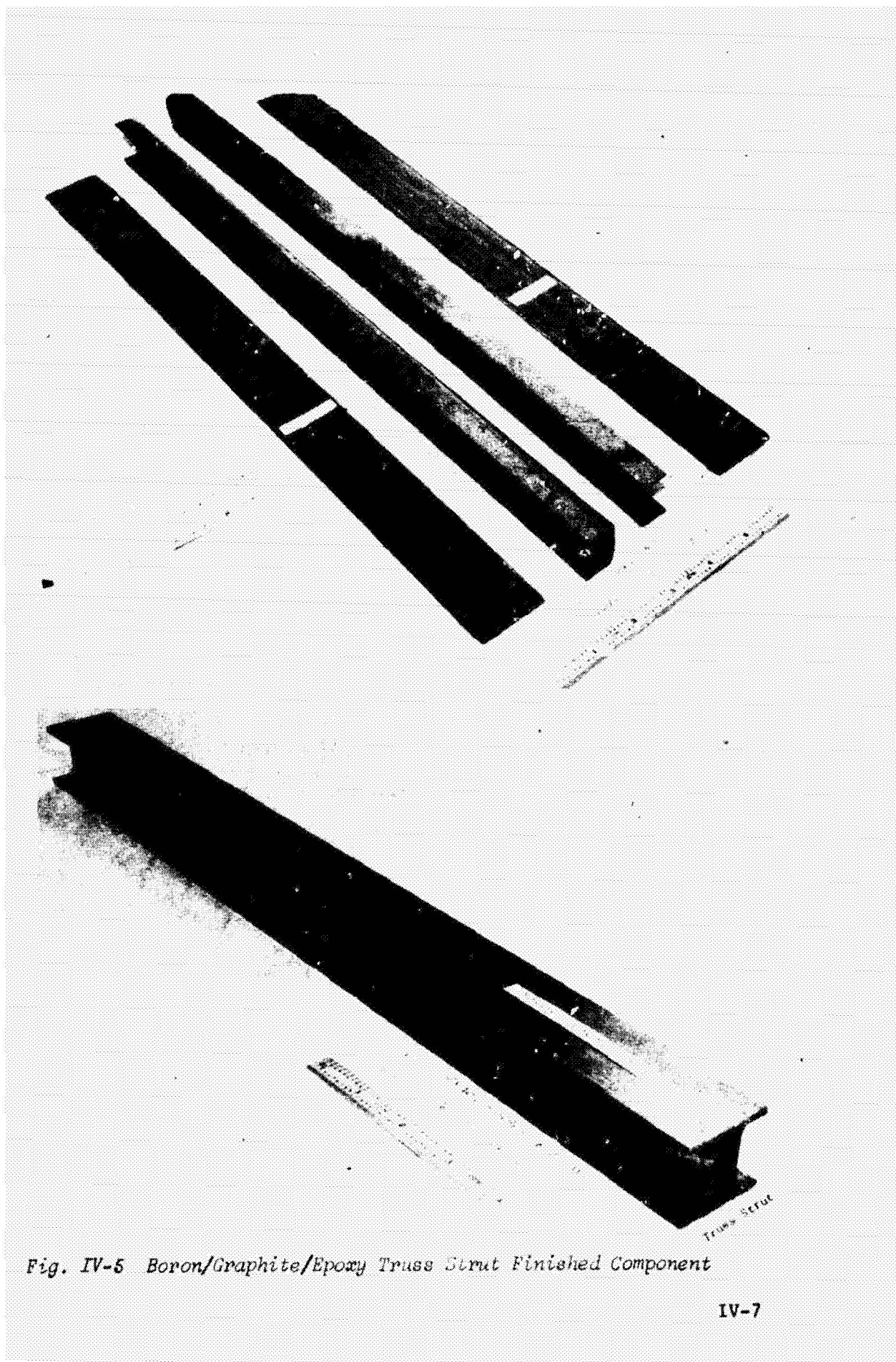


Fig. IV-5 Boron/Graphite/Epoxy Truss Strut Finished Component

#### 4. Honeycomb Sandwich Panels

A variety of honeycomb sandwich panels and panel components were fabricated during Phase I. In all cases, skin/core bonding was accomplished using thin FM-24 reticulating adhesive. The initial goal was to minimize bond line thickness while maintaining good filleting and bond strength. The sandwich core used in all cases was 1/8-5052-0.0007-3.1 lightweight aluminum Hexcel honeycomb core. Core selection was based on providing lightweight, small cell size and adequate strength and stiffness. Sandwich faceskins were made using fiberglass cloth, boron/epoxy, graphite/epoxy, aluminum, and titanium.

a. *FM-24 Reticulating Adhesive* - Four honeycomb sandwich panels were fabricated to evaluate FM-24 reticulating adhesives with film thicknesses of 0.178 mm (0.007 in.) and 0.089 mm (0.0035 in.). Two of the panels used 0.178 mm (0.007 in.) adhesive, one reticulated prior to cure. Two similar panels were fabricated using the 0.089 mm (0.0035 in.) adhesive. Each of the four panels had overall dimensions of 17.8 cm by 12.7 cm (7.0 in. by 5.0 in.) and were 2.54 cm (1.0 in.) deep. They all used 1/8-5052-0.0007, 50-kg/m<sup>3</sup> (3.1-lb/ft<sup>3</sup>) aluminum honeycomb core and 0.330-mm (0.013-in.) thick glass/phenolic faceskins. Reticulation of the film adhesive on two of the panels was accomplished as follows:

- 1) Apply FM-24 film adhesive to one side of cleaned aluminum core.
- 2) Place for 30 sec in an oven that is preheated to 149°C (300°F).
- 3) Remove and place adhesive side down on a Teflon film.
- 4) Allow to cool for 3 min.
- 5) Apply film to other side of cleaned core.
- 6) Place for 60 sec in an oven that is preheated to 149°C (300°F).
- 7) Remove and place the side which was just reticulated face down on a Teflon film.

The core with reticulated adhesive on both sides is then sandwiched between two cleaned glass/phenolic faceskins and cured under vacuum bag plus 17.2 N/cm<sup>2</sup> (25 psi) autoclave pressure for 60 min at 121°C (250°F). Reticulated cores for 0.178 mm (0.007 in.) and 0.089 mm (0.0035 in.) films are shown in Fig. IV-6.



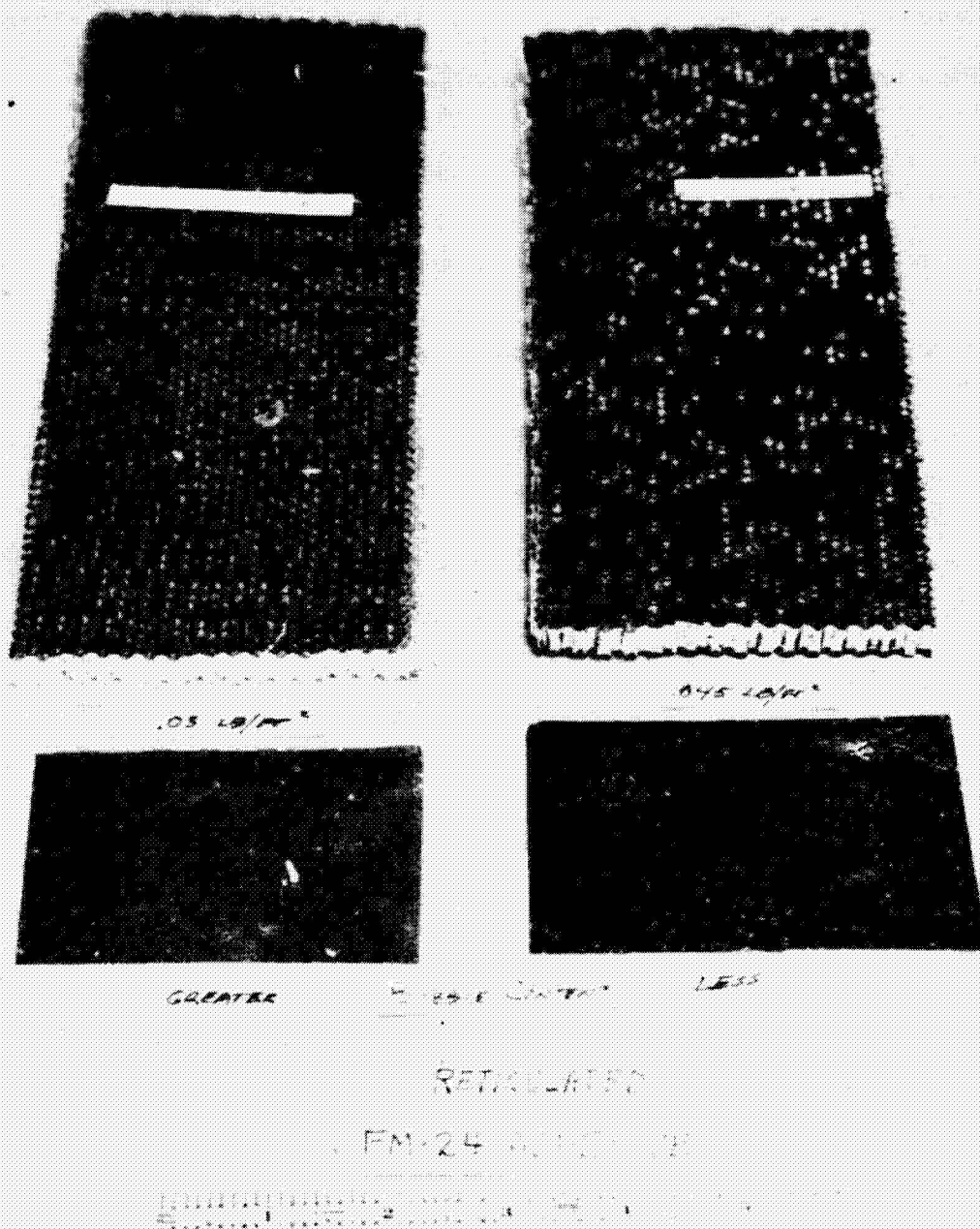


Fig. IV-6 FM-24 Reticulated Adhesive

Layup of the two panels that were not reticulated was accomplished as follows:

- 1) Warm one of the cleaned glass/phenolic faceskins to 66°C (150°F) and then apply the FM-24 film adhesive.
- 2) Apply FM-24 film adhesive to the other cleaned faceskin at room temperature.
- 3) Sandwich the cleaned honeycomb core between the faceskins with skin that was warmed on top.

These panels were then cured using the cure cycle used previously on the reticulated panels.

Following cure, the four panels were cut into 5.08 cm by 5.08 cm (2 in. by 2 in.) specimens for flat tensile tests.

*b. Lightweight Aluminum Honeycomb Core* - The honeycomb sandwich core material used throughout Phase I was hexagonal aluminum honeycomb designated 1/8-5052-0.0007-3.1. This core shown in Fig. IV-7, contains 5052 alloy aluminum foil 0.0018 cm (0.0007 in.) thick and has 0.318-cm (1/8-in.) hexagonal cells. At 50 kg/m<sup>3</sup> (3.1 lb/ft<sup>3</sup>), it is the lightest available aluminum core with 0.318 cm (1/8 in.) cells. This small cell size is required to prevent intercell buckling of the thin face skins used on the various development sandwich panels. The 0.0018 cm (0.0007 in.) thick foil used to fabricate this particular core provides low core weight; however, it presents handling problems that must be considered when evaluating it for use on relatively large structural panels. Typical core damage caused by normal handling is shown in Fig. IV-7. This type of damage is present in as-received 1.22 by 2.44 m (4 by 8 ft) expanded sheets and is also caused by normal handling during fabrication. None of the honeycomb sandwich panels fabricated during Phase I contained core with damaged cells because the relatively small panel size of 43.2 cm by 40.6 cm (17 in. by 16 in.) allowed for selection of good core. Also, each core was machined to final thickness from a basic 1 in. thick core. The task of preventing core damage on larger sizes, however, would definitely require special handling and quality control methods.

It was necessary during the honeycomb sandwich development program to machine the lightweight aluminum honeycomb core. This is typically accomplished by filling the honeycomb cells with an easily removed rigid material to support the cell walls during machining. The filler materials investigated were--Rigidex and Brak-Away plaster. The Brak-Away plaster provides adequate support but is very hard to remove from the cells after machining and tends to oxidize the aluminum. The Rigidex also provides

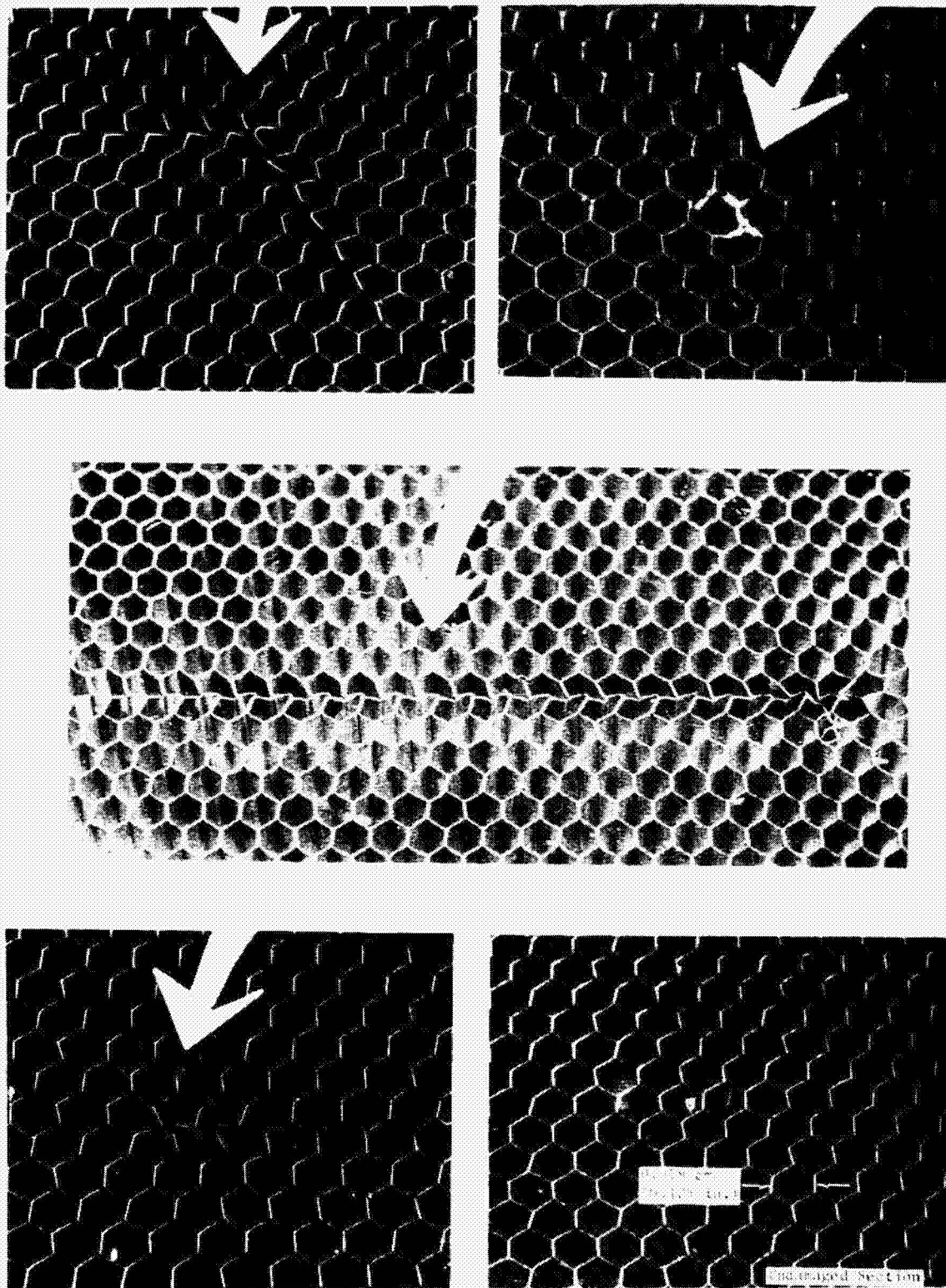


Fig. IV-7 Aluminum Honeycomb Core Damage



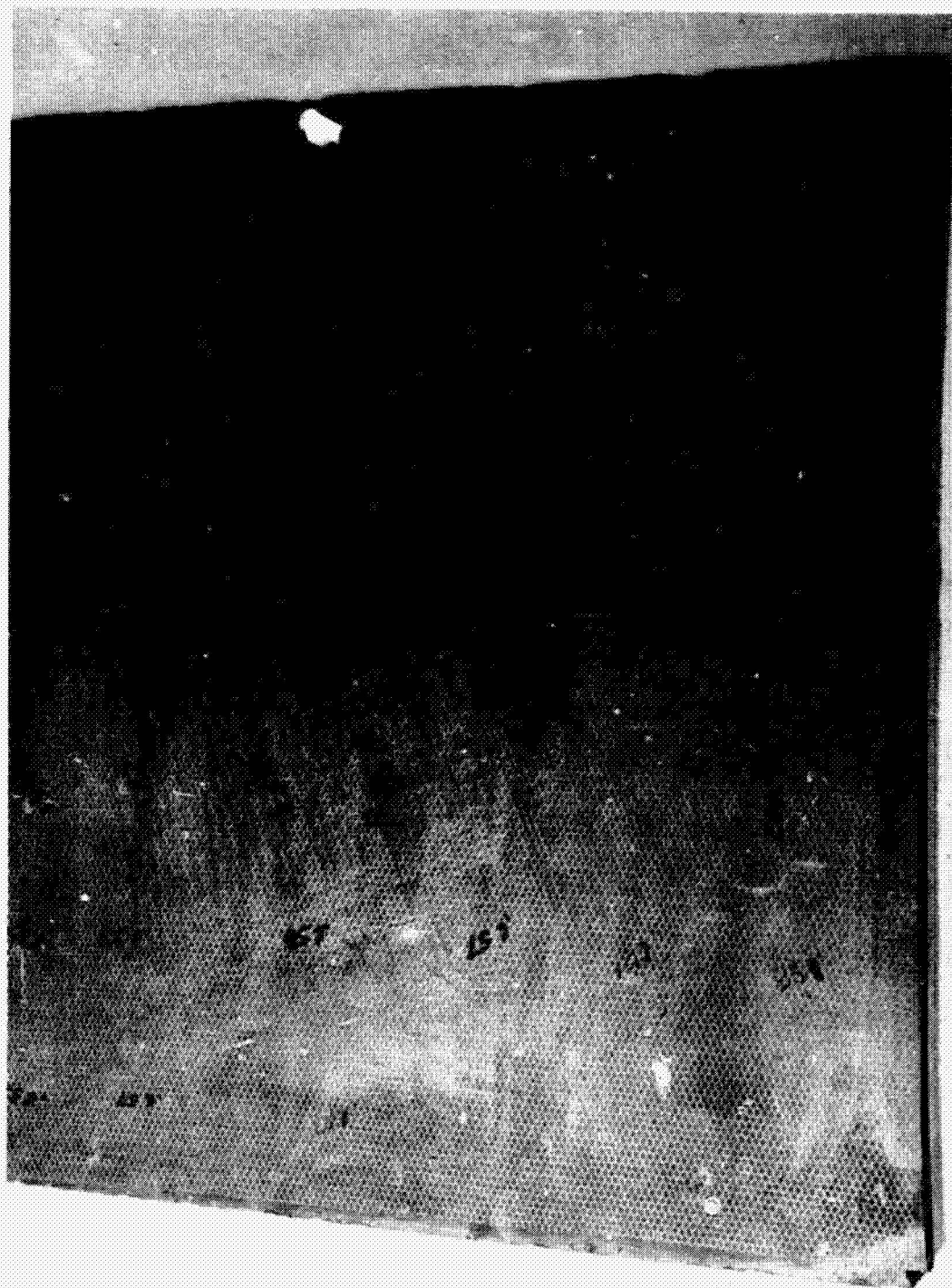
good support, but is easily melted out after machining and does not oxidize the aluminum. The aluminum core is alkaline-cleaned following the removal of the Rigidex material. All of the cores used in the honeycomb sandwich development test panels were machined using the Rigidex support and surface milling method. This involved pouring hot Rigidex material into the core, allowing it to harden and then milling the surfaces to the desired core thickness. The milling was done using a large drill press with a 10.4-cm (4-in.) diameter single point planer head cutter rotated at 2400 rpm. The filled core is passed under the cutter at a rate of approximately 5.2 cm (2 in.) per sec making rough cuts of 0.076 cm (0.030 in.) per pass and finish cuts of 0.0076 to 0.0254 cm (0.003 to 0.010 in.) per pass. Finished thickness tolerance of -0.000 and 0.0076 cm (+0.003 in.) can be achieved on these relatively small cores. Following machining, the Rigidex is removed by heating in an oven and the core is cleaned to prepare it for the final sandwich bonding operation. The cleaning operation for the aluminum core is as follows:

<u>Step</u>	<u>Operation</u>	<u>Duration, min</u>
1	Degrease	2 to 3
2	Alkaline Clean	4 to 5
3	Rinse	3 to 4
4	Deoxidizer Etch	1
5	Rinse	2 to 4

The machined core, with Rigidex still in place, used on test panel Boron-GL-17-1, is shown in Fig. IV-8. Measured final thicknesses are also shown.

### *c. Faceskin Fabrication*

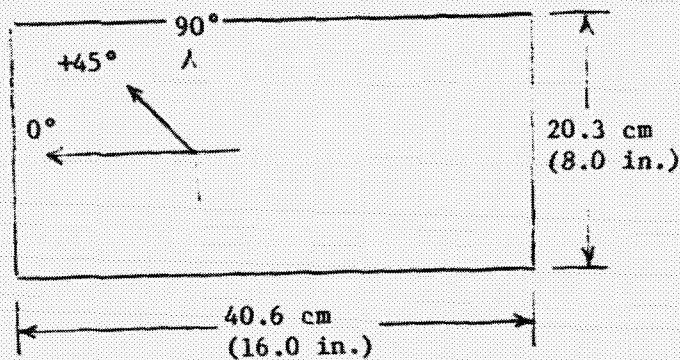
*Composite Development Skins* - Several laminate configurations using various combinations of boron, graphite, fiberglass, and epoxy were laminated and cured to determine potential fabrication problems. The specific configurations investigated are shown schematically in Fig. IV-9. Selection of the particular configurations for preliminary evaluation was highly influenced by available raw materials. The lamination angle associated with each lamina represents the angle that the fibers in a unidirectional prepreg make with a zero reference for a particular layup. In the case of a woven-cloth prepreg, such as the fiberglass cloth, the angle is associated with the reference zero and the fibers in the warp direction of the cloth. This definition is necessary for cloth prepreg because, in general, they do not contain an equal proportion of fiber in the warp and fill direction.

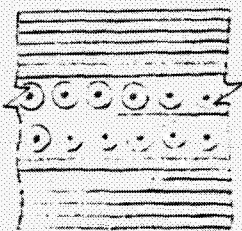


*Fig. IV-8 Machined Honeycomb Core*

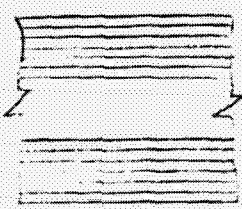
*Fig. IV-8*



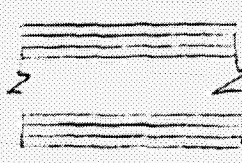


1. 

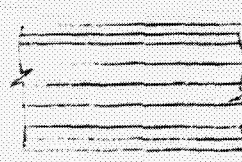
0° 104 GL 0.001 in.
90° 104 GL 0.001 in.
+45° 104 GL 0.001 in.
-45° 104 GL 0.001 in.
+45° 104 GL 0.001 in.
-45° 104 GL 0.001 in.
0° B/E 0.005 in.

Symmetric
2. 

0° 104 GL 0.001 in.
90° 104 GL 0.001 in.
+45° 104 GL 0.001 in.
-45° 104 GL 0.001 in.
+45° 104 GL 0.001 in.
-45° 104 GL 0.001 in.
0° HTS GR/E 0.005 in.

Symmetric
3. 

0° 104 GL 0.001 in.
+45° 104 GL 0.001 in.
-45° 104 GL 0.001 in.
0° HTS GR/E 0.005 in.

Symmetric
4. 

0° 104 GL 0.001 in.
90° 104 GL 0.001 in.
+45° HM GR/E 0.002 in.
-45° HM GR/E 0.002 in.

Symmetric

Fig. IV-9 Laminate Configurations

The fabricated skins were 20.3 cm (8 in.) wide and 40.6 cm (16 in.) in length and were cured using the vacuum bag system shown in Fig. IV-10. Future process development work will be associated with refinement of the vacuum bag system to produce proper fiber/resin ratios, fiber alignment, and surface finish. The time/temperature/pressure cure cycle used for each skin is diagrammed in Fig. IV-11. This is the recommended cure cycle for Fiberite's X-904 epoxy resin which was used on the graphite/epoxy materials and the fiberglass cloth. The laminates combining boron/epoxy prepreg and fiberglass cloth prepreg contained two epoxy systems X-904 and Narmco's 5505. The Narmco system appeared to cure properly with the X-904 cure cycle, however, mechanical property tests would be required to fully assess the characteristics of the combined resin system. Three 20.3 cm by 40.6 cm (8 in. by 16 in.) skins of each of four laminate configurations were cured. The back or smooth side of one skin of each of the four configurations is shown in Fig. IV-12. Flatness of the cured skins was assured through the use of symmetric layup configurations and long time cool-down following cure to minimize thermal gradients.

*Laminates for Thin Laminate Process Study* - A series of 12, 38.1 cm by 30.5 cm (15 in. by 12 in.) thin composite laminates were fabricated for the ultra-lightweight material study. The laminate configuration and cure processes used are defined in Section II.B of this report. Techniques developed during this fabrication of these laminates and results of the material process study were used during fabrication of faceskins for the honeycomb sandwich development test panels.

*Development Test Panel Faceskins* - The series of honeycomb sandwich development test panels consisted of twelve, 44.4 cm by 41.9 cm (17.5 in. by 16.5 in.) panels with a total of six different faceskin materials (laminates). The faceskin configurations and panel designations are shown in Fig. IV-13. The fibrous-composite faceskins were fabricated two at a time on the layup tool shown in Fig. IV-14 using the vacuum bag system diagrammed. Each laminate was subjected to a compaction cycle prior to cure which consisted of heating the vacuum-bagged laminate to 356°K (180°F), holding at that temperature for 20 min and hand rolling (compacting) the laminate immediately upon removal from the oven. The laminate was then placed in an autoclave and subjected to the appropriate time/temperature/pressure cure cycle. The cure cycles used were those found to be most successful during the material process study.

The aluminum faceskins were chem-milled to final thickness from 0.051 cm (0.020 in.) thick 6061-T6 sheet material and the titanium face skins from 0.041 cm (0.016 in.) thick 6Al-4V titanium sheet.



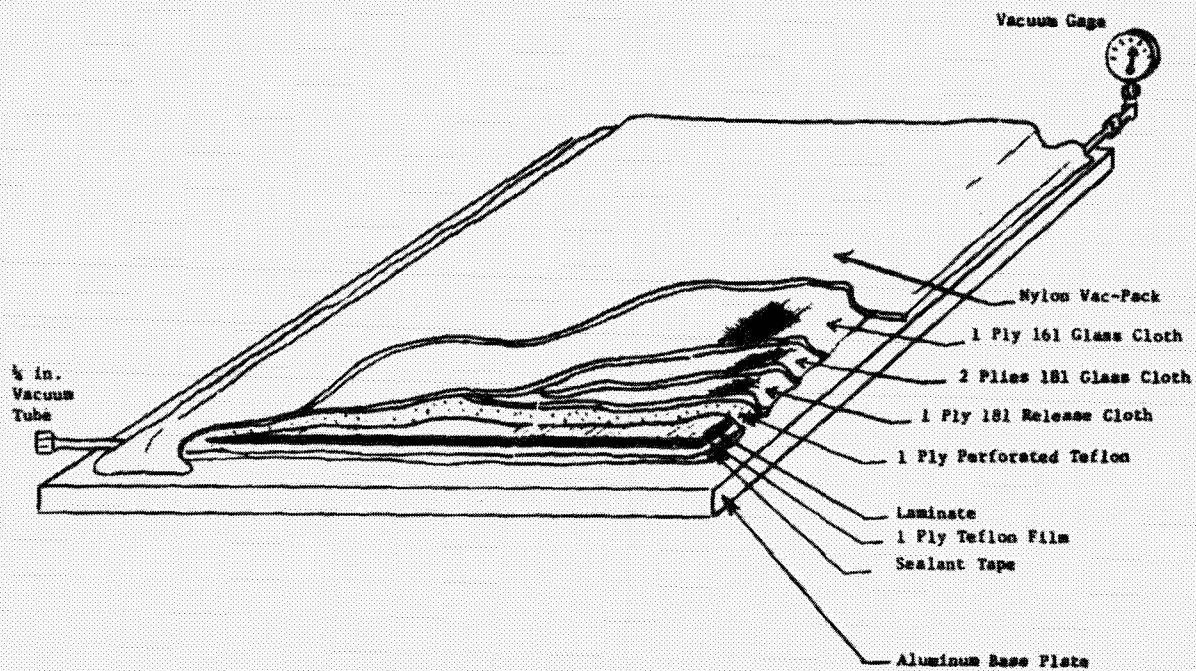


Fig. IV-10 Vacuum Bag System

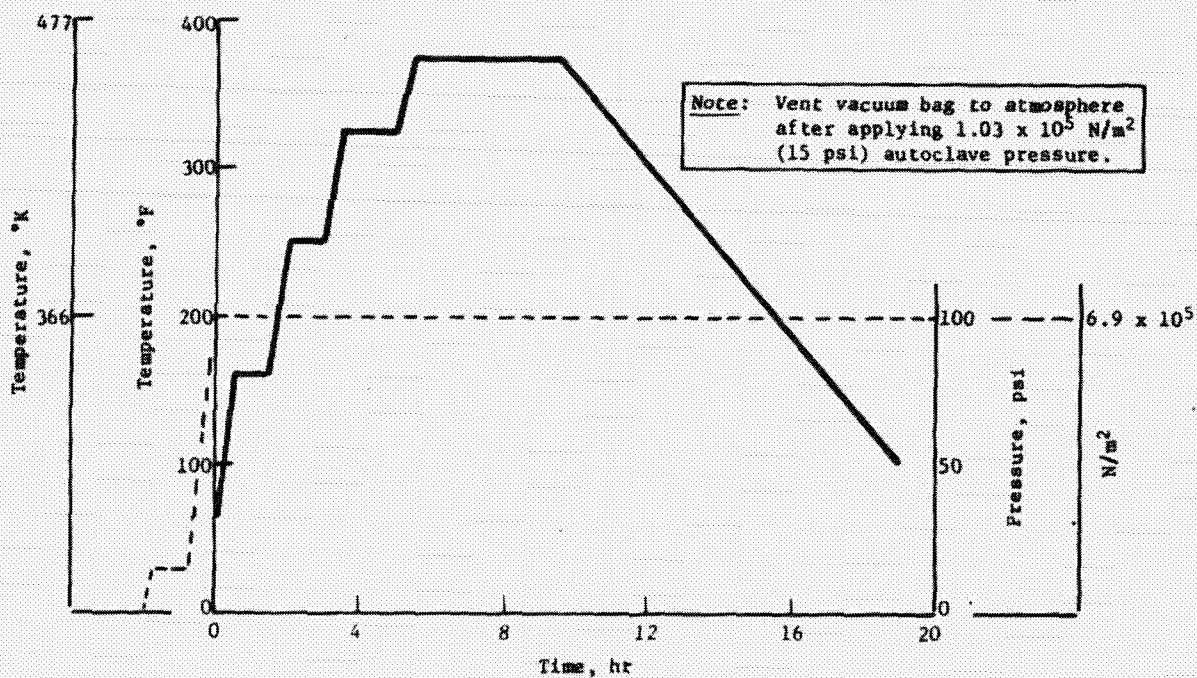


Fig. IV-11 Time/Temperature/Pressure Cure Cycle

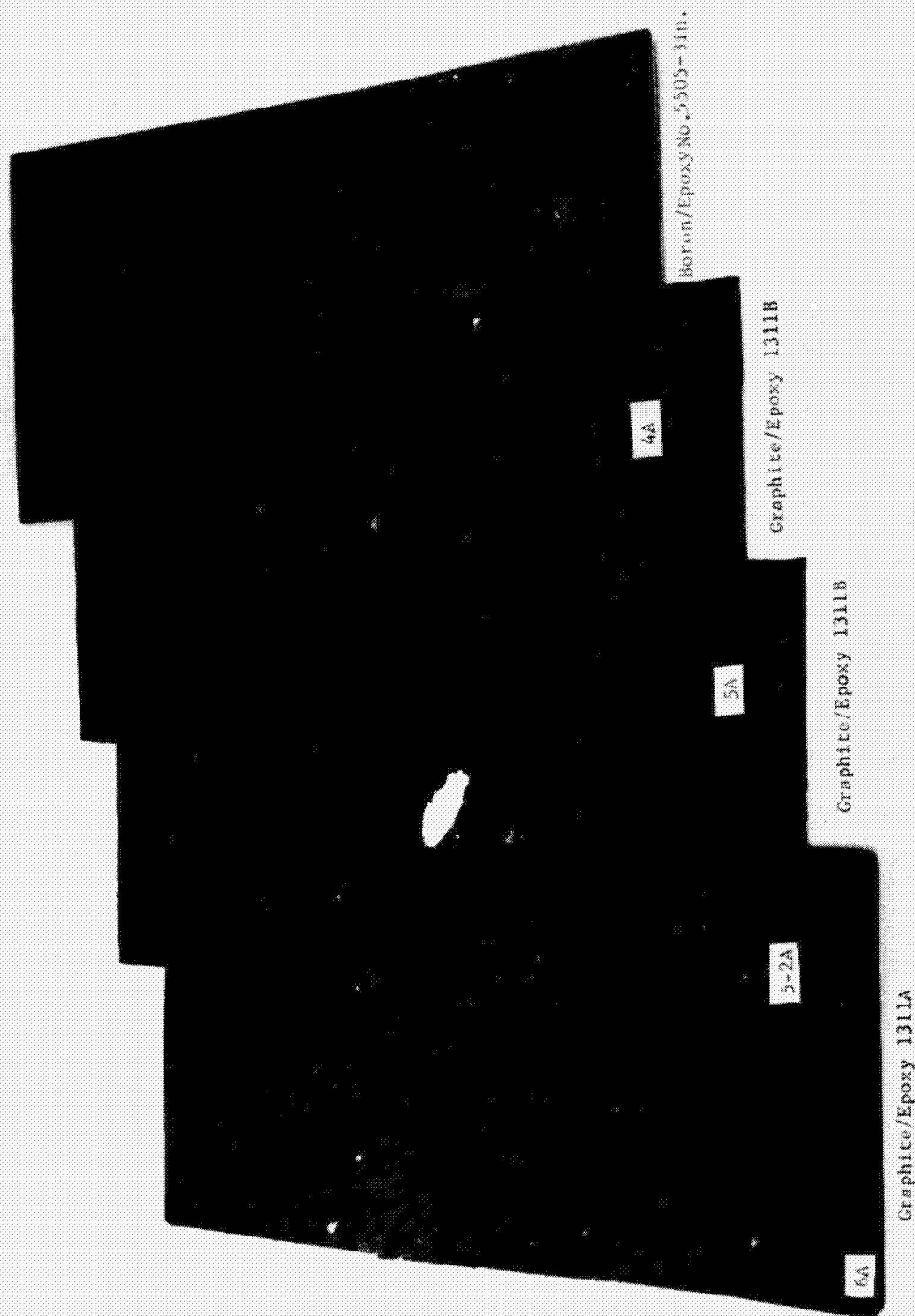


Fig. IV-12

Fig. IV-12 Cured Laminates



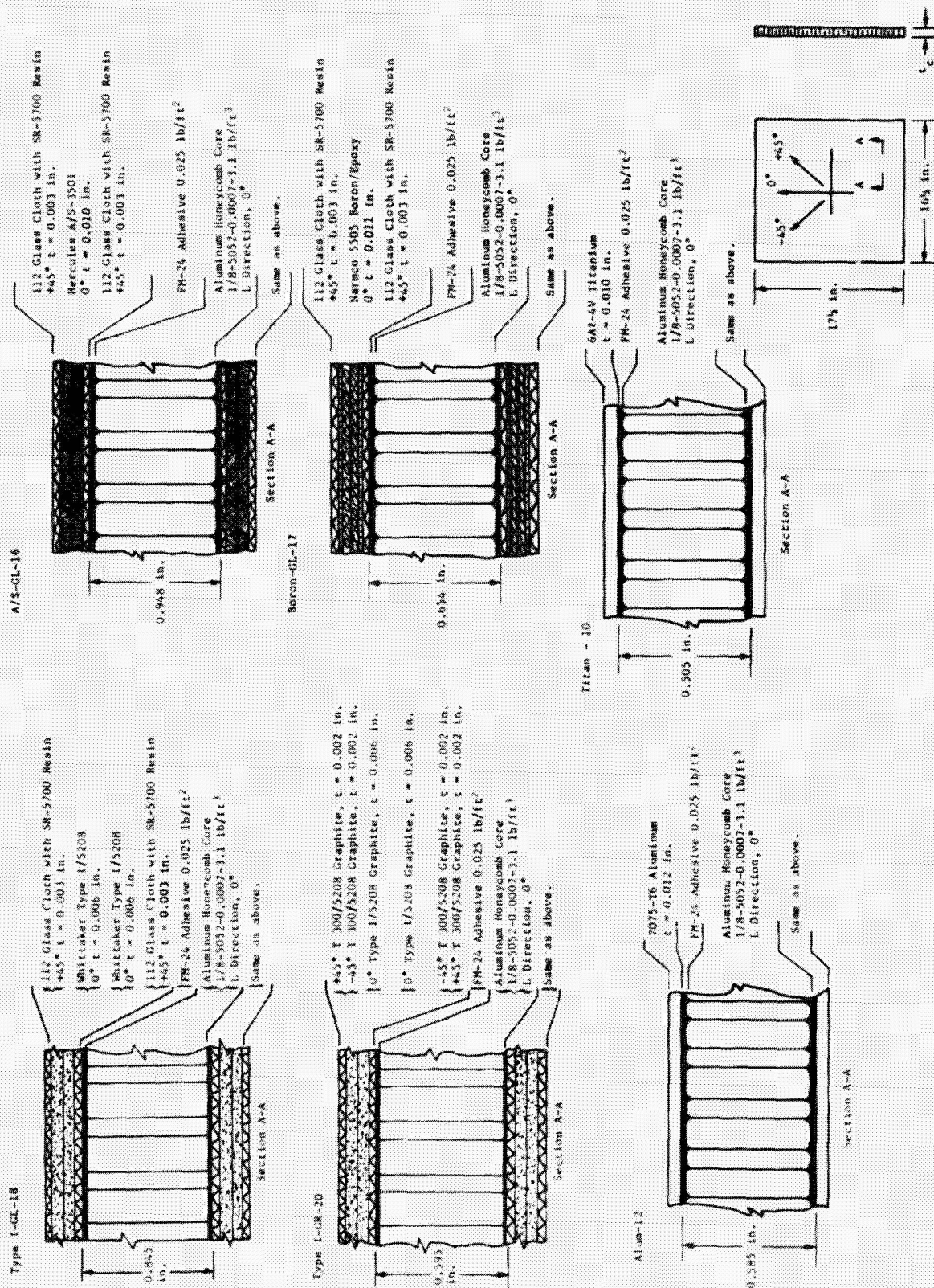


Fig. IV-13  
IV-18

ORIGINAL PAGE IS  
OF POOR QUALITY

Fig. IV-13 Sandwich Face Skin Configurations



Fig. IV-14 Faceskin Layup Tool



d. *Development Test Panels* - The machined aluminum honeycomb cores, FM-24 adhesive film, and the faceskins were used to fabricate twelve 44.4 cm by 41.9 cm (17.5 in. by 16.5 in.) honeycomb sandwich panels, two of each of the six basic designs. The fibrous-composite faceskins were prepared for bonding by very lightly abrading the rough side and cleaning with MEK solvent. The sandwich panel consists of the cleaned honeycomb core with the layer of 0.0089 cm (0.0035 in.) thick FM-24 film adhesive applied to each surface and the composite faceskins, rough side towards core, applied to the film adhesive. The assembled sandwich is cured in an autoclave under vacuum bag plus 3 to 4 psi autoclave pressure at 250°F for 60 min.

Three test specimens, one compression panel, one long beam bend specimen, and one short beam shear specimen were cut from each sandwich panel as shown in Fig. IV-15. Fiberglass laminate doubler plates were bonded to the ends of each compression panel before delivering all specimens to the structural test laboratory.

Photomicrographs of a section from each of the six types of sandwich panel are shown in Fig. IV-16 and Fig. IV-17. The photos in Fig. IV-16 are approximately 10X and reveal the amount of adhesive film filleting obtained. The 100X photos shown in Fig. IV-17 reveal the layer compaction and cured thickness.

## 5. Aluminum Isogrid Panel

The isogrid panel shown in Fig. IV-18 was machined out of 2014-T6 aluminum plate, one-half in. thick. The plate was held in place with a vacuum chuck. A flycutter was used first to clean up the two flat faces of the plate. A two flute 1.59 cm (5/8 in.) diameter end mill was then used to rough cut the plate and final milling was performed using a 0.318 cm (1/8 in.) end mill with a 0.081 cm (0.032 in.) radius. It was noticed during the milling that the material tended to distort at the area being machined. This was probably due to the residual stresses inherent in the -T6 aluminum temper. A final light milling pass eliminated the slight distortion.

For large production quantities of this type of an article, several alternate machining methods are recommended over the hand-operated procedure. Numerically-controlled tape machines lend themselves to this type of work very well. The tediousness of the job is taken away from the operator and the reproducibility of the job is increased. However, a considerable amount of time is still

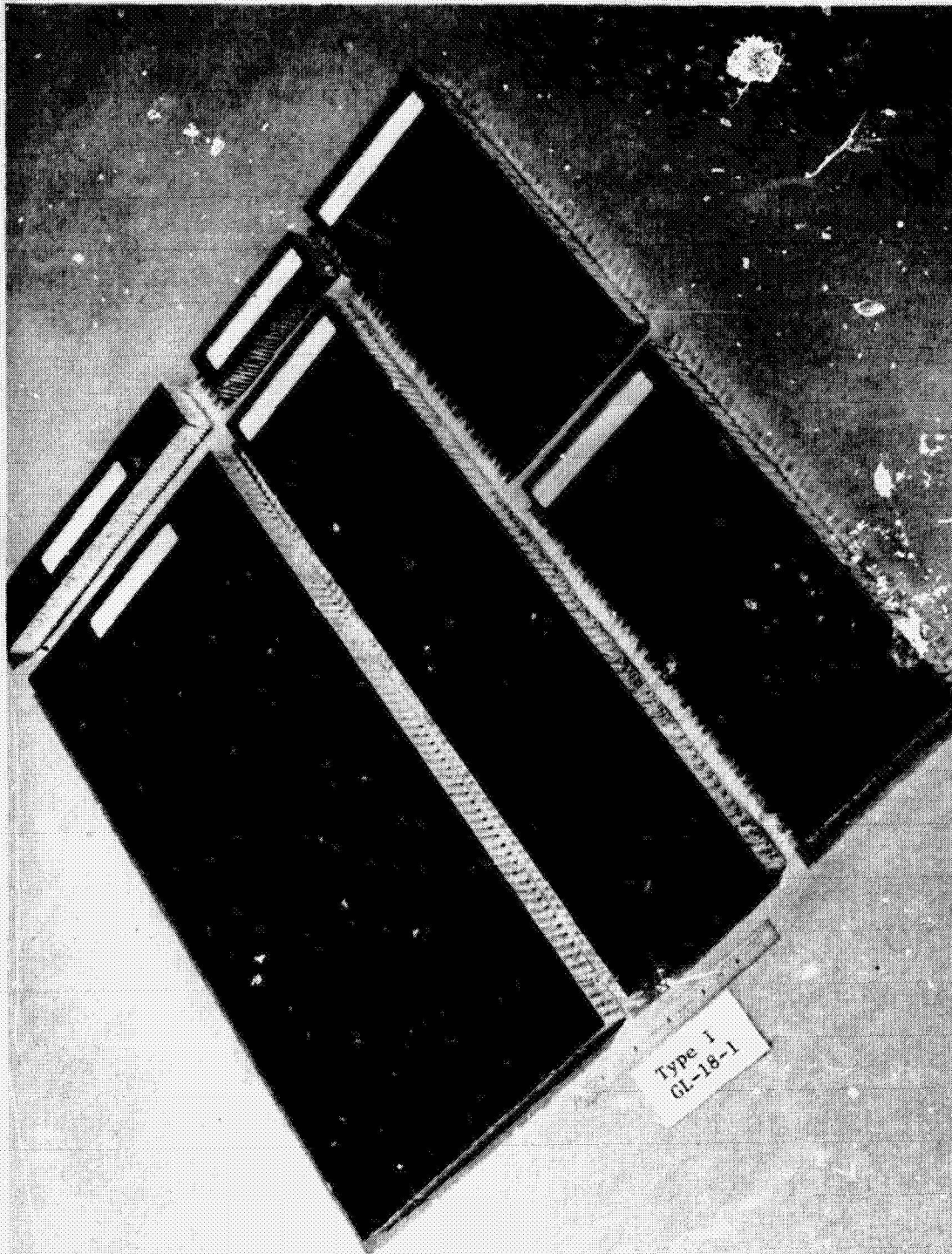


Fig. IV-15 Composite Development Test Panels Type I - GL-18-1

Fig. IV-15





A/S - GL-18-1

45° Style 112 Glass Cloth/5208 Epoxy  
 0<sub>2</sub> A/S Graphite/3501 Epoxy,  
 45° Style 112 Glass Cloth/5208 Epoxy  
 FM-24 Film Adhesive



Type I - GL-18-1

45° Style 112 Glass Cloth/5208 Epoxy  
 0<sub>2</sub> Type I Graphite/5208 Epoxy  
 45° Style 112 Glass Cloth/5208 Epoxy  
 FM-24 Film Adhesive



Type I - GR-20-1

+45° T 300 Graphite/5208 Epoxy  
 -45° T 30° Graphite/5208 Epoxy  
 0<sub>2</sub> Type I Graphite/5208 Epoxy  
 -45° T 300 Graphite/5208 Epoxy  
 +45° T 300 Graphite/5208 Epoxy  
 FM-24 Film Adhesive



Boron - GL-17-1

45° Style 112 Glass Cloth/5208 Epoxy  
 0<sub>2</sub> 5505/4 Boron/Epoxy  
 45° Style 112 Glass Cloth/5208 Epoxy  
 FM-24 Film Adhesive



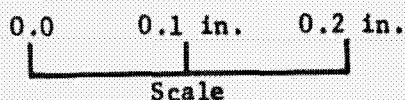
Alum - 12-1

6061-T6 Aluminum  
 FM-24 Film Adhesive



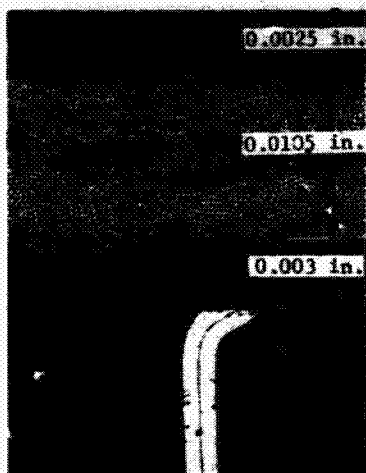
Titan - 10-1

6Al-4V Titanium  
 FM-24 Film Adhesive

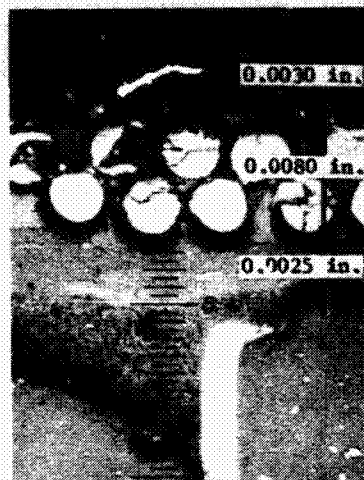


Honeycomb Sandwich  
 Development Test Panels

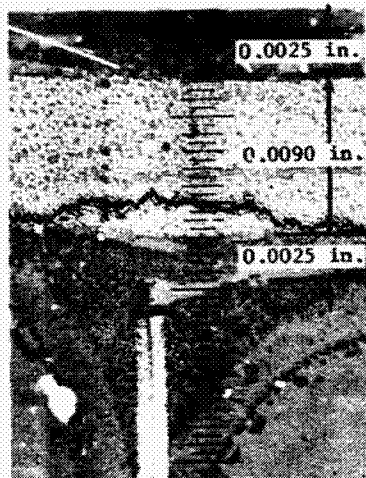
Fig. IV-16 Honeycomb Sandwich Test Panels, 10X Photomicrographs



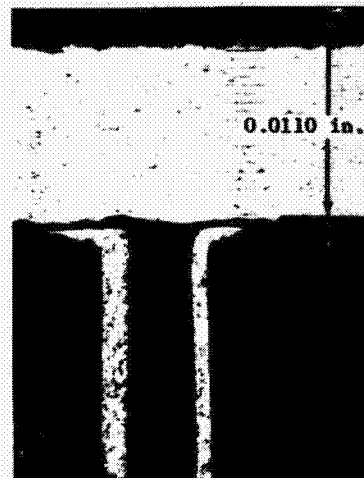
A/S - GL-18-1



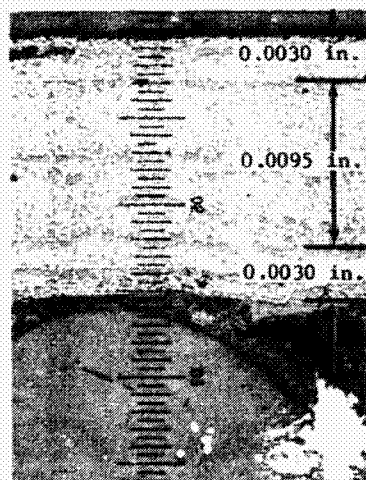
Boron - GL-17-1



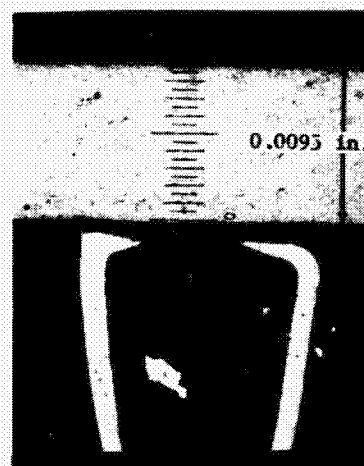
Type I - GL-18-1



Alum-12-1



Type I - GR-20-1



Titan - 10-1

100X Photos

Fig. IV-17 Honeycomb Sandwich Test Panels, Photomicrographs

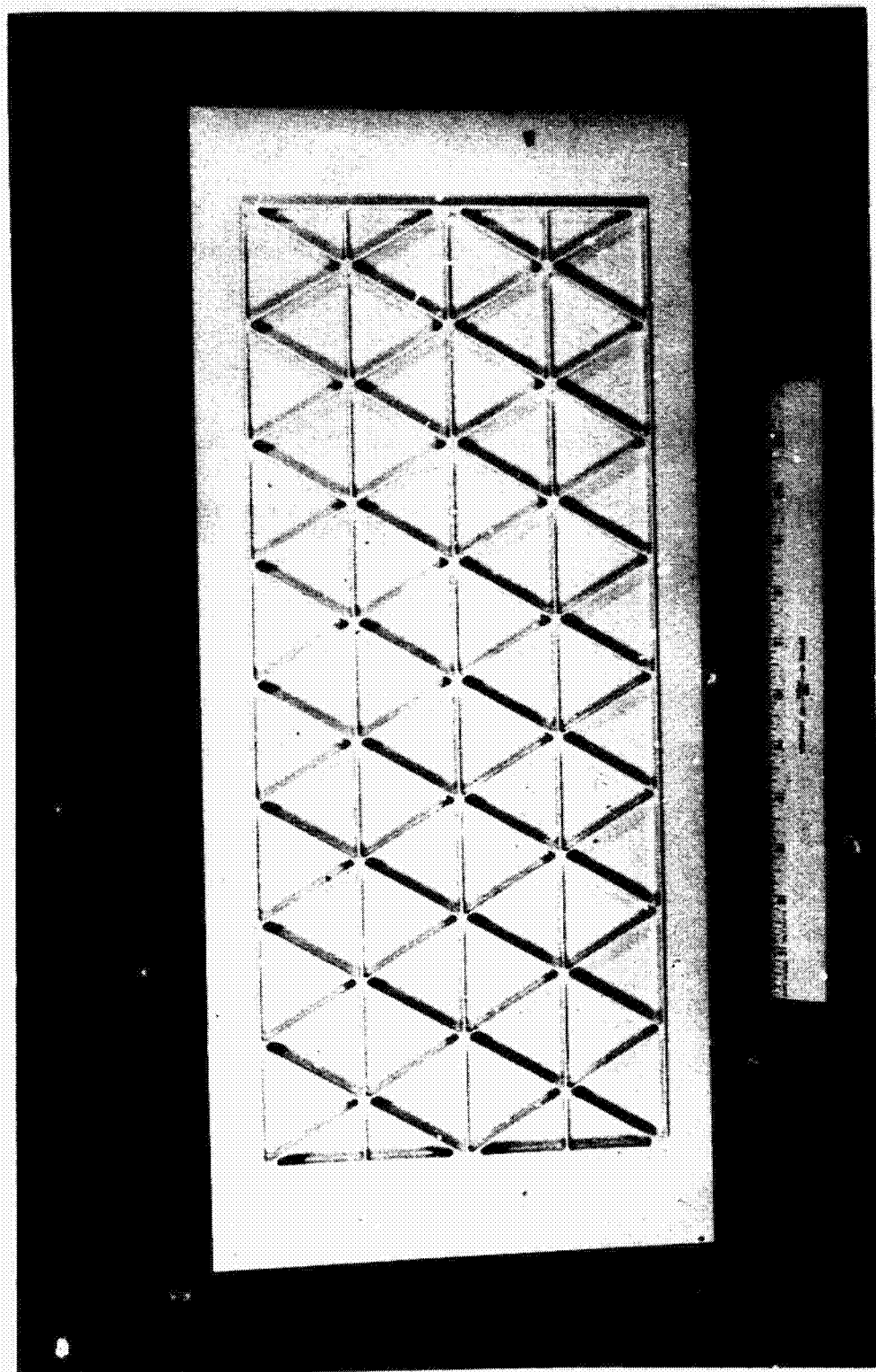


Fig. IV-18 Isogrid Test Panel

Fig. IV-18

required on each panel. Electrodischarge machining (EDM) has the increased advantage of reducing the time for machining each panel, but does require maintenance of the carbon electrode. A final method is electrochemical machining. The process is rapid with no wear on the brass electrode. The largest drawback is the high initial cost of the electrode and the cost of purchasing the machine.

#### 6. Aluminum Truss Section

Several I section aluminum components, some of which are shown in Fig. IV-19, related to the aluminum truss skirt concept were fabricated. They are approximately 1 in. square with 0.102 cm (0.040 in.) thick webs and 0.102 cm (0.040 in.) to 0.216 cm (0.085 in.) thick flanges. Machining was performed on a vertical mill using a 1.59 cm (5/8 in.) single end mill for aluminum. Rough cutting used a spindle speed of 1115 rpm and finish milling 660 rpm, both at a feed of approximately 3 in. per min. The slower speed served to reduce the heat build-up near the end mill. Three cuts were used to reach the web thickness, constantly blowing the aluminum chips away. The latter process was important throughout the machining. Because of the thin (0.040 in.) flanges, a milling technique known as "climb cutting" was used to push the flange away from the end mill against a rigid backup bar. Once one side of the I-beam was finished, a support was inserted into the finished side to provide rigid backing for machining the final side.

These truss segments were assembled to form a typical section, shown in Fig. IV-20, of the aluminum truss concept. The I-Beams were welded together using a TIG process with low amperage settings and argon gas. The filler wire was 4043 aluminum. The technique finally used was to weld the frame and shear tie together first, then weld the assembly to the stringer from the open area opposite the shear tie. Difficulty was experienced with the fusion weld due to the limited working area of the joint. Movement of the welding tip was difficult due to the constrictions of the I-beam structure.

The doubler was attached by spot welding. Again, the constraints of the structure caused access problems to perform the welding. Standard welding heads would not fit between the I-beam flanges to put pressure on the weld area. To solve the problem, a small



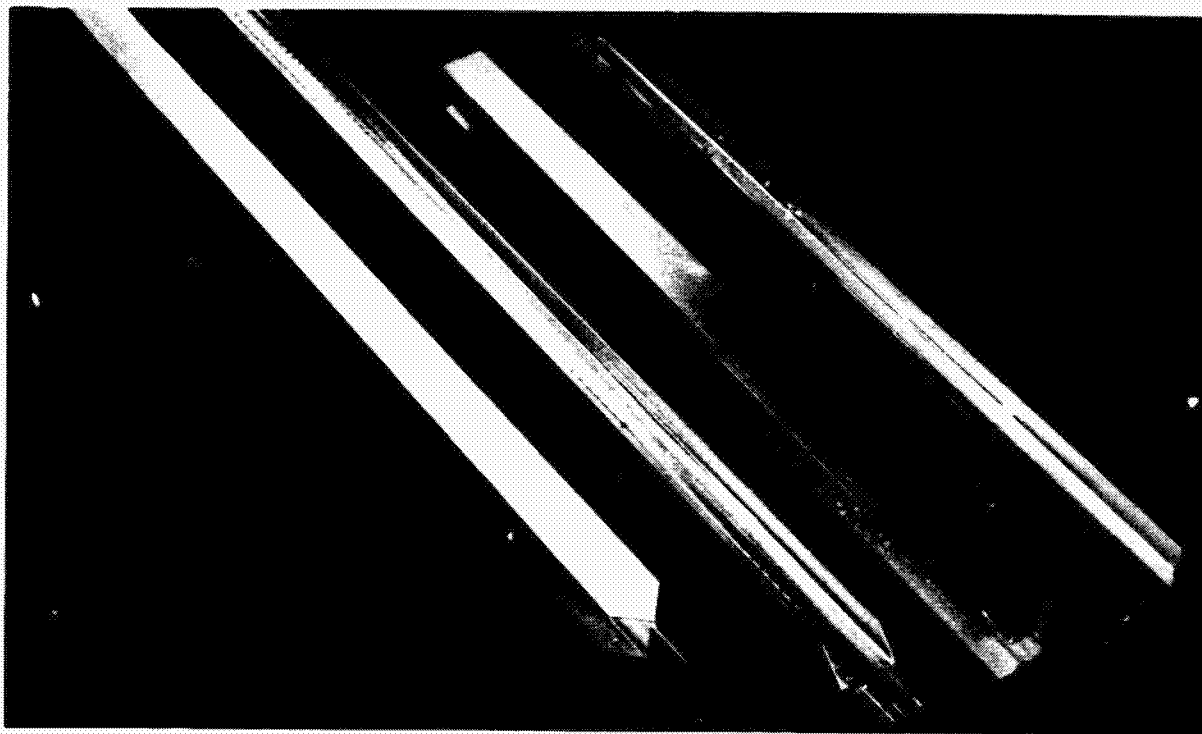


*Fig. IV-19 Aluminum Truss Components*

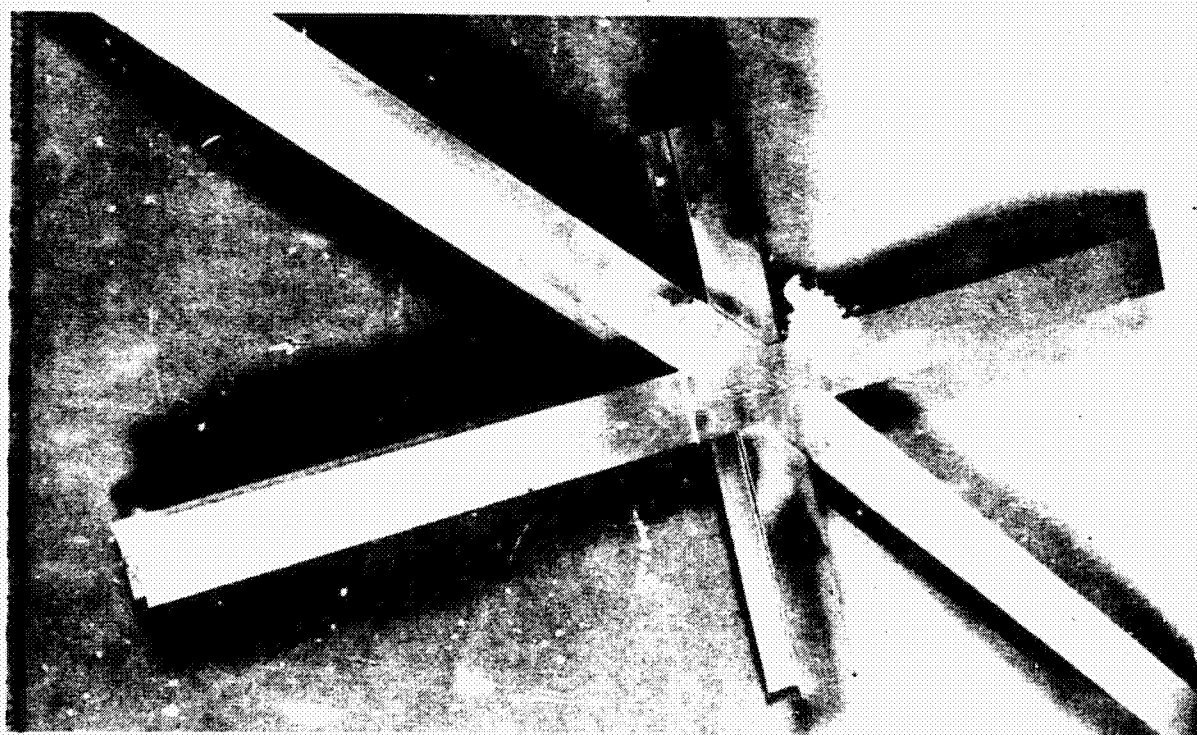


*Fig. IV-20 Aluminum Truss Joint*

block of copper was made to fit snugly between the flanges. Then, two standard vertical weld heads were used to put vertical pressure on the outside of both top and bottom doublers. In this manner, both doublers were welded at the same time.

## B. LARGE PHASE II STRUCTURES

Three of the structural concepts evaluated during Phase I were selected, in cooperation with the NASA-COR, for further evaluation in Phase II. The selected concepts, aluminum honeycomb sandwich (Alum-12), graphite/epoxy honeycomb sandwich (Type I-GR-20), and the aluminum truss were subjected to further fabrication development and structural testing on larger panels.

The selection of three concepts from those evaluated was difficult because most of them are viable candidates with each having specific advantages and disadvantages. A flow diagram of the selection process is shown in Fig. IV-21. Of the honeycomb sandwich panels with metal faceskins, the aluminum concept was selected because it has low weight potential and uses relatively inexpensive face skin material. The honeycomb sandwich designs with fibrous-composite faceskins all have similar weight potential and adequate strength. The one using all graphite faceskins (Type I-GR-20) was selected for further evaluation because it has the lowest weight potential of all designs evaluated during Phase I. The three truss concepts given consideration all have low weight potential. The aluminum truss was selected over the other two because of its lower cost and reliability. The aluminum truss was also selected over the aluminum skin/stringer/frame and the aluminum isogrid. This selection was the most difficult to make because all three of these concepts have similar advantages and disadvantages. The aluminum truss concept does have lower weight potential and was, therefore, selected for further evaluation.

The aluminum honeycomb sandwich concept uses 0.025 cm (0.010 in.) thick 2014-T6 aluminum faceskins bonded to 1.51 cm (0.595 in.) thick 1/8-5052-0.0007-3.1 aluminum hexcel core using 0.035-inch-thick FM-24 film adhesive. The graphite/epoxy honeycomb sandwich concept uses identical core and adhesive but has 0.041 cm (0.016 in.) thick, six layer graphite/epoxy faceskins. The aluminum truss concept uses basic 3.81 by 2.86 cm (1 1/2 by 1 1/8 in.) 2024-T81 aluminum tubing with 0.125 cm (0.049 in.) wall thickness. These basic tubes are chem milled to different web and flange thicknesses for the individual truss components. The joint attachment is made using doubler plates mechanically fastened with CR-2251 6-2 bulbed cherrylock rivets. A 0.010 cm (0.004 in.) thick fiberglass sheet is bonded to the inner and outer surfaces of the truss to provide meteoroid protection.

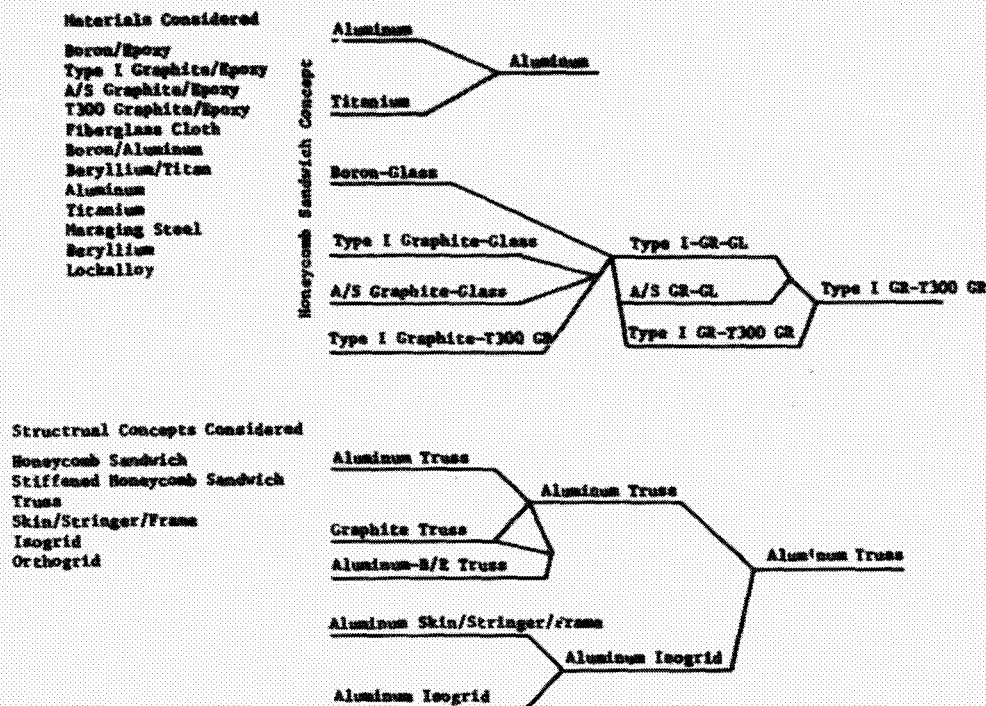


Fig. IV-21 Structural Concept Selection for Phase II Work

Three panels, a 1.83 by 0.915 m (6 by 3 ft) development panel, a 1.83 by 0.915 m (6 by 3 ft) compression test panel, and a 0.915 by 0.915 m (3 by 3 ft) shear test panel were fabricated for each of the three structural concepts. Successful test of these panels will help to verify the predicted potential of these light-weight shell concepts.

# 1. Graphite/Epoxy Honeycomb Sandwich Panels

a. *Faceskin Fabrication* - The graphite/epoxy faceskin required for the basic layup of sandwich panels is shown schematically and in a typical photomicrograph in Fig. IV-22. Layup of one of the skins during application of the fifth layer is shown in Fig. IV-23.

Care must be taken during layup to make good splices between adjacent strips of prepreg in a particular layer. Some degree of overlapping or gapping is unavoidable, however, a method of pre-cure compaction was developed during Phase II which eliminates preceivable seams or ridges in the cured faceskin.

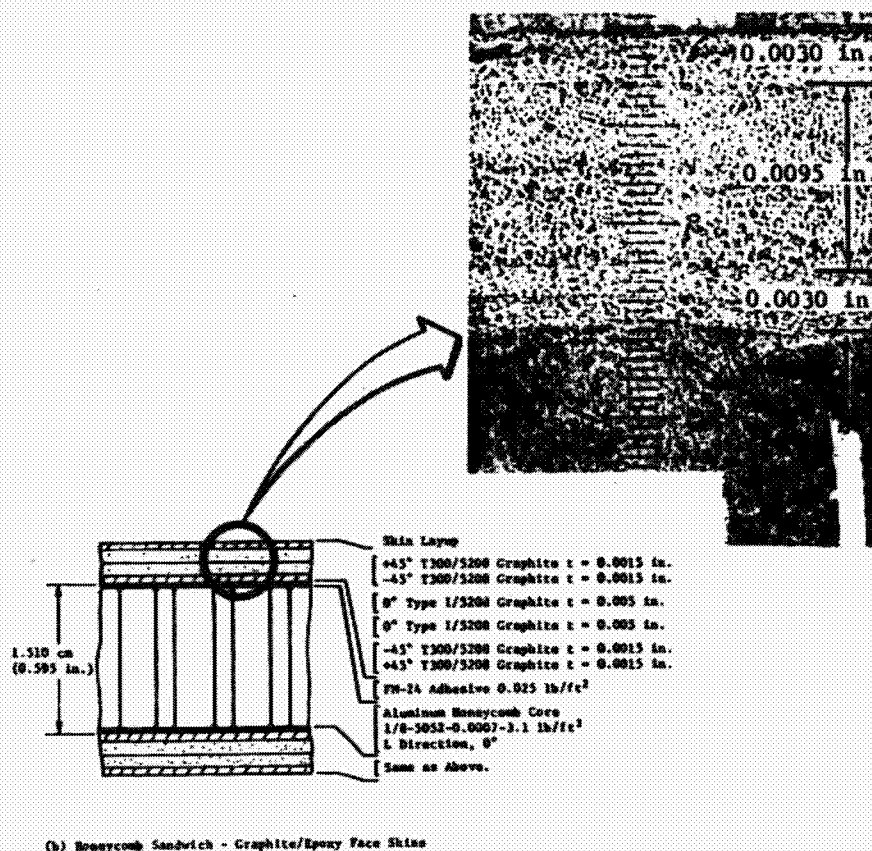


Fig. IV-22 Graphite/Epoxy Panel Configuration

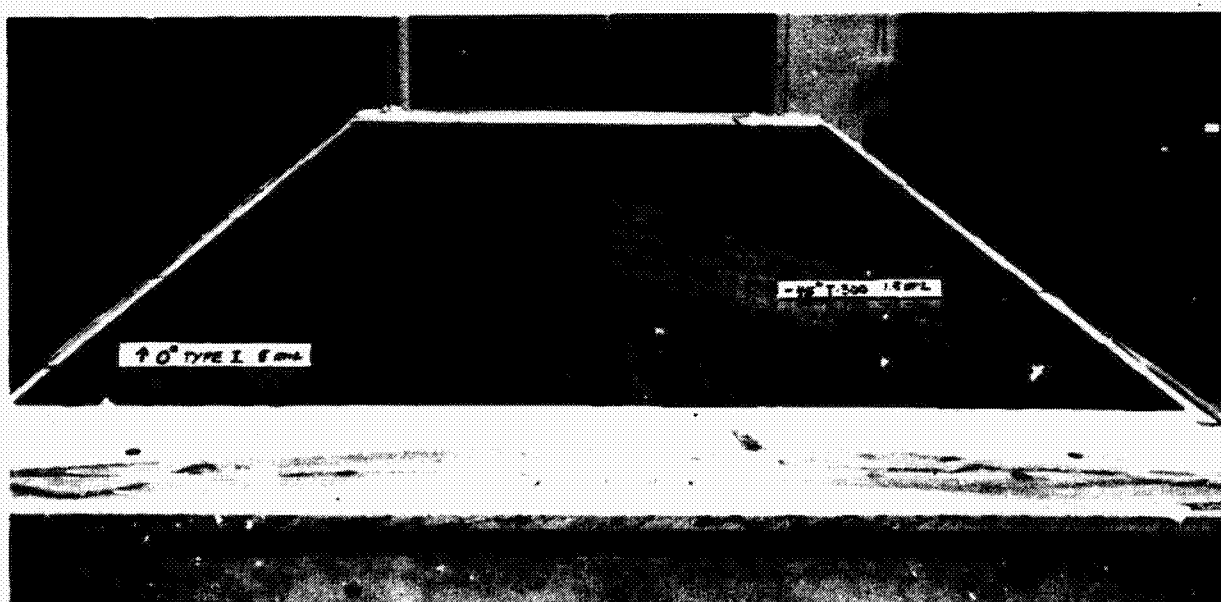
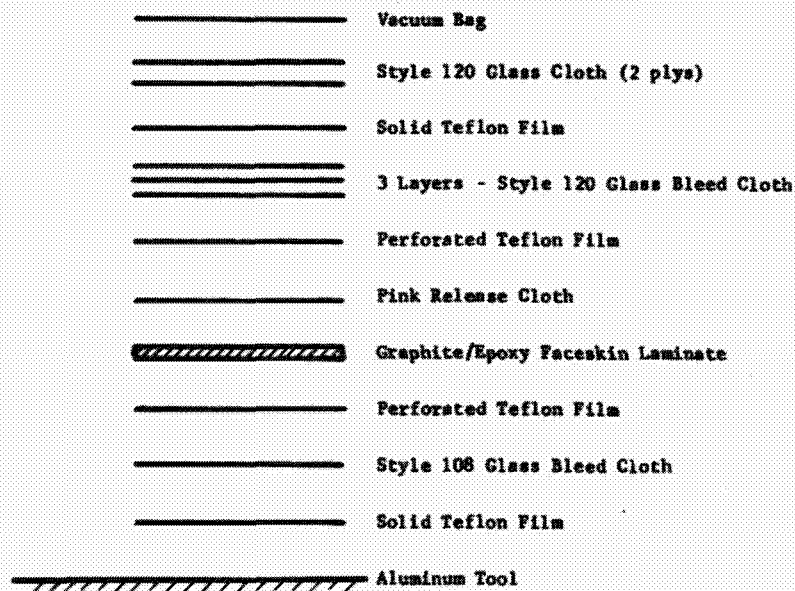


Fig. IV-23 Graphite/Epoxy Faceskin Layup



The vacuum bag system used for all graphite/epoxy faceskins is shown schematically in Fig. IV-24. Again, this system was shown to be satisfactory during Phase I development work. Prior to cure, the fully bagged part was heated in the autoclave to 180°F in 34 minutes, held for 10 minutes and immediately removed from the autoclave. The heated layup was then compacted with Teflon paddles as shown in Fig. IV-25 to remove ridges and irregularities caused during layup. The compacted part was then placed back in the autoclave and cured using the Narmco 5208 cure cycle. The desired and actual cure history of one of the graphite/epoxy faceskins is shown in Fig. IV-26. A fully cured faceskin is shown in Fig. IV-27. Pertinent data about the five fabricated graphite/epoxy faceskins are listed in Table IV-1. The average thickness of the five sheets is slightly higher than hoped for due to proportionally smaller edge resin bleed for the larger laminates.

#### Vacuum Bag System for Graphite/Epoxy Faceskins



#### Process:

1. Compaction Cycle
  - a. Vacuum bag system shown above
  - b. Full vacuum pressure
  - c. Heat to 180°F in 45 min.
  - d. Hold at 180°F for 10 min.
  - e. Remove from autoclave and hand roll  
(Note: Do not remove bag system)
2. Cure Cycle
  - a. After compaction, with same bag system, place in autoclave
  - b. Cure per NARMCO 5208 cure cycle

Fig. IV-24 Graphite/Epoxy Faceskins Vacuum Bag System

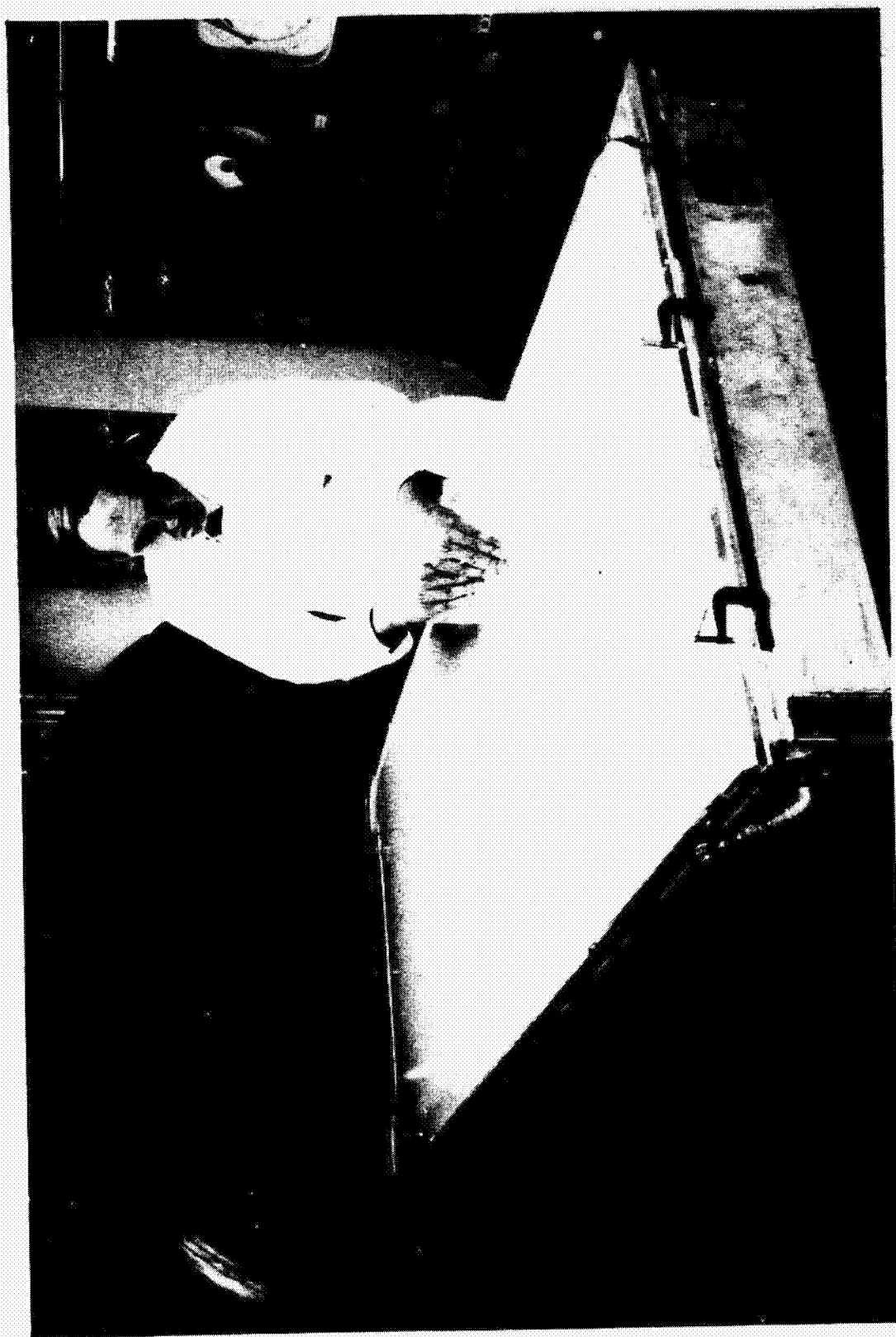


*Fig. IV-25*

*Fig. IV-25 Graphite/Epoxy Faeskin Compaction*

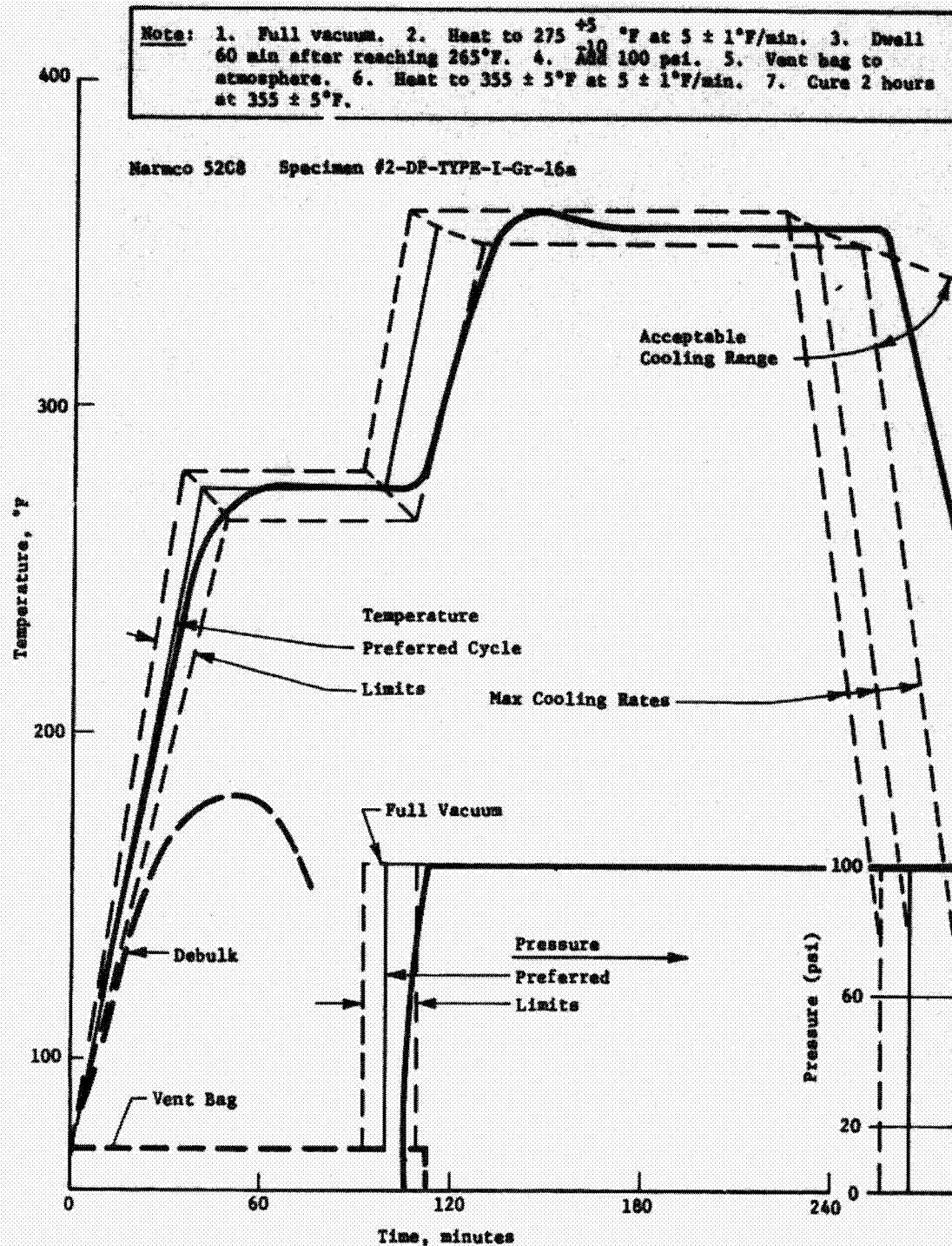


Fig. IV-26 Graphite/Epoxy Facoskin Cure Cycle



Fig. IV-27 Cured Graphite/Epoxy Faceskin

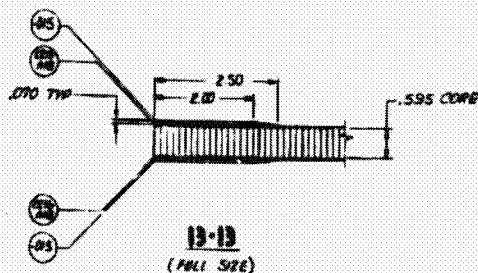
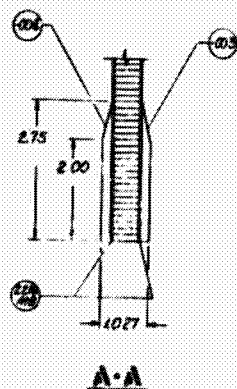
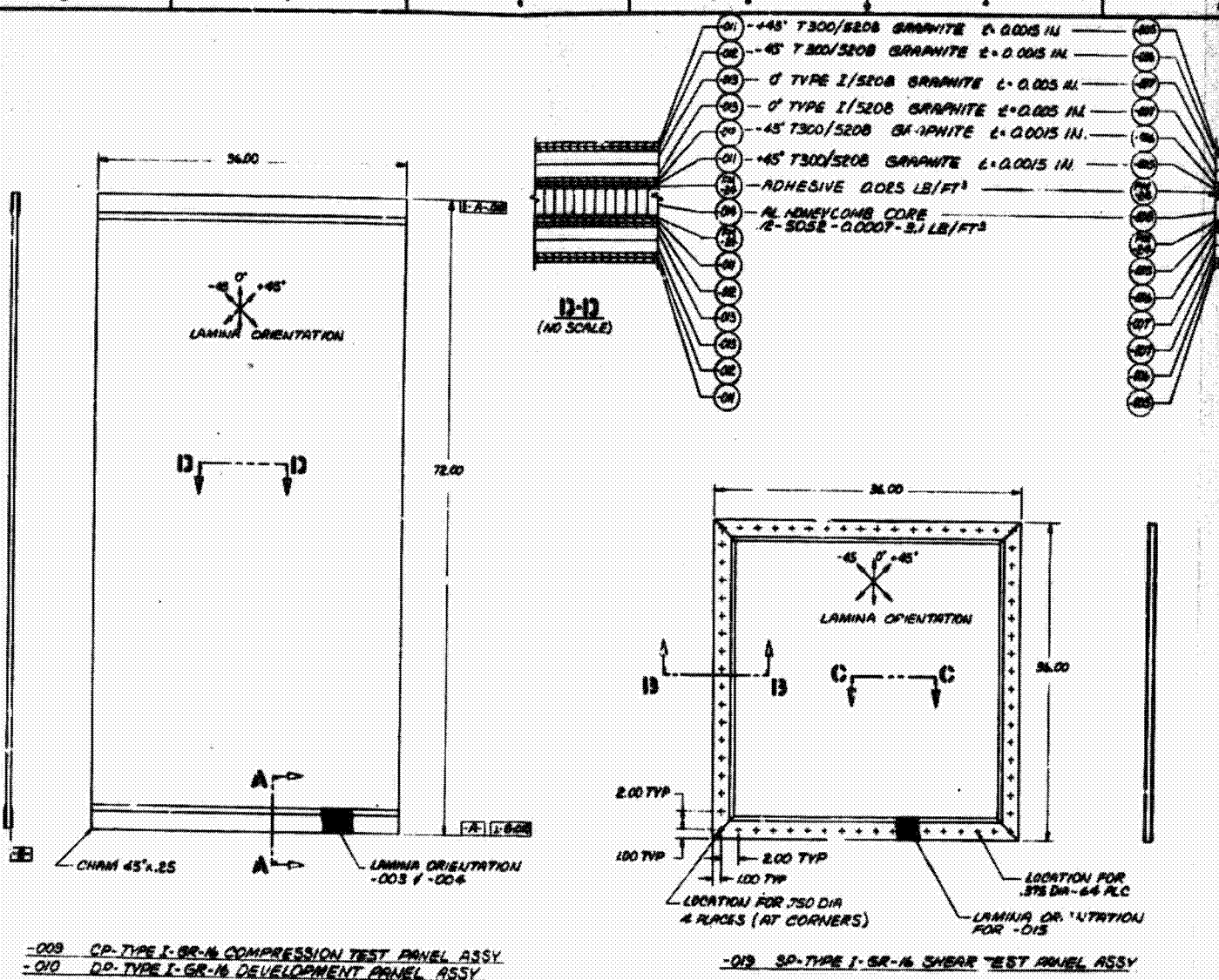
Table IV-1 Graphite/Epoxy Faceskins

Faceskin Laminate Designation	Length, cm (in.)	Width, cm (in.)	Weight, kg (lb)	Average Thickness, cm (in.)
DP-Type I-Gr-16a	187.50 (73.88)	92.30 (36.37)	—	0.046 (0.018)
DP-Type I-Gr-16B	187.50 (73.88)	92.30 (36.37)	—	0.046 (0.018)
CP-Type I-Gr-16a	187.50 (73.88)	92.30 (36.37)	1.226 (2.70)	0.046 (0.018)
CP-Type I-Gr-16b	187.50 (73.88)	92.30 (36.37)	1.260 (2.78)	0.046 (0.018)
SP-Type I-Gr-16	187.40 (73.77)	92.40 (36.34)	1.025 (2.26)	0.038 (0.015)

b. *Sandwich Panel Fabrication* - The five faceskin laminates were used in the fabrication of three honeycomb sandwich panels, a development panel (DP-Type I-Gr-16), a compression test panel (CP-Type I-Gr-16) and a shear test panel (SP-Type I-Gr-16). The fabrication drawing for these panels, include fiberglass edge reinforcement for introduction of test loads, is shown in Fig. IV-28. The vacuum bag system used for each sandwich panel is shown schematically in Fig. IV-29. It is important that the aluminum baseplate used be very flat because the final cured panel flatness will be highly dependent on tool quality. The layup tool with the top faceskin of a graphite/epoxy panel being put in place is shown in Fig. IV-30. Also shown is the autoclave used to apply pressure and temperature for panel cure. The actual and recommended cure cycle for the panel designated CP-Type I-Gr-16 is shown in Fig. IV-31. The cured panel, without fiberglass end reinforcement, is shown in Fig. IV-32. The fiberglass reinforcement for introduction of test loads was bonded to the cleaned, fully cured panel using room temperature curing epoxy adhesive. The shear test panel, SP-Type I-Gr-16, with fiberglass reinforcement in place is shown in Fig. IV-33. This test panel sustained handling damage as shown in Fig. IV-34 following panel fabrication. The damage consists of a hole in one faceskin, approximately 0.63 by 0.63 cm (0.25 by 0.25 in.) in size. Local core damage to a depth of approximately 0.25 cm (0.10 in.) was also apparent. This accidental damage provided unscheduled but interesting damage repair information on the lightweight graphite/epoxy panels. The hole was patched with a 2.74 cm (1.0 in.) square  $\pm 45^\circ$  graphite/epoxy laminate as shown in Fig. IV-34. The area to be patched was cleaned locally and room temperature curing epoxy adhesive applied to the surface and into the fractured area. The patch was then applied and allowed to cure in place under local pressure.

The average weight of the three graphite/epoxy panels fabricated was 2.32 kg/m<sup>2</sup> (0.476 lb/ft<sup>2</sup>). This is very close to what was expected based on Phase I small panel development work.

ORIGINAL PAGE IS  
OF POOR QUALITY

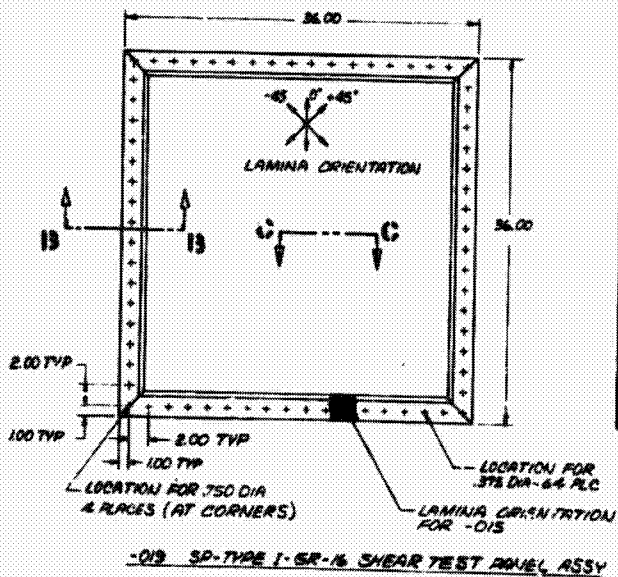
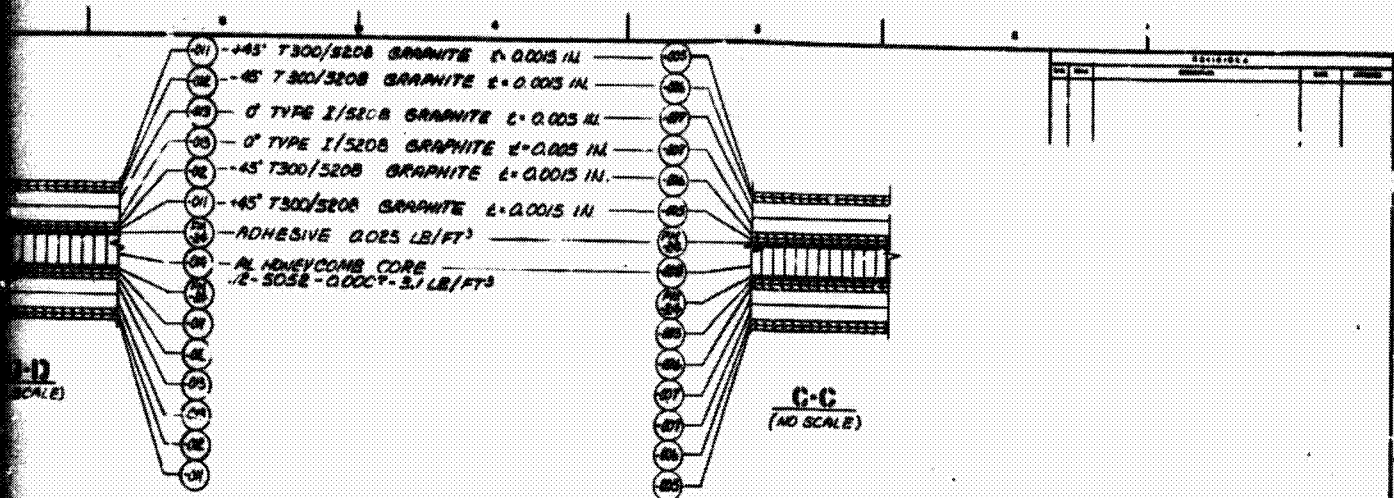


5. WHITTAKER CORP COSTA MESA, CA.
4. MELCOR CORP LOS ANGELES, CA
3. AMERICAN CYANAMIDE, MORRISVILLE, NC.
2. THALCO CO. LOS ANGELES, CA.
1. MINNESOTA MINING & MFG CO ST PAUL, MINN

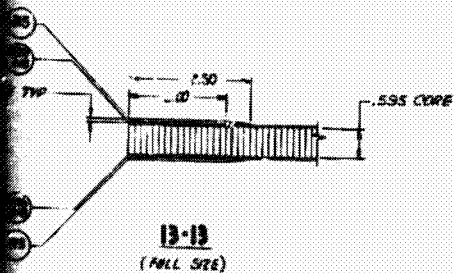
NOTES:

FOLDOUT FRAME





ORIGINAL PAGE IS  
OF POOR QUALITY



ITEM	QTY	DESCRIPTION	UNIT	REMARKS
1	1	STRIP	IN.	2.00
2	1	ADHESIVE	LB/FT²	0.025
3	1	GRAPHITE	IN.	0.0015
4	1	GRAPHITE	IN.	0.0015
5	1	GRAPHITE	IN.	0.0015
6	1	GRAPHITE	IN.	0.0015
7	1	GRAPHITE	IN.	0.0015
8	1	GRAPHITE	IN.	0.0015
9	1	GRAPHITE	IN.	0.0015
10	1	GRAPHITE	IN.	0.0015
11	1	GRAPHITE	IN.	0.0015
12	1	GRAPHITE	IN.	0.0015
13	1	GRAPHITE	IN.	0.0015
14	1	GRAPHITE	IN.	0.0015
15	1	GRAPHITE	IN.	0.0015
16	1	GRAPHITE	IN.	0.0015
17	1	GRAPHITE	IN.	0.0015
18	1	GRAPHITE	IN.	0.0015
19	1	GRAPHITE	IN.	0.0015
20	1	GRAPHITE	IN.	0.0015
21	1	GRAPHITE	IN.	0.0015
22	1	GRAPHITE	IN.	0.0015
23	1	GRAPHITE	IN.	0.0015
24	1	GRAPHITE	IN.	0.0015
25	1	GRAPHITE	IN.	0.0015
26	1	GRAPHITE	IN.	0.0015
27	1	GRAPHITE	IN.	0.0015
28	1	GRAPHITE	IN.	0.0015
29	1	GRAPHITE	IN.	0.0015
30	1	GRAPHITE	IN.	0.0015
31	1	GRAPHITE	IN.	0.0015
32	1	GRAPHITE	IN.	0.0015
33	1	GRAPHITE	IN.	0.0015
34	1	GRAPHITE	IN.	0.0015
35	1	GRAPHITE	IN.	0.0015
36	1	GRAPHITE	IN.	0.0015
37	1	GRAPHITE	IN.	0.0015
38	1	GRAPHITE	IN.	0.0015
39	1	GRAPHITE	IN.	0.0015
40	1	GRAPHITE	IN.	0.0015
41	1	GRAPHITE	IN.	0.0015
42	1	GRAPHITE	IN.	0.0015
43	1	GRAPHITE	IN.	0.0015
44	1	GRAPHITE	IN.	0.0015
45	1	GRAPHITE	IN.	0.0015
46	1	GRAPHITE	IN.	0.0015
47	1	GRAPHITE	IN.	0.0015
48	1	GRAPHITE	IN.	0.0015
49	1	GRAPHITE	IN.	0.0015
50	1	GRAPHITE	IN.	0.0015
51	1	GRAPHITE	IN.	0.0015
52	1	GRAPHITE	IN.	0.0015
53	1	GRAPHITE	IN.	0.0015
54	1	GRAPHITE	IN.	0.0015
55	1	GRAPHITE	IN.	0.0015
56	1	GRAPHITE	IN.	0.0015
57	1	GRAPHITE	IN.	0.0015
58	1	GRAPHITE	IN.	0.0015
59	1	GRAPHITE	IN.	0.0015
60	1	GRAPHITE	IN.	0.0015
61	1	GRAPHITE	IN.	0.0015
62	1	GRAPHITE	IN.	0.0015
63	1	GRAPHITE	IN.	0.0015
64	1	GRAPHITE	IN.	0.0015
65	1	GRAPHITE	IN.	0.0015
66	1	GRAPHITE	IN.	0.0015
67	1	GRAPHITE	IN.	0.0015
68	1	GRAPHITE	IN.	0.0015
69	1	GRAPHITE	IN.	0.0015
70	1	GRAPHITE	IN.	0.0015
71	1	GRAPHITE	IN.	0.0015
72	1	GRAPHITE	IN.	0.0015
73	1	GRAPHITE	IN.	0.0015
74	1	GRAPHITE	IN.	0.0015
75	1	GRAPHITE	IN.	0.0015
76	1	GRAPHITE	IN.	0.0015
77	1	GRAPHITE	IN.	0.0015
78	1	GRAPHITE	IN.	0.0015
79	1	GRAPHITE	IN.	0.0015
80	1	GRAPHITE	IN.	0.0015
81	1	GRAPHITE	IN.	0.0015
82	1	GRAPHITE	IN.	0.0015
83	1	GRAPHITE	IN.	0.0015
84	1	GRAPHITE	IN.	0.0015
85	1	GRAPHITE	IN.	0.0015
86	1	GRAPHITE	IN.	0.0015
87	1	GRAPHITE	IN.	0.0015
88	1	GRAPHITE	IN.	0.0015
89	1	GRAPHITE	IN.	0.0015
90	1	GRAPHITE	IN.	0.0015
91	1	GRAPHITE	IN.	0.0015
92	1	GRAPHITE	IN.	0.0015
93	1	GRAPHITE	IN.	0.0015
94	1	GRAPHITE	IN.	0.0015
95	1	GRAPHITE	IN.	0.0015
96	1	GRAPHITE	IN.	0.0015
97	1	GRAPHITE	IN.	0.0015
98	1	GRAPHITE	IN.	0.0015
99	1	GRAPHITE	IN.	0.0015
100	1	GRAPHITE	IN.	0.0015

Fig. IV-28 Graphite/Epoxy Sandwich Panels

FOLDOUT FRAME

IV-35 and IV-36

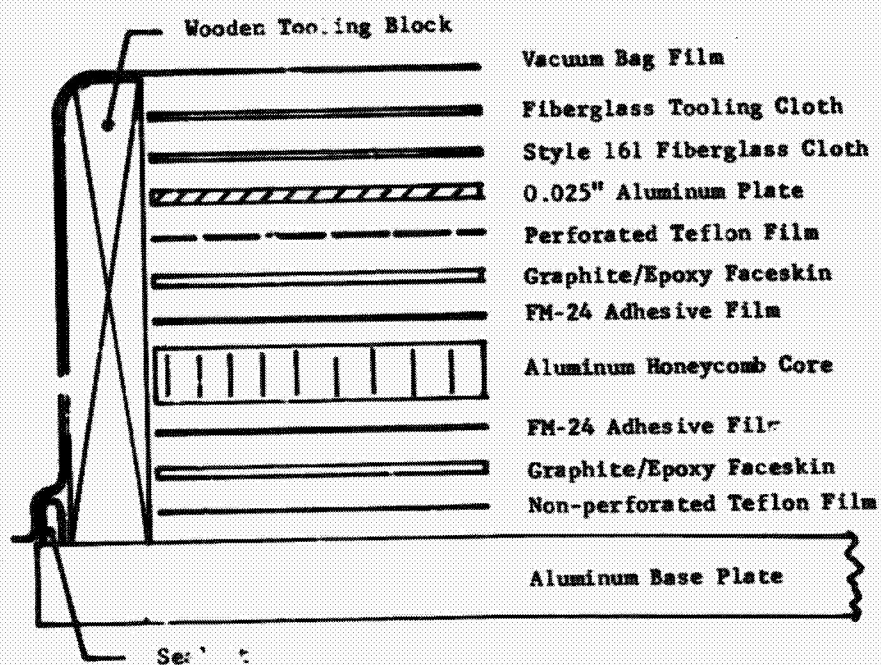


Fig. IV-29 Graphite/Epoxy Sandwich Panel Vacuum Bag System

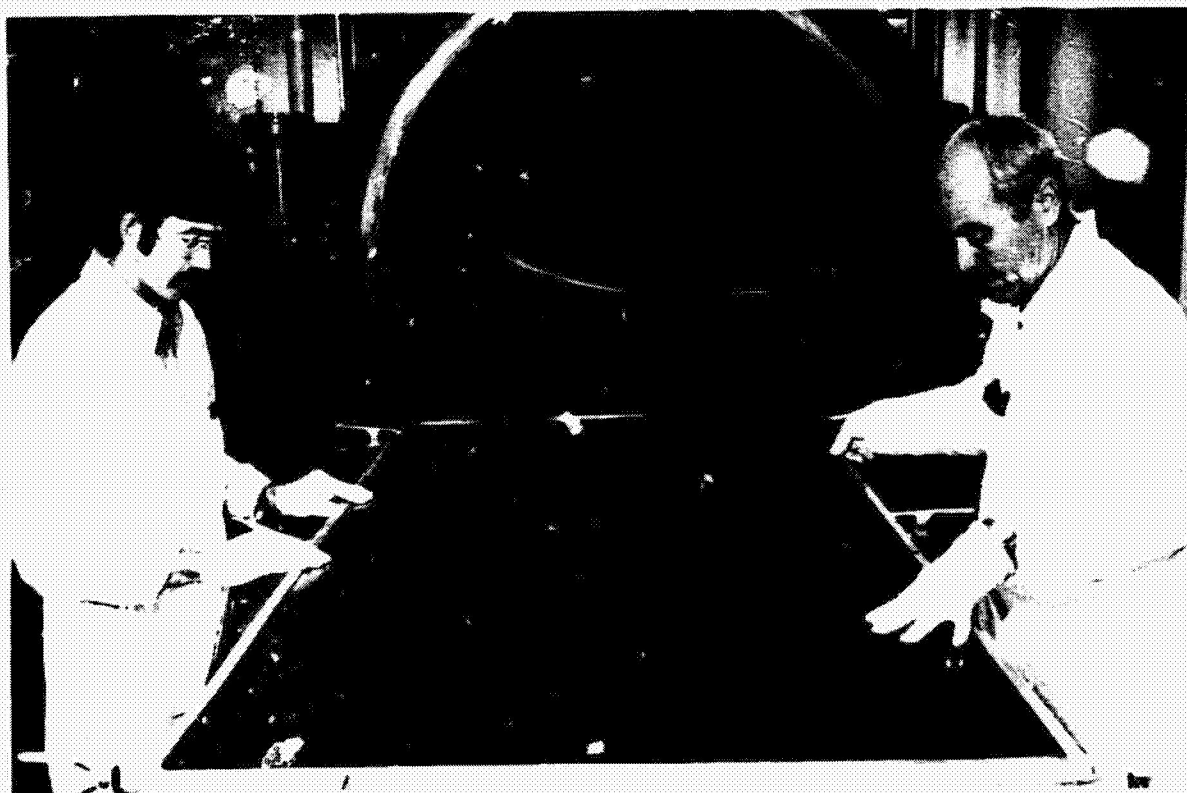


Fig. IV-30 Graphite/Epoxy Sandwich Panel Layup



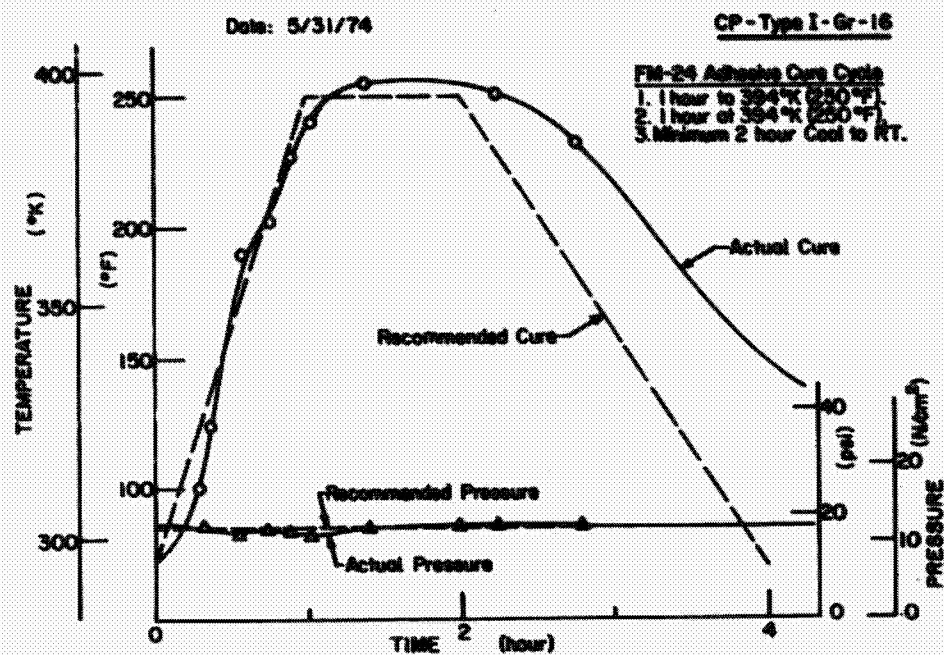


Fig. IV-31  
Cure Cycle for Graphite/Epoxy Sandwich Panel CP-Type I-Gr-16

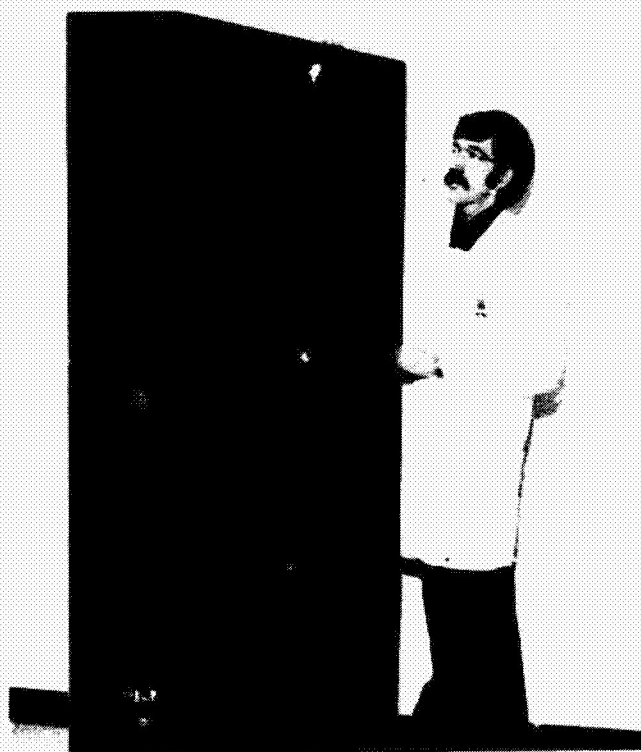


Fig. IV-32  
Graphite/Epoxy Compression Test Panel  
CP-Type I-Gr-16



Fig. IV-36

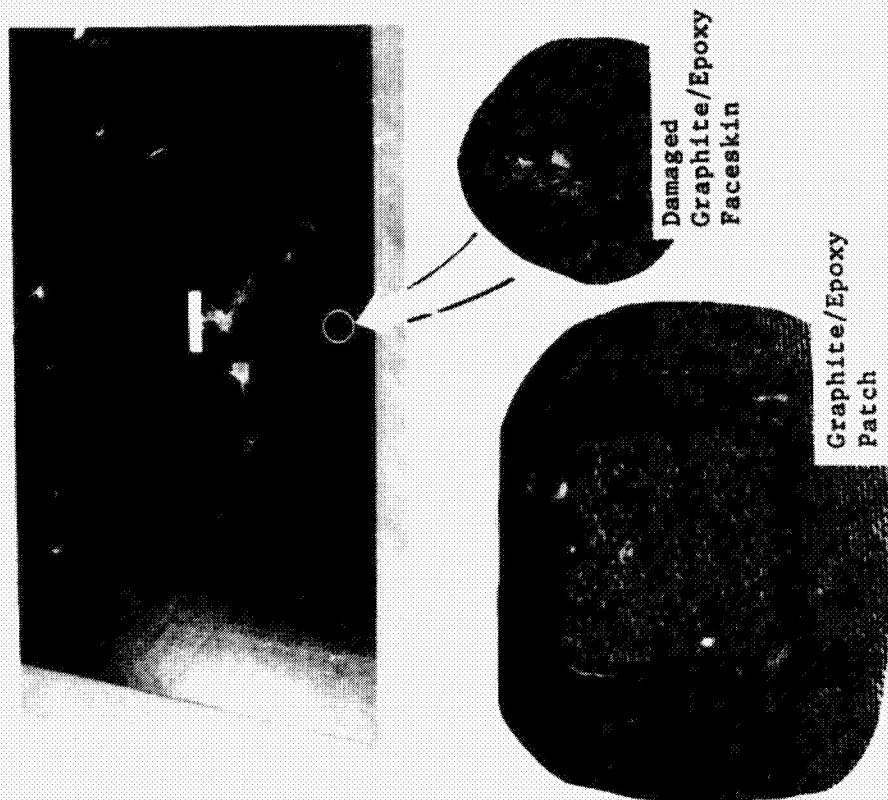


Fig. IV-34

Fig. IV-34 Shear Panel Damage and Repair

Fig. IV-33  
Graphite/Epoxy Shear Test Panel SP-Type I-Gr-16

## 2. Aluminum Honeycomb Sandwich Panels

a. *Faceskin Fabrication* - The basic panel configuration for the aluminum honeycomb concept and a typical photomicrograph of a 0.028 cm (0.011 in.) thick faceskin bonded to aluminum hexcel core is shown in Fig. IV-35. All of the faceskins for the aluminum honeycomb sandwich panels were fabricated by chemically milling 0.101 cm (0.040 in.) thick 2014-T6 aluminum sheet down to 0.025 cm (0.010 in.) with a tolerance of -0.000 and +9.005 cm (+0.002 in.) on the finished thickness. Thickness data and comments on the seven 1.83 by 0.915 m (6 by 3 ft) aluminum sheets that were chemically milled are listed in Table IV-2. Faceskins numbered 2 and 3 were used to fabricate the 1.83 by 0.915 m (6 by 3 ft) development panel. These sheets were slightly thicker than originally desired. Experience gained in chemically milling these sheets resulted in the development of techniques required to be able to meet thickness tolerances. Faceskins numbered 4 and 5 with average thickness of 0.0290 cm (0.0114 in.) were used to fabricate the (6 ft by 3 ft) panel for compression testing and number 1, with average thickness of 0.0284 cm (0.0112 in.) was used to make the 0.915 by 0.915 m (3 by 3 ft) shear test panel.

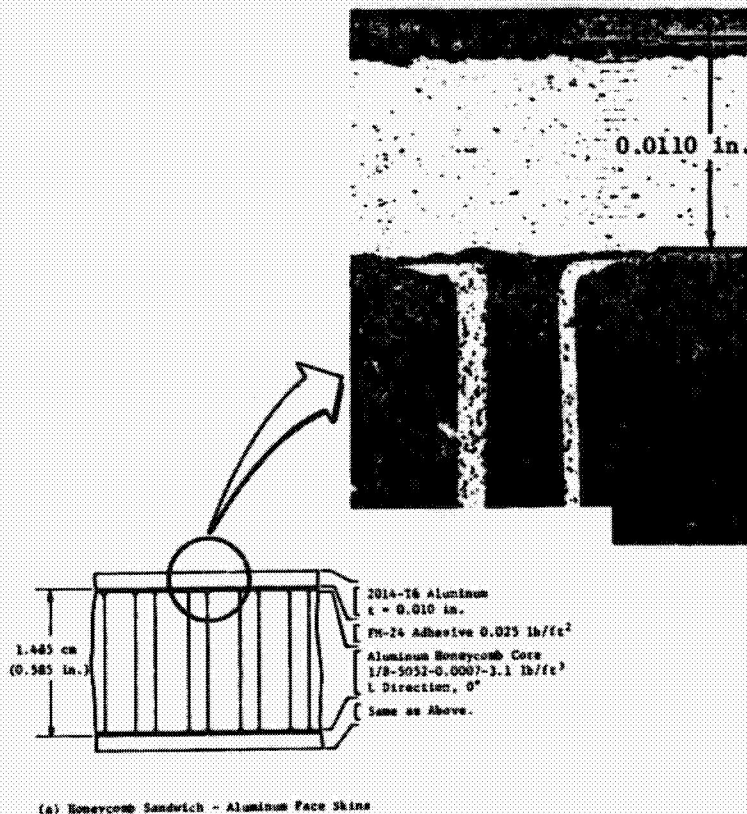


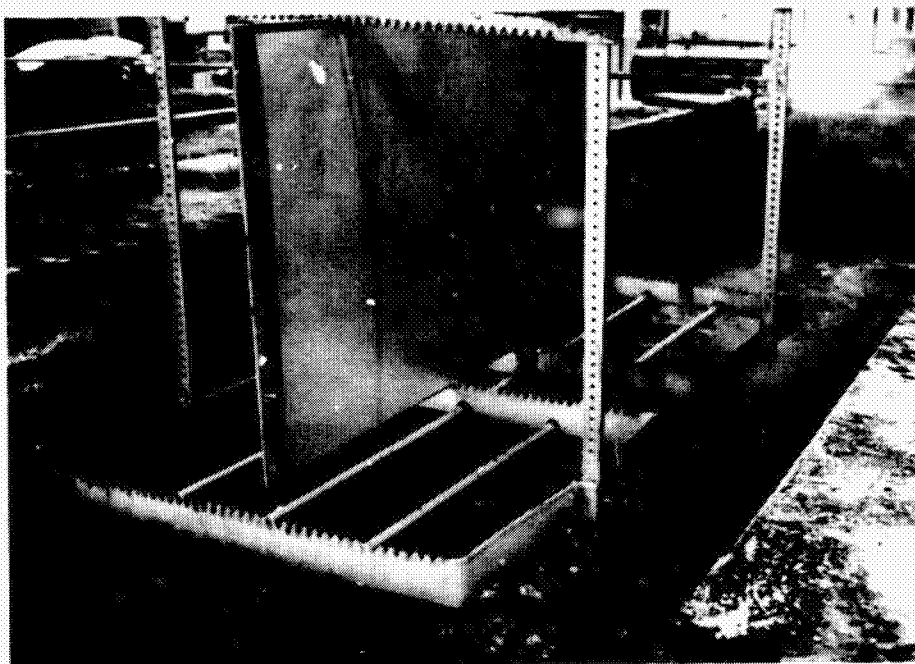
Fig. IV-35 Aluminum Panel Configuration

Table IV-2 Aluminum Faceskins

Sheet Number	Minimum Thickness, cm (in.)	Maximum Thickness, cm (in.)	Average Thickness, cm (in.)	Comments
1	0.0267 (0.0105)	0.0302 (0.0119)	0.0284 (0.0112)	Good
2	0.0292 (0.0115)	0.0340 (0.0134)	0.0307 (0.0121)	Slightly Thick
3	0.0284 (0.0112)	0.0335 (0.0132)	0.0307 (0.0121)	Slightly Thick
4	0.0269 (0.0106)	0.0300 (0.0118)	0.0290 (0.0114)	Good
5	0.0277 (0.0109)	0.0307 (0.0121)	0.0290 (0.0114)	Good
6	0.0249 (0.0098)	0.0302 (0.0115)	0.0279 (0.0110)	One Small Wrinkle
7	0.0256 (0.0101)	0.0305 (0.0120)	0.0282 (0.0111)	Two Small Wrinkles

The step-by-step fabrication process used to chemically mill the aluminum sheets was presented previously in the Interim Report. A typical panel just before being immersed in the etchant solution is shown in Fig. IV-36, and same panel immediately after removal is shown in Fig. IV-37.

Chemically milling large aluminum sheets to thin (0.010 in.) gage with reasonable finished thickness tolerance and surface quality requires that the starting blank be free of surface irregularities and have uniform thickness. The thickness tolerance on the 0.101 cm (0.040 in.) 2014-T6 aluminum sheets used was approximately  $\pm 0.0013$  cm ( $\pm 0.0005$  in.) and the chem-milled sheets had a tolerance of  $\pm 0.002$  cm ( $\pm 0.001$  in.). Thickness variation caused by chem milling is associated with etchant being in contact with the bottom portion longer than the top portion during dipping and removal operations. This effect is minimized by rotating the part after each material removal operation.



*Fig. IV-36*  
*Aluminum Sheet before Immersion into Chem-Mill*  
*Etchant Solution*

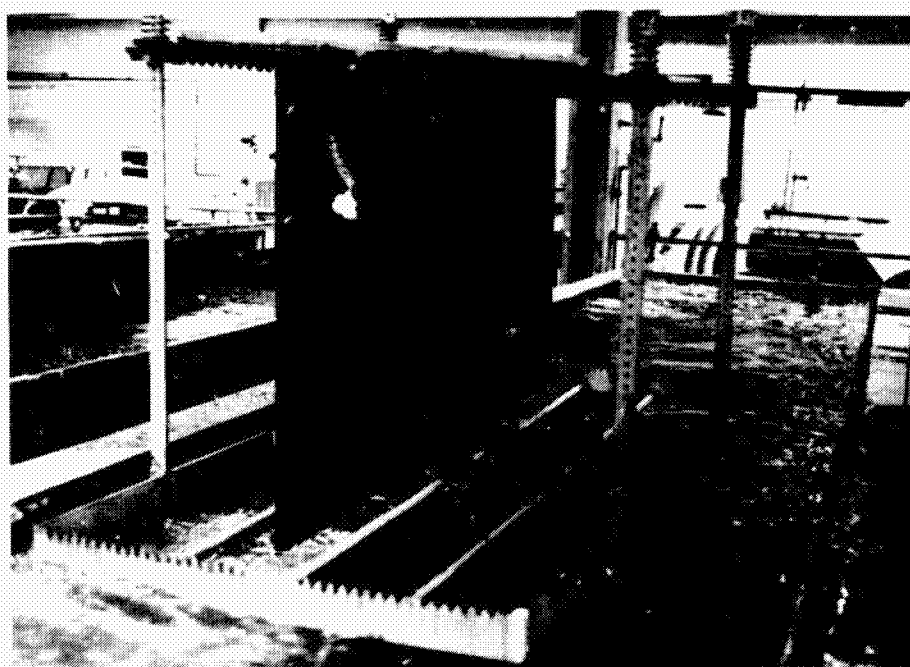
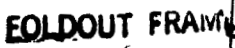


*Fig. IV-37*  
*Aluminum Sheet Being Removed from Chem-Mill*  
*Etchant Solution*

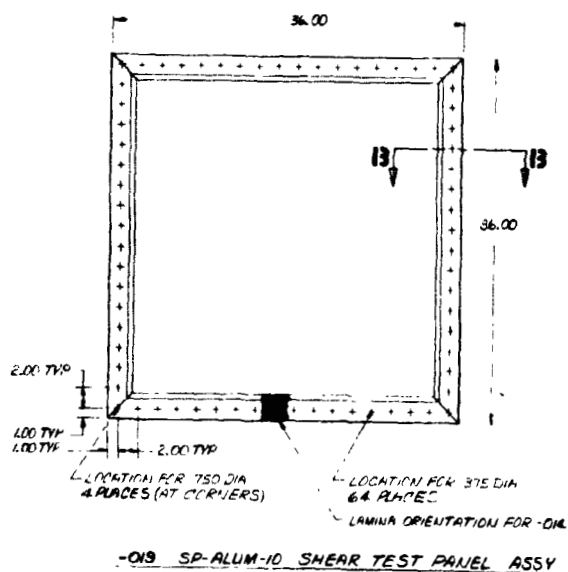
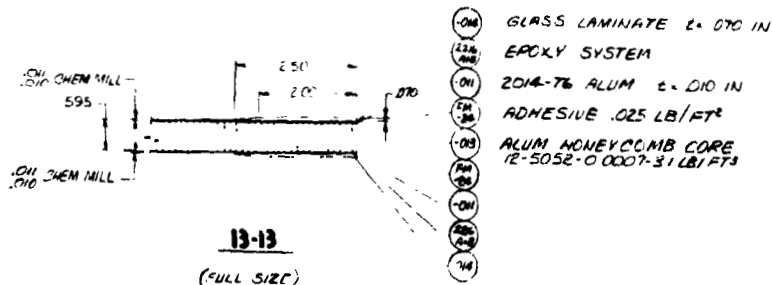


The thin aluminum sheets are very flexible and, therefore, were attached to a plywood board during the chem mill operation. The sheet is chem milled from one side with the side adjacent to the plywood board masked off to prevent etchant attack. Removing material from one rather than both sides results in better thickness control, however, it does cause some curvature of the finished skin due to release of residue stress. This curvature is not structurally degrading since it requires very little force to flatten the sheets.

b. *Sandwich Panel Fabrication* - Three aluminum sandwich panels, a development panel (DP-ALUM-10), a compression test panel (CP-ALUM-10) and a shear test panel (SP-ALUM-10), shown in Fig. IV-38 were fabricated. The development panel was fabricated using the same cure cycle and vacuum bag system as previously described for the graphite/epoxy panels. The cleaning processes used were those found to be satisfactory during Phase I work. The development panel revealed two problems that were subsequently solved. First, the midspan core splice caused a very slight but perceivable local curvature in the upper aluminum skin. This did not happen on previously fabricated graphite/epoxy panels because of their higher local faceskin stiffness. The core splice was eliminated on the compression test panel. A requirement for core splice on large panels would necessitate the use of either thicker faceskins or a local bonded on doubler. Also, the development panel exhibited more overall panel warpage that was considered desirable. This problem was solved by modifying the FM-24 panel cure cycle as shown in Fig. IV-39. The slower heat up to maximum temperature results in reduced thermal gradients and consequently flatter finished panels. The compression test panel and the shear test panel were cured using this modified cure cycle. The maximum out of flatness dimension was reduced from 0.152 cm (0.060 in.) on the development panel to 0.023 cm (0.009 in.) on the compression test panel. The average measured weight of the three aluminum sandwich panels, without end attachment capability, was 2.52 kg/in.<sup>2</sup> (0.516 lb/ft<sup>2</sup>). This is a typical panel weight for 0.025 cm (0.010 in.) minimum gage aluminum and  $\pm 0.0025$  cm ( $\pm 0.001$  in.) chem-mill tolerance. The finished compression and shear test panels are shown in Fig. IV-40 and IV-41, respectively



ORIGINAL PAGE IS  
OF POOR QUALITY



ORIGINAL PAGE IS  
OF POOR QUALITY

ITEM	QUANTITY	DESCRIPTION	UNIT	REMARKS
018	1	SP-ALUM-10 SHEAR TEST PANEL ASSY	EA	
019	1	SP-ALUM-10 SHEAR TEST PANEL ASSY	EA	
020	1	SP-ALUM-10 SHEAR TEST PANEL ASSY	EA	
021	1	SP-ALUM-10 SHEAR TEST PANEL ASSY	EA	
022	1	SP-ALUM-10 SHEAR TEST PANEL ASSY	EA	
023	1	SP-ALUM-10 SHEAR TEST PANEL ASSY	EA	
024	1	SP-ALUM-10 SHEAR TEST PANEL ASSY	EA	
025	1	SP-ALUM-10 SHEAR TEST PANEL ASSY	EA	
026	1	SP-ALUM-10 SHEAR TEST PANEL ASSY	EA	
027	1	SP-ALUM-10 SHEAR TEST PANEL ASSY	EA	
028	1	SP-ALUM-10 SHEAR TEST PANEL ASSY	EA	
029	1	SP-ALUM-10 SHEAR TEST PANEL ASSY	EA	
030	1	SP-ALUM-10 SHEAR TEST PANEL ASSY	EA	
031	1	SP-ALUM-10 SHEAR TEST PANEL ASSY	EA	
032	1	SP-ALUM-10 SHEAR TEST PANEL ASSY	EA	
033	1	SP-ALUM-10 SHEAR TEST PANEL ASSY	EA	
034	1	SP-ALUM-10 SHEAR TEST PANEL ASSY	EA	
035	1	SP-ALUM-10 SHEAR TEST PANEL ASSY	EA	
036	1	SP-ALUM-10 SHEAR TEST PANEL ASSY	EA	
037	1	SP-ALUM-10 SHEAR TEST PANEL ASSY	EA	
038	1	SP-ALUM-10 SHEAR TEST PANEL ASSY	EA	
039	1	SP-ALUM-10 SHEAR TEST PANEL ASSY	EA	
040	1	SP-ALUM-10 SHEAR TEST PANEL ASSY	EA	
041	1	SP-ALUM-10 SHEAR TEST PANEL ASSY	EA	
042	1	SP-ALUM-10 SHEAR TEST PANEL ASSY	EA	
043	1	SP-ALUM-10 SHEAR TEST PANEL ASSY	EA	
044	1	SP-ALUM-10 SHEAR TEST PANEL ASSY	EA	
045	1	SP-ALUM-10 SHEAR TEST PANEL ASSY	EA	
046	1	SP-ALUM-10 SHEAR TEST PANEL ASSY	EA	
047	1	SP-ALUM-10 SHEAR TEST PANEL ASSY	EA	
048	1	SP-ALUM-10 SHEAR TEST PANEL ASSY	EA	
049	1	SP-ALUM-10 SHEAR TEST PANEL ASSY	EA	
050	1	SP-ALUM-10 SHEAR TEST PANEL ASSY	EA	
051	1	SP-ALUM-10 SHEAR TEST PANEL ASSY	EA	
052	1	SP-ALUM-10 SHEAR TEST PANEL ASSY	EA	
053	1	SP-ALUM-10 SHEAR TEST PANEL ASSY	EA	
054	1	SP-ALUM-10 SHEAR TEST PANEL ASSY	EA	
055	1	SP-ALUM-10 SHEAR TEST PANEL ASSY	EA	
056	1	SP-ALUM-10 SHEAR TEST PANEL ASSY	EA	
057	1	SP-ALUM-10 SHEAR TEST PANEL ASSY	EA	
058	1	SP-ALUM-10 SHEAR TEST PANEL ASSY	EA	
059	1	SP-ALUM-10 SHEAR TEST PANEL ASSY	EA	
060	1	SP-ALUM-10 SHEAR TEST PANEL ASSY	EA	
061	1	SP-ALUM-10 SHEAR TEST PANEL ASSY	EA	
062	1	SP-ALUM-10 SHEAR TEST PANEL ASSY	EA	
063	1	SP-ALUM-10 SHEAR TEST PANEL ASSY	EA	
064	1	SP-ALUM-10 SHEAR TEST PANEL ASSY	EA	
065	1	SP-ALUM-10 SHEAR TEST PANEL ASSY	EA	
066	1	SP-ALUM-10 SHEAR TEST PANEL ASSY	EA	
067	1	SP-ALUM-10 SHEAR TEST PANEL ASSY	EA	
068	1	SP-ALUM-10 SHEAR TEST PANEL ASSY	EA	
069	1	SP-ALUM-10 SHEAR TEST PANEL ASSY	EA	
070	1	SP-ALUM-10 SHEAR TEST PANEL ASSY	EA	
071	1	SP-ALUM-10 SHEAR TEST PANEL ASSY	EA	
072	1	SP-ALUM-10 SHEAR TEST PANEL ASSY	EA	
073	1	SP-ALUM-10 SHEAR TEST PANEL ASSY	EA	
074	1	SP-ALUM-10 SHEAR TEST PANEL ASSY	EA	
075	1	SP-ALUM-10 SHEAR TEST PANEL ASSY	EA	
076	1	SP-ALUM-10 SHEAR TEST PANEL ASSY	EA	
077	1	SP-ALUM-10 SHEAR TEST PANEL ASSY	EA	
078	1	SP-ALUM-10 SHEAR TEST PANEL ASSY	EA	
079	1	SP-ALUM-10 SHEAR TEST PANEL ASSY	EA	
080	1	SP-ALUM-10 SHEAR TEST PANEL ASSY	EA	
081	1	SP-ALUM-10 SHEAR TEST PANEL ASSY	EA	
082	1	SP-ALUM-10 SHEAR TEST PANEL ASSY	EA	
083	1	SP-ALUM-10 SHEAR TEST PANEL ASSY	EA	
084	1	SP-ALUM-10 SHEAR TEST PANEL ASSY	EA	
085	1	SP-ALUM-10 SHEAR TEST PANEL ASSY	EA	
086	1	SP-ALUM-10 SHEAR TEST PANEL ASSY	EA	
087	1	SP-ALUM-10 SHEAR TEST PANEL ASSY	EA	
088	1	SP-ALUM-10 SHEAR TEST PANEL ASSY	EA	
089	1	SP-ALUM-10 SHEAR TEST PANEL ASSY	EA	
090	1	SP-ALUM-10 SHEAR TEST PANEL ASSY	EA	
091	1	SP-ALUM-10 SHEAR TEST PANEL ASSY	EA	
092	1	SP-ALUM-10 SHEAR TEST PANEL ASSY	EA	
093	1	SP-ALUM-10 SHEAR TEST PANEL ASSY	EA	
094	1	SP-ALUM-10 SHEAR TEST PANEL ASSY	EA	
095	1	SP-ALUM-10 SHEAR TEST PANEL ASSY	EA	
096	1	SP-ALUM-10 SHEAR TEST PANEL ASSY	EA	
097	1	SP-ALUM-10 SHEAR TEST PANEL ASSY	EA	
098	1	SP-ALUM-10 SHEAR TEST PANEL ASSY	EA	
099	1	SP-ALUM-10 SHEAR TEST PANEL ASSY	EA	
100	1	SP-ALUM-10 SHEAR TEST PANEL ASSY	EA	

Fig. IV-38 Aluminum Sandwich Panels

FOOTNOT FRAME

IV-45 and IV-46

PRECEDING PAGE BLANK NOT FILMED



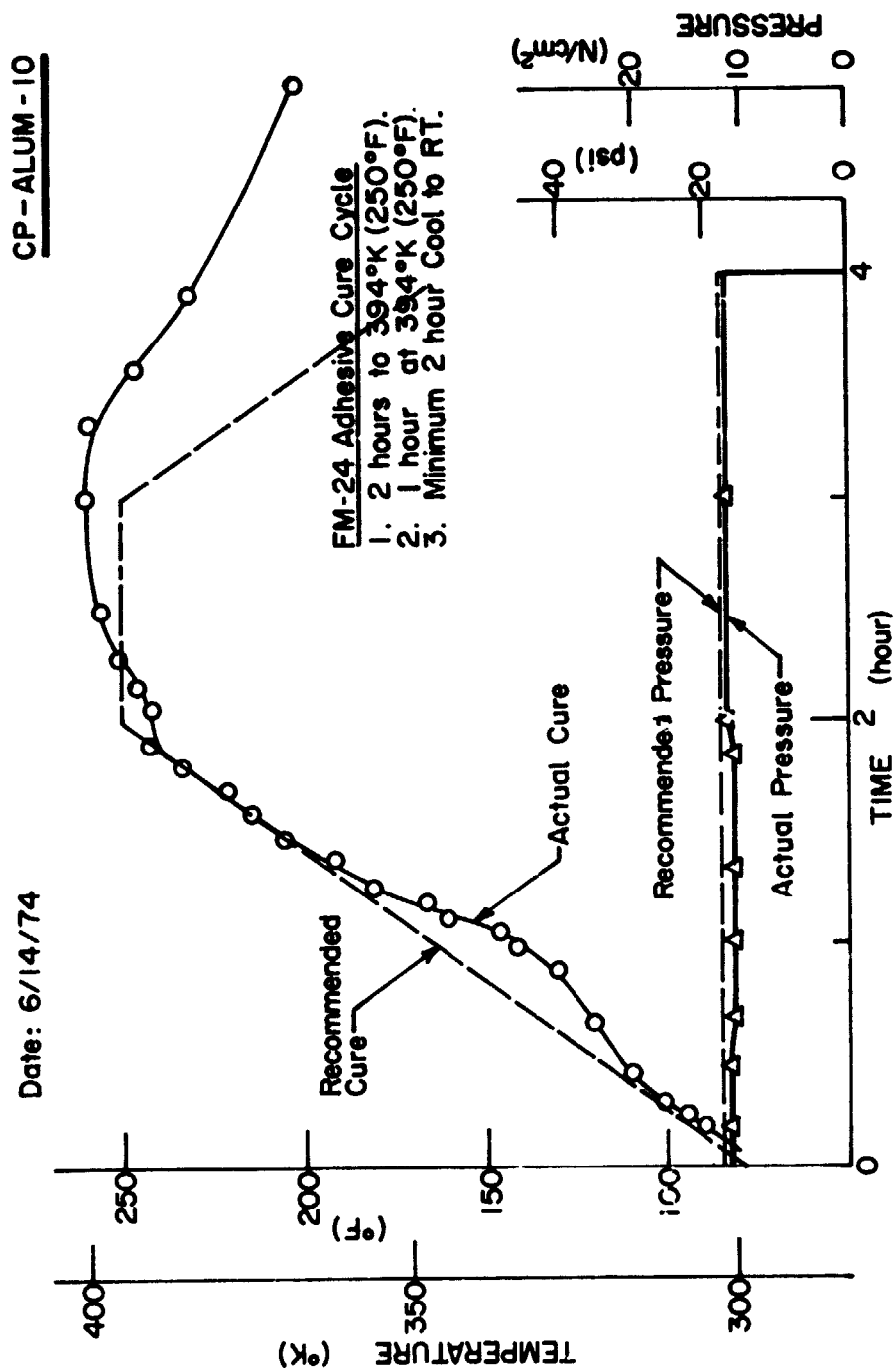


Fig. IV-35

Fig. IV-39 Modified FM-24 Cure Cycle for Aluminum Sandwich Panels

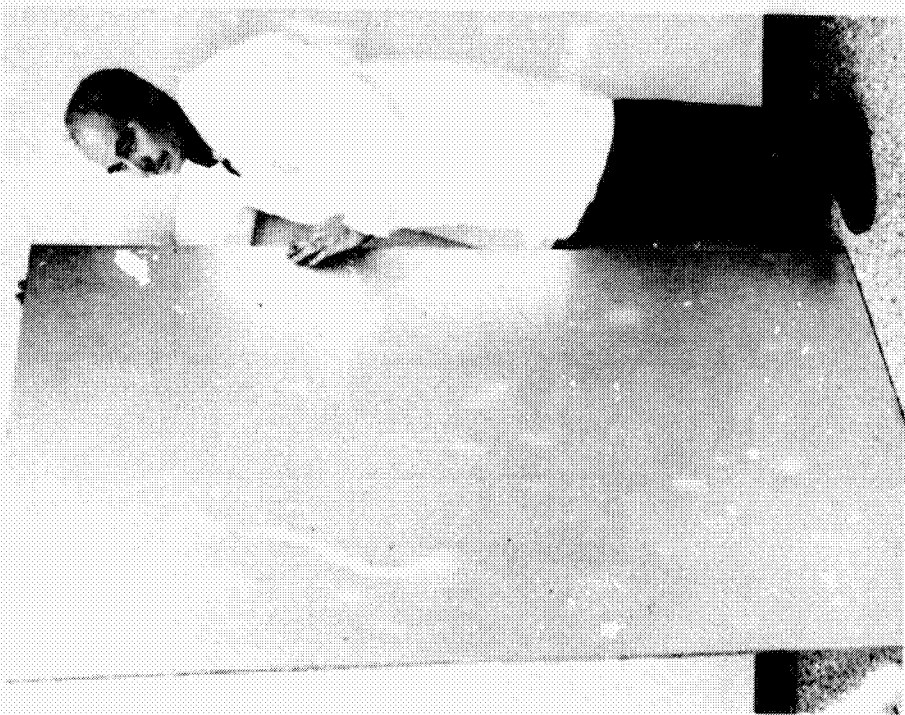


Fig. IV-40  
IV-48

Fig. IV-40  
Aluminum Sandwich Compression Panel  
CP-Alum-10

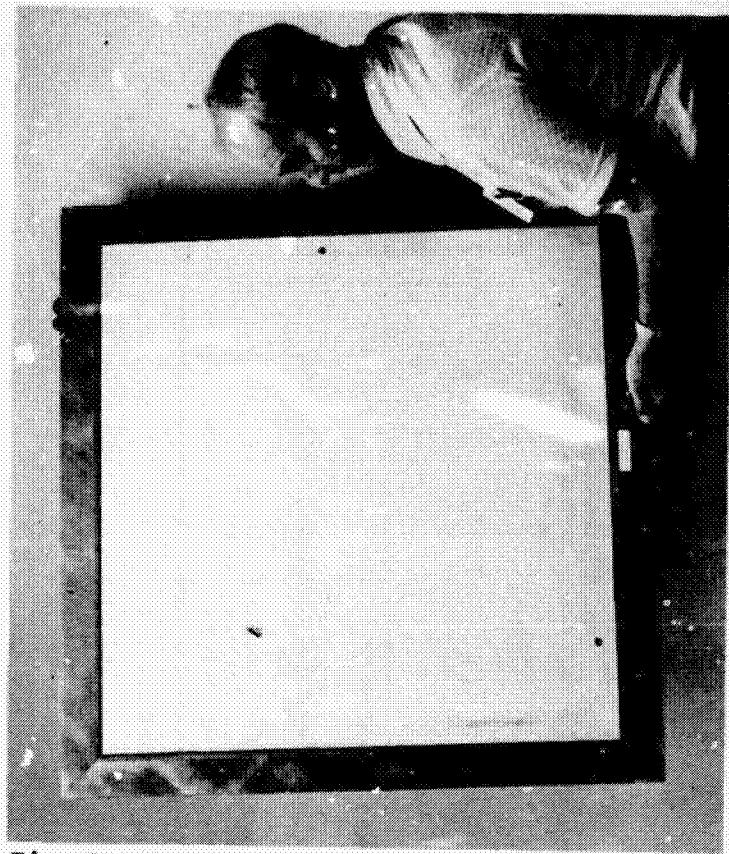


Fig. IV-41

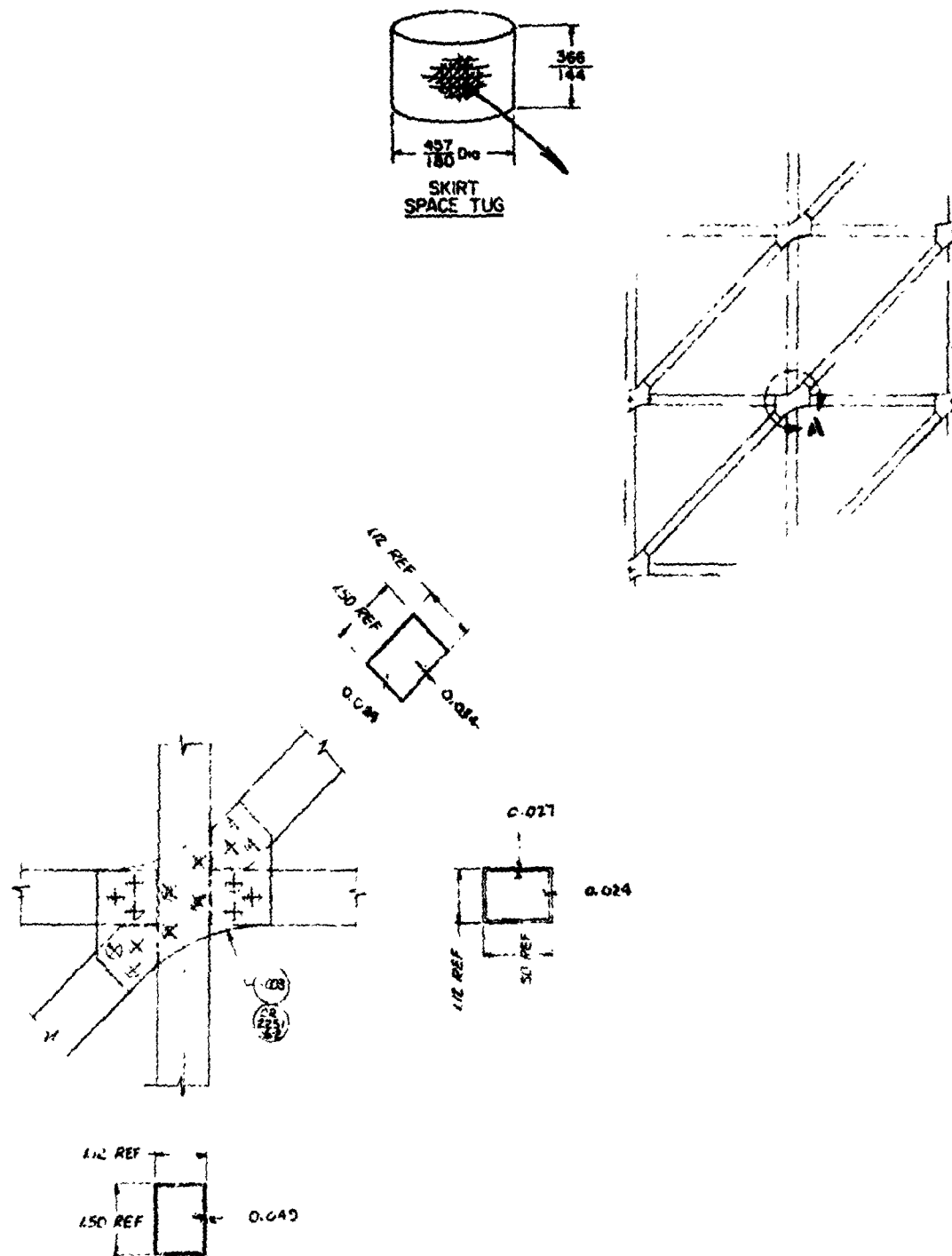
Fig. IV-41 Aluminum Sandwich Shear Panel SP-Alum-10

### 3. Aluminum Truss Fabrication

The aluminum truss configuration shown in Fig. IV-42 contains tubular aluminum truss members mechanically fastened at the joints using doubler plates and blind cherry rivet fasteners. The inner and outer surfaces of the truss are covered with thin (0.010 cm) fiberglass cloth sheets to provide meteoroid protection. The flanges and webs of the truss horizontal and diagonal members are chemically milled to final dimensions. A set of detailed drawings was used during fabrication of three truss sections. The three components are a development panel (DP-ALUM-Truss), a compression test panel (CP-Alum-Truss) and a shear test panel (SP-Alum-Truss). Basic truss components are vertical stringers, selectively chem-milled horizontal frames and diagonal stiffeners, joint doubler plates and blind cherrylock rivets.

a. *Detail Fabrication* - The aluminum doubler plates were made from 0.127 cm (0.050 in.) thick 2014-T6 aluminum alloy. Doublers were laid out by hand, cut and filed to size. Then one of each type was used as a drill template. Pilot holes (0.040 in. diameter) were drilled into the template. The remaining doublers were stacked with the template on top, clamped and drilled.

All tubular details were initially cut 0.25 in. oversize. The vertical stringer tubes were simply trimmed at the ends to final size. The horizontal and diagonal members that required chem-milling were given a flash etch in an alkaline solution, water rinsed, submersed in an iridite solution for 10 minutes, water rinsed and wiped dry. Each tube was then plugged at one end with a silicone rubber plug that was expanded, once inside the tube, by compressing with two wing nuts on threaded rod. A silicone rubber plug with a stainless steel vent tube sealed the other end and was held in place with lead tape. The sealed tubes were individually dipped into a commercially available maskant solution (organoceram) that was thinned with xylene. Depending on the thickness of the maskant, two or three coats produced a fully covered tube. Using a template, maskant on the sides to be chem-milled the deepest was cut away. A four tube assembly was mounted in a stainless steel fixture as shown in Fig. IV-43, before chem milling. The tubes and fixture were immersed into the alkaline solution at 358K (185°F) and two sides of each tube chem milled. The chem milling rate was approximately 0.0013 in./minute (0.005 in./minute). The vent tubes provided an escape route for the hot, expanding air inside the tubes. Thickness was checked periodically during chem milling, and when a thickness was reached equalling the difference in thickness between the two sides, the maskant on the final two sides was cut away. Chem milling proceeded on all four sides until the desired chem mill depth was reached. The chem-milled details showed a smooth fillet from the chem milled area into the original surface. A shallow, rounded ridge ran lengthwise at the tube corners separating the sides of the tube.



DETAIL A

Fig. IV-42 Aluminum Truss Configuration

ORIGINAL PAGE IS  
OF POOR QUALITY

The chem milled tube details were then cut to final size as shown in Fig. IV-44. All tubes details were aged to the -T81 condition at  $433 \pm 5K$  ( $320 \pm 10^{\circ}F$ ) for 18 hr.

b. *Panel Assembly* - The panel assembly tool was simply a modified mill cutting table which provided a flat surface and a means of securing detail parts prior to attachment. The doublers at the ends of each long vertical stringer member were first attached using a weld bond technique. This process involved spot welding through a thin layer of adhesive to produce a high strength light-weight joint. Each end of the tube was first abrasively cleaned and wiped with a solvent, on both the inside and outside. The adhesive (Hysol ADX-347) was applied to the outside of each tube on both sides. Both doublers for that joint were positioned and clamped in place. The spot welding was then performed as shown in Fig. IV-45 on both doublers at once using a corner bar machined to fit the inside of the tube. The vertical members, stringers, were next aligned in the fixture and clamped in place. The four horizontal end details were aligned with the doublers on the stringers, clamped in place and riveted. The remaining details were positioned, clamped in place and riveted. To ensure proper fit-up between tube details, doublers and rivets, each end of each tube was marked in pencil with a centerline and two parallel guidelines 0.508 cm (0.200 in.) from the side of the tube. Once the tube was positioned properly and clamped, the lines could be seen through the pilot holes in the doubler. The doubler was moved so that the middle pilot hole was centered on the center line and the outer two holes were between the two parallel side lines. In this way the as-fastened rivet did not extend onto the corner radius. Once the doublers were fitted to a joint, pilot holes were drilled through the doubler into the tube detail part. When enough holes were drilled to secure the doubler in place, "clicco" clamps were inserted and the remaining pilot holes drilled. The next step was to drill full size holes 0.510 cm (0.201 in.) in diameter, insert large "cliccos", removing the smaller ones, and finish drilling all holes (Fig. IV-46). The doubler was then removed and all holes finished to size using a 0.520 cm (0.205 in.) reamer. The holes were deburred and the surfaces cleaned. The doubler was repositioned using the large "cliccos" and the rivets attached. The panel was then taken out of the fixture and turned to rivet the opposite side. The panel was shimmed in the fixture as shown in Fig. IV-47 so that the rivet heads did not touch the assembly table. The same procedure was used to finish the second side. The completed panel was wiped with a solvent and the adhesive cured in an oven at  $250^{\circ}F$  for 1 hr. The compression test panel without fiberglass meteoroid protection layers is shown in Fig. IV-48.

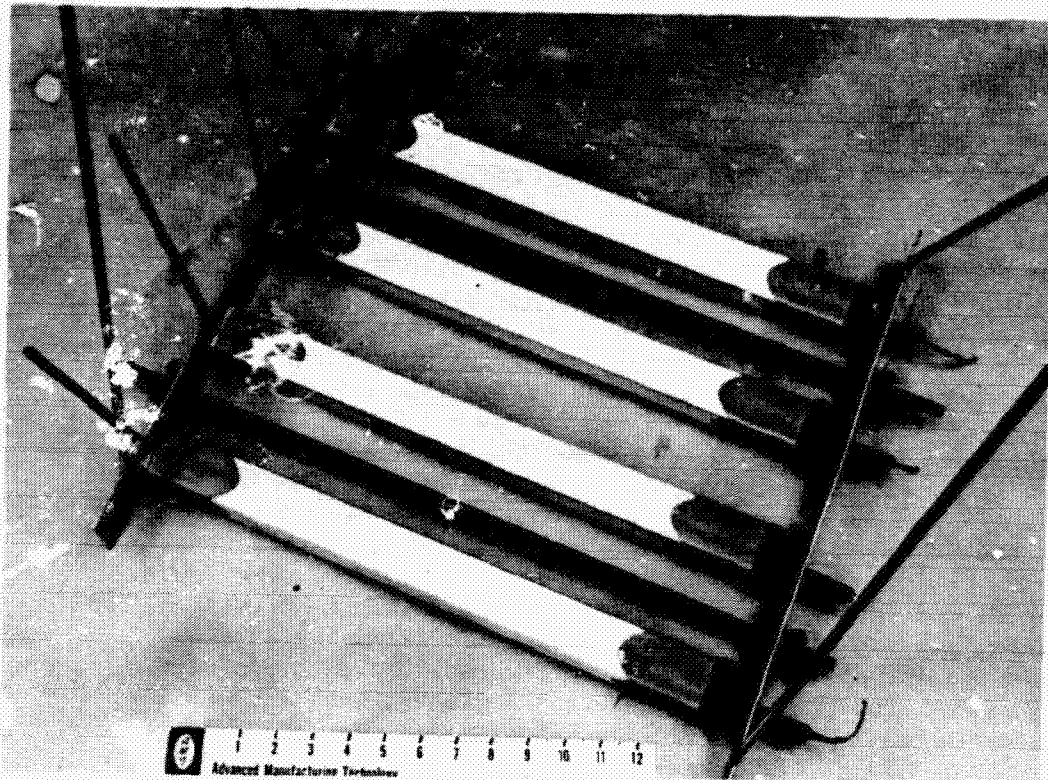


Fig. IV-43 Aluminum Truss Component Chem Milling

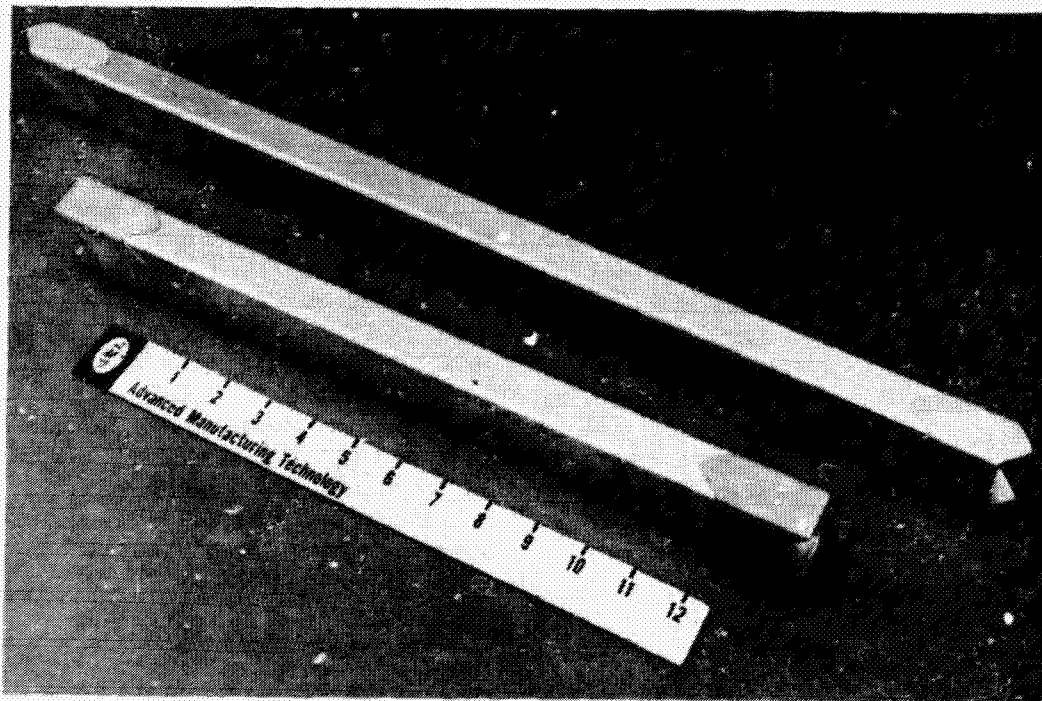


Fig. IV-44 Aluminum Truss Members

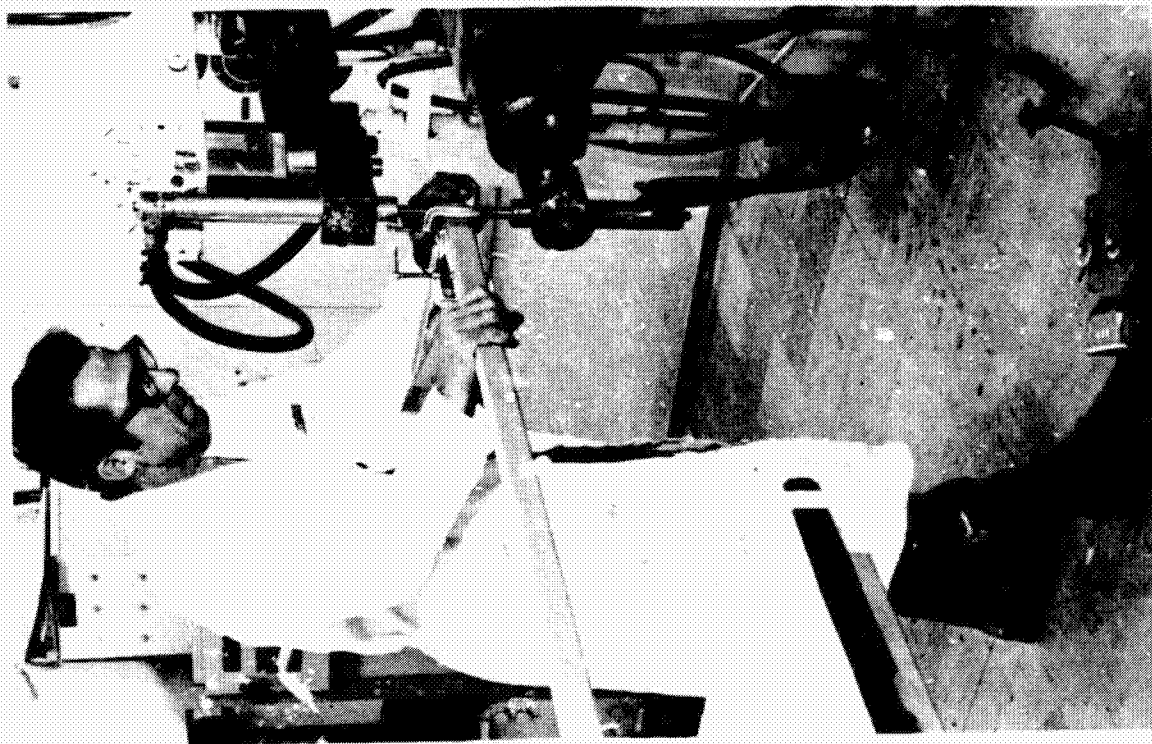


Fig. IV-45

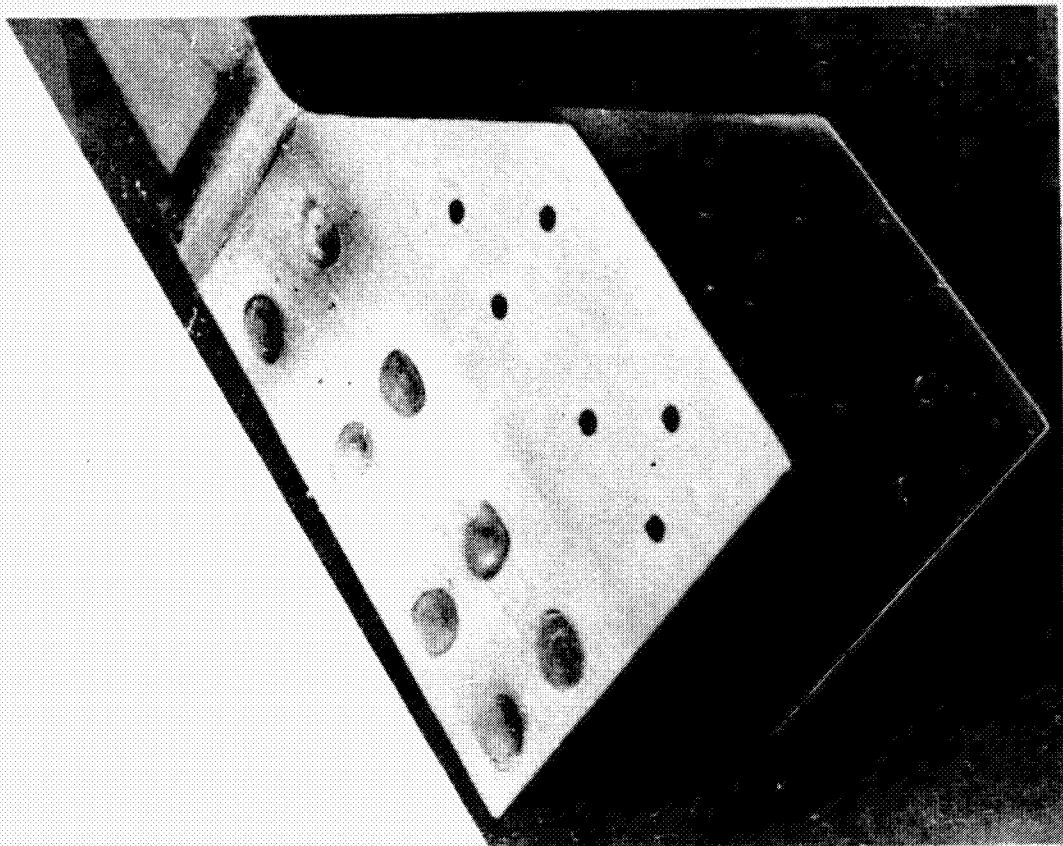
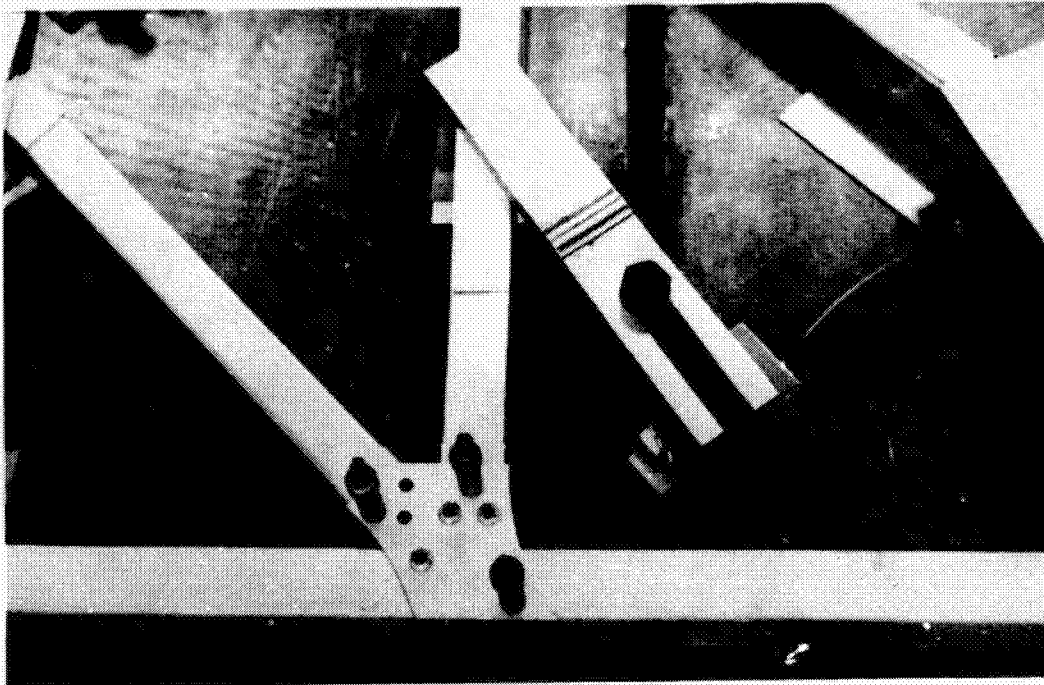
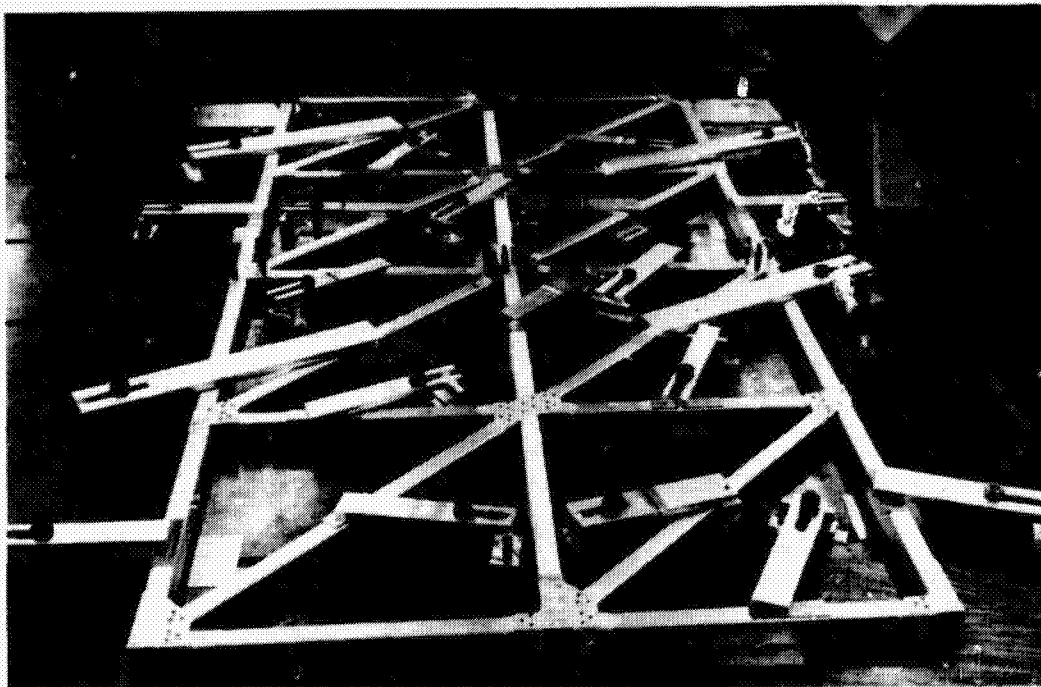


Fig. IV-45 Aluminum Truss Stringer Weld-Bond





*Fig. IV-46 Aluminum Truss Joint Assembly*



*Fig. IV-47 Aluminum Truss Assembly Fixture*

c. *Fiberglass Meteoroid Protection* - The completed aluminum development truss was covered on both front and back surfaces as shown in Fig. IV-49 with 0.010 cm (0.004 in.) thick fiberglass cloth for meteoroid protection. The cloth layers consist of precured single plys of style 120 glass cloth. The translucent layer of cured cloth was positioned on the truss and held with tape while holes were cut to accommodate the doubler plates. The trimmed layer was then removed, the truss members cleaned, adhesive added to the truss component surfaces and the cloth layer repositioned for bonding.

The average measured weight of the three truss panels, without special end attachment provisions, was 3.07 kg/in.<sup>2</sup> (0.629 lb/ft<sup>2</sup>).

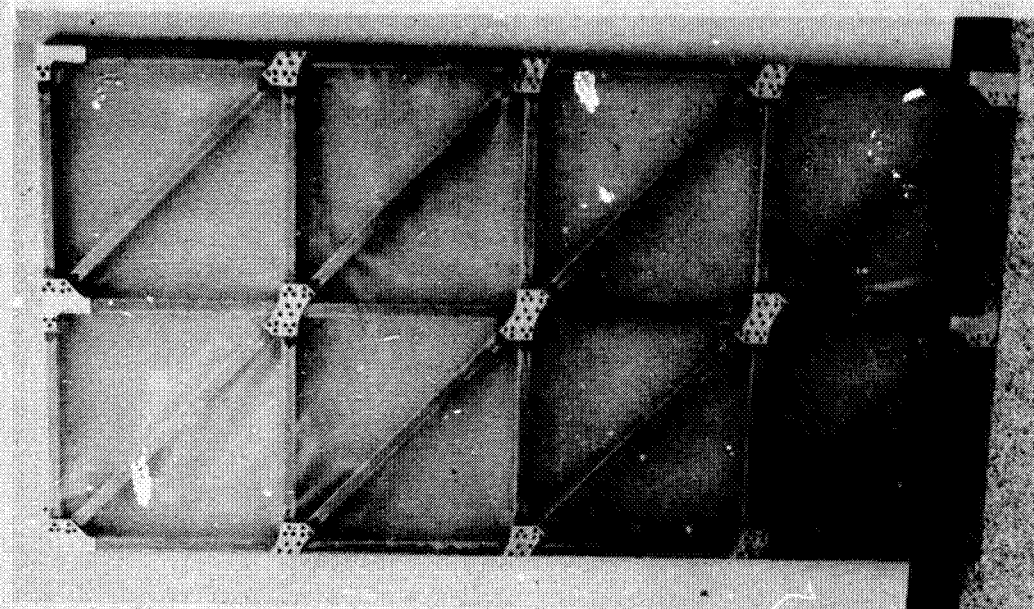


Fig. IV-49

Fig. IV-49  
Aluminum Truss with Fiberglass  
Meteoroid Protection Layers

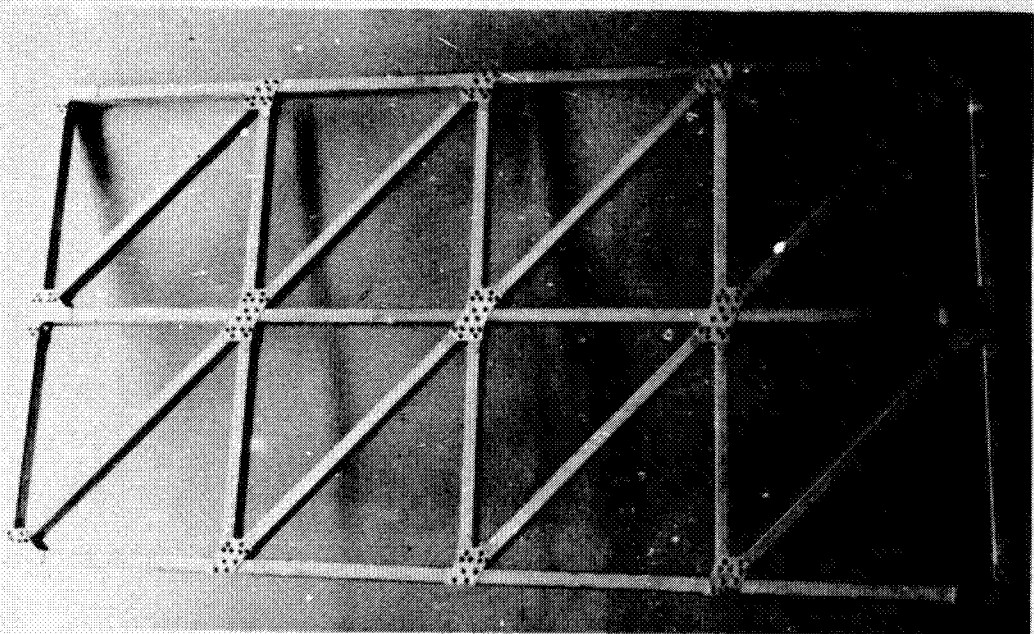


Fig. IV-48

Fig. IV-48  
Aluminum Truss Compression Test Panel  
without Fiberglass Cloth

An aluminum honeycomb sandwich panel, identical in basic construction to the Phase II test panels, was fabricated with a wide variety of included defects to determine the effectiveness of two nondestructive evaluation (NDE) methods, ultrasonic and radiographic inspection. This control panel was divided into four quadrants as shown in Fig. V-1 each containing different types of defects. In addition, a honeycomb core splice was made down the center of the panel, with the core splice adhesive purposely containing defects as shown in Fig. V-2. Also shown in Fig. V-2 is the core damage introduced to quadrant B and two strands of style 120 fiberglass cloth, one coated for use as a release cloth and the other untreated bleed cloth. Two additional strands of these same materials are shown in Fig. V-3 located on top of the FM-24 adhesive film. Also shown are the gaps and overlaps in the FM-24 film introduced into quadrant A. The side of the aluminum faceskin that was placed against the adhesive film is shown in Fig. V-4 with the grease spot, faceskin scratch and faceskin dent visible. In addition, a single drop of water was included in one of the core cells of quadrant D. This control panel was assembled and subjected to a cure cycle identical to that of the aluminum sandwich panels for Phase II structural testing.

The completed control panel was ultrasonically and radiographically inspected by Martin Marietta quality assurance personnel without prior knowledge of the location, type or extent of included defects. Ultrasonic C scans of the four quadrants are shown in Fig. V-5 thru V-8. The C scan of quadrant A shows the core splice. The C scan of quadrant B, shown in Fig. V-6 revealed anomalies at the locations of local core cell wall surface crushing and buckling but did not reveal core cell wall wrinkling through the depth of the core. Neither the faceskin dent or scratch were revealed on the C scan of quadrant C, shown in Fig. V-7. The faceskin dent was flattened out by the pressure applied during panel fabrication and, therefore, would not be expected to reveal a C scan anomaly. The grease spot introduced into quadrant D is readily detectable on the C scan shown in Fig. V-8. The location of the water drop in the core cell is also shown due to the apparent bond problem caused by the resultant steam during panel cure at 250°F. The location of the 0.25-in. gap in the core splice is also indicated on this C scan. The included fiberglass cloth strands with bond release coating are vaguely detectable; however, the untreated cloth strands are not detectable.



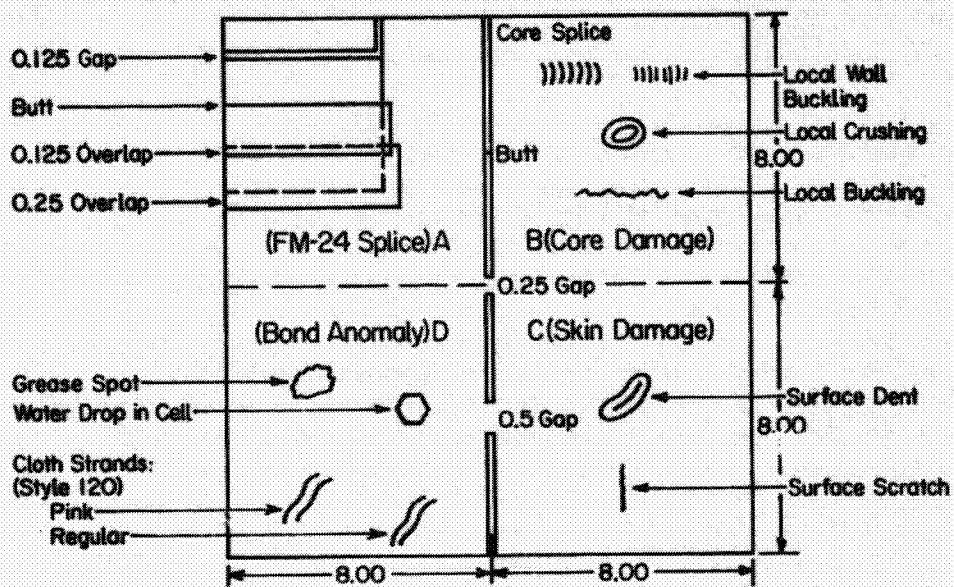


Fig. V-1 Aluminum Sandwich Panel Quality NDE Standards Panel

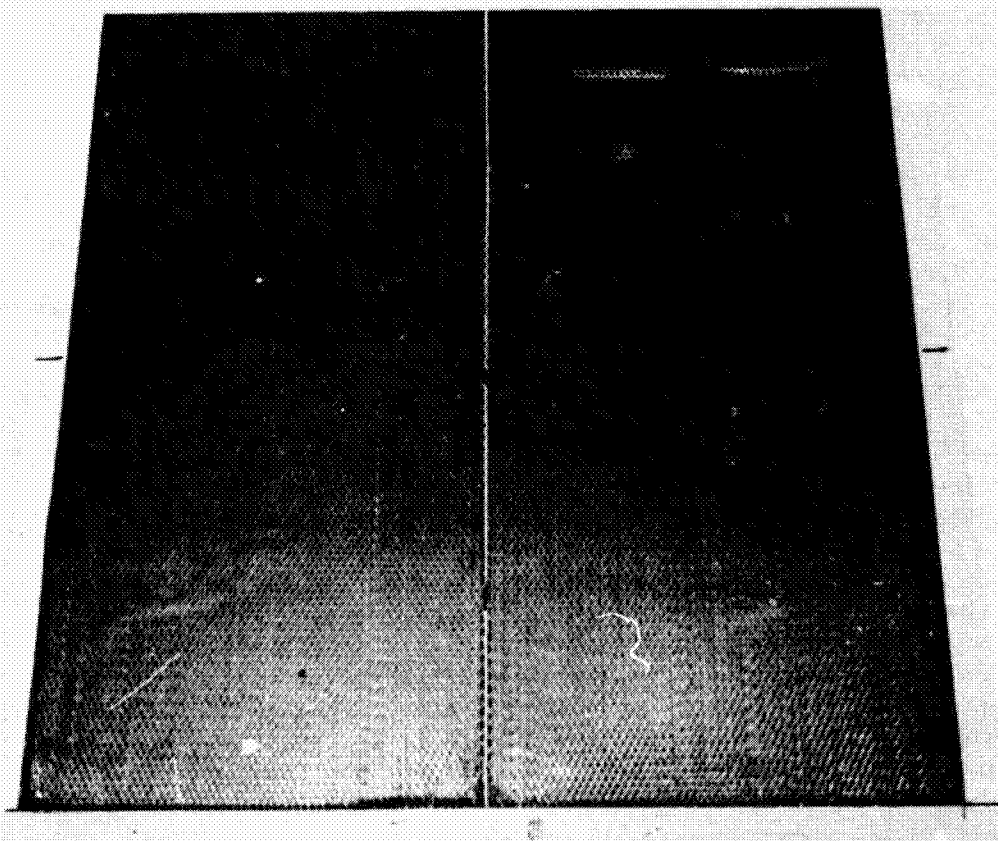
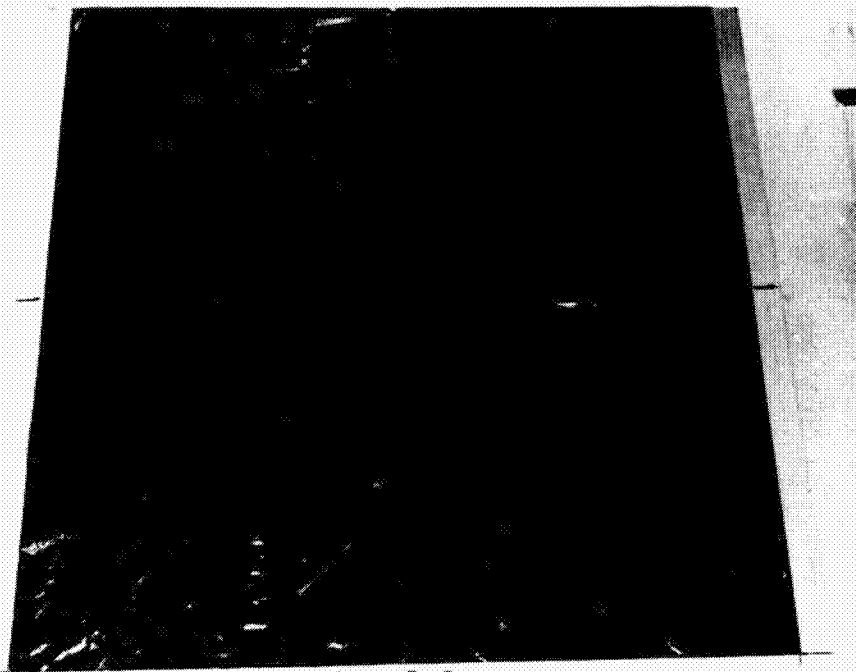
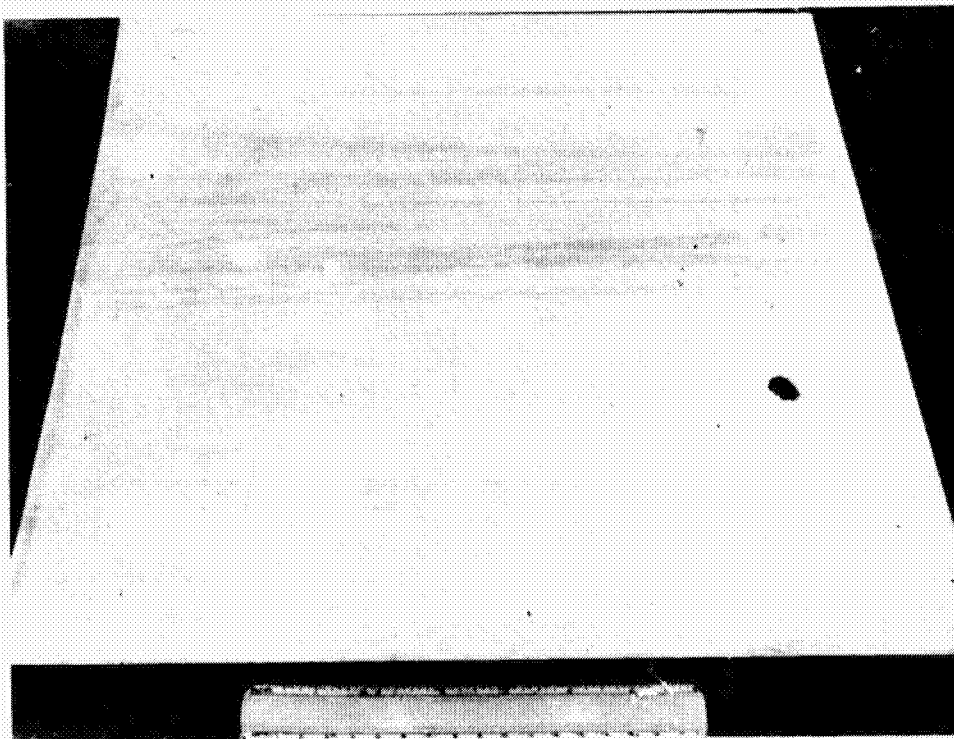


Fig. V-2 Quality NDE Standards Panel Aluminum Core



IT 28

*Fig. V-3 Quality NDE Standards Panel FM-24 Adhesive Film*



*Fig. V-4 Quality NDE Standards Panel Aluminum Faceskin*

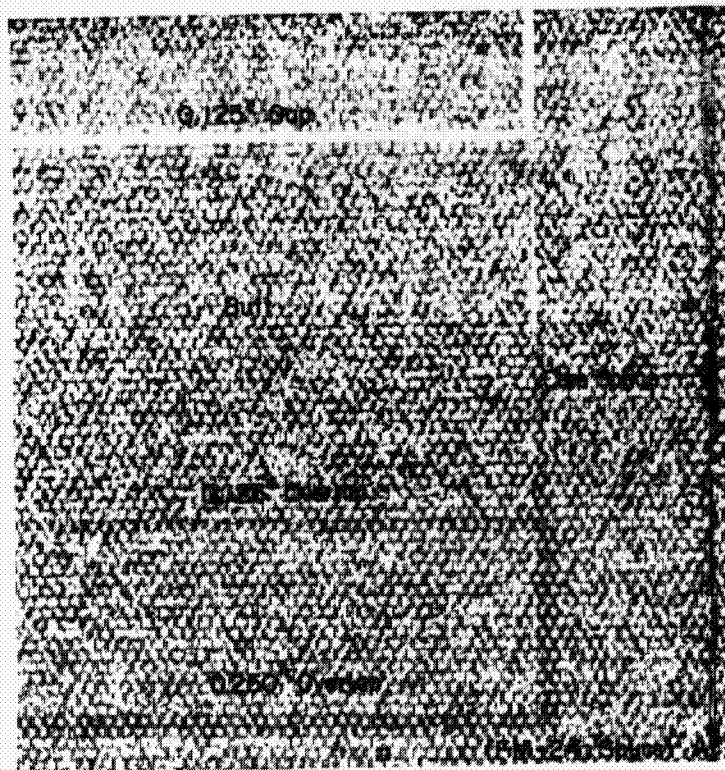


Fig. V-5  
Ultrasonic C Scan Aluminum Honeycomb  
Sandwich Panel Quadrant A, FM-24 Splice

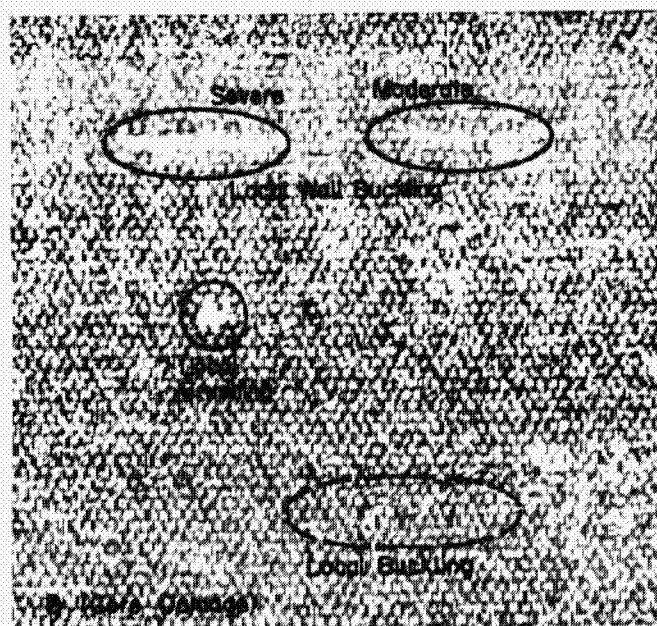


Fig. V-6  
Ultrasonic C Scan Aluminum Honeycomb  
Sandwich Panel Quadrant B, Core Damage



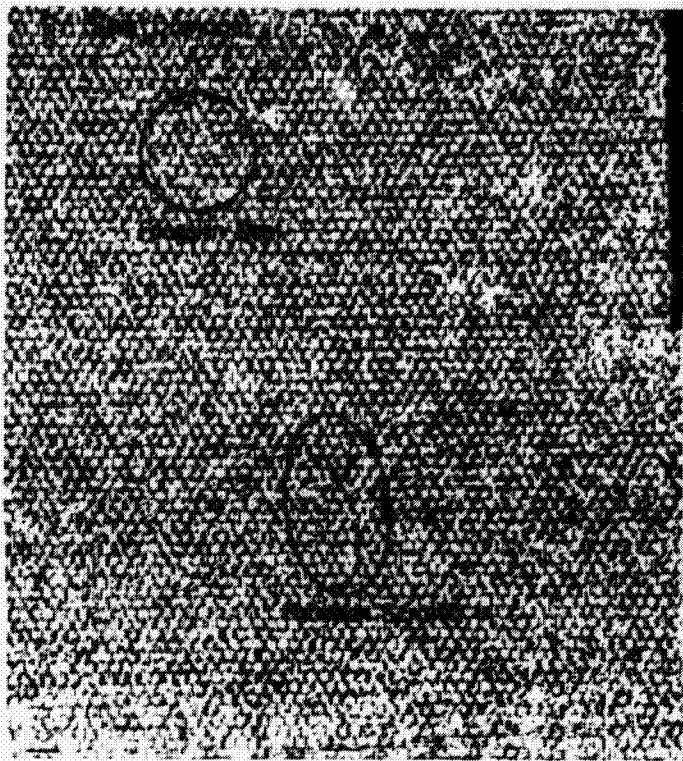


Fig. V-7  
 Ultrasonic C Scan Aluminum Honeycomb  
 Sandwich Panel Quadrant C, Skin Damage

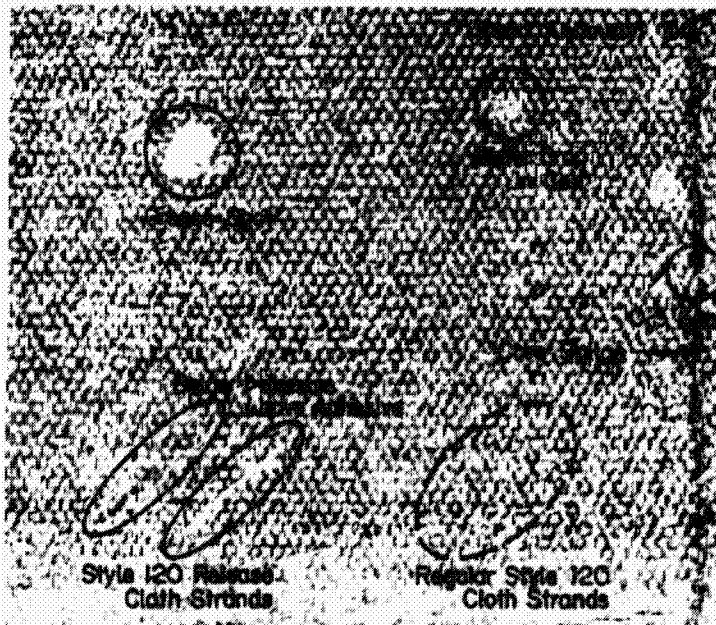


Fig. V-8  
 Ultrasonic C Scan Aluminum Honeycomb  
 Sandwich Panel Quadrant D, Bond Anomaly

The control panel was then radiographically inspected to evaluate this NDE method. The only defects that were detectable were the core damage areas of quadrant B. An X-ray of this quadrant is shown in Fig. V-9. All four of the core defects indicated are readily detectable using appropriate X-ray viewing equipment.

In conclusion, the results of the NDE study are very encouraging. All of the included defects that would be expected to be of concern for maintaining structural integrity were detected by one or both of the inspection techniques.

#### Local Wall Buckling



Severe



Moderate



Local Crushing



Local Buckling

#### B - Core Damage

*Fig. V-9*  
*X-Ray Aluminum Honeycomb Sandwich Panel Quadrant B,*  
*Core Damage*

## VI. STRUCTURAL TEST

---

### A. SMALL PHASE I STRUCTURES

#### 1. Honeycomb Sandwich Core/Skin Bond Tests

The material proposed for use in bonding honeycomb core to face skins is FM-24 reticulating film adhesive. Reticulation of the adhesive film involves applying it in film form to the surface of a honeycomb core and heating it. This causes the film to break at the center of each core cell and migrate to the cell wall. Honeycomb sandwich bond tension tests were performed to determine the relative merits of two different thickness of film adhesive and to evaluate the effect of reticulating the adhesive. Six flat tension specimens from each of four honeycomb sandwich panels were tested. The test results are summarized in Table VI-1. Panels 14 and 15 were bonded using 0.178 mm (0.007 in.) thick FM-24 film adhesive with panel 14 reticulated and panel 15 unreticulated. Panels 18 and 19 were bonded using 0.089 mm (0.0035 in.) thick FM-24 film adhesive with panel 18 reticulated and panel 19 unreticulated. The failed specimens from panel 15, shown in Fig. VI-1, indicate the type of failure obtained on all of the test specimens. In all cases the failure was in the aluminum honeycomb core, which was 1/8-5052-0.0007-3.1 aluminum Hexcel.

The test results indicate that the 0.089 mm (0.0035 in.) thin film adhesive is adequate for use in lightweight honeycomb sandwich construction. This is desirable since the core/faceskin bond adhesive weight can be a significant portion of the total weight of honeycomb sandwich panels with thin faceskins and lightweight core. Also, the tests indicate that it is not necessary to reticulate the film adhesive to obtain adequate strength, which eliminates a fabrication step with resultant lower fabrication cost.

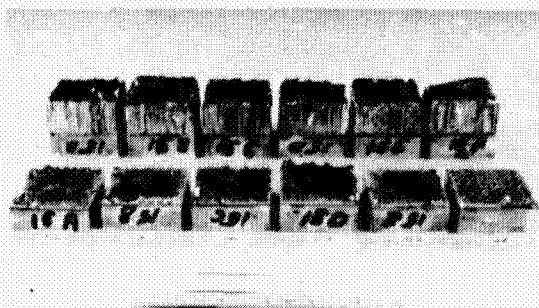


Fig. VI-1  
Failed Flat Bond Tensile Specimens,  
Panel 15, Unreticulated

Table VI-1 Honeycomb Sandwich Flat Tension Test Results

Panel Number	Specimen Number	Bond Area, cm <sup>2</sup> (in. <sup>2</sup> )	Ultimate Load, N (lb)	Bond Tensile Stress, N/cm <sup>2</sup> (psi)
14 Reticulated	14A	25.8 (4.0)	12,721 (2,860)	493 (715)
	14B	25.8 (4.0)	11,898 (2,675)	461 (669)
	14C	25.8 (4.0)	12,677 (2,850)	492 (713)
	14D	25.8 (4.0)	12,988 (2,920)	503 (730)
	14E	25.8 (4.0)	11,787 (2,650)	457 (663)
	14F	25.8 (4.0)	13,033 (2,930)	505 (733)
15 Unreticulated	15A	25.8 (4.0)	12,632 (2,840)	489 (710)
	15B	25.8 (4.0)	12,788 (2,875)	496 (719)
	15C	25.8 (4.0)	13,077 (2,940)	507 (735)
	15D	25.8 (4.0)	12,588 (2,830)	488 (708)
	15E	25.8 (4.0)	12,899 (2,900)	500 (725)
	15F	25.8 (4.0)	12,855 (2,890)	498 (723)
18 Reticulated	18A	25.8 (4.0)	11,431 (2,570)	443 (643)
	18B	25.8 (4.0)	12,499 (2,810)	485 (703)
	18C	25.8 (4.0)	12,477 (2,805)	483 (701)
	18D	25.8 (4.0)	12,410 (2,790)	481 (698)
	18E	25.8 (4.0)	11,476 (2,580)	445 (645)
	18F	25.8 (4.0)	11,787 (2,650)	457 (663)
19 Unreticulated	19A	25.8 (4.0)	12,232 (2,750)	474 (688)
	19B	25.8 (4.0)	12,321 (2,770)	478 (693)
	19C	25.8 (4.0)	12,276 (2,760)	476 (690)
	19D	25.8 (4.0)	12,143 (2,730)	471 (683)
	19E	25.8 (4.0)	12,232 (2,750)	474 (688)
	19F	25.8 (4.0)	11,876 (2,670)	462 (670)

## 2. Honeycomb Sandwich Composite Stiffeners

A candidate structural concept for lightweight shell structures is one in which a honeycomb sandwich with thin faceskins contains thin integral stiffeners. These stiffeners are located directly beneath each faceskin, as shown in Fig. VI-2.

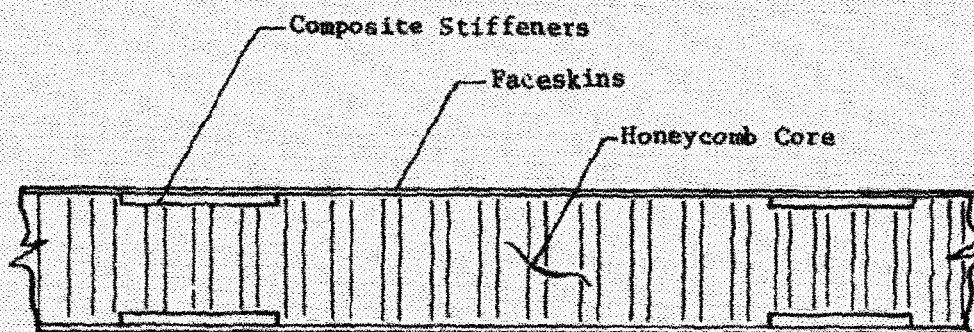


Fig. VI-2 Sandwich Stiffener Location

Three candidate stiffeners were loaded to failure in axial tension to aid in preliminary evaluation of the basic structural concept. A tensile load was applied to each specimen as shown in Fig. VI-3. Axial strain was monitored during the test using an SR-4 strain gage located at the center of each specimen. Overall specimen deflection was monitored using a linear motion deflection transducer attached at the ends of the specimens. Plots of load versus deflection for the three tests are shown in Fig. VI-4. Test data and calculated stress levels for each of the three specimens are given in Table VI-2. Design ultimate load for the test specimens was 6240 N (1400 lb). The boron/epoxy specimen, 1D, failed in tension at a load of 7000 N (1570 lb) across the titanium shim insert at the chem milled step as shown in Fig. VI-5. Two of the boron/epoxy layers are discontinuous at this point and therefore the load is resisted by the two outer layers of boron/epoxy and the 0.152 mm (0.006 in.) titanium. The high tensile strength graphite/epoxy specimen, 3D, failed in a similar manner at a load of 9550 N (2140 lb). The high modulus graphite/epoxy specimen, 2E, failed at a load of 2450 N (550 lb), which is significantly lower than the design ultimate load. The failure occurred at the end of the titanium shim insert. It is very possible that some of the graphite fibers are not well aligned in this region.



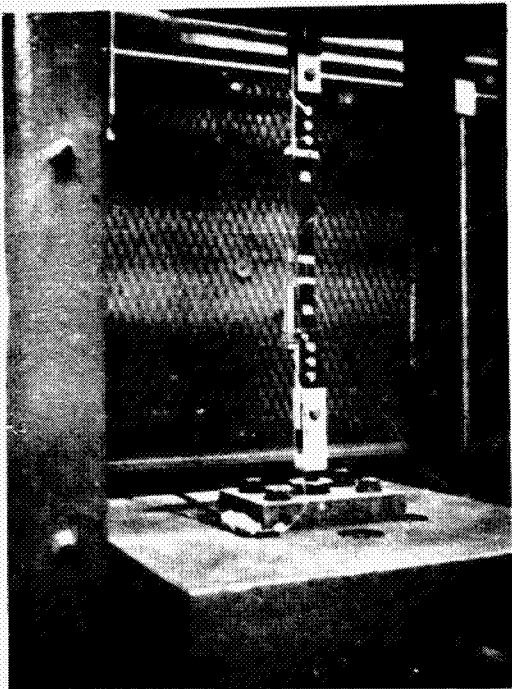


Fig. VI-3 Test Setup

Table VI-2 Test Results

Specimen Number	1D	2E	3D
Composite Material	Boron/Epoxy	HM Graph/ Epoxy	HTS Graph/ Epoxy
Failure Load, N (lbf)	7,000 (1,570)	2,450 (550)	9,550 (2,140)
Strain at Failure, $\mu$ in./in.	2,060	1,970	3,070
Composite Area, $\text{cm}^2$ ( $\text{in}^2$ )	0.181 (0.028)	0.129 (0.020)	0.187 (0.029)
Composite Stress, $\text{N/m}^2 \times 10^3$ (psi)	387,000 (56,100)	189,000 (27,200)	508,000 (73,800)
Young's Modulus, $\text{N/m}^2 \times 10^3$ (ksi)	187,000 (27,200)	95,000 (13,800)	165,000 (24,000)
Bearing Area, $\text{cm}^2$ ( $\text{in}^2$ )	0.872 (0.0135)	0.872 (0.0135)	0.872 (0.0135)
Bearing Stress, $\text{N/m}^2 \times 10^3$ , psi	802,000 (116,200)	281,000 (40,700)	1,092,000 (158,500)



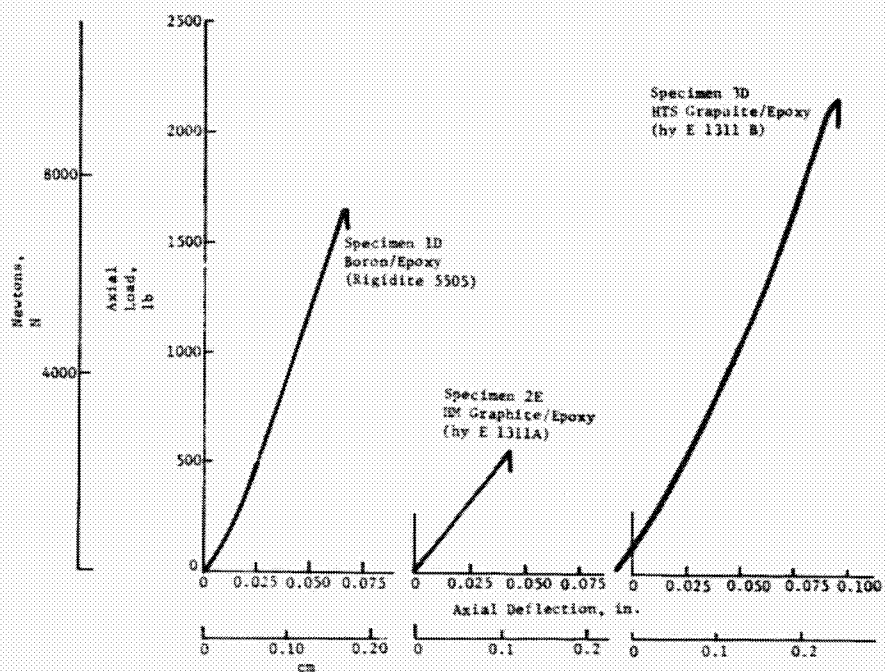


Fig. VI-4 Composite Stiffner Straps, Load Deflection Curves

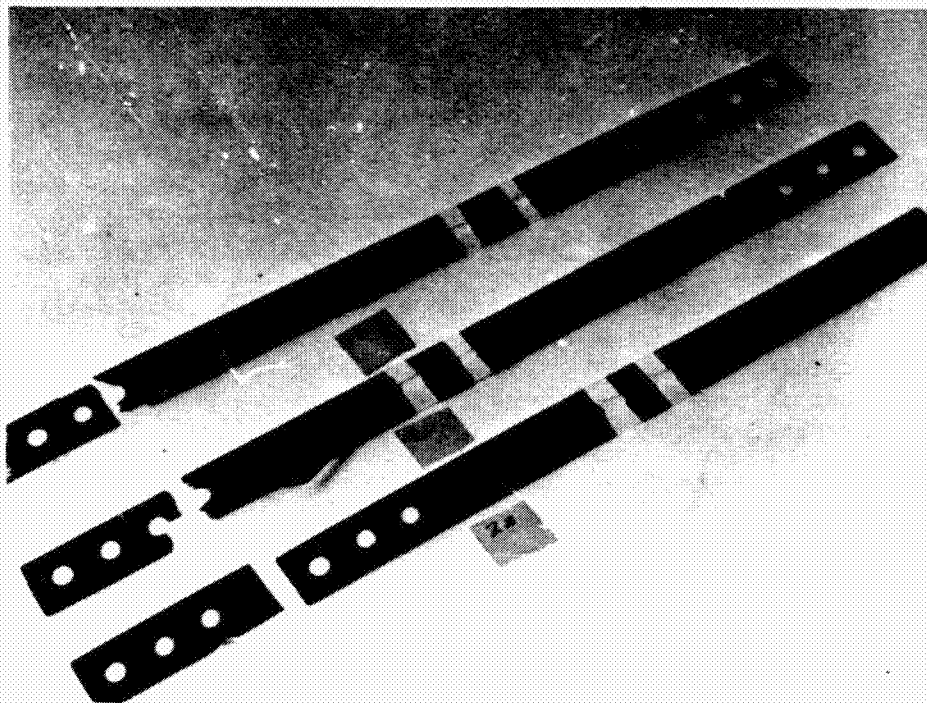
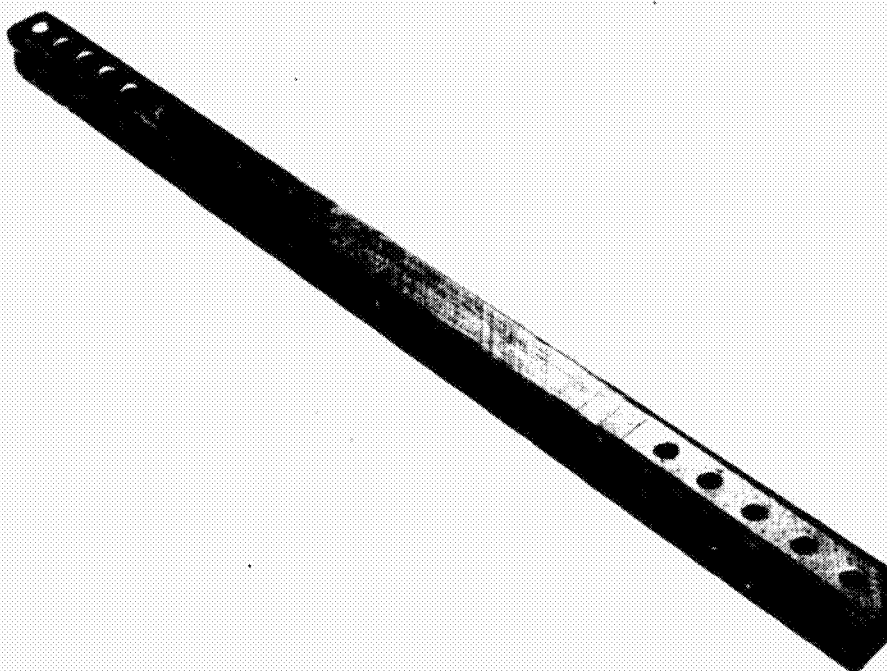


Fig. VI-5 Failed Specimens

### 3. Graphite/Epoxy Truss Struts

Two graphite/epoxy truss struts representative of the axial truss members of a lightweight truss skirt concept were structurally tested. Both specimens were of identical construction. They are approximately 2.85 cm (1.12 in.) by 2.85 cm (1.12 in.) square and 61.0 cm (24.0 in.) long. The primary material is Hercules A/S/3501 graphite/epoxy oriented axially and at  $\pm 45^\circ$  from the axial direction. The ends of the specimens contain thin titanium shim inserts distributed over the last 16.5 cm (6.50 in.) of each end. Load is transferred to the specimens through five 3/8-in.-diameter bolts at each end of the specimen. Figure VI-6 is a photo of specimen 1. The test setup for specimen 1 is shown in Fig. VI-7. Overall axial deflection was monitored using a G. L. Collins Linear Motion Transducer connected to an X-Y plotter, which produced a continuous plot of axial load versus axial deflection. Each specimen was also instrumented with two BLH SR-4 axial strain gages at midspan. Axial load was applied using a BLH 150K Tension-Compression test machine.

Load deflection curves for each of the two specimens are shown in Fig. VI-8. Design ultimate load for the specimens was 55,000 N (12,350 lb). Specimen 1 failed at 52,600 N (11,800 lb) or 95.5% of design ultimate, and specimen 2 failed at 46,400 N (10,400 lb) or 84% of design ultimate. Strain gage results are plotted in Fig. VI-9. The primary failure mode for both specimens was micro-buckling of the thin titanium shims from the compressive stress due to bolt bearing. The failed section of specimen 1 is shown in Fig. VI-10. The bearing stress on the titanium shims of specimens 1 and 2 at failure, assuming that all of the load is resisted by the titanium, was  $751 \times 10^6 \text{ N/m}^2$  (109,000 psi) and  $657 \times 10^6 \text{ N/m}^2$  (96,300 psi), respectively. These stress levels are significantly lower than those obtained previously on thicker graphite/epoxy laminates with a greater number of shim inserts. The reduction is attributed to the damage caused to the shim inserts nearest the surface of a laminate during machining. The subject test specimens have only four shim inserts in each laminate at the ends and therefore damage to the outer two results in a large percentage reduction.



*Fig. VI-6 Graphite/Epoxy Truss Strut Test Specimen 1*



*Fig. VI-7 Test Setup*

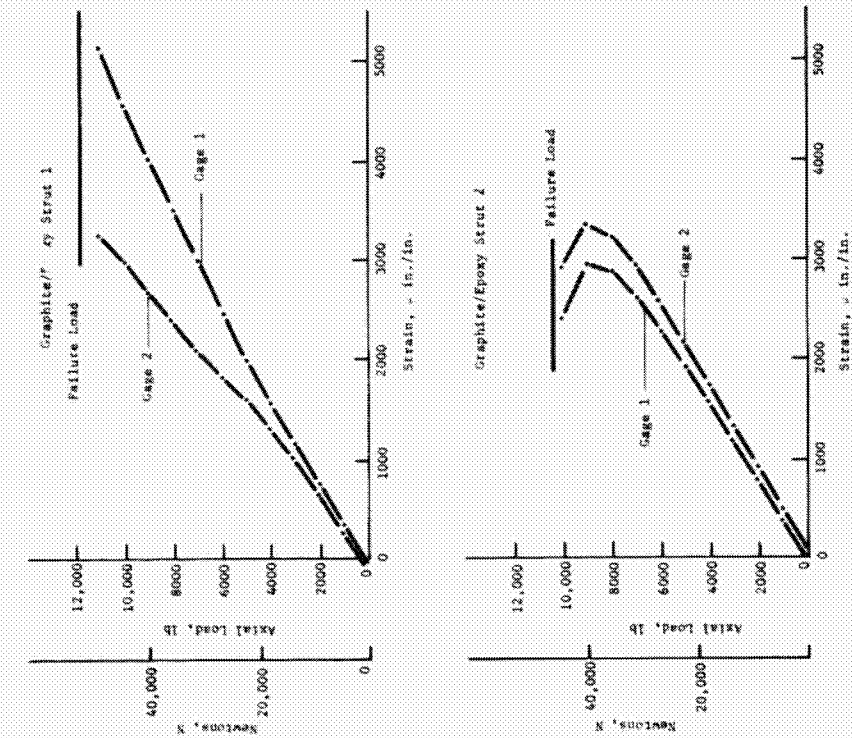


Fig. VI-9 Strain Gage Plots

Fig. VI-9

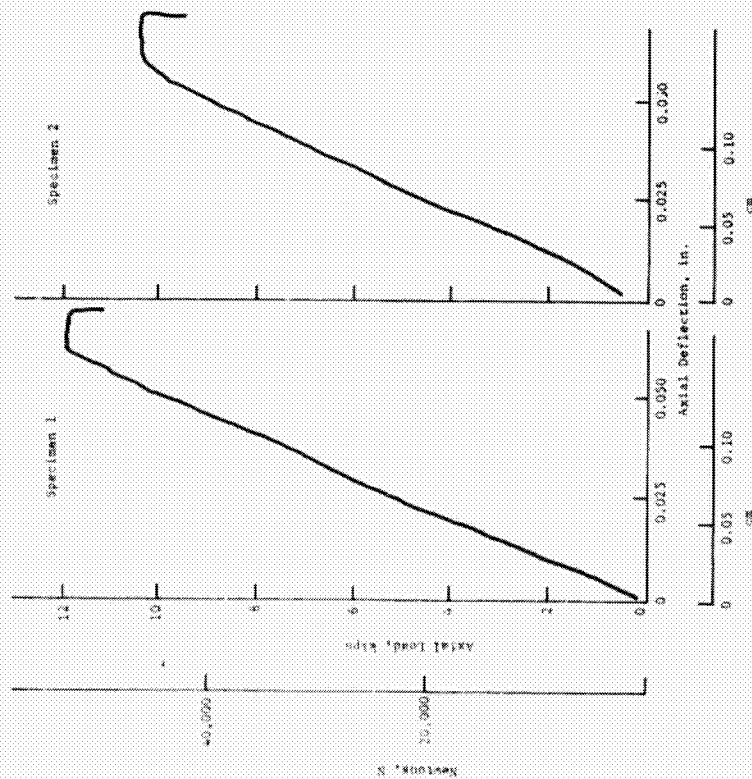


Fig. VI-8  
Load Deflection Curves,  
Graphite/Epoxy Columns

Fig. VI-8

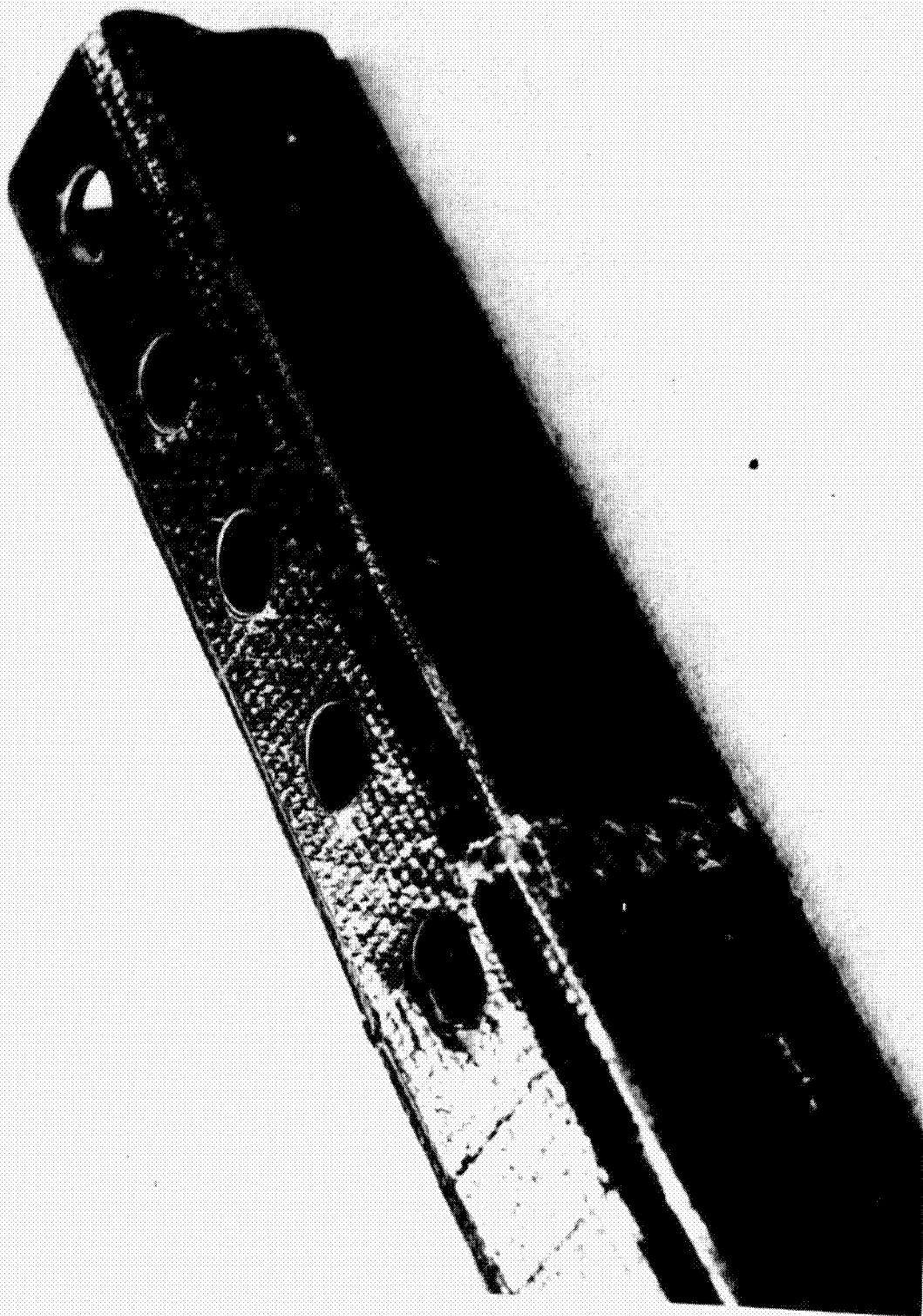


Fig. VI-10

Fig. V-10 Failed Section, Specimen 1

#### 4. Honeycomb Sandwich Panels

Six sets of honeycomb sandwich panels were structurally tested. A set of specimens consist of two 40.70x20.35 cm (16x8 in.) compression panels, two 40.70x10.17 cm (16x4 in.) long beam bending specimens, and two 20.35x10.17 cm (8x4 in.) short beam shear specimens. All specimens that form one set have a core thickness, skin thickness, and skin material selected from the design and analysis study. A summary of the materials and pages involved is given in Table VI-3.

*Table VI-3 Honeycomb Panel Definition*

Panel Set Designation	Core Thickness, cm (in.)	Total Skin Thickness, cm (in.)	Face Skin Material	
			±45° Torsion Material	0° Axial Material
A/S-GL-18	2.410 (0.948)	0.0407 (0.0160)	2 Layers, Style 112 Fiberglass Cloth/5208 Epoxy	2 Layers, Unidirectional, Type A/S Graphite/5208 Epoxy
Type I-GL-18	2.145 (0.845)	0.0368 (0.0145)	2 Layers, Style 112, Fiberglass Cloth/5208 Epoxy	2 Layers, Unidirectional, Modmor Type I Graphite/5208 Epoxy
Type I-GR-20	1.510 (0.595)	0.0394 (0.0155)	4 Layers, Unidirectional, Thornel T-300 Graphite/5208 Epoxy	2 Layers, Unidirectional, Modmor Type I Graphite/5208 Epoxy
Boron-GL-17	1.660 (0.654)	0.0381 (0.0150)	2 Layers, Style 112, Fiberglass Cloth/5200 Epoxy	2 Layers, Unidirectional, Narmco 5505/4 Boron/Epoxy
Alum-12	1.425 (0.585)	0.0254 to 0.0216 (0.0100 to 0.0085)	6061-T6 Aluminum	
Titan-10	1.280 (0.505)	0.0228 to 0.0203 (0.0090 to 0.0080)	6Al-4V Titanium	



Each of the test specimens was instrumented with four strain gages located as shown in Fig. VI-11.

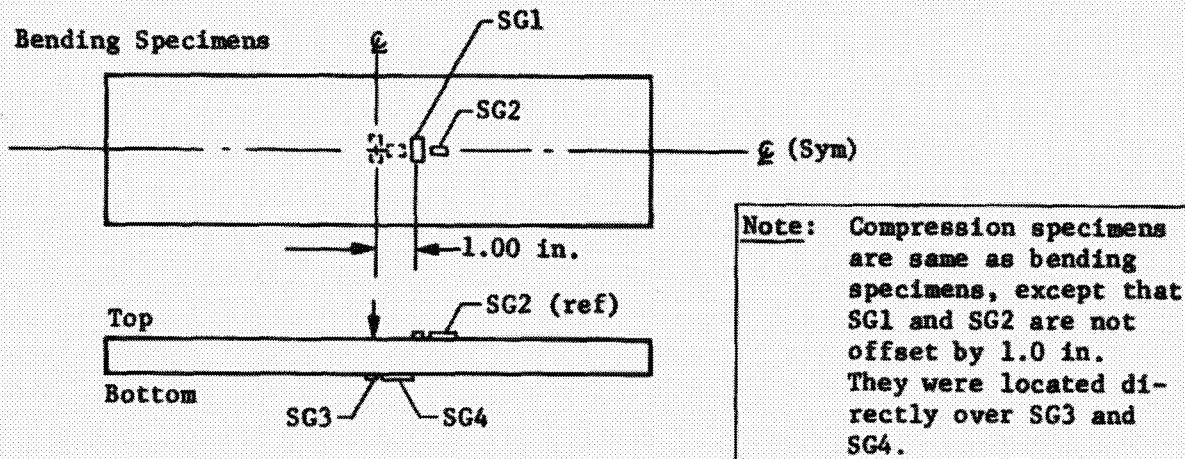


Fig. VI-11 Strain Gage Locations

a. *Axial Compression Tests* - A total of 12 honeycomb sandwich specimens, two from each of the six panel sets, were tested in axial compression. The basic panel size is 40.70x20.35 cm (16x8 in.) and each test specimen has fiberglass doubles bonded to the end region for introduction of test loads. A typical test setup for the compression tests is shown in Fig. VI-12. Plots of axial load versus deflection for the 12 tests are shown in Fig. VI-13. Compression panel test results are summarized in Table VI-4. The average skin stress at failure is calculated by dividing the failure load by the total cross-sectional area of the two face skins. The Young's modulus shown was calculated by using average stress and average measured axial strain at a load within the linear portion of the load-deflection curves. Plots of load versus strain for all of the sandwich panel tests are shown in Appendix A. Typical examples of the type of failure obtained are shown in Fig. VI-14.

b. *Long Beam Bend Tests* - The specimens are 40.60 cm (16.0 in.) long by 10.15 cm (4.0 in.) wide. Twelve specimens, two from each of the six panel sets, were tested in three point bending. The test setup (Fig. VI-15), includes a beam support fixture that provides free rotation of the beam ends. The distance between beam supports was 38.1 cm (15.0 in.) in all cases with the load applied at mid-span. Each specimen was instrumented with four axial strain gages located as shown previously in Fig. VI-11. A load distribution pad consisting of three aluminium strips was used under the

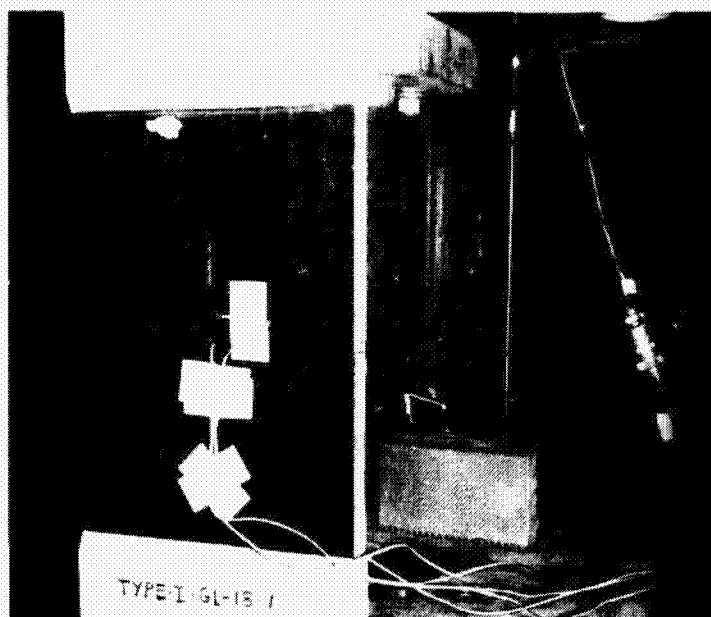


Fig. VI-12 Axial Compression Test Setup

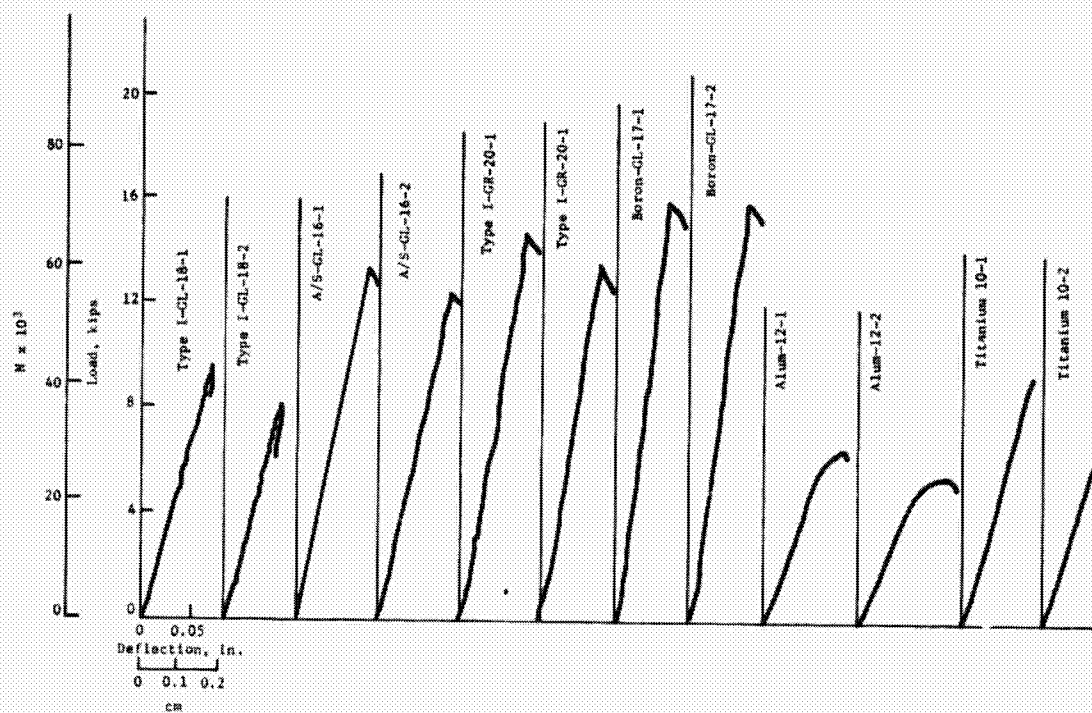


Fig. VI-13  
Load Deflection Curves, Honeycomb Sandwich Compression Tests

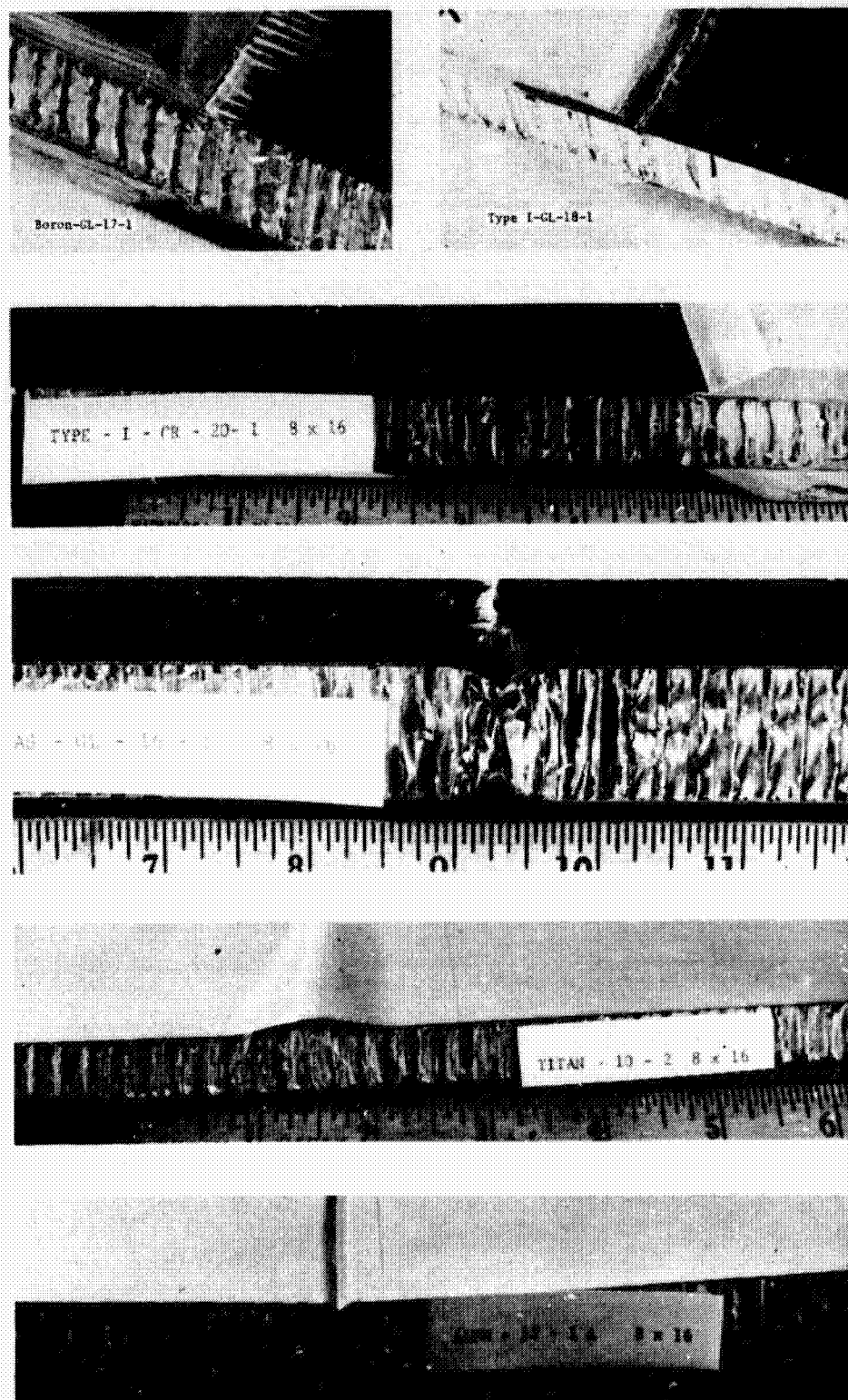


Fig. VI-14 Typical Failures, Honeycomb Sandwich Compression Tests

Table VI-4 Honeycomb Sandwich Compression Panel Test Results

Honeycomb Panel Designation <sup>1</sup>	Core Thickness <sup>2</sup> , cm (in.)	Face Skin Thickness <sup>2</sup> , cm (in.)	Compressive Failure Load		Avg Skin Stress at Failure <sup>4</sup> , N/m <sup>2</sup> x 10 <sup>3</sup> (psi)	Measured Face Skin Axial Young's Modulus <sup>5</sup> , N/m <sup>2</sup> x 10 <sup>9</sup> (psi x 10 <sup>6</sup> )
			Total Weight, N (lb)	N/cm (lb) per Inch Width <sup>3</sup>		
A/S-GL-18-1	2.410 (0.948)	0.0406 (0.0160)	54,500 (12,250)	2680 (1532)	329,500 (47,800)	73.6 (10.68)
-2	2.410 (0.948)	0.0406 (0.0160)	59,000 (13,250)	2900 (1656)	357,000 (51,800)	77.6 (11.25)
Type I-GL-18-1	2.145 (0.845)	0.0368 (0.0145)	42,500 (9,550)	2090 (1195)	284,000 (41,200)	126.2 (18.30)
-2	2.145 (0.845)	0.0368 (0.0145)	35,600 (8,000)	1750 (1000)	237,000 (34,400)	125.5 (18.20)
Type I-GR-20-1	1.510 (0.595)	0.0393 (0.0155)	65,000 (14,600)	3200 (1825)	405,000 (58,800)	111.8 (16.20)
-2	1.510 (0.595)	0.0393 (0.0155)	59,800 (13,450)	2950 (1682)	274,000 (54,200)	106.9 (15.50)
Boron-GL-17-1	1.660 (0.654)	0.0380 (0.0150)	70,200 (15,750)	3455 (1970)	452,000 (65,600)	151.4 (21.95)
-2	1.660 (0.654)	0.0380 (0.0150)	70,200 (15,750)	3455 (1970)	452,000 (65,600)	147.2 (21.35)
Alum-12-1	1.485 (0.585)	0.0254 (0.0100)	28,400 (6,380)	1400 (797)	275,000 (39,900)	69.8 (10.12)
-2	1.485 (0.585)	0.0216 (0.0085)	24,000 (5,400)	1180 (675)	273,500 (39,700)	70.2 (10.16)
Titan-10-1	1.280 (0.505)	0.0228 (0.0070)	41,000 (9,220)	2020 (1153)	441,000 (64,000)	105.2 (15.25)
-2	1.280 (0.505)	0.0203 (0.0080)	28,750 (6,460)	1415 (808)	348,000 (50,500)	102.7 (14.90)

<sup>1</sup>All test panels are 40.60 cm (16.0 in.) high by 20.30 cm (8.0 in.) wide.

<sup>2</sup>Measured thicknesses.

<sup>3</sup>Design ultimate combined loading is 1225.8 N/cm (700 lb/in.) axial compression with 245.2 N/cm (140 lb/in.) torsion.

<sup>4</sup>Based on total skin thickness.

<sup>5</sup>From measured axial face skin strain.

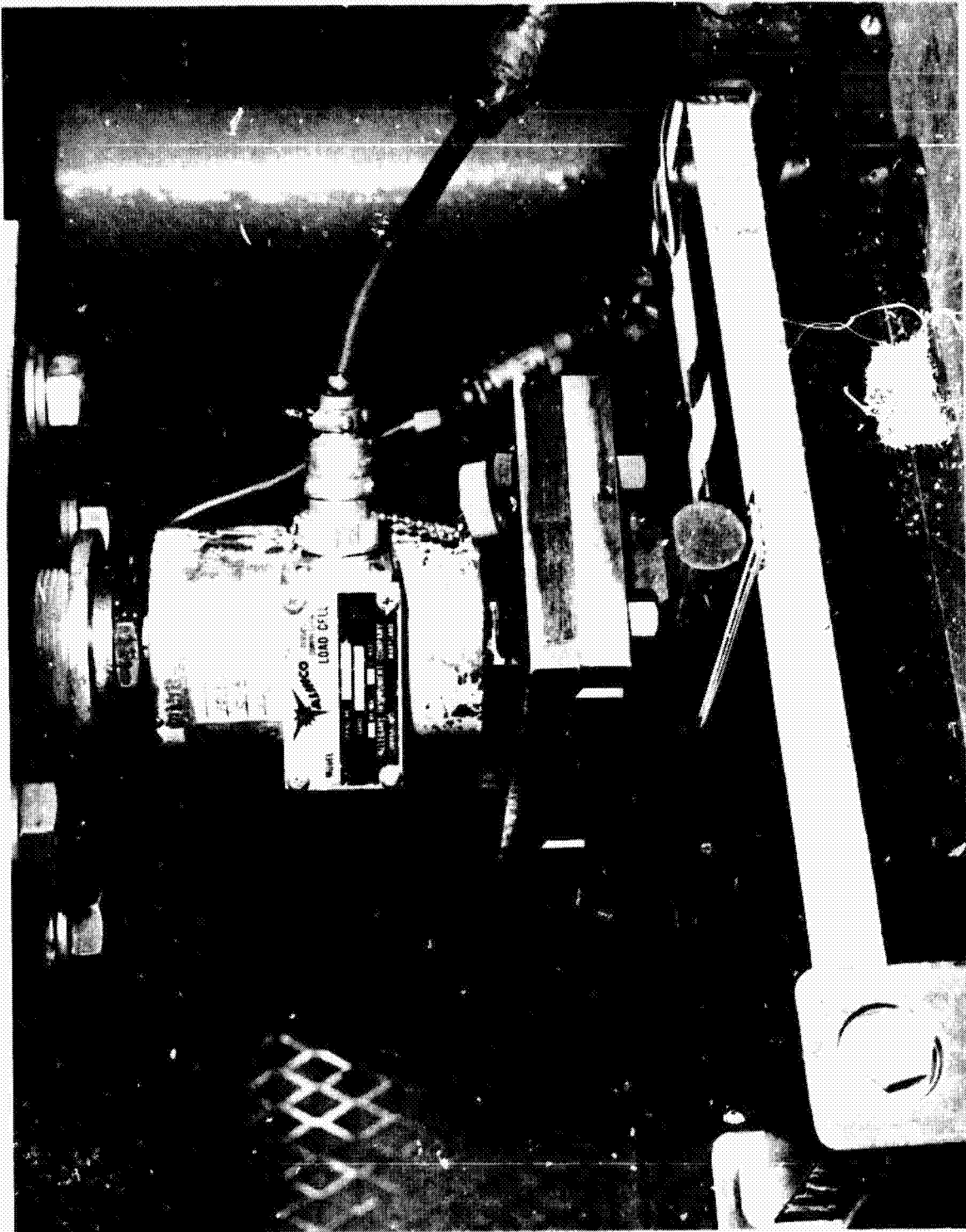


Fig. VI-16 Long Beam Bending Test Setup

load introduction rod. This proved to be an inadequate load distribution pad and caused a local core crushing failure of the first specimen tested (Type I-GL-18-2). For subsequent tests, a larger 10.15x4.44x0.317 cm (4x1.75x0.125 in.) pad was used with satisfactory results. Plots of applied load versus midspan deflection for the 12 tests are shown in Fig. VI-16. Test results for this series are summarized in Table VI-5. The maximum faceskin stress shown was calculated by dividing the total load carried by the bottom (tension) faceskin at midspan by the tension faceskin cross sectional area. The faceskin Young's modulus shown was calculated by dividing the midspan stress by measured strain at a load level within the linear portion of the load-deflection curves. Plots of load versus strain for the long beam bending tests were given in Ref. 1. Specimen failure in all cases, except for the specimen that failed because of the inadequate load distribution pad, was caused by fracture of the top (compression) skin near beam midspan. Examples of typical failures are shown in Fig. VI-17.

c. *Short Beam Shear Tests* - These specimens are 20.30 cm (8.0 in.) long by 10.15 cm (4.0 in.) wide. Twelve specimens, two from each of the six panel sets were tested in three point bending. The test setup, shown in Fig. VI-18, uses the same beam support fixture previously used for the long beams, except that the supports are adjusted to 15.23 cm (6.0 in.) between centers. The load was applied at midspan through the load distribution pad as shown. Each specimen was instrumented with four axial strain gages located as shown previously in Fig. VI-11. Plots of applied load versus midspan deflection for the 12 tests are shown in Fig. VI-19.

Test results for this series of tests are summarized in Table VI-6. The core shear stress at failure, shown in Table VI-6, was calculated by dividing one-half the applied load by the core cross sectional area. The failed specimen shown in Fig. VI-20 is typical of the type of failure on all specimens. In all cases the core shear stress at failure was above the minimum strength value shown in the Hexcel Design Manual, TSB-120.



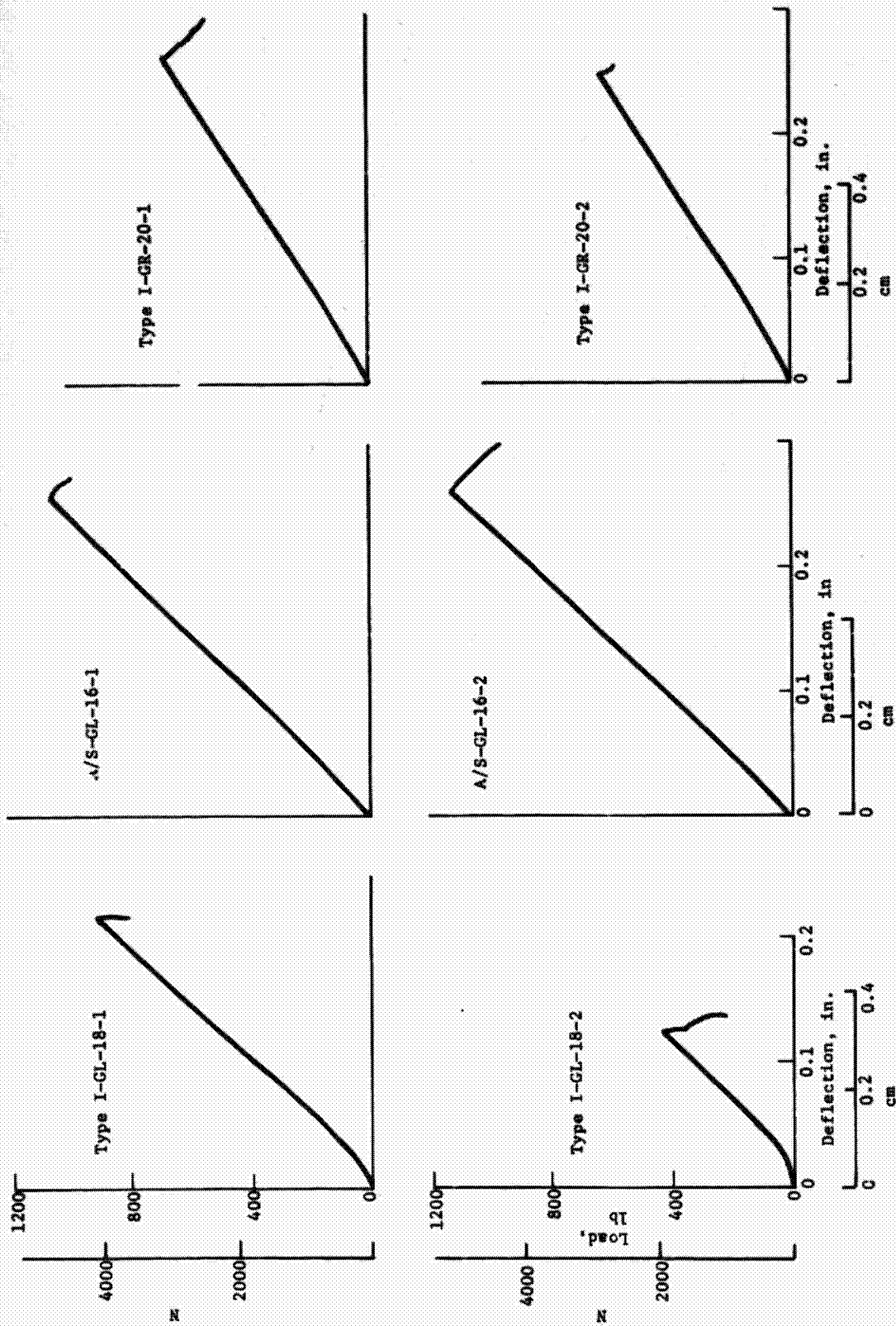


Fig. VI-16

Fig. VI-16 Load Deflection Curves, Honeycomb Sandwich Long Beam Bending Tests

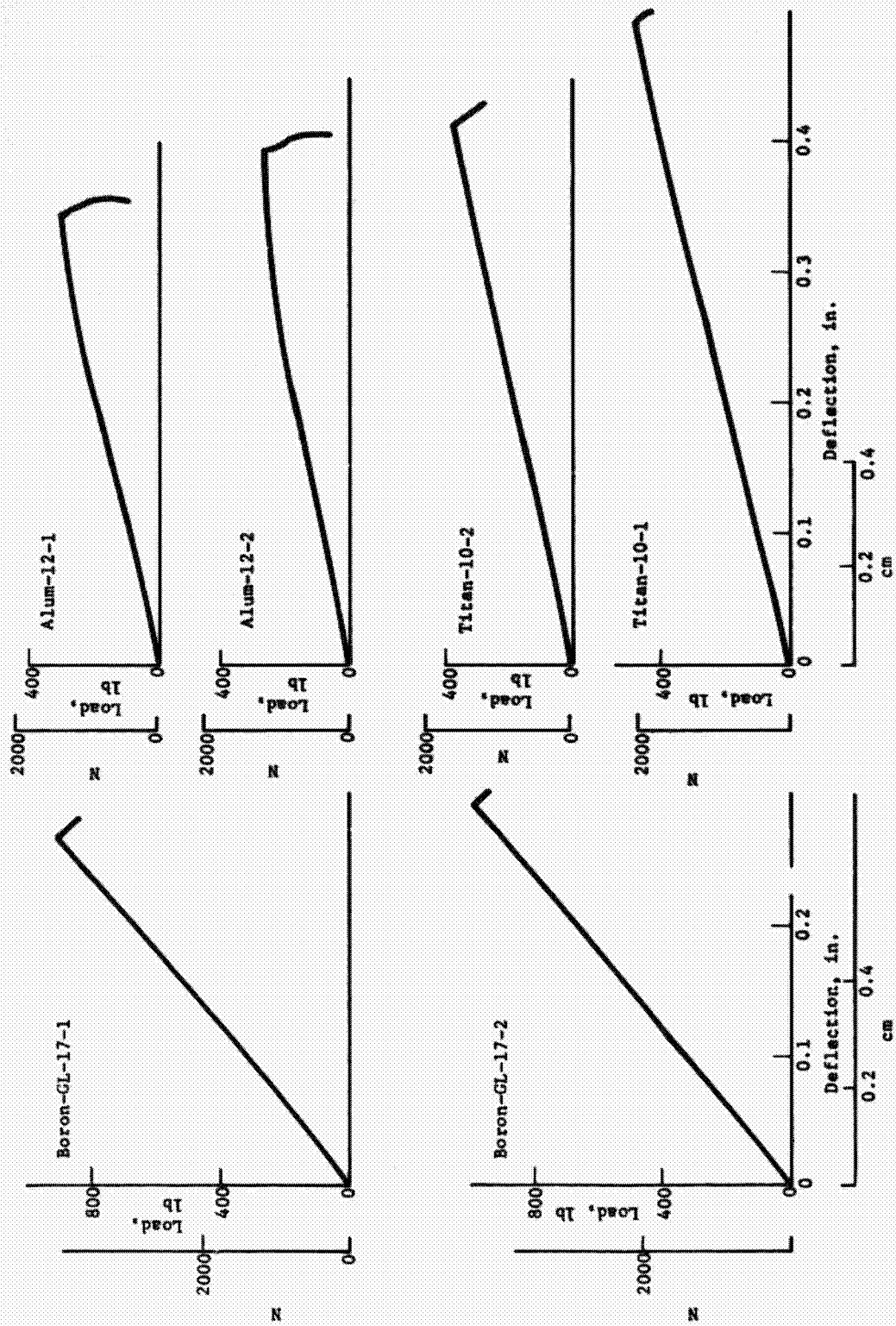


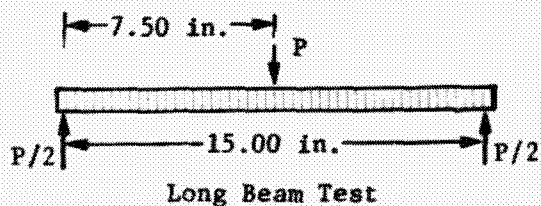
Fig. VI-16 (concl)

Fig. VI-16 (concl)

Table VI-5 Honeycomb Sandwich Long Beam Bending Test Results

Honeycomb Panel Designation <sup>1</sup>	Core Thickness <sup>2</sup> , cm (in.)	Face Skin Thickness, cm (in.)	Long Beam Failure Load, N (lb)	Max. Skin Stress at Failure <sup>3</sup> , N/m <sup>2</sup> x 10 <sup>3</sup> (psi)	Measured Face Skin Axial Young's Modulus <sup>4</sup> , N/m <sup>2</sup> x 10 <sup>9</sup> (psi x 10 <sup>5</sup> )
A/S-GL-18-1	2.410 (0.948)	0.0406 (0.0160)	4600 (1035)	434,000 (62,900)	87.0 (12.61)
-2	2.410 (0.948)	0.0406 (0.0160)	4900 (1100)	462,000 (66,900)	85.7 (12.43)
Type I-GL-18-1	2.145 (0.845)	0.0368 (0.0145)	4000 (900)	467,500 (67,800)	139.3 (20.20)
-2	2.145 (0.845)	0.0368 (0.0145)	1860 (418) <sup>5</sup>	217,000 (31,500) <sup>5</sup>	127.2 (18.45)
Type I-GR-20-1	1.510 (0.595)	0.0393 (0.0155)	2940 (660)	452,000 (65,500)	132.0 (19.15)
-2	1.510 (0.595)	0.0393 (0.0155)	2690 (605)	414,000 (60,000)	132.0 (19.15)
Boron-GL-17-1	1.660 (0.654)	0.0380 (0.0150)	4000 (900)	579,000 (84,000)	153.1 (22.20)
-2	1.660 (0.654)	0.0380 (0.0150)	4430 (995)	617,000 (89,500)	143.5 (20.80)
Alum-12-1	1.485 (0.585)	0.0254 (0.0100)	1335 (300)	325,500 (47,700)	77.3 (11.20)
-2	1.485 (0.585)	0.0216 (0.0085)	1180 (265)	338,500 (49,100)	73.2 (10.60)
Titan-10-1	1.280 (0.505)	0.0228 (0.0070)	2090 (470)	657,000 (95,300)	118.3 (17.15)
-2	1.280 (0.505)	0.0203 (0.0080)	1557 (350)	552,000 (80,000)	117.5 (17.05)

<sup>1</sup>All test beams are 40.60 cm (16.0 in.) long by 10.15 cm (4.0 in.) wide.  
<sup>2</sup>Measured thicknesses.  
<sup>3</sup>Based on total skin thickness.  
<sup>4</sup>From measured axial face skin strain.  
<sup>5</sup>Premature failure due to inadequate test load pad.



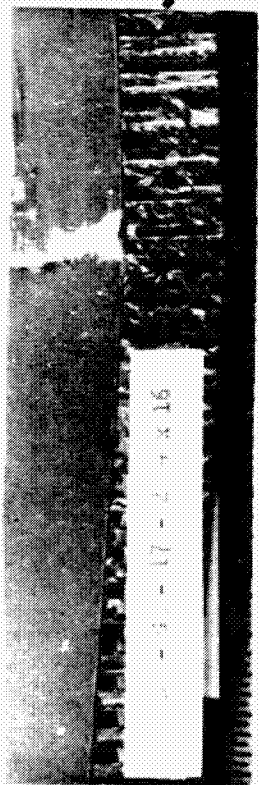
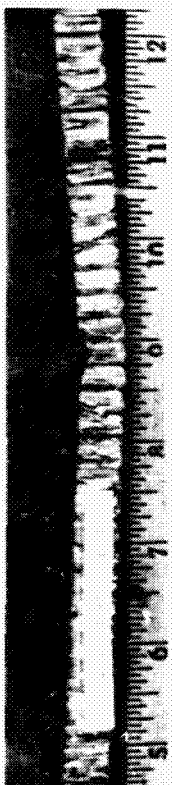
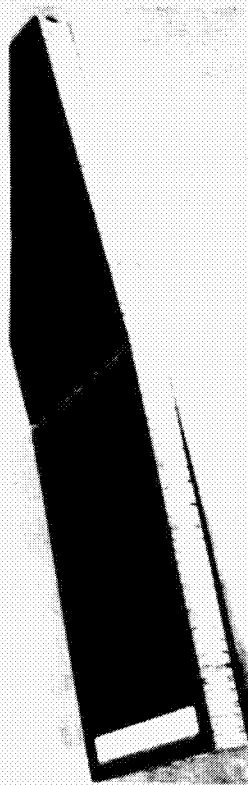
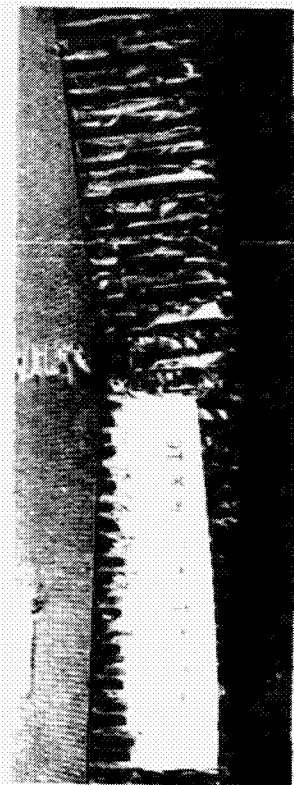
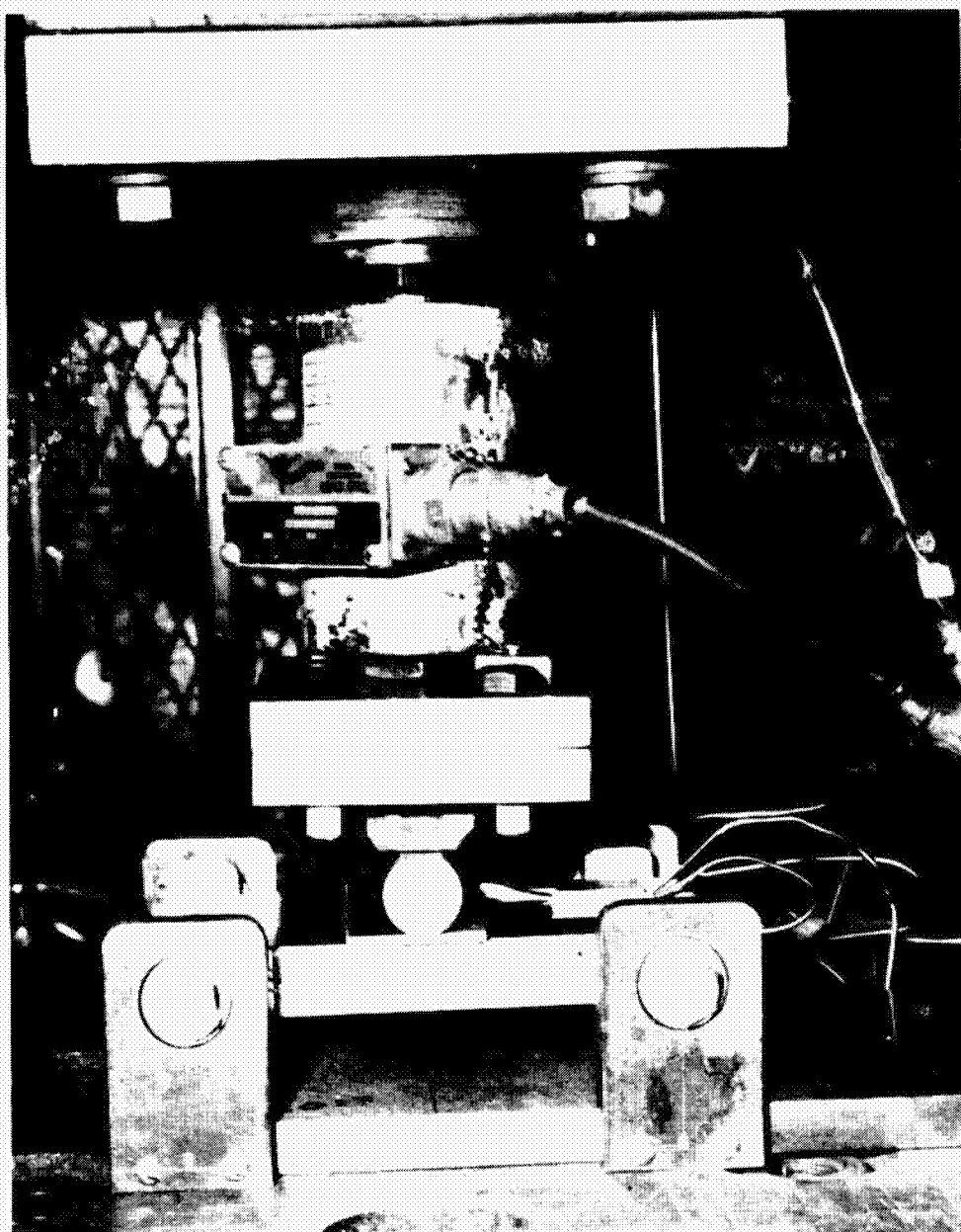


Fig. VI-17

Fig. VI-17 Typical Failures, Honeycomb Sandwich Long Beam Bending Tests



*Fig. VI-18 Short Beam Shear Test Setup*

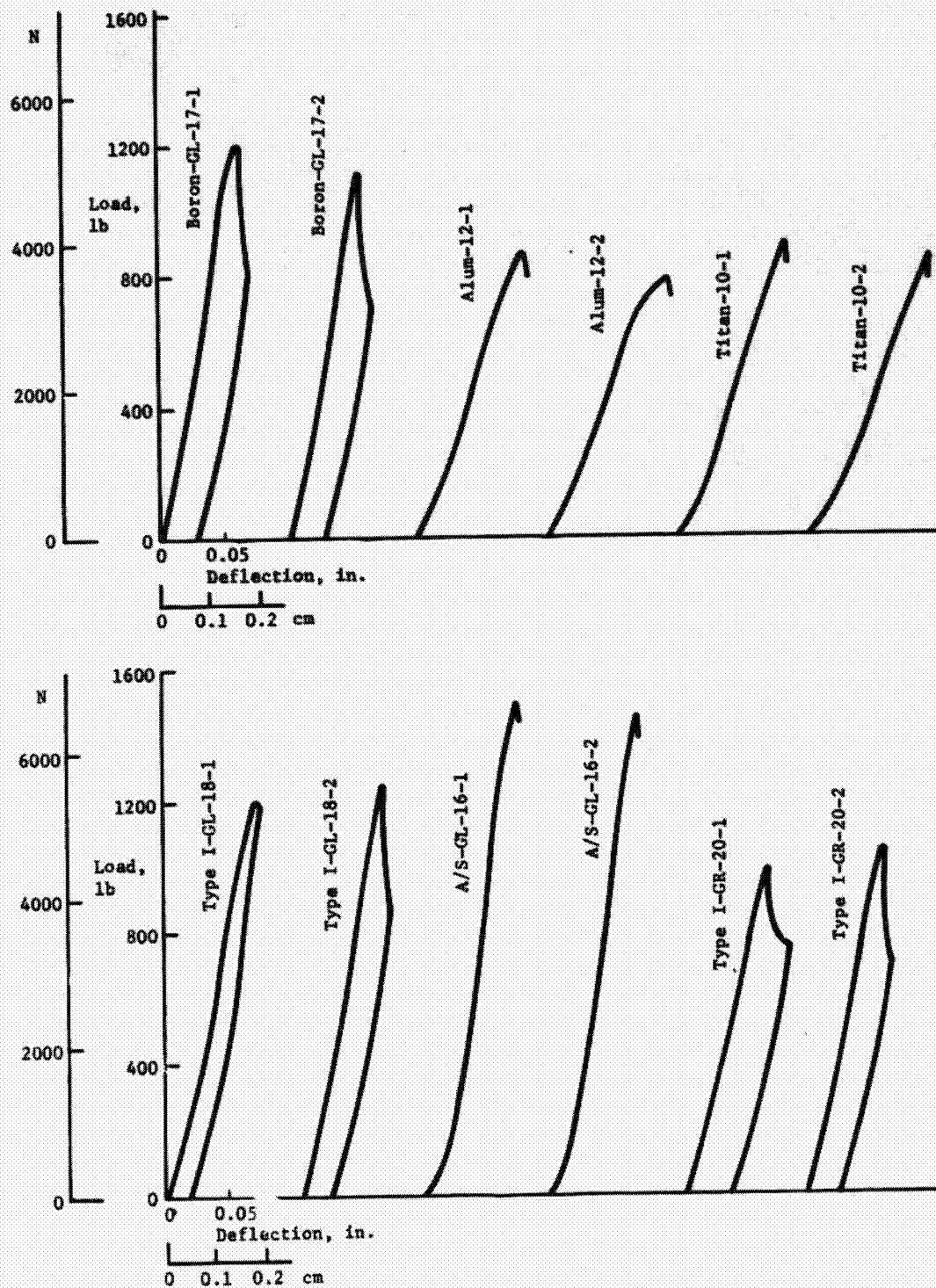


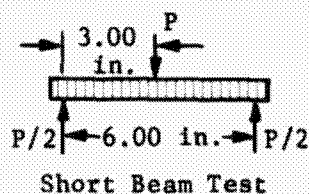
Fig. VI-19 Load Deflection Curves, Honeycomb Sandwich Short Beam Shear Tests

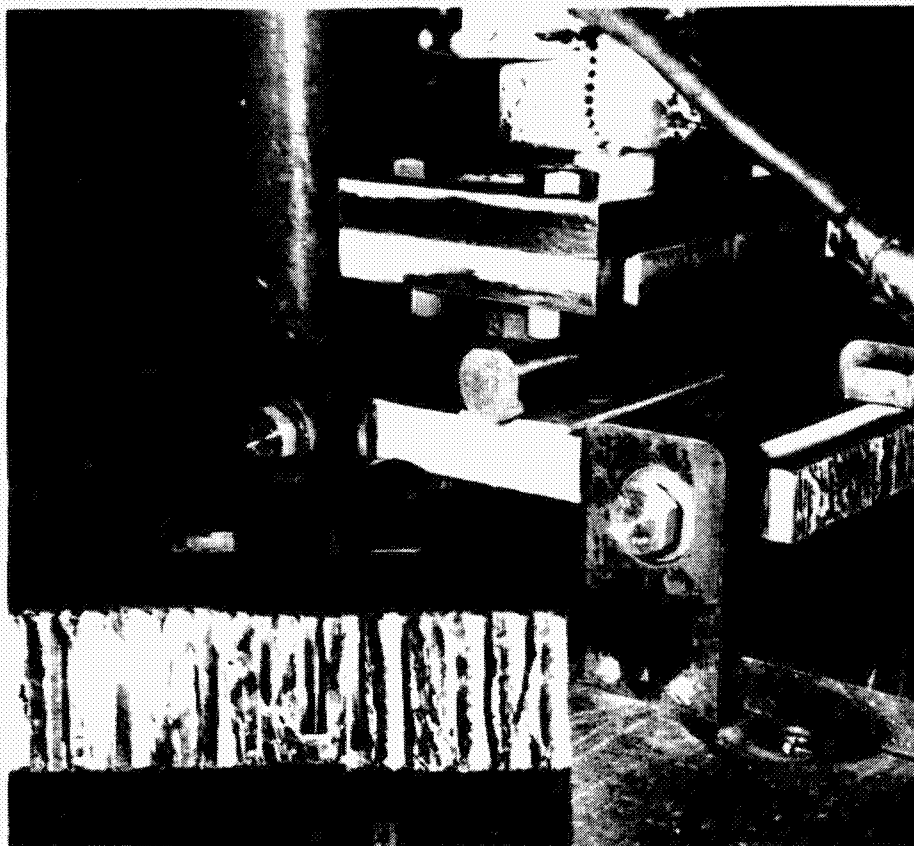


Table VI-6 Honeycomb Sandwich Short Beam Shear Test Results

Honeycomb Panel Designation <sup>1</sup>	Core Thickness <sup>2</sup> , cm (in.)	Face Skin Thickness <sup>2</sup> , cm (in.)	Beam Failure Load, N (lb)	Core Shear Stress at Failure <sup>3</sup> , N/m <sup>2</sup> x 10 <sup>3</sup> (psi)
A/S-GL-18-1	2.410 (0.948)	0.0406 (0.0160)	6450 (1450)	1317 (191)
-2	2.410 (0.948)	0.0406 (0.0160)	6340 (1425)	1295 (188)
Type I-GL-18-1	2.145 (0.845)	0.0368 (0.0145)	5260 (1180)	1200 (174)
-2	2.145 (0.845)	0.0368 (0.0145)	5430 (1220)	1241 (180)
Type I-GR-20-1	1.510 (0.595)	0.0393 (0.0155)	4210 (945)	1365 (198)
-2	1.510 (0.595)	0.0393 (0.0155)	4560 (1025)	1490 (216)
Boron-GL-17-1	1.660 (0.654)	0.0380 (0.0150)	5210 (1170)	1545 (224)
-2	1.660 (0.654)	0.0380 (0.0150)	4850 (1090)	1435 (208)
Alum-12-1	1.485 (0.585)	0.0254 (0.0100)	3740 (840)	1241 (180)
-2	1.485 (0.585)	0.0216 (0.0085)	3340 (750)	1104 (160)
Titan-10-1	1.280 (0.505)	0.0 <sup>2</sup> (0.0090)	3870 (870)	1483 (215)
-2	1.280 (0.505)	0.0203 (0.0080)	3600 (810)	1380 (200)

<sup>1</sup>All test beams are 20.30 cm (8.0 in.) long by 10.15 cm (4.0 in.) wide.  
<sup>2</sup>Measured thicknesses.  
<sup>3</sup>Shear strength of 1/8-5052-0.007 core, 155 psi min 210 psi typ from Hexcel TSB 120.





*Fig. VI-20 Failed Short Beam Shear Specimen*

#### 5. Aluminum Isogrid Panel

A flat, aluminum isogrid panel 57.22 cm (22.53 in.) long by 25.54 cm (10.05 in.) wide, shown in Fig. VI-21, was tested in axial compression. The panel was supported during tests in a test fixture shown in Fig. VI-22. The panel edges were supported against lateral deformation and the end compression load was applied through bolted and bonded aluminum end angles. The panel was instrumented with eight strain gages located as shown in Fig. VI-23. Axial deformation was monitored using a linear motion transducer and lateral deformation at the panel center was monitored using a dial indicator. Plots of deformation versus load and strain versus load are given in Fig. VI-24 and VI-25, respectively. The panel failed at an applied load of 82,400 N (18,500 lb) due to local crippling of the axially aligned ribs, shown in Fig. VI-26.

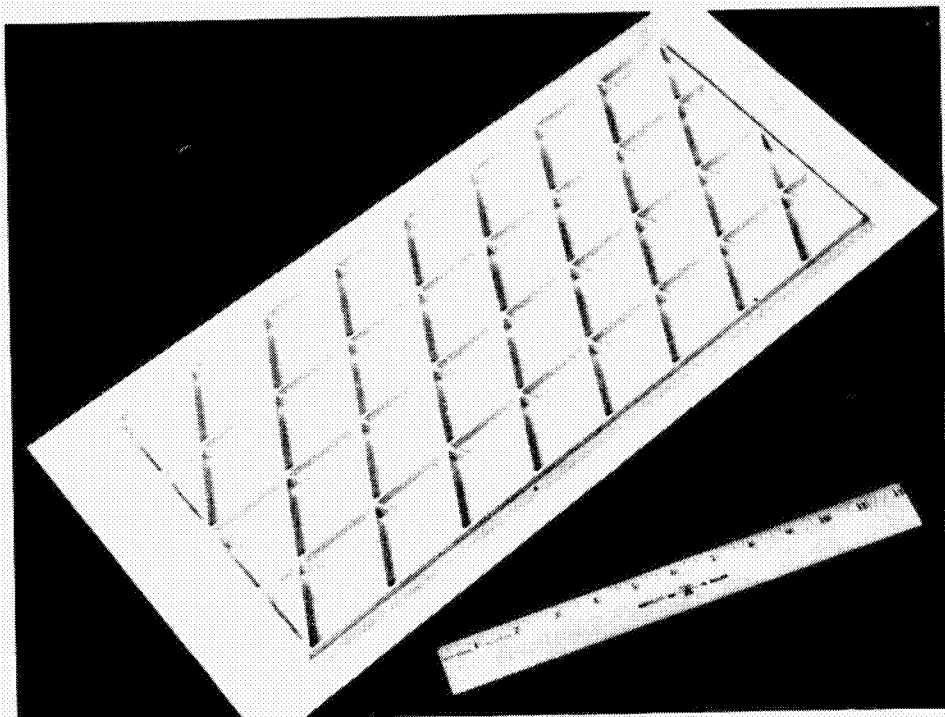


*Fig. VI-21 Aluminum Isogrid Test Panel*

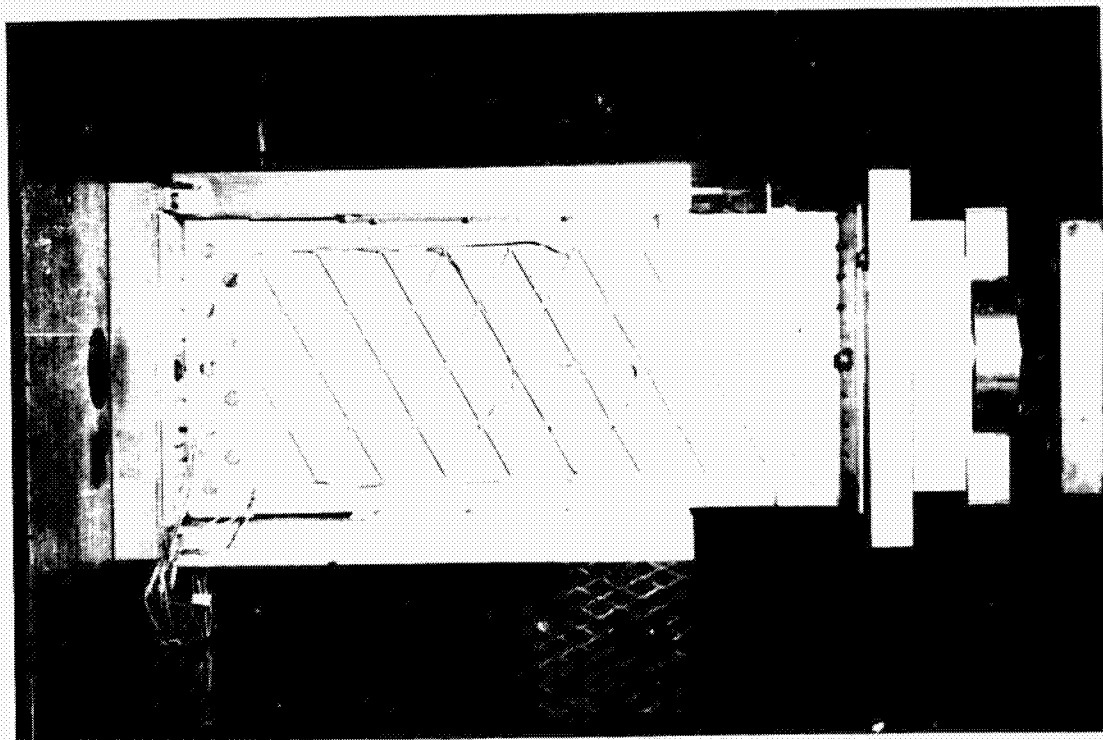


*Fig. VI-22 Aluminum Isogrid Panel Test Setup*

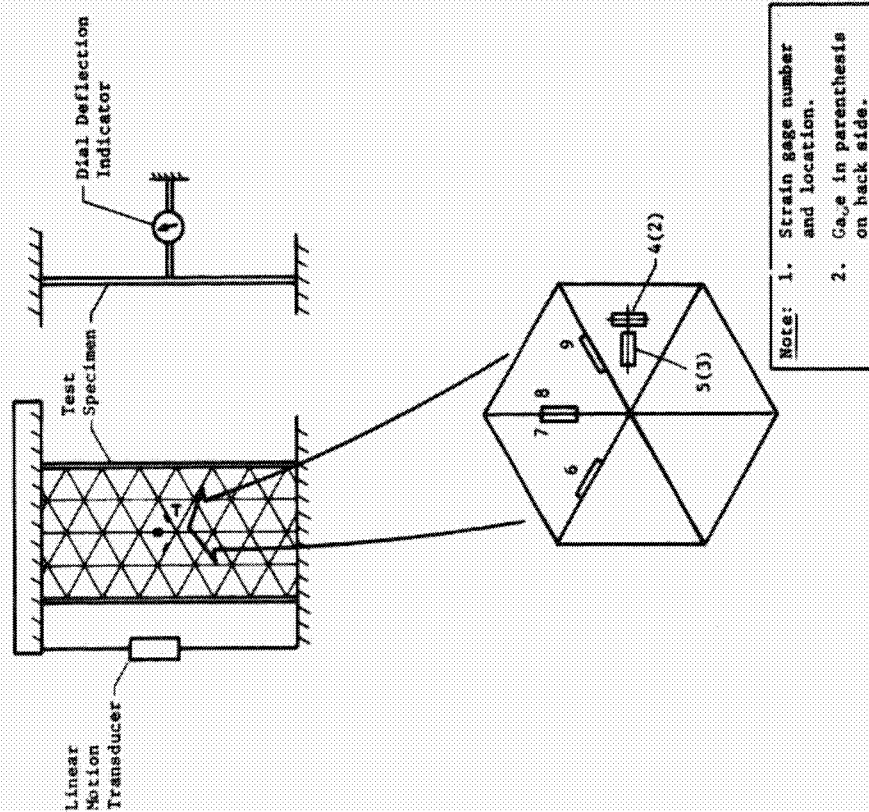


Fig. VI-23 Aluminum Iosgrid Instrumentation

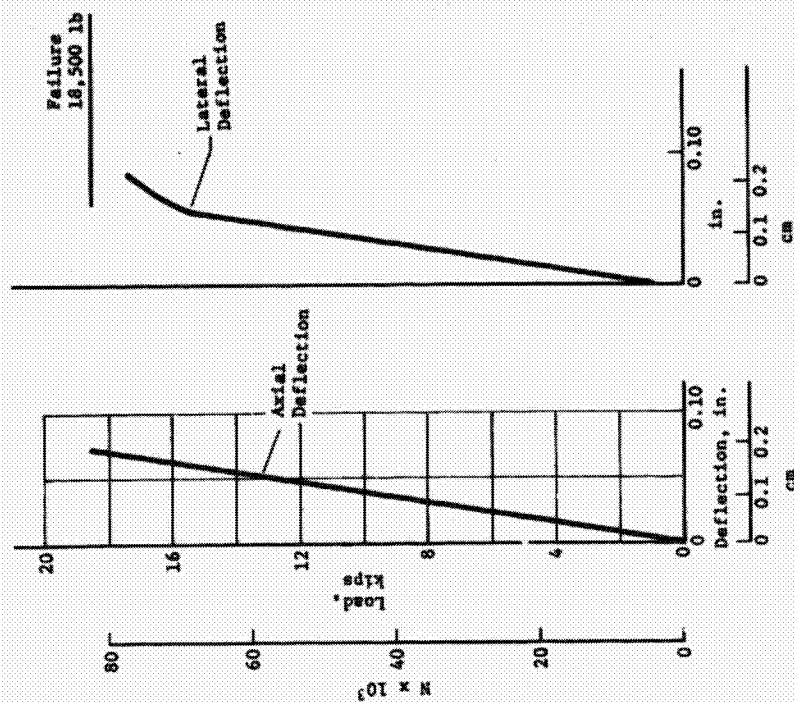


Fig. VI-24 Load Deflection Curves, Aluminum Iosgrid Panel

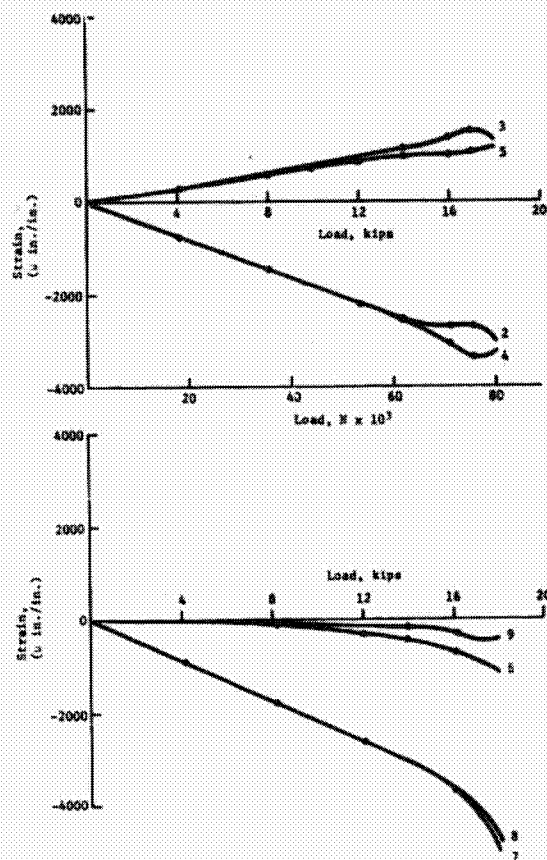


Fig. VI-25  
Strain Gage Plots, Aluminum  
Isogrid Panel

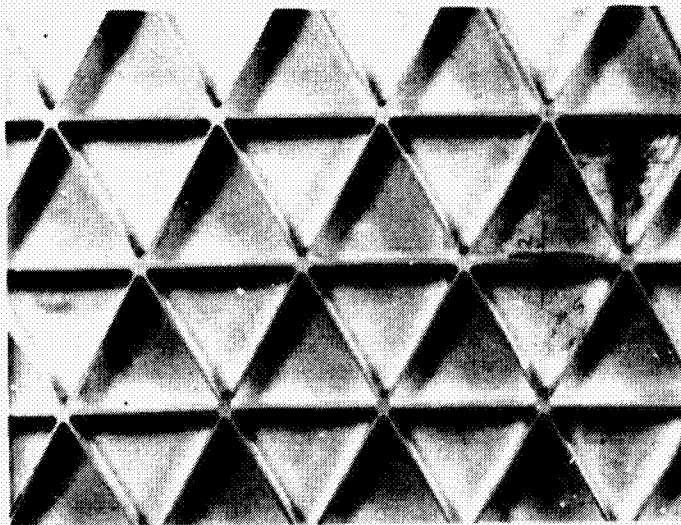


Fig. VI-26 Failed Panel, Aluminum Isogrid

## B. LARGE PHASE II STRUCTURES

The design and analysis study conducted during Phase I was concerned with a 3.66 m (144 in.) tall by 4.51 m (180 in.) diameter cylindrical shell structure subjected to combined loading of 1225.8 N/cm (700 lb/in.) axial compression and 245.2 N/cm (140 lb/in.) torsion. Preliminary evaluation of candidate concepts was aided by structural tests of small development panels. Three of the concepts were selected for further evaluation during Phase II. The development test panels for each of the three selected concepts consist of a flat 1.83 by 0.92 m (6 by 3 ft) compression panel and a flat 0.92 by 0.92 m (3 by 3 ft) shear panel. The compression panels were supported along all four edges and subjected to uniform axial compressive loading until failure. The shear panels were loaded to failure in pure shear, using an appropriate test support fixture. Unfortunately, the critical failure mode of the lightweight, large diameter cylinders designed during Phase I is overall instability at the combined design ultimate loading. The overall buckling characteristics of the flat test panels are not related to larger cylindrical shell buckling behavior and, therefore, had to be investigated before structural test.

### 1. Compression Test Panel Overall Buckling

The buckling load of a rectangular sandwich plate with isotropic faceskins under uniaxial compression can be predicted from the expression.

$$[1] \quad P = k \frac{\pi^2 D}{b^2},$$

where  $b$  is the panel width and  $D$  is the bending stiffness per unit run calculated from

$$[2] \quad D = \frac{EI}{(1-\nu^2)},$$

where  $E$  is Young's modulus,  $I$  is moment of inertia and  $\nu$  is Poisson's ratio. The buckling coefficient,  $k$ , depends on the boundary support, panel geometry and sandwich core shear stiffness. The shear stiffness is defined to be

$$[3] \quad s = \frac{b^2 S}{\pi^2 D},$$

where  $S$  is the transverse shear stiffness of the sandwich plate.



To determine the effect of core shear stiffness on panel buckling, the shear stiffness of the core in the warp or weak direction was used to calculate  $S$  from

$$[4] \quad S = G_w \left( \frac{c + f}{c} \right)^2,$$

where  $G_w$  is the core shear modulus,  $c$  is the core depth and  $f$  is the faceskin thickness. The resulting calculated value of  $s$  for the aluminum sandwich compression panel was such that the buckling load reduction due to core shear stiffness was less than 5% and was, therefore, neglected. The buckling coefficient,  $k$ , for the aluminum sandwich compression panel with  $a/b = 2$ , is dependent on the side boundary conditions of the plate. Values of  $k$  for several boundary conditions can be found in.<sup>16</sup> The structural test fixture will provide neither perfectly fixed nor simply supported boundary condition, therefore, calculations were made for these extremes with test values expected to fall between them if the designs prove to be buckling, rather than strength, critical. The value of  $k$  for simple support boundary conditions,  $a/b = 2$  and  $1/s \approx 0$  is given in Fig. 4.2 of<sup>16</sup> to be 4.0. This results in a calculated panel buckling load from Equation [1] of 1333 N/cm (762 lb/in.).

If it is assumed that the panel boundaries are perfectly fixed, the  $k$  value from Fig. 4.11 of<sup>16</sup> is 7.0 and the corresponding buckling load is 2325 N/cm (1337 lb/in.).

Similar calculations can be made for the orthotropic graphite/epoxy panel. Assuming negligible core shear effect, Equation [1] is again applicable, however, the bending stiffness  $D$  is replaced by

$$[5] \quad \bar{D} = \sqrt{D_x D_y},$$

where

$$[6] \quad D_x = \frac{E_x I_x}{(1 - \nu_{xy} \nu_{yx})} \quad \text{and} \quad D_y = \frac{E_y I_y}{(1 - \nu_{xy} \nu_{yx})}$$

which takes into account the orthotropic nature of the graphite/epoxy faceskins.

The case of simply supported rectangular plates with  $D_x \neq D_y$ , loaded in uniaxial compression, is discussed in section 5.3 of<sup>16</sup> and curves for  $k$  are shown in Fig. 5.7 of that reference. The buckling coefficient for the graphite/epoxy sandwich test panel is 3.1, which yields a critical buckling load for simple support boundary conditions of 922 N/cm (566 lb/in.). The case of fixed

boundary conditions with  $D_x \neq D_y$ , is presented in.<sup>17</sup> The value of  $k$  for this condition is 6.0, which yields a critical buckling load of 1915 N/cm (1096 lb/in.).

The critical overall buckling behavior of the aluminum truss can also be determined by calculating smeared  $D_x$  and  $D_y$  bending stiffnesses and treating the equivalent orthotropic panel. The critical buckling load, assuming simple support edge condition, calculated from Equation [1] is 1505 N/cm (858 lb/in.) and for the fixed edge support is 2900 N/cm (1660 lb/in.).

## 2. Shear Panel Overall Buckling

The buckling load of sandwich panels loaded in pure shear can be predicted from

$$[7] \quad P = k \frac{\pi^2 \bar{D}}{b^2},$$

where  $\bar{D}$  and  $b$  are as defined for compression buckling and  $k$ , the buckling coefficient, is determined from the boundary conditions, panel geometry and core shear stiffness. The appropriate values of  $k$  for simple support and fixed boundary conditions for the aluminum honeycomb shear panel taken from the NASA Design Structures Manual, (Fig. C2.1.5-14) are 9.5 and 15, respectively, if it is assumed that core shear stiffness is adequate. The calculated critical buckling loads are 3170 N/cm (1815 lb/in.) for simple support boundary conditions and 5000 N/cm (2868 lb/in.) for fixed boundary support.

Buckling coefficients for the graphite/epoxy panel are not readily available; however, it can be easily shown that the test panel is strength, rather than buckling, critical. If, for example, the lowest bending stiffness,  $D_y$ , is used rather than  $\bar{D} = \sqrt{D_x D_y}$  and the isotropic buckling coefficients of 9.5 and 15 used again, the critical buckling loads are 1260 N/cm (721 lb/in.) and 1990 N/cm (1139 lb/in.) for simple and fixed support, respectively. Full development of panel strength would cause failure at approximately 1340 N/cm (766 lb/in.). Because the  $D_x$  bending stiffness is five times greater than the  $D_y$  value, it can be conservatively assumed that the true critical buckling load is much higher than the critical strength load.

Similarly, the overall buckling load for the aluminum truss shear panel can be shown to be significantly higher than the critical strength value by considering smeared  $D_x$  and  $D_y$  bend stiffnesses.

If the lowest bending stiffness,  $D_y$ , is used rather than  $\bar{D} = \sqrt{D_x D_y}$ , the critical buckling loads are 3710 N/cm (2120 lb/in.) and 5860 N/cm (3350 lb/in.) for simple and fixed support respectively. These values are significantly higher than the expected critical strength value of 996 N/cm (570 lb/in.).

### 3. Local Instability

Another possible mode of failure for each of the six test panels is local instability. In the case of the sandwich panels this includes intercell buckling and face wrinkling and for the truss panels, local crippling of the tubular members.

a. *Honeycomb Sandwich Face Wrinkling* - The wrinkling phenomenon is a short wave faceskin buckling highly dependent on the transverse normal stiffness of the core. The critical faceskin load,  $P$ , can be calculated<sup>16</sup> from

$$[8] \quad P = 1.52 f (G_c E_{cz} E_f)^{1/3},$$

where  $f$  is the faceskin thickness,  $G_c$  the core shear modulus,  $E_{cz}$  the core transverse normal stiffness, and  $E_f$  the faceskin stiffness. The calculated critical faceskin wrinkling load for the aluminum sandwich panel is 8660 N/cm (4900 lb/in.) or a faceskin stress of 168,500 N/cm<sup>2</sup> (245,000 psi). Similar calculations for the graphite/epoxy sandwich panels yield 16,080 N/cm (9180 lb/in.) and 198,000 N/cm<sup>2</sup> (287,000 psi) if the faceskin stiffness  $E_f$  is taken to be the axial faceskin modulus,  $E_x$ , of the graphite/epoxy laminate.

b. *Honeycomb Sandwich Intercell Buckling* - The stress level at which a sandwich faceskin loaded in compression buckles locally within an individual hexagonal cell can be calculated<sup>16</sup> from the expression

$$[9] \quad \sigma_{cr} = 3E (f/d)^2,$$

where  $E$  is the faceskin modulus,  $f$  is the faceskin thickness, and  $d$  is the cell size. The calculated values for the aluminum and graphite/epoxy sandwich panels are 132,000 N/cm<sup>2</sup> (192,000 psi) and 540,000 N/cm<sup>2</sup> (785,000 psi), respectively. The value for the graphite/epoxy panels was calculated using the faceskin axial Young's modulus  $E_x$ .

c. *Truss Tube Local Crippling* - The critical local crippling stress of thin walled rectangular tubing can be calculated from

$$[10] \quad \sigma_{cr} = k_h \frac{\pi^2 E}{12(1-\nu^2)} \left( t_w / h_w \right)^2,$$

where E is Young's modulus,  $\nu$  is Poisson's ratio,  $t_w$  is web thickness,  $h_w$  is web height, and  $k_h$  is a coefficient dependent on stiffener geometry available from the NASA Structures Design Manual (Fig. 4.2.2-5). The calculated critical stress values for the truss stringers, horizontals and diagonals are 33,100 N/cm<sup>2</sup> (48,100 psi), 10,280 N/cm<sup>2</sup> (14,900 psi), and 10,500 N/cm<sup>2</sup> (15,310 psi), respectively.

#### 4. Material Strength and Stiffness

Mechanical properties of the materials used in fabricating the compression and shear test panels are listed in Table VI-7. The aluminum sandwich panel used 2014-T6 aluminum faceskins that were chemically milled from 0.102 cm (0.040 in.) down to 0.025 cm +0.005 cm (0.010 in. +0.002 in.) -0.000 cm (-0.000 in.). It has compression and shear ultimate values of 40,000 N/cm<sup>2</sup> (58,000 psi) and 26,850 N/cm<sup>2</sup> (39,000 psi) respectively. The rectangular aluminum tubing used in the truss structure was 2024 alloy that was received in the T3 hardened condition and heat treated to the T81 condition. This yielded tubing with ultimate compression and shear strength values of 39,250 N/cm<sup>2</sup> (57,000 psi) and 24,100 N/cm<sup>2</sup> (35,000 psi), respectively. The graphite/epoxy laminates used as faceskins on the sandwich panels consist of two layers of axial Type I/5208 material sandwiched between four symmetric layers of  $\pm 45^\circ$  T-300/5208 material. A typical cured faceskin thickness was 0.041 cm (0.016 in.) of which 0.023 cm (0.009 in.) was axial material and 0.018 cm (0.007 in.) was  $\pm 45^\circ$  material. The axial strength and stiffness shown in Table IV-7 for this laminate was taken from Phase I small panel test results, while other values are estimated from material properties of the constituents.

Table VI-7 Material Properties

Property	Aluminum Sandwich Faceskins,* 2014-T6	Aluminum Truss Tubes,* 2024-T81	Graphite/Epoxy Sandwich Faceskins, Type I/T-300/5208
Compression Ultimate $\sigma_{cy}$ , N/cm <sup>2</sup> (psi)	27,300 (39,000)	39,900 (57,000)	37,800 <sup>a</sup> (54,000)
Shear Ultimate $\tau_u$ , N/cm <sup>2</sup> (psi)	27,300 (39,000)	24,500 (35,000)	16,800 (24,000)
Axial Young's Modulus $E_x$ , N/cm <sup>2</sup> (psi)	7,350,000 (10,500,000)	7,350,000 (10,500,000)	11,090,000 (15,850,000)
Transverse Young's Modulus $E_y$ , N/cm <sup>2</sup> (psi)	7,350,000 (10,500,000)	7,350,000 (10,500,000)	1,918,000 (2,740,000)
Shear Modulus $G_{xy}$ , N/cm <sup>2</sup> (psi)	2,800,000 (4,000,000)	2,800,000 (4,000,000)	1,750,000 (2,500,000)
Poisson's Ratio $\nu_{xy}$	0.33	0.33	0.25
*Values taken from MIL- Handbook 58, September 1971.			

5. Test Results Summary

The calculated theoretical critical loads and the actual test loads for the six panel structural tests are listed in Table VI-8. The honeycomb sandwich compression panel with aluminum faceskins shown in the test fixture in Fig. VI-27 was critical in overall panel buckling. The panel was loaded to 1285 N/cm (735 lb/in.) without failure. The test was terminated at that point because excessive center panel normal deflection indicated the onset of panel buckling. Terminating the test within the elastic strain range allows for possible future retest under different test conditions. The test information is sufficient to predict an overall buckling load, from a Southwell plot (Fig. VI-28) of test data, of 1607 N/cm (918 lb/in.). Similarly, the test of the sandwich compression panel with graphite/epoxy faceskins was terminated at an applied load of 1268 N/cm (725 lb/in.) without failure. A Southwell plot of test data shown in Fig. VI-29 was used to predict a buckling load of 1362 N/cm (779 lb/in.). The critical failure mode of the aluminum truss compression panel was local



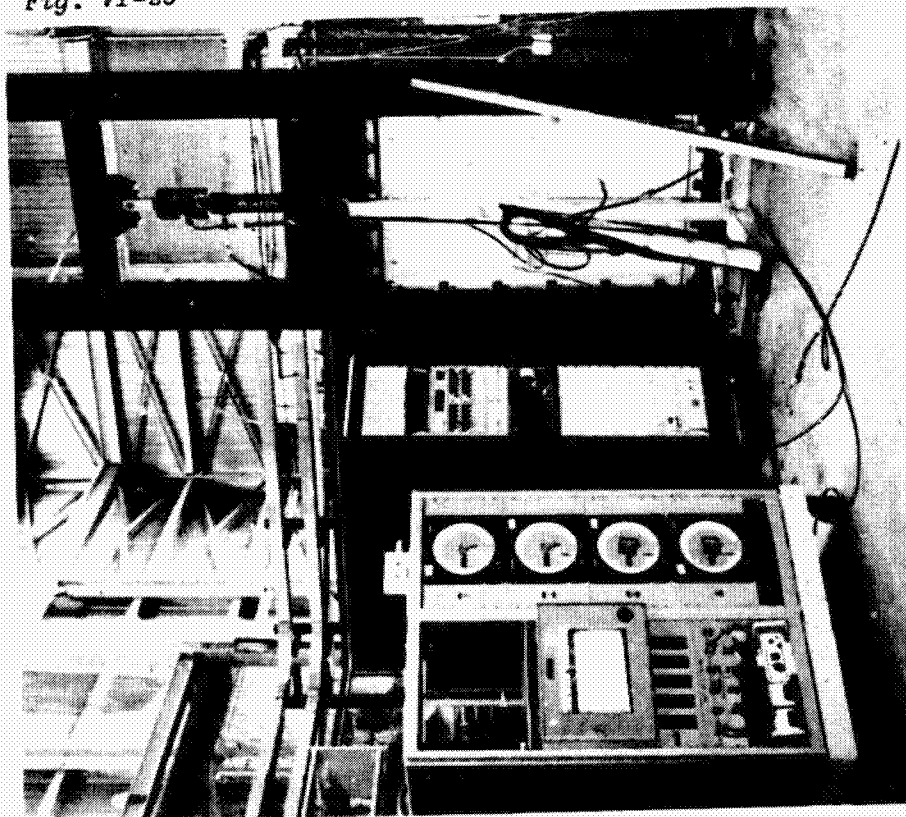


Fig. VI-27

Fig. VI-27 Sandwich Panel Compression Test Fixture

Fig. VI-28

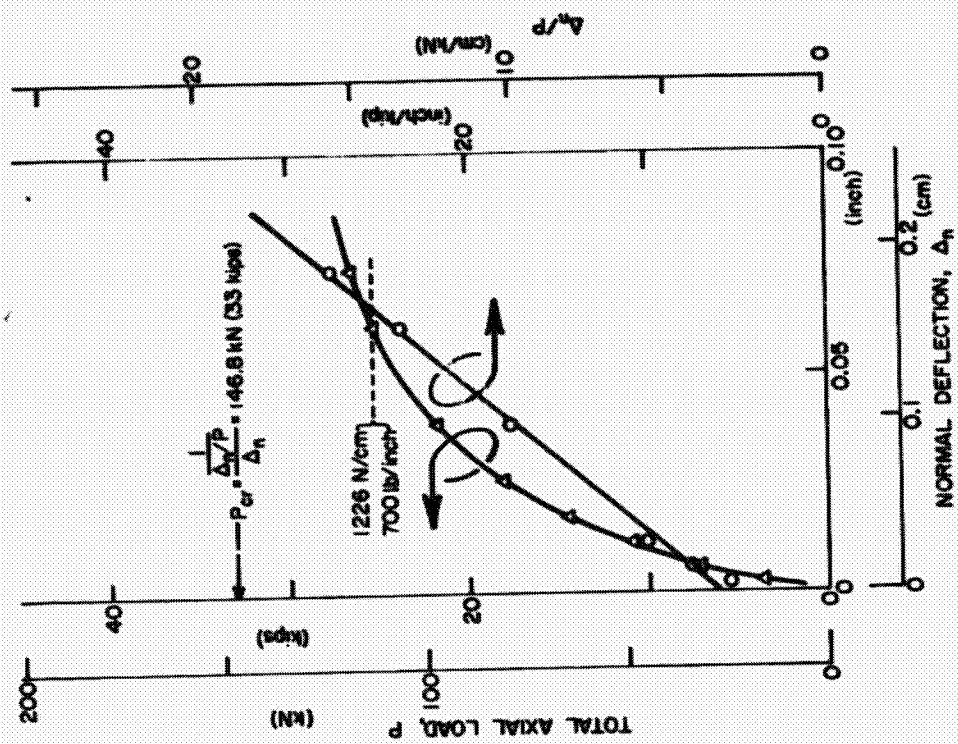


Fig. VI-28  
Southwell Plot, Aluminum Panel  
Compression Test, CP-Alum-10



Table VI-8

Table VI-8 Theoretical and Experimental Panel Loads

Test Specimen	Theoretical Critical Loads, N/cm (lb/in.)					Structural Test Load, N/cm (lb/in.)	Comment
	Critical Overall Buckling Loads		Critical Local Buckling Load	Critical Strength			
	Fixed Support	Simple Support					
Aluminum Sandwich Compression Panel	2327 (1330)	1333 (762)	6,720 (3,840)	2231 (1275)	1286 (735)	No failure, 918 lb/in. predicted Southwell buckling load	
Graphite/Epoxy Sandwich Compression Panel	1918 (1096)	990 (566)	16,065 (9,180)	3027 (1730)	1268 (725)	No failure, 779 lb/in. predicted Southwell buckling load	
Aluminum Truss Compression Panel	2905 (1660)	1501 (858)	1,239 (708)	1470 (840)	1072 (613)	Stringer local buckling failure	
Aluminum Sandwich Shear Panel	5005 (2860)	3176 (1815)	6,720 (3,840)	1501 (858)	1594 (911)	Material strength failure above yield stress	
Graphite/Epoxy Sandwich Shear Panel	4795 (2740)*	3045 (1740)*	11,725 (6,700)	1340 (766)	1520 (869)	Material strength failure	
Aluminum Truss Shear Panel	5878 (3359)*	3710 (2120)*	278 (159)	997 (570)	592 (310)	Diagonal member local buckling at 140 lb/in., catastrophic failure at 310 lb/in.	

\*Estimated using  $\bar{D} = \sqrt{D_x D_y}$  and  $K_s = 9.5$ ,  $K_f = 15.0$

instability of the stringer segments. Simultaneous catastrophic failure of all three stringer sections (Fig. VI-30) occurred at a test load of 1073 N/cm (613 lb/in.). Local buckling failure occurred at a stress level approximately 13% lower than was predicted.

The aluminum sandwich shear panel failed (Fig. VI-31) at 1594 N/cm (911 lb/in.) with faceskin principal strains all well beyond the elastic yield strain. Similarly, the graphite/epoxy shear panel failure occurred at material strain levels indicative of full development of material strength. The failure did not initiate at the faceskin repair patch as can be seen in Fig. VI-32. The overall panel shear load at failure was 1520 N/cm (869 lb/in.). The critical failure mode of the aluminum truss shear panel was local instability of the diagonal truss members. Initial buckling occurred at an effective shear load of 245 N/cm (140 lb/in.), however, initial buckling did not cause catastrophic failure due to the low stress level at which it occurred. The panel failed catastrophically (Fig. VI-33) at 542 N/cm (310 lb/in.). Strain gage and deflectometer data were presented previously in<sup>18</sup>.

In summary, both of the honeycomb sandwich concepts, aluminum and graphite/epoxy, use faceskins which are minimum gage as determined by fabricability, handleability, available raw material size, quality assurance and damage sensitivity and each has adequate strength and stiffness. The aluminum truss concept requires only slight design modification to satisfy strength requirements, however, the redesigned truss would still have a smaller margin of safety than the sandwich panel concepts.

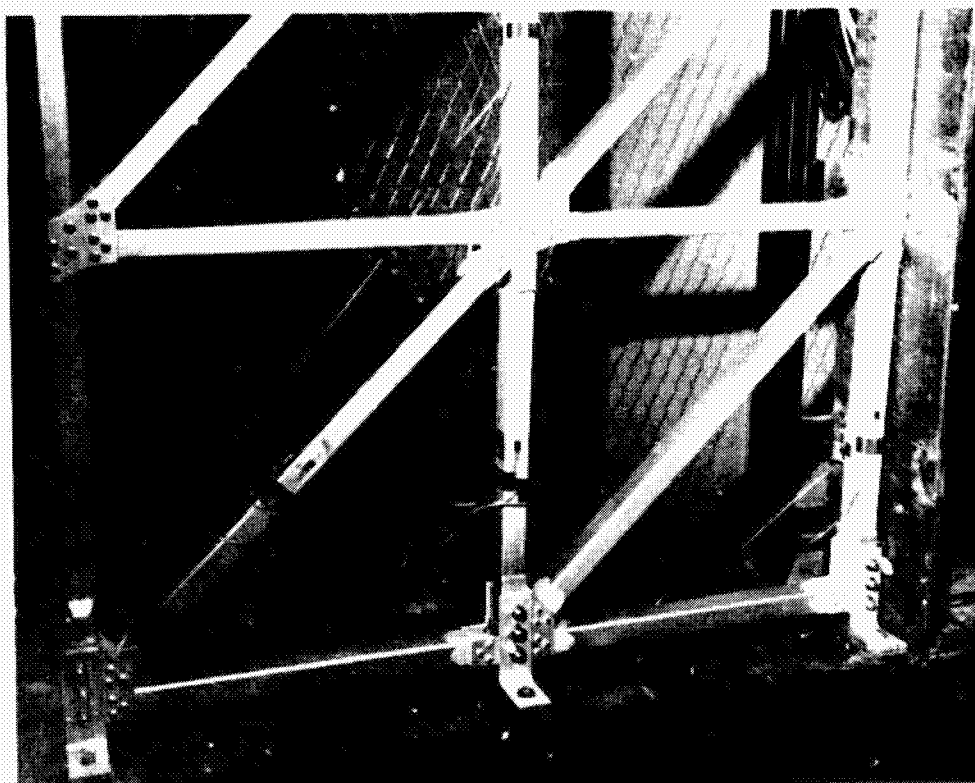


Fig. VI-29

Fig. VI-30  
Aluminum Truss Compression Test Local  
Stringer Buckling

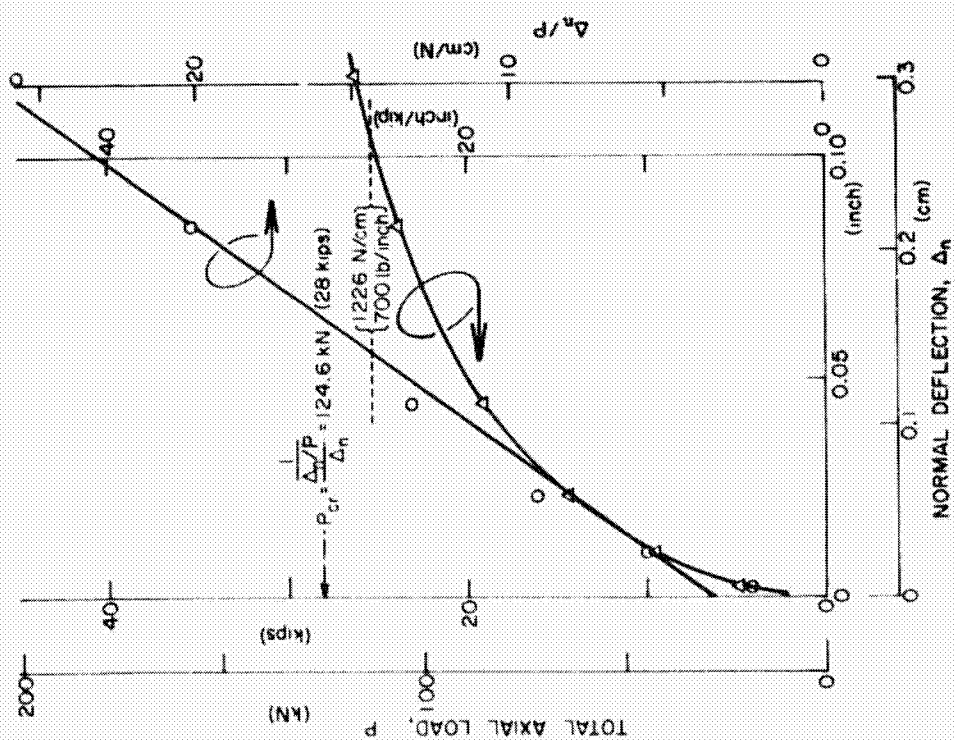


Fig. VI-30

Fig. VI-30  
Graphite/Epoxy Panel  
Compression Test, CP-Type 1-50-16

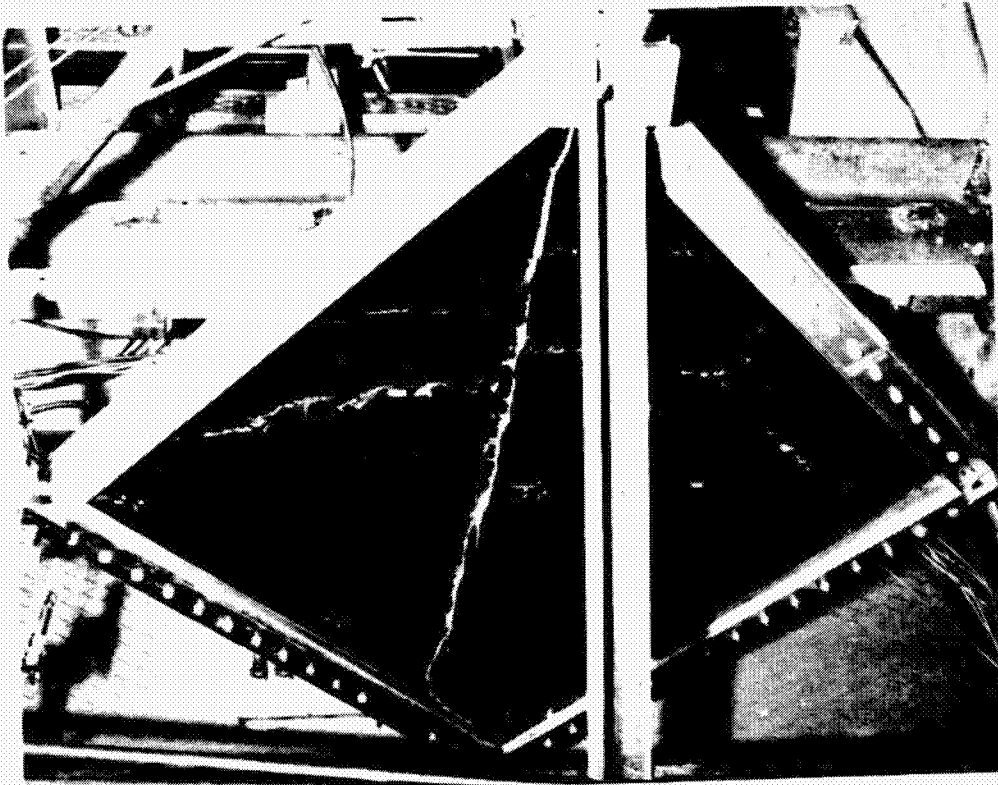


Fig. VI-32  
Graphite/Epoxy Sandwich Shear Panel Failed  
Specimen

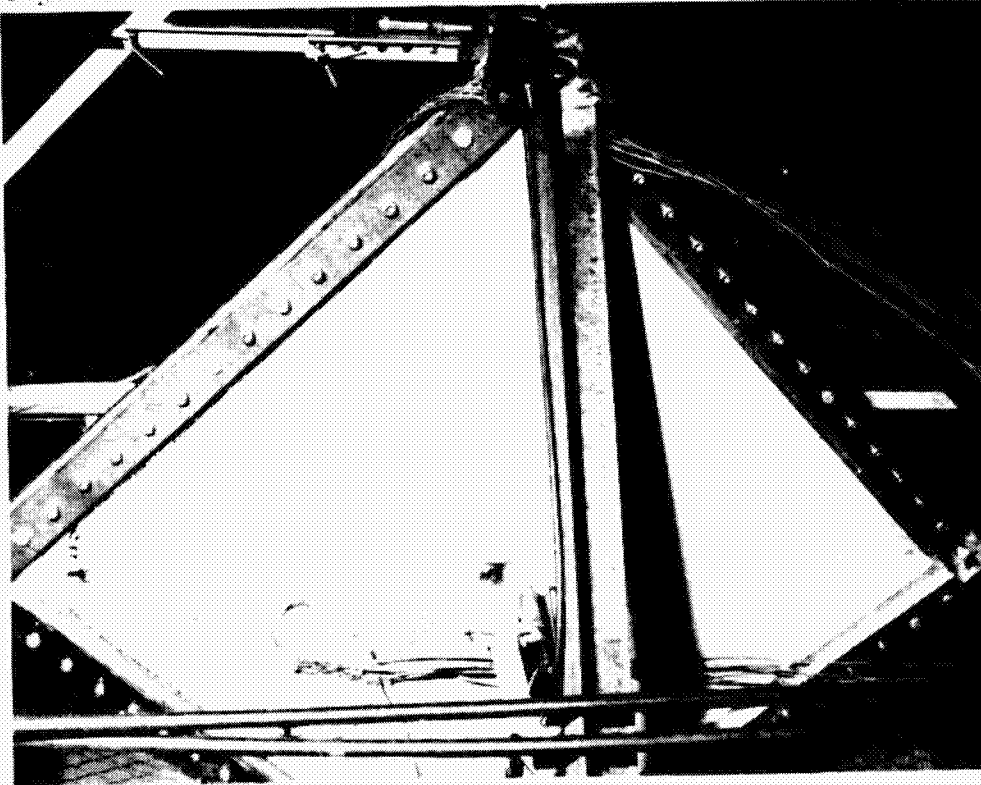
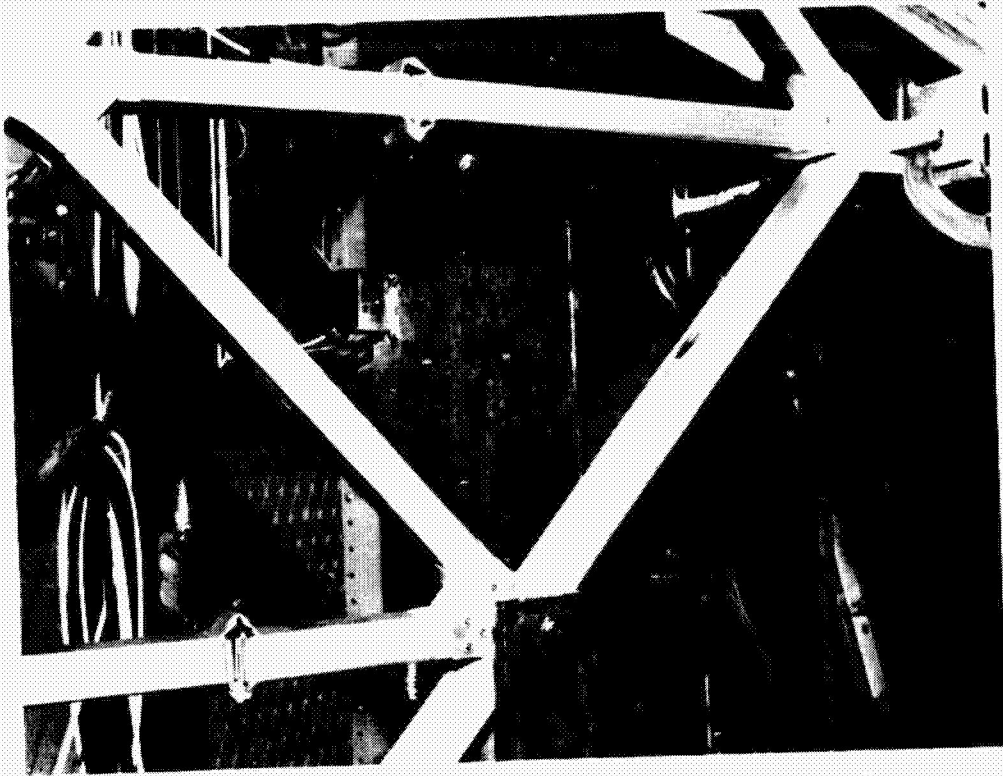


Fig. VI-31  
Aluminum Sandwich Shear Panel Failed  
Specimen

Fig. VI-32

Fig. VI-31



*Fig. VI-33 Aluminum Truss Shear Test Local Buckling Failure*

## VII. CONCLUSIONS AND RECOMMENDATIONS

---

The initial objective of the work to be performed under this contract was to determine the feasibility of achieving Space Tug body structural weights so that optimum performance of that vehicle can be achieved. The results of the work are very encouraging because more than one structure/material concept was shown to provide reliable, lightweight shell structure within original weight guidelines. In addition, at least one of the concepts uses state-of-the-art manufacturing technology and conventional materials, thereby, minimizing total structure cost. Notable conclusions from several aspects of the contract are summarized.

### A. CONCLUSIONS

#### 1. Structural Weight

The lowest structural weight is provided by the honeycomb sandwich concept with graphite/epoxy faceskins with a cylinder area weight of  $2.78 \text{ kg/m}^2$  ( $0.570 \text{ lb/ft}^2$ ), which includes edge attachment weight estimated from preliminary closeout designs. The sandwich concept with aluminum faceskins, at  $2.88 \text{ kg/m}^2$  ( $0.590 \text{ lb/ft}^2$ ), is only slightly heavier. This concept is lower cost because of the less expensive faceskin material, however, the graphite/epoxy concept provides more reserve strength due to minimum material gages involved. The aluminum truss concept with fiberglass meteoroid protection yields a weight of  $3.12 \text{ kg/m}^2$  ( $0.640 \text{ lb/ft}^2$ ), including attachment capability. The truss concept provides more damage resistance than the sandwich concept and is more versatile for secondary attachment or design modification.

#### 2. Strength and Stiffness

The three concepts were all designed to be buckling critical when used in the design of a 4.57 m (15 ft) diameter by 3.66 m (12 ft) high cylinder subjected to combined loading of 1225.8 N/m (700 lb/in.) axial compression and 245.2 N/m (140 lb/in.) torsion. The ultimate strengths of panels small enough to cause a strength failure for singly applied axial compression and torsion are listed below for the three concepts.



Structural Concept	Ultimate Strength, kg/m (lb/in.)	
	Axial Compression	In-Plane Shear
Honeycomb Sandwich with Graphite/Epoxy Faceskin	2840 (1682)	1556 (889)
Honeycomb Sandwich with Aluminum Faceskin	2275 (1300)	1585 (905)
Aluminum Truss with Fiber-glass Meteoroid Protection	1035 (613)	507 (300)

The apparent excessive strength of the sandwich panels is actually caused by minimum gage restrictions of the materials involved. Excessive strength can be taken advantage of in the final design by permitting a larger amount of local structural damage.

#### Minimum Useful Gages and Sizes

The design of the subject cylindrical structure for loads representative of those expected on Space Tug body structure was restricted in most cases by the minimum useful material gage or size. Fabrication of a wide variety of structural panels using many different structural materials has provided information on the useful sizes of many of these materials. This information is tabulated below for the materials involved.

Material	Minimum Recommended Thickness (inches)	Comments
Aluminum	0.0250 0.0100 0.0030	Stiffener local sections Honeycomb sandwich faceskins Nonstructural, damage protection
Titanium	0.0080	Honeycomb sandwich faceskins
Style 104 fiberglass cloth/ epoxy	0.0008	Nonstructural, crack retention
Style 112 fiberglass cloth/ epoxy	0.0030 0.0045	Balanced shear ply, structural Damage protection
T-300 Graphite/ Epoxy	0.0015 0.0030	Unidirectional, structural ±45° shear ply, structural
HM Graphite/ Epoxy	0.0050 0.0100	Unidirectional, structural ±45° shear ply, structural
Boron/ Epoxy	0.0050 0.0100	Unidirectional, structural ±45° shear ply, structural

4. Sandwich Panel Damage Resistance

Although a rigorous program of damage sensitivity and damage effects was not included within the scope of this program, an overall "feel" for the relative merits of the structural concepts fabricated was developed over the course of work. The honeycomb sandwich panels using 1/8-5052-0.0007-3.1 aluminum hexcel core with many different thin faceskin materials were all very susceptible to "denting" from a relatively low energy impact. If this denting causes a significant reduction in load-carrying capability it may be necessary to do any or all of the following: (1) reduce design allowables; (2) use special handling and fabrication techniques; or (3) add a nonload-carrying damage protection surface to the panels.

5. Analytical Capability

An existing computer program, HOLBOAT, which calculates the critical buckling load of an anisotropic cylindrical shell under combined loading, was expanded to include cylinders stiffened with discrete stringers and frames. A user's manual was also written and submitted to NASA-MSFC along with copies of the computer program. The modified program provides a very versatile, inexpensive analytical test for flight hardware design.

6. Sandwich Panel Nondestructive Evaluation (NDE)

Ultrasonic evaluation and radiographic examination of a "control" sandwich panel provided encouraging preliminary results for NDE of lightweight sandwich panels. All of the included imperfections that caused lack of adhesive bond were detected by ultrasonic inspection. Irregularities in the aluminum honeycomb core were easily detected by X-ray.

B. RECOMMENDATIONS

Lightweight structure technology has been enhanced through successful completion of this contract. The successful conclusion of this work also clarifies the next steps necessary in proceeding toward flight hardware fabrication. Recommendations for future work aimed at full verification of lightweight Space Tug structures are summarized.

1. Structural Damage and Associated Reliability

The structural panels fabricated and tested to date have been of relatively small size and have been handled very carefully to minimize damage so that maximum strength could be achieved. A problem inherent in the lightweight structures required for Space Tug is that they are more susceptible to damage than conventional aerospace structures. It is recommended, therefore, that a test program be initiated that investigates the susceptibility of the candidate structural designs to damage, the effects of damage on the ultimate strength, and methods and efficiency of damage repair techniques.

2. Quality Assurance Methods

Achieving high reliability flight hardware will require methods aimed at verifying structural integrity of the finished product. This will include nondestructive evaluation (NDE) of structural components using methods consistent with the structural concept involved. This may include, for example, ultrasonic C scans of bonded structures, such as honeycomb sandwich panels. It is recommended, therefore, that a program be initiated to investigate methods of verifying the structural integrity of finished structures without causing degradation.

3. Honeycomb Sandwich Panel Closeouts

Investigation of lightweight methods of efficiently attaching honeycomb sandwich panels and introducing loads was not included under the original format of this contract. This presents a special problem for lightweight sandwich construction using minimum gage materials because of manufacturing tolerances and criticality of relatively small geometrical mismatch. It is recommended, therefore, that a design, fabrication, and test program be initiated that is aimed at developing minimum weight, reliable, attachment methods for sandwich panels with aluminum and graphite/epoxy faceskins.

4. Structural Design Computer Program

The modified HOLBOAT buckling analysis computer program provides a general tool for the prediction of overall buckling of large, stiffened cylindrical shells under combined loading. This analysis tool can be incorporated into a design computer program that fully designs a cylindrical shell structure. The design program would handle a wide variety of stiffener geometries and would incorporate realistic design information, such as material minimum gages and experimental buckling reduction factors. The general design scheme would be an iterative approach balancing overall and local stability using the input design information,

such as load direction and magnitude, material types and properties, skin, stringer, and frame type, or general shape and geometrical restraints. It is therefore recommended that this design computer program and an appropriate user's manual be developed to aid in rapid, low-cost preliminary design trade studies as well as final design.

5. Fabrication and Test of Full Size Skirt

The feasibility of achieving Space Tug body structural weight within required limits has been demonstrated through successful work under this contract. In general, the original concern was the exceedingly light weight of candidate structural concepts and the resulting difficulty with ultrathin material gage, geometrical tolerance control, damage sensitivity, and fabricability. Work during Phase I identified many structural configurations with potential of satisfying the design goals. Relatively small panels representing the leading candidates were fabricated and tested to aid in further screening. Three of the configurations evaluated during Phase I were selected for further evaluation during Phase II. Fabrication and test of 1.83x0.95 m (6x3 ft) compression panels and 0.95x0.95 m (3x3 ft) shear panels provided manufacturing feasibility information and further verified the predicted full-scale skirt structural weight.

The next logical step in the development of lightweight shell structure for Space Tug is the fabrication and test of a full size skirt. This skirt would contain typical access doors to demonstrate door design techniques and verify proposed analysis methods. The full size skirt would also provide information on attachment methods, manufacturing handling techniques, real tolerances, and final assemble tooling.

## VIII. REFERENCES

---

1. *Phase I Design, Fabrication, and Test of Lightweight Shell Structure, Interim Report.* MCR-74-92. Martin Marietta Corporation, Denver, Colorado, March 1974.
2. *Graphite Composite Applications.* Rockwell International, Space Division, SD73-SA-0400, Contract NAS7-200. March 22, 1973.
3. E. M. Lenoe *et al.*: "Preliminary Evaluation of Test Standards for Boron/Epoxy Laminates. *Composite Materials: Testing and Design.* ASTM STP-660, 1969, pp 122 thru 139.
4. *Buckling of Thin-Walled Circular Cylinders.* NASA SP-8007; NASA Space Vehicle Design Criteria (Structures), August 1968.
5. A. Holston, Jr., A Feldman, and D. A. Stang: "HOLSTON's Buckling of Anisotropic Tubes," *Stability of Filament-Wound Cylinders under Combined Loading.* AFFDL-TR-67-55 Martin Marietta Corporation, Denver, Colorado, May 1967.
6. *Metallic Materials and Elements for Aerospace Vehicle Structures,* MIL-HDBK-5B. September, 1971.
7. S. Cheng and B. P. C. Ho: "Stability of Heterogeneous Aeolotropic Cylindrical Shells under Combined Loading." *AIAA Journal*, Vol 1, No. 4, April 1963, pp 892-898.
8. B. P. C. Ho and S. Cheng: "Some Problems in Stability of Heterogeneous Aeolotropic Cylindrical Shells under Combined Loading." *AIAA Journal*, Vol 1, No. 7, July 1963, pp 1603-1607.
9. W. Flugge: *Stresses in Shells.* Springer-Verlag, Berlin, Germany, 1962.
10. *User's Manual HOLBOAT Computer Program.* MCR-74-426, Martin Marietta Corporation, Denver, Colorado, October 1974.
11. *Astronautic Structures Manual,* National Aeronautics and Space Administration, Marshall Space Flight Center, August 15, 1970.
12. M. B. Harmon and R. R. Meyer *et al.*: *Isogrid Design Handbook.* NASA CR-124075. McDonnell Douglas Astronautics Company, February 1973.
13. A. Holston, Jr.: "Buckling of Inhomogeneous Anisotropic Cylindrical Shells by Bending." *AIAA Journal*, Vol 6, No. 10, October 1968, pp 1837-1841.

14. R. M. Jones: "Buckling of Circular Cylindrical Shells with Multiple Orthotropic Layers and Eccentric Stiffeners." *AIAA Journal*, Vol 6, No. 12, December 1968, pp 2301-2305.
15. *Buckling of Thin-Walled Circular Cylinders* (NASA SP-8007), NASA Space Vehicle Design Criteria (Structures), August 1968.
16. F. F. Plantems: *Sandwich Construction*. John Wiley & Sons, New York, 1966.
17. C. C. Chang, I. K. Ebcioğlu, and C. H. Hsight: "General Stability Analysis of Orthotropic Sandwich Panels for Four Different Boundary Conditions." *ZAMM*, 42, September 9, 1962, pp 373-389.
18. *Test Results Report, Lightweight Shell Structure Development Panels*. MCR-74-460. Martin Marietta Corporation, Denver, Colorado, September 1974.



# APPENDIX - CONVERSION FACTORS

Basic Si Units		
Physical Concept	Measurement	Abbreviation
Length	meter	m
Mass	kilogram	kg
Time	second	sec
Force	Newton	N
Thermodynamic Temperature	degree Kelvin	°K
Density	kilograms/meter <sup>3</sup>	kg/m <sup>3</sup>

Prefixes		
Factor By Which Unit Is Multiplied	Prefix	Symbol
10 <sup>6</sup>	mega	M
10 <sup>3</sup>	kilo	k
10 <sup>2</sup>	hecto	h
10	deca	da
10 <sup>-1</sup>	deci	d
10 <sup>-2</sup>	centi	c
10 <sup>-3</sup>	milli	m
10 <sup>-6</sup>	micro	μ

Conversion Factors		
To Convert From	To	Multiply By
Celsius (temp)	Kelvin	$t_K = t_C + 273.15$
Fahrenheit (temp)	Kelvin	$t_K = (5/9) (t_F + 459.67)$
foot	meter	$3.048 \times 10^{-1}$
inch	meter	$2.54 \times 10^{-2}$
pound mass (lbm avoirdupois)	kilogram	$4.536 \times 10^{-1}$
pound mass force (lbf)	Newton	4.44822
lbm/inch <sup>3</sup>	kilogram/meter <sup>3</sup>	$2.768 \times 10^4$
psi	Newton/meter <sup>2</sup>	$6.895 \times 10^3$